

SCALE AND ABSTRACTION: THE SENSITIVITY OF
FIRE-REGIME SIMULATION TO NUISANCE PARAMETERS

IAN DAVID DAVIES



Australian
National
University

September 2014



Ian David Davies: *Scale and Abstraction: The Sensitivity of Fire-Regime Simulation to Nuisance Parameters*, September 2014



DECLARATION

This thesis contains no material which has been accepted for the award of any other degree or diploma in any university. To the best of the author's knowledge, it contains no material previously published or written by another person, except where due reference is made in the text.

Canberra, September 2014

A handwritten signature in cursive script, reading "Ian David Davies", written over a horizontal line.

Ian David Davies

ABSTRACT

Fire plays a key role in ecosystem dynamics and its impact on environmental, social and economic assets is increasingly a critical area of research. Fire regime simulation models are one of many approaches that provide insights into the relative importance of factors driving the dynamics of fire-vegetation systems. The components of these systems: climate, weather, terrain and ignition, mediated through vegetation, operate over vast temporal and spatial scales when compared to that of human observation. Simulation provides a valuable way in which systems operating over these scales can be investigated, where analytical solutions may be intractable, data scarce or unavailable or field experiments prohibitively expensive or otherwise impractical.

Fire propagates as a contagious process and simulation offers an approach to capture this important behaviour explicitly. The patterns of fire regimes that emerge from such models are simply the sum of many fire events over time, each shaped by the changing weather, terrain and vegetation influencing the spreading fire. However, when formulating these models, space and time must be made discrete, and this entails introducing 'nuisance parameters': parameters necessary for the model formulation but not otherwise of interest. The most obvious of these are time step and spatial resolution. However, when points are traversed by fire during a simulation, how they are connected (number of neighbours) and their arrangement (the distance and angle to each neighbour) can also be considered as nuisance parameters required to describe a discrete geometry.

Thus fire growth simulations are discrete approximations of continuous non-linear systems, and it might be expected that the values chosen for these nuisance parameters will be important. While it is well known that discrete geometries have consequences for the shape and area of simulated fires, to my knowledge, no research has investigated the consequence this may have for estimates of the relative importance of the various drivers of fire regimes, which is after all, the key application of these models. Identifying the significance of spatio-temporal resolution and spatial representation has implications for model performance, the scales to which they can be realistically applied and our confidence in their findings.

I will argue in this thesis that nuisance parameters can be demonstrated to be unimportant for this class of model within some reasonable limits. I use the idea of 'importance' to underline the need for context with such an assertion. With sufficient replication, any parameter can be found statistically significant. A parameter is important, on the other hand, if different values produce qualitatively different

outcomes. A qualitatively different outcome would be, for example, that climate is found to be the most important determinant of fire regimes with one set of nuisance parameters but fuel management the most important with some other set.

Models are commonly either re-parameterised to account for changes in resolution or scaling-up methods applied if such exist. I will further argue that such differences as there are in model outputs due to spatial resolution, cannot be accounted for by either re-parameterising or using an approach that allows resolution to vary over the spatial extent as has been done in other fields.

A set of experiments were devised using a published fire regime simulation model, that I modified, verified and validated, to isolate just those aspects of the model's sensitivity to resolution and discrete geometries that are unavoidable or intrinsic to these choices. This new model (FIREMESH) is used to test the above hypotheses, using published experimental treatments that can stand as yardsticks by which formal estimates of the importance of nuisance parameters can be made.

As estimated by the model, neither spatio-temporal resolution nor any of the various choices available for discrete geometries, altered the model predictions with one exception: the use of spatial models that have only four neighbours between locations. This adds considerable confidence to the robustness of this type of model. This finding holds for measures of the amount of fire in the landscape (average inter-fire interval), arguably, the major component of fire regimes. As expected, it is spatial resolution that has the greatest impact on running times for the model but this study finds that neither calibration, nor taking an approach that allows resolution to vary over the spatial extent, can account for differences in model outputs that arise from running simulations at coarser resolutions.

All models are abstractions and a good model should ideally hold over levels of abstraction. This is rarely the case, but within the range of the abstraction of space and time used here, this study shows that findings made by models of this type are relatively robust with regard to these aspects of abstraction and can, with some confidence, be constructed more simply. However, abstracting systems for the purpose of study is unavoidably subjective. The difficulty of providing objective measures of levels abstraction is a critical bottleneck in finding suitable system representations. An important area of further research is the development of approaches to model construction that allow fast, flexible and objective measures of abstraction choices. This means recognising modelling studies themselves as dynamic systems, where ideas from many disciplines must be captured in an appropriate and reusable form to allow an agile response, as questions change in the light of new findings and new research requirements.

ACKNOWLEDGMENTS

This study has been undertaken at the Fenner School of Environment and Society, Australian National University with financial support from an Australian Postgraduate Research Award and a CSIRO Flagship PhD Scholarship. I have many people to thank for their assistance during my research. In particular I would like to thank my supervisor Geoff Cary for encouragement, challenging ideas and new perspectives, not only during this study but over the course of many years. He has always been available for discussion and always with good grace and humour. I also owe a great debt of gratitude to Malcolm Gill, someone who has experienced the development of fire science first hand in both Australia and around the world, and who has been generous with his time in providing guidance, always accompanied by insight and precision. Both Geoff Cary and Malcolm Gill have provided stimulating discussion on many facets of the impact of fire on the environment and society both before and during this study.

Of particular value has been the opportunity to take part in an intentional model comparison study with researchers from Australia, North America and France. This has been a stimulating group whose ideas have in many ways led to this study. I thank members of that group, Bob Keane, Russ Parsons, Mike Flannigan and Geoff Cary for the opportunity to present my initial ideas at a joint workshop at the start of this study in 2012.

I thank all members of my panel, Geoff Cary, Malcolm Gill, Steve Roxburgh and Jacques Gignoux for their detailed review of the draft of this thesis and for joint discussions over the course of the project. This work has benefited greatly from their insights and I have learnt much of what is required to undertake original research from these discussions. Of course, any errors and omissions remain my own.

I am grateful to Phil Zylstra for fire map data of the Australian Alps and for discussions of related work. Thanks also go to John Stein for his expertise in preparing terrain data on which this study is based, to Luciana Porfirio and Brendan Mackey for access to Landform 7 data and to Clem Davis for discussions on weather and climate data for SE Australia. I also would like to thank Bob Forrester for statistical advice during this study, Joel Kelso for correspondence on fire spread on irregular grids and Lachie McCaw for discussions and data comparing rates of fire spread from Project Vesta and McArthur's Forest Fire Danger Meter. Geoff Cary has also been generous in providing both source code and data from the original version of FIRESCAPE (from some 16 years past) together with data from more recent studies with

which to validate the model used in this study. I also thank Professor Michael Barnsley for enthusiastic and animated discussions on fractal landscapes and look forward to continuing these discussions in the future.

Finally, it is difficult to imagine how a project such as this could succeed without support of family and friends. In particular I owe a great deal to my wife Anne for support, encouragement and her professional editing skills in reviewing the initial draft of this thesis. I am hugely in debt and now must get to work.

CONTENTS

1	HYPOTHESES AND KEY CONCEPTS	1
1.1	Introduction and hypothesis	1
1.2	Fire models	4
1.2.1	Current research interest	4
1.2.2	Scales at which fire growth models are applied	5
1.2.3	Important applications of fire growth models	6
1.3	The fire regime concept	7
1.3.1	Intensity	8
1.3.2	Frequency	10
1.3.3	Seasonality	11
1.3.4	Type	11
1.3.5	Spatial considerations	12
1.4	Systems and models as abstractions	13
1.4.1	Grounded abstractions	14
1.4.2	Scale	16
1.4.3	Physical-biological duality	17
1.4.4	Landscapes	18
1.4.5	Spatial representation: Models of space	18
1.5	Approach of this study	21
2	DATA REQUIREMENTS: TERRAIN, VEGETATION, WEATHER AND REPLICATION	25
2.1	Overview of the model's data requirements	25
2.2	Terrain and vegetation	26
2.3	Climate	29
2.3.1	Extrapolating to other elevations	34
2.4	Replication of input data	36
2.4.1	Stochastic weather replication	36
2.4.2	Stochastic terrain replication	37
2.5	Matching available data to model requirements	42
2.6	Concluding remarks	43
3	FIREMESH: ITS ORIGINS IN FIRESCAPE AND SUBSEQUENT MODIFICATIONS	45
3.1	Overview	45
3.2	Model	45
3.2.1	Model assumptions	46
3.2.2	Weather data	47
3.2.3	Models of space	48
3.2.4	Models of time	48
3.2.5	Projecting one-dimensional fire models to two dimensions	50
3.2.6	Fire spread by lofted embers and firebrands	52
3.2.7	Ellipse properties	53

3.2.8	Implementation in FIRESCAPE	58
3.2.9	Project Vesta	62
3.2.10	Implementation in FIREMESH	62
3.3	Concluding remarks	65
4	EXAMINING THE OPTIMAL USE OF TEMPORAL AND SPATIAL DATA	69
4.1	Temporal and spatial resolution	69
4.1.1	Temporal resolution	70
4.1.2	Spatial resolution	74
4.1.3	Summary of findings	77
4.2	Mesh creation	77
4.2.1	Definition of equivalent spatial resolutions	77
4.2.2	Regular meshes	77
4.2.3	Triangulated Irregular Networks (TIN)	79
4.2.4	Generating even and uneven density Triangulated Irregular Networks	81
4.3	Concluding remarks	89
5	MODEL VERIFICATION	91
5.1	Introduction	91
5.2	Consistency across resolutions using regular mesh configurations	92
5.3	Consistency across spatial resolution using triangulated irregular networks	93
5.4	Measuring area	101
5.5	Wind direction	108
5.6	Comparison of methods in deriving fire shape on Triangular Irregular Networks	111
5.7	Wind and slope interactions	114
5.8	Wind, slope, elevation and fuel	117
5.9	Terrain projection	121
5.10	Fuel change with time since last fire	122
5.11	Summary of findings	125
6	MODEL AND DATA VALIDATION	127
6.1	Introduction	127
6.2	Validation	130
6.2.1	Synthetic and Observed data	130
6.2.2	Simulation time required for stability of model outputs	131
6.2.3	Broad measures of comparison with FIRESCAPE	132
6.2.4	Ignition Neighbourhoods: Model skill in realized niche generation	140
6.3	Replication of published experiments	142
6.3.1	Sensitivity to variation in terrain, fuel pattern, climate and weather	143
6.3.2	Relative importance of fuel management, ignition management and weather	157

6.4	Summary of findings	167
7	RELATIVE IMPORTANCE OF SPATIO-TEMPORAL RESOLUTION	169
7.1	Introduction	169
7.2	Factors common to all experiments	169
7.3	Data analysis	172
7.4	Testing spatial and temporal resolution	175
7.4.1	Methods	175
7.4.2	Results	176
7.4.3	Discussion	180
7.4.4	Calibration	192
7.5	Summary of findings for spatio-temporal resolution	193
8	SPATIAL REPRESENTATION: EXAMINING DIFFERENT FORMS OF DISCRETE SPACE	197
8.1	Hypothesis (ii): Relative importance of neighbourhood number	198
8.1.1	Purpose	198
8.1.2	Methods	198
8.1.3	Results	198
8.1.4	Discussion	203
8.2	Hypothesis (iii): Importance of regular/irregular spatial representation	208
8.2.1	Purpose	208
8.2.2	Methods	208
8.2.3	Results	208
8.2.4	Discussion	213
8.3	Hypothesis (iv): Optimal sampling of space using a prior adapted mesh	216
8.3.1	Purpose	216
8.3.2	Method	216
8.3.3	Results	217
8.3.4	Discussion	221
8.4	Summary of findings for spatial representation	223
9	SYNTHESIS AND FUTURE DIRECTIONS	227
9.1	Synthesis	227
9.2	Generality of findings	231
9.3	Future directions	233
	REFERENCES	237
A	FIREMESH: OVERVIEW, DESIGN CONCEPTS AND DETAILS	259
A.1	Purpose	259
A.2	Entities, state variables, and scales	259
A.3	Process overview and scheduling	261
A.4	Design concepts	262
A.5	Initialization	269
A.6	Input data	270

A.7 Submodels	271
A.8 References	274

LIST OF FIGURES

Figure 1.1	Level of interest in simulation modelling	5
Figure 1.2	Consequences of interpolating wind vectors	15
Figure 1.3	Graphic depicting a nested hierarchy of ecological entities	17
Figure 1.4	Neighbourhood number density distribution for Delaunay triangulations	20
Figure 1.5	Regular and variable distribution of vertices in a discrete landscape	21
Figure 2.1	Study location	27
Figure 2.2	Observed fire size distribution	28
Figure 2.3	Density distributions of elevation, slope and aspect for the study site	29
Figure 2.4	Map of fuel steady state values	30
Figure 2.5	Monthly weather data (Canberra Airport 1985–2011)	31
Figure 2.6	Relative proportion of wind and modelled fire runs	32
Figure 2.7	Yearly weather data (Canberra Airport 1985–2011)	33
Figure 2.8	Empirically derived temperature lapse rates	35
Figure 2.9	Multi-scale standard deviations in elevation for the Brindabella digital elevation model	39
Figure 2.10	Brindabella Ranges and derived fractal landscape	40
Figure 2.11	Comparison of aspects between real and fractal landscapes	41
Figure 3.1	Simulated fire burning on five different mesh configurations	49
Figure 3.2	Time / space diagram	51
Figure 3.3	Simple elliptical fire growth model	54
Figure 3.4	Ellipse metrics	54
Figure 3.5	Empirical length-to-breadth ratio functions	56
Figure 3.6	Back-fire rate of spread	57
Figure 3.7	Ellipse parameters required to shift the point from which the fire is assumed to propagate	58
Figure 3.8	Ellipse areas arising from three methods of calculating the back-fire rate of spread	60
Figure 3.9	Three examples of fire shapes for 9 wind speeds using FFDM	61
Figure 3.10	Forward rate of spread of the head fire relative to wind speed and its modification	63

Figure 3.11	Three examples of fire shapes for 9 wind speeds using modified FFDM	64
Figure 3.12	Isochrones showing the updated position of the fire front at half-hourly intervals	65
Figure 3.13	Polygons outlining burnt areas	66
Figure 3.14	Three magnifications of the same simulated fire showing the heterogeneity of conditions over the course of the fire	66
Figure 3.15	Simulated fires burning at two different time steps	67
Figure 3.16	A simulated fire spreading over a Delaunay mesh triangulation with an irregular displacement of vertices	67
Figure 4.1	Changes in head-fire rate of spread at three different time steps on two days of contrasting fire danger	71
Figure 4.2	Cumulative area burnt for time steps of 0.5 and 3 hours for two periods of contrasting fire danger	72
Figure 4.3	Differences in the vector sum of fire spread	73
Figure 4.4	A short transect of the study area showing the rate of spread at each location determined by spatial components of fire spread	75
Figure 4.5	A transect of the study area showing R_h for each location for a fire moving from left to right	76
Figure 4.6	Taxicab geometric system	78
Figure 4.7	Mesh minimum energy produced using the Capacity-Constrained Delaunay Triangulation	82
Figure 4.8	Sequence of steps in converting a digital image into a Delaunay triangulation	84
Figure 4.9	Four surfaces depicting the steps involved in creating a surface of the rate of change in the rate of spread of a head fire	85
Figure 4.10	A Delaunay triangulation using the Capacity-Constrained Delaunay Triangulation algorithm	86
Figure 4.11	A Voronoi tessellation	87
Figure 4.12	Density distribution of $\Delta R_h / \Delta S$	88
Figure 4.13	Density distribution of angles between neighbouring vertices	89
Figure 5.1	Four, six and eight neighbour meshes at three hour time steps	95
Figure 5.2	Fire spread on triangulated irregular meshes with even and uneven distribution of vertex locations	96

Figure 5.3	Simulated and expected fire perimeter of a 24 hour fire	96
Figure 5.4	Simulated and expected fire perimeters on even Triangular Irregular Network meshes	97
Figure 5.5	Simulated and expected fire perimeters uneven Triangular Irregular Network meshes	98
Figure 5.6	Mean and standard deviation of the radii of 10 replicate simulations with an even distribution of vertices	99
Figure 5.7	Mean and standard deviation of the radii of 10 replicate simulations with uneven distribution of vertices	100
Figure 5.8	Inherent error arising if area is calculated using mesh length traversed	102
Figure 5.9	Complex polygon surrounding the fire perimeter of an 8 neighbour mesh	103
Figure 5.10	A tessellation of space using a combination of octagons and squares	103
Figure 5.11	Comparison of simulated and expected fire area at four spatial resolutions	105
Figure 5.12	Polygons placed around the perimeter of circular fires on 4, 6 and 8 neighbour meshes	106
Figure 5.13	Comparison of two methods of calculating area of fire foot prints on five mesh configurations	107
Figure 5.14	Approximations to an elliptical fire shape using meshes with a variety of geometries	108
Figure 5.15	Area burnt on a variety of mesh configurations	110
Figure 5.16	Comparison of fire shapes arising on a TIN mesh using the equations for rate of spread of the head-fire from the Mark V Forest Fire Danger Meter	112
Figure 5.17	Comparison of fire shapes arising on a TIN mesh using the equations for rate of spread of the head-fire from the modified Mark V Forest Fire Danger Meter	113
Figure 5.18	Slope and wind speed relationship on a triangulated irregular mesh	115
Figure 5.19	Slope and wind speed relationship on a regular N-8 mesh	116
Figure 5.20	Twenty simulations with testing each of the spatial factors affecting fire spread tested independently and together	118
Figure 5.21	Two simulations under constant conditions of slope and wind speed at two different time steps	119

Figure 5.22	Rate of spread of the fire front and its complex interaction over time and space with fuel, temperature and temporal resolution	120
Figure 5.23	Fire shapes arising from projected and un-projected fire travel distances	121
Figure 5.24	A sample of 360 simulations performed under various wind directions and fuel treatment blocks	123
Figure 5.25	Average area burnt for 100 random fires under identical condition on a triangulated irregular network mesh	124
Figure 6.1	Observed and synthetic monthly weather data	131
Figure 6.2	Time series of various measures of frequency, intensity and seasonality for 1,000 year simulations with FIREMESH	133
Figure 6.3	Patterns of inter-fire intervals produced by the original version of FIRESCAPE	135
Figure 6.4	Patterns of mean fireline intensity produced by the original version of FIRESCAPE	136
Figure 6.5	Average inter-fire intervals for FIRESCAPE and FIREMESH in four landform classifications	137
Figure 6.6	Fire size distributions for three variants of FIREMESH from 1,000 year simulations	138
Figure 6.7	Relative change in average fireline intensity by slope class	139
Figure 6.8	Average distance (metres) to the 25th, 50th and 75th percentile of ignition points for three replicates of each site classification	142
Figure 6.9	Selection of ten weather years	145
Figure 6.10	Comparison of the daily average temperature and precipitation of 40 years of weather data generated by a synthetic weather generator and observed half-hourly data from Canberra Airport	146
Figure 6.11	Relative importance of factors affecting area burnt from Cary <i>et al.</i> (2006)	148
Figure 6.12	Differences and similarities between FIRESCAPE and FIREMESH in determining ignition rates and the response of ln-transformed area burnt to climate and terrain treatments	150
Figure 6.13	Changes in ln-transformed area burnt over treatment levels for Climate, Terrain and Weather for two variants of FIREMESH	152
Figure 6.14	Comparison of two variants of FIREMESH in determining the relative importance of factors affecting area burnt	153

Figure 6.15	Relative importance of factors affecting fireline intensity after Cary <i>et al.</i> (2006)	155
Figure 6.16	Relative importance of factors affecting area burnt in summer after Cary <i>et al.</i> (2006)	156
Figure 6.17	Relative importance of factors affecting area burnt after Cary <i>et al.</i> (2009)	160
Figure 6.18	Relative importance of factors affecting edge area burnt after Cary <i>et al.</i> (2009)	161
Figure 6.19	Ln-transformed area burnt (ha) for four levels of ignition management effort for FIRESCAPE, FMF (synthetic weather), FMM (observed weather) and FMV (observed weather with modifications to rates of fire spread)	163
Figure 6.20	Fire-size density distribution for FMM (observed weather) and FMV (observed weather with modifications to rates of fire spread) summed for all factors and replicates combined	164
Figure 6.21	Relative importance of factors affecting fireline intensity after Cary <i>et al.</i> (2009)	165
Figure 6.22	Relative importance of factors affecting area burnt in summer after Cary <i>et al.</i> (2009)	166
Figure 7.1	Density distributions of precipitation, minimum and maximum temperature and the resulting Forest Fire Danger Index	170
Figure 7.2	Examples of random 625 ha. block fuel treatments	172
Figure 7.3	Distribution of the residuals of key measures of FIREMESH model outputs	174
Figure 7.4	Relative importance of factors affecting fire frequency, intensity and seasonality	178
Figure 7.5	Relative importance of factors affecting fire frequency analysed separately for different spatial and temporal resolutions	179
Figure 7.6	Change in fire frequency, intensity and seasonality for each factor and each level of treatment	180
Figure 7.7	Seasonal variation in area burnt that arises from and empirical lightning distribution and a null model	183
Figure 7.8	Changes in the number of fires (successful ignition per 1,000 years) and the average fire duration (days)	184
Figure 7.9	Area burnt per annum with time steps ranging from 0.5 to 7 hours in mountainous terrain	185

Figure 7.10	Two simulations of 1,000 year duration on flat and mountainous terrain with spatial resolution from 100 to 1,000 metres 187
Figure 7.11	Relative change in area burnt for three 1,000 year simulations on flat terrain over spatial resolutions from 100 to 1000 metres 188
Figure 7.12	Fire size density distributions for each of five treatments and five replicates 190
Figure 7.13	Fire size distributions for a wide range of spatial and temporal resolutions 191
Figure 7.14	Simulation efficiency over a large range of temporal and spatial resolutions 192
Figure 7.15	Nine simulated fires burning under identical weather, fuel and terrain conditions with different combinations of temporal and spatial resolution 194
Figure 8.1	Relative importance of neighbour number in affecting fire frequency, intensity and seasonality 200
Figure 8.2	Relative importance of factors affecting of fire frequency analysed separately for each neighbourhood number 201
Figure 8.3	Changes over treatment levels in fire frequency, intensity and seasonality 202
Figure 8.4	Simulation efficiency with four, six and eight neighbour mesh configurations averaged over all treatments 203
Figure 8.5	Fire size density distribution of simulated fires with four, six and eight neighbours 205
Figure 8.6	Fire size density distribution of simulated fires with four, six and eight neighbours, constrained by landscape size 206
Figure 8.7	The effect of landscape size on simulated measures of fire frequency 207
Figure 8.8	Relative importance of factors affecting fire frequency, intensity and seasonality using different forms of spatial representation 210
Figure 8.9	Relative importance of factors affecting fire frequency with regular and irregular lattices analysed separately 211
Figure 8.10	Changes over treatment levels in fire frequency, intensity and seasonality 212
Figure 8.11	Fire size density distributions for spatial representations using a regular eight-neighbour mesh and a Triangular Irregular Network 214

Figure 8.12	The simulation efficiency for spatial representations using a regular eight-neighbour mesh and a triangular irregular network	215
Figure 8.13	Simulated average annual area burnt for two mesh configurations at three spatial resolutions	218
Figure 8.14	Relative importance of factors affecting fire frequency, intensity and seasonality for a spatially optimised mesh	219
Figure 8.15	Relative importance of factors affecting fire frequency for regular and optimised meshes analysed separately	220
Figure 8.16	Simulated annual area burnt over a large range of spatial resolution comparing a Triangulated Irregular Network (TIN) with a Poisson-Disk distribution of vertices (Even TIN) with a TIN with an optimised arrangement of vertices	222
Figure 9.1	Proposed workflow for rapid model development currently under development	236
Figure A.1	Mesh class	261
Figure A.2	Classes and relationships in the event-driven time model	263
Figure A.3	Objects and their relationships in the time model of FIREMESH	264
Figure A.4	Sequence diagram for the three implemented processes that operate during simulation	265
Figure A.5	State transition diagram for a Vertex in FIREMESH	266
Figure A.6	FIREMESH using the Ecosystem Ontology (Gignoux et al. 2011)	268
Figure A.7	Empirically derived temperature lapse rates	270
Figure A.8	Ellipse parameters required to shift the point from which the fire is assumed to propagate	275

LIST OF TABLES

Table 1.1	Fireline intensity control categories	9
Table 2.1	Fuel accumulation rates	29
Table 5.1	FIREMESH parameter values relevant to this chapter	93
Table 5.2	Errors reported between expected and simulated maximum distance travelled	94

Table 5.3	Simulated and expected differences for 4, 6 and 8 neighbour geometries of a circular fire	104
Table 6.1	Comparison of simulated seasonal proportions of fire occurrence between FIRESCAPE and three variants of FIREMESH	140
Table 6.2	Experimental design after Cary et al. (2006)	144
Table 6.3	Experimental factors that were found important in explaining variation in ln-transformed area burnt by FIREMESH and five other models	147
Table 6.4	Experimental design after Cary et al. (2009)	158
Table 6.5	Experimental factors that were found important in explaining variation in ln-transformed area burnt by FIREMESH and five other models	159
Table 6.6	Experimental factors that were found important in explaining variation in ln-transformed <i>edge area burnt</i> by FIREMESH and five other models	162
Table 7.1	Experimental design for a factorial experiment to measure the importance of spatio-temporal resolution against published experimental factors in fire regime simulation modelling	176
Table 7.2	Calibrated parameter values for slope and fire-line extinguishment	193
Table 8.1	Experimental design for a factorial experiment to measure the importance of neighbourhood number resolution against published experimental factors in fire regime simulation modelling	199
Table 8.2	Experimental design for a factorial experiment to measure the importance of regular/irregular spatial representation against published experimental factors in fire regime simulation modelling	209
Table 8.3	Experimental design for a factorial experiment to measure the importance of optimal vertex placement against published experimental factors in fire regime simulation modelling	217
Table A.1	Fuel accumulation rates	271
Table A.2	Evapo-transpiration table for Canberra	272

HYPOTHESES AND KEY CONCEPTS

1.1 INTRODUCTION AND HYPOTHESIS

Much of fire science is motivated in some way by the question of how fire regimes – the history of fires and their attributes – alter in response to environmental and social change. While the dynamics of fire has been an integral part of environmental variability over the course of evolution (Bond and Keeley 2005; Keeley *et al.* 2011; Pausas *et al.* 2012), it was not always seen as such (Krebs *et al.*, 2010). Rather, fire has been viewed in the past as an externality that resets the ‘normal’ seral sequence in vegetation development. Measuring the relative importance of the factors that influence fire is central to understanding the consequences that societal and environmental change may have upon fire regimes in the future.

How, for example, might changing patterns of rainfall affect fire regimes given that fire frequency is constrained in drier regions by fuel accumulation and in wetter regions by changes in the length of periods of weather likely to promote combustion (Matthews *et al.* 2012; Pausas and Fernández-Muñoz 2012; Batllori *et al.* 2013; Koutsias *et al.* 2013; King *et al.* 2013)? Alternatively, do changes in the rate of human-caused ignitions have a greater or lesser impact on the long-term risk to social, economic and environmental assets than say, climate change, and last but not least can fuel management strategies offset the effect of a changing climate on fire regimes (Flannigan *et al.* 2000; Amiro *et al.* 2001; Bradstock *et al.* 2012)? As fire plays such a fundamental role in shaping the terrestrial biosphere, how do we balance assessments of the long-term risk to these environmental, social and economic assets in order to apportion limited resources to mitigation in a cost effective manner (Rummer 2008; Gill *et al.* 2013; Milne *et al.* 2014)? These are just some of the questions for which an understanding of the relative importance of the drivers of fire is essential.

The components of these systems: climate, weather, terrain and ignition, mediated through vegetation, operate over vast temporal and spatial scales when compared to that of human observation. Simulation provides a valuable way in which systems operating over these scales can be investigated, where analytical solutions may be intractable, data scarce or unavailable or field experiments prohibitively expensive or otherwise impractical. Fire regime simulation models are only one of many approaches to making such assessments (see for example: McCarthy *et al.* 2002; Krawchuk *et al.* 2009; Thonicke *et al.* 2010; Moreno and Chuvieco 2013). However, simulation offers the only

means by which empiricism can be reduced (Gignoux *et al.*, 2011), an important concern when understanding system behaviour beyond the bounds of observation. In addition, as fire is a contagious process, simulation is particularly relevant as contagion is implemented explicitly; that is, simulation links the drivers of fire events directly to the generation of spatial patterns of fire regimes (Thompson and Calkin, 2011). Such models must be simple enough to generate fire events over large temporal and spatial extents within a tractable time. They must also, as do all spatial simulation models, introduce two parameters that have no equivalent in the real world: time step and spatial grain. These parameters are analogous to 'nuisance parameters' in statistics (Gignoux *et al.*, 2011); parameters necessary to the model but not of direct interest (Basu, 1977). While there has been research into the effect of temporal and spatial resolution on the accuracy of predictions of individual fires (Jones *et al.* 2003; Hu and Ntaimo 2006; Cui *et al.* 2008), none has been done within the context of the purpose of fire regime models in addressing the questions above. If this is the case, then a large body of work that has been done over the past two decades may be called into question (for example see: Van Wagten-donk, 1996; Bennetton *et al.*, 1998; Pausas, 1999; Cary *et al.*, 2006; King *et al.*, 2006, 2008b; Cary *et al.*, 2009; Perera and Cui, 2010; Scheller *et al.*, 2011; Syphard *et al.*, 2011; King *et al.*, 2011; Bradstock *et al.*, 2012; Keane *et al.*, 2013a; King *et al.*, 2012, 2013).

Therefore, the first question addressed by this thesis is: in what way does spatio-temporal resolution change simulated fire regimes and, in particular, does this affect how such simulation modelling will rank the relative importance of drivers of fire behaviour?

Simulation is the application of the model of a system over time (Banks *et al.*, 2000). The fire growth simulations discussed in this work are discrete approximations of systems displaying non-linear and discontinuous behaviour. They are non-linear not only because the forcing variables are irregular (slope, fuel, wind speed and direction, humidity and temperature) but also because the model's response to those variables is non-linear, such as response to slope, fuel moisture and, in some models, wind speed. They are discontinuous because there always exists some point at which a fire will either continue to burn or extinguish. However, it remains unclear if in practice, the fire model's overall response will be non-linear with respect to space and time, as the effects of these two domains may either reinforce or cancel measures of fire velocity.

Simulation models must not only make time and space discrete, but must also propose a model of space (apart from its resolution), referred to here as spatial representation. Three such models are commonly employed by fire growth simulations: (i) vector (Finney (2004); Tymstra *et al.* (2010)), (ii) raster (e.g. Cary and Banks (2000); Perera *et al.* (2008); Trunfio *et al.* (2011)) and (iii) mesh, a model of space rep-

resented by an irregular triangular network (Heil and Brych (1978); Peucker *et al.* (1978)) as proposed by Johnston *et al.* (2008). Vector models simulate the growth of the fire perimeter with a vector composed of a variable number of discrete points, the number increasing as the fire perimeter grows (see Figure 1 in Finney (2004)). Vector fire growth models achieve fire shapes very close to their theoretically expected shape (the shape they intended to create without artefacts of the spatial representation intervening). Nevertheless, they have a computational burden too great to perform experiments that require tens of millions of simulated fires, such as those in the present study (see Bose *et al.* 2009; Sousa *et al.* 2012). While vector models are at times used in studies of vegetation dynamics, the regions where they are applied have fewer fires and thus lower computational demands than the region in the present study (e.g. Keane *et al.*, 1996).

If the approach taken by vector models is, for the most part, too computationally intensive for fire regime simulations, we are restricted to a spatial representation that comprises a fixed set of locations and a decision as to (i) how many neighbours each location has and (ii) whether or not those locations are placed on regular or irregular grids. It has long been recognized that discrete geometries limit the way simulated fires propagate (Feunekes 1991; Caballero 2006; Johnston *et al.* 2008; Perera *et al.* 2008; Trunfio 2004; Trunfio *et al.* 2011; Avolio *et al.* 2012). In fact, more research appears to have been done on this topic than on the importance of spatial and temporal resolution despite the observation by Green *et al.* (1983a) that simple rectangles may be adequate to depict a fire shape template for many purposes. If the observation of Green *et al.* (1983a) is correct, and spatial representation found to be relatively unimportant, then fire models designed to analyse the relative importance of the factors influencing fire would be a fundamentally easier task than may have been supposed. If the contrary is found, then again, this may call some previous work in this field into question.

Therefore, the second question is: in what way do fundamentally different ways of representing space change simulated fire regimes and, in particular, does this affect how simulation modelling would rank the relative importance of drivers of fire behaviour?

The above two questions can be expressed in the terminology of formal null hypotheses as:

- 1 Ranking the relative importance of the drivers of fire by simulation modelling is insensitive to a wide range of spatio-temporal resolutions; and
- 2 Ranking the relative importance of the drivers of fire by simulation modelling is insensitive to fundamentally different approaches to spatial representation.

'Importance' is used here with the same meaning as in three international fire model comparison studies (Cary *et al.* 2006, 2009; Keane *et al.* 2013a). Importance, in those studies, was measured by the proportion of variation explained in area burnt by experimental factors in a standardized general linear analysis of simulated data on area burnt. These studies compared the magnitude of variance explained by factors such as terrain, weather, climate, ignition suppression and a variety of fuel treatments by an ensemble of fire regime models from North America and Australia. The purpose of that work was to examine whether or not there was a consensus among these independently developed models as to how they rank the environmental and anthropogenic drivers of fire. The focus in those studies on importance rather than significance has been supported more recently by White *et al.* (2014). The use of frequentist statistics to test a hypothesis can be meaningless in simulation modelling because altering any parameter is likely to be significant if sufficient replications are produced. In an analysis of variance (ANOVA), it is the magnitude of the partitioned variance that provides insight into the importance of experimental factors and their interactions (White *et al.*, 2014). The above hypotheses are accepted or rejected based upon a threshold of relative variance explained (i.e. the Sum of Squares divided by the total Sum of Squares) in landscape wide averages of fire frequency, fireline intensity and seasonality. The experimental factors used to test these hypotheses include treatments from the literature by which to gauge the relative importance of spatial-temporal resolution and various forms of spatial representation.

1.2 FIRE MODELS

1.2.1 *Current research interest*

The increasing interest in fire modelling, and fire simulation models in particular, is indicative of the importance of understanding the role of fire in the dynamics of socio-ecological systems in a world experiencing unprecedented rates of change in land-use and climate since the dawn of the Holocene (Caldararo 2002; Vannière *et al.* 2008). This research focus has been enabled by the exponential increase in readily accessible computing power and spatial satellite data available to researchers over the past 25 years (Sullivan, 2009a). However, a continuation of this growth in computing power cannot be taken for granted (Mann, 2000) and model parsimony is therefore an important consideration on these grounds alone. A search of Scopus (<http://www.scopus.com/>) indicates an increasing trend in the use of models in fire research between the mid 1980's and the present (Figure 1.1). Not all simulation studies use the term 'simulation' as a

keyword and therefore this result should only be taken as indicative.

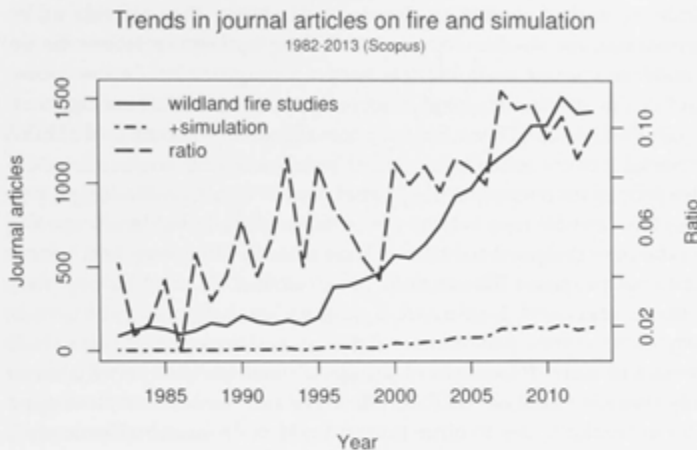


Figure 1.1: A Scopus search (<http://www.scopus.com/>) showing the trend of increase in interest in simulation modelling of wildland fire. The solid line charts the number of publications with the keywords ((forest OR wildland) AND fire) OR bushfire. The dotted/dashed line (+simulation) is the same query with the addition of the keyword 'simulation'. The dashed line is the ratio of the two. About 10% of publications in this field discuss simulation in 2013. Note that this was a keyword search only. It can be assumed the many papers may discuss fire simulation modelling without the use of these keywords.

Growing research interest in this area can also be gauged from the number of models published in recent times. A three paper review of fire models published between 1990 and 2007 (Sullivan 2009a,b,c) discussed approximately 70 published models of simulations and mathematical analogues. Keane *et al.* (2004), in a study on model classification, lists 45 landscape fire succession models, a term coined by Keane to identify models that simulate fire and vegetation interactions.

1.2.2 Scales at which fire growth models are applied

Sullivan 2009a,b,c discussed fire spread models classified as either physical, semi-physical, empirical or semi-empirical. However, the model used in this study (FIREMESH) is more clearly positioned in terms of a classification based on the scale of the model's application, which implies the model's degree of simplification or abstraction.

The model classification study of Keane *et al.* (2004) identifies three spatial resolutions for landscape fire vegetation models (fine <50 m, mid < 500 m and coarse > 500 m). Models designed to understand

the dynamics of combustion and turbulence at very fine spatial and temporal scales (FIRETEC: Linn *et al.*, 2002) are computationally intensive and cannot realistically be applied to temporal and spatial scales typical of vegetation dynamics. However, they provide an essential tool for the development of scaling-up laws to lessen the dependence coarser scale models have on empiricism. At the coarse end of the spectrum, global models such as MCFIRE (Lenihan *et al.*, 1998), GLOB-FIR (Thonicke *et al.*, 2001) and more recently, SPITFIRE (Thonicke *et al.*, 2010) have spatial resolutions too coarse to model fire propagation as explicitly spatial, that is as a true landscape process (see Section 1.4.4 below). Some relatively detailed landscape fire models are designed for the analysis of individual fires and for operational purposes (Keane *et al.* 1996; Clark *et al.* 2004; Finney 2004; Tolhurst *et al.* 2008; Tymstra *et al.* 2010) and are on the edge of tractability of fire regime generation - that is, simulations over thousands of years and many thousands of square kilometres. The model used in this study is based on FIRESCAPE (Cary and Banks, 2000) and operates at similar scales to other fine and mid-scale models (Keane *et al.*, 2004). Examples of this class of model are Mladenoff and He 1999; Lavorel *et al.* 2000; Li 2000; Hargrove *et al.* 2000; Pausas and Ramos 2006; King 2004; Perera *et al.* 2008; Sturtevant *et al.* 2009; Trunfio *et al.* 2011 and Avolio *et al.* 2012.

1.2.3 Important applications of fire growth models

A key use of fire models is to examine the long-term risks posed by fire to social, economic and environmental assets under treatments related to climate change (Cary and Banks 2000; Tymstra *et al.* 2007; Bradstock *et al.* 2012) and land management scenarios (Finney 2001; King *et al.* 2008b; Bradstock *et al.* 2012). Risk over the shorter term (e.g. modelling individual fire events) can be assessed using more computationally intensive models such as FARSITE: Finney (2004), PROMETHEUS: Tymstra *et al.* (2010) and PHOENIX: Tolhurst *et al.* (2008) as used in Anon (2013).

The cost of fire to social, economic and environmental assets is large as is the cost of fire management. In the USA, suppression costs for the US Forest Service alone were over \$US 1 billion in 2006 (Abt *et al.*, 2009) while in Australia, Ashe *et al.* (2009) estimate the total cost of bushfires at 1.3% of GDP. Bradstock *et al.* (2012) report an indicative cost of \$AUD 200 million per annum is required to achieve a 50% reduction in risk. Fire growth models are an important component in unplanned fire decision support systems (Noonan-Wright *et al.* 2011; Rodríguez y Silva and González-Cabán 2010). They generate the fire regime and fire effects that underpin risk analysis (Thompson and Calkin, 2011) that in turn informs cost/benefit analyses. Cost/benefit analysis is an increasingly important area of research as governments

attempt to balance the allocation of finite resources and ever expanding community expectations with regard to risk exposure (Milne *et al.*, 2014).

Fire models of a variety of types play a role in carbon accounting. Fire affects carbon stocks directly by the release of combustion products and indirectly by altering vegetation age structure. While fire regimes remain substantially unchanged, fire effects on carbon balance will remain stable (Flannigan *et al.*, 2009). However, the sensitivity of carbon stocks to altered fire regimes varies greatly between biomes. For example, fire is a primary driver of boreal forests, a biome that represents 20% of the global vegetation cover (Flannigan *et al.*, 2009). The types of fire models used in carbon accounting span many scales from global, (Thonicke *et al.*, 2010), to the work of King *et al.* (2011), which coupled the landscape fire regime simulation model FIRESCAPE (Cary and Banks, 2000) with the FullCAM carbon cycle model (Richards and Evans, 2004). These coupled models estimated a significant reduction in carbon stores in SE Australia under SRES climate scenarios.

1.3 THE FIRE REGIME CONCEPT

The performance of the model used in this study is measured against three fire regime attributes: frequency, intensity and seasonality. A fire regime is a measure that encapsulates the primary attributes of fire in the landscape, changes in which are an indicator of potential impacts on ecosystem function, biodiversity and society. Being a metric, it is value-neutral and only within a defined context can potential impacts be meaningful. This has not always been the case. The theory of vegetation dynamics proposed by Clements (1916) dominated ecological thinking during the first half of the 20th century (Krebs *et al.*, 2010). This theory conceives of vegetation as a super-organism progressing deterministically through seral stages to an idealized climax state. Clements described vegetation in the field in terms of deviation from this ideal. Though criticized by Gleason 1917; Whittaker 1953 and somewhat by Tansley (1935), the idea of an orderly development fitted well with the views of nations undergoing industrialization (Krebs 2010). Fire was seen as a disturbance that interrupted or reset the natural development of the super-organism rather than an integral component of the environment within which life has evolved (Krebs *et al.*, 2010). During the colonial period of the 19th century, the aims of colonialists and other newly arrived people were inevitably at odds with those of the indigenous populations as regards fire (Zylstra 2006; Krebs *et al.* 2010; Gammage 2011). In Europe, there was also conflict between different sectors of society and the use of fire, notably shepherds and owners of forests or buildings (Krebs *et al.*, 2010). The dominance of Clements and the values of owners of cap-

ital combined to view fire as an externality of vegetation dynamics. The appreciation of fire, and disturbance more generally, as an integral part of environmental variability arrived when 'the fire regime concept in the 1960s became primarily a system for describing, quantifying and characterizing fire occurrence, without any value connotations. A fire regime is neither negative nor positive and may refer to any fire frequency, including fire exclusion.' (Krebs *et al.*, 2010, p.59). Measuring and classifying components of environmental variation such as climate zones (Peel *et al.*, 2007), biomes (Olson *et al.*, 2001), forest types (Specht, 1970) and disturbance regimes (Pickett and White 1985; Bradstock 2010) is a powerful way of understanding and managing the complex dynamics of socio-ecological systems.

While the definition of terms will vary with context, it would seem natural that to make scientific progress there must be a common understanding of shared terms. Terminology is especially difficult in ecology as the subject spans many, if not all, traditional disciplines. Spies *et al.* (2012) note that 'One problem impeding the development of a better understanding of fire effects at ecologically relevant spatio-temporal scales is that terminology associated with the fire behaviour and impacts are often used inconsistently or incorrectly'. Gignoux *et al.* (2011) list a number of examples where the meaning of terms has caused confusion and debate. With this in mind, defining fire regime by focusing on pyrological attributes without regard to a fire's antecedent and subsequent conditions can help clarify a complex and potentially confusing chain of causal relations. Gill (1975) has made one of the first clear definitions of fire regime (Krebs *et al.*, 2010). He defined it as the history of fire at a point measured by the frequency, seasonality, intensity and type (below or above ground fire). Gill (1975) makes no reference to the temporal extent of the measures, their statistical distribution (means, variance or trends) nor what degree of change in these variables may constitute a 'shift' in regime. These are all rightly left to context. In other words, it is the history of fire at a point without regard to the reasons why fire may or may not have occurred or the effects that flow from it. In particular, Gill (1975) does not include area as a fire regime attribute, and this is a key difference between Gill (1975) and other writers on the topic (for example: Heinzelman 1981; Christensen 1993). To include area is to mix the concept of a fire regime (history of fire at a point) with that of a fire mosaic. Area is rather a matter for measurements of the spatial autocorrelation of point attributes for fire regimes as shown by Gill *et al.* (2003) in identifying patch structure in the savannas of northern Australia.

1.3.1 Intensity

Fireline intensity (Byram, 1959) is a measure of the rate of energy released per unit of fireline length (I) (kW.m^{-1}), a product of the heat

Table 1.1: Broad thresholds of fire suppression effectiveness in relation to fireline intensity (after Alexander *et al.*, 2000)

INTENSITY ($\text{kW} \cdot \text{m}^{-1}$)	CONTROL REQUIREMENTS
< 500	Ground crews with hand tools
500 – 2000	Water under pressure and /or heavy machinery
200 – 4000	Helitanks and airtankers using chemical fire retardants
> 4000	Very difficult if not impossible to control

of combustion (H) ($\text{kJ} \cdot \text{kg}^{-1}$), the fuel weight (W) ($\text{kg} \cdot \text{m}^{-2}$) and the rate of spread of the fire (R) ($\text{m} \cdot \text{s}^{-1}$) and is therefore some indication of how difficult a fire may be to control (Table 1.1).

$$I = H.W.R \quad (1.1)$$

In practice, not all fuel is available for combustion and for forest systems there are different traditions in the methods of estimating the proportion of fuel that can burn under particular conditions. In North America the rate at which fuel dries after rain is classified by the size of fuel elements. This approach is fundamental to many fire models and the lack of data in Australia on fuel element sizes may be one reason why North American models are not routinely applied in Australia (Opperman *et al.*, 2006). Nevertheless, the fuel element size approach has been found to perform poorly in fire prediction (Keane *et al.*, 2013b). Fires in Australian forest surface fuels use an empirical equation (drought factor) based on the time and amount of the last rain event to estimate the proportion of fuel available for combustion (McArthur 1967; Noble *et al.* 1980). Note that drought factor affects intensity by modifying the rate of spread (R) rather than fuel weight (W) in Equation 1.1. This approach of estimating fuel availability has also been questioned (McCarthy, 2003) suggesting that this area is one that may introduce significant uncertainty in rate of spread and therefore fireline intensity estimates. In systems where grass is a major component of fuel, curing times are the critical factor in determining the proportion of fuel available for combustion (Cheney *et al.*, 1998). In the present study, however, discussion is confined to surface fuels in Australian eucalypt forests.

In practice, fireline intensity is difficult to measure directly and is more often measured indirectly by estimating fuel weight and rate of spread, heat of combustion (H) being well conserved in Australian eucalypt litter (McArthur and Cheney, 1972). Rate of spread can be measured using:

- i Temperature probes and triangulation (Moore *et al.*, 1995), markers placed on the perimeter of fires at constant intervals (Steph-

ens *et al.*, 2008) or fishing line placed across the path of experimental fires as was done in Project Vesta (Gould *et al.*, 2007);

- ii Reconstructions of fire perimeters at particular times from observations (e.g. Cruz *et al.*, 2012).
- iii Measurement of fuels, their ignitibility, sustainability and combustability (Gill and Zylstra, 2005) together with meteorological data and the geometry of the fuel array.

Intensity can be directly inferred by:

- i Empirical relationships with flame height and length (Van Wilgen, 1986; Burrows, 1997 and see review by Alexander and Cruz, 2012); and
- ii Relationships with the effects of fire on vegetation (severity) such as scorch height (Burrows, 1997) and leaf char height (Williams *et al.*, 1998) or satellite observations.

The term 'severity' is often used instead of, or confounded with, intensity (Feller 1996; Spies *et al.* 2012). Though the term 'severity' itself has ambiguity (see debate following Odion and Hanson (2008), the generally agreed meaning of severity is the magnitude of the immediate effects of fire such as mortality, seed release, resprouting, biomass consumed and changes in soil properties (Keeley, 2009). The confounding of severity and intensity may have to do with the experience of researchers working in forest types with stand replacement fires as opposed to forests with strong resprouting potential. Keeley (2009) also makes a case for disentangling aspects of intensity into fireline intensity and energy flux; the total energy released into the environment per unit time per unit area. Energy flux can have profound effects on plant mortality and soil and microbial properties. For example, a study by Doerr *et al.* (2006) found that water repellency changes after fire were inversely proportional to intensity, contrary to laboratory studies. The authors note that this may have been due to inferring energy flux from intensity which was in turn inferred from severity as estimates of biomass consumed. Shea *et al.* (2004) include 'duration' as a disturbance regime attribute, the equivalent of residence time, in their definition of disturbance. Some fire resistance strategies of plants are very dependent on short residence times (J. Gignoux, pers. comm., 2014). To compute fire residence time requires knowledge of both the leading and trailing edge of the fire front, which could perhaps be inferred from fuel element size and the rate of spread.

1.3.2 Frequency

Frequency at a point is the number of times a location burns over a period of observation and is often determined from fire scars and

tree ring data (McBride 1983; Swetnam *et al.* 1993; Cary and Banks 2000). Changes in inter-fire intervals (mean and variance) can have consequences for plants adapted to particular fire regimes (Morrison *et al.* 1995), including no fire at all (Gill, 1975). Frequency can affect reproductive success by being more or less frequent than life-history attributes such as age at maturity and seed pool and plant longevity (Gill, 1975; Noble and Slatyer, 1980). The life-history attributes of fauna are much less studied than flora (Whelan *et al.*, 2002; Keith *et al.*, 2002), but no less important (Short and Smith, 1994; Bradstock *et al.*, 2005; Clarke, 2008; Banks *et al.*, 2013).

1.3.3 Seasonality

Changes in seasonality may arise due to changes in ignition densities over time from all sources (Price and Rind, 1994; Kuleshov *et al.*, 2002; Russell-Smith *et al.*, 2007), rainfall and drought patterns (Pausas and Fernández-Muñoz, 2012), the curing times of grasses (King *et al.*, 2012) and extended periods of high fire danger (Hennessy *et al.*, 2005; Lucas *et al.*, 2007). The general trend in Australia is for the peak fire season to shift from August-September in the tropical north towards February in Tasmania and other southern regions with a Mediterranean climate (Luke and McArthur, 1978). Fire seasonality affects severity as the response of flora and fauna to the time of year at which they are burnt can vary. Enright and Lamont (1989) have found significant differences in germination rates of co-occurring *Banksia* species between autumn and winter fires. Fires late in the fire season may increase mortality of early recruits (Gill, 2008). Wright and Clarke (2007) found '*seedlings of woody species were significantly more abundant following summer than winter fires*' in central Australia while an interesting example of the effect of seasonality on mortality of resprouting mallee can be found in Noble (1997) p. 51 in Gill (2008). Early season fires may affect breeding success of fauna as animals may be less mobile at this time (Neumann 1992 in Gill, 2008).

1.3.4 Type

Fires can be of two types in this sense, above or below ground. Below ground fires burn without flame, potentially for long periods (the coal seam fire at Mt Wingen NSW has reportedly been burning for 6,000 years! - <http://www.smithsonianmag.com/travel/fire-in-the-hole>) and kill plants through root destruction. In Australia at least, they are rare compared to above ground fires (Gill, 2008) and while they may have profound effects (Wein, 1981) they are not modelled in the present study.

1.3.5 *Spatial considerations*

Identifying patches with a common fire regime attribute can provide valuable insights into patch dynamics (Gill *et al.*, 2003) and inform conservation management (Parr and Andersen, 2006). Strictly speaking, if fire history is taken over a long enough time, all locations will differ by some measure of the fire regime and thus the spatially correlated fire regime attributes will have utility only for a particular purpose. Spatial attributes may be useful in pin-pointing areas where intensity, frequency and seasonality may be of a different order and indicate changes in the relative importance of the drivers of fire. Fiorucci *et al.* (2008) showed that by disaggregating bi-modal fire size distributions into their constituent uni-modal parts, they could identify regions with differing fire regime classes. Slocum *et al.* (2007) used fire size-class distributions to disentangle the impact of natural and anthropogenic ignitions on fire regimes in the Everglades National Park.

An additional spatial attribute of a fire event is its shape complexity. Changes in fire shape complexity may simply be correlated with fire size (Eberhart and Woodard, 1987; Burton *et al.*, 2009; Anderson, 2012) which in turn is likely associated with increasing intensity (Gill and Allan, 2008). In a fire simulation model, if fire shape is recorded as a polygon then fire shape complexity can be measured as the ratio of the polygon length to the perimeter of a circle of the same area (Hengl, 2006).

As the proportion of large fires in a region increases, the fire frequency at each point in the landscape will regress to the mean of the whole landscape. However, what constitutes a large fire depends on scale of observation and the question being asked. Gill and Allan (2008) suggest large fires are those that, combined, contribute more than 50% of the total area burnt over the time and area of interest. For example, in the Australian Alps, two fires (those of 1939 and 2003) account for more than 70% of area burnt since 1927 (data courtesy P. Zylstra).

An interesting measure of landscape heterogeneity is that proposed by Brookhouse *et al.* (2010), which has implications for both landscape and species diversity. The authors define a point measure of distance to structural complement (DiSCo), which is the minimum distance from a point that encounters all structural elements defined within a landscape from a finite set. In a fire model, the set of structural elements could be defined as say, a set of fuel age classes and the DiSCo measure, the minimum distance from a point to all fuel age classes. This provides a relatively simple point classification of patch complexity. A low DiSCo index indicates high diversity of the chosen fire regime attribute at fine scale and may have application to fire and habitat studies such as Leavesley *et al.* (2010).

In summary, over the past 100 years, fire has come to be seen as an integral component of the environmental variability within which life has evolved. A fire regime is the history of fire at a point measured by its pyrological attributes: frequency, intensity, seasonality and type. As noted, below ground fires are not modelled in this study and the remaining three attributes of frequency, intensity and seasonality are the response variables by which the importance of experiment factors in this thesis is measured.

1.4 SYSTEMS AND MODELS AS ABSTRACTIONS

The hypotheses posed in the introduction are questions about levels of abstraction. Ideally, a good model is independent of the level of abstraction but this is rarely the case (Gignoux *et al.*, 2011). In its most general sense, abstraction is simply the process by which we identify what is relevant: *'that part of the universe under consideration'* (Carnot 1824 in Gignoux *et al.* 2011) or *'to isolate systems for the purpose of study'* (Tansley, 1935, p 300). However, abstraction can also refer to the method by which models are formulated (Zucker, 2003). Two models can be differently formulated (algebraically or geometrically for example) yet be at the same level of abstraction if both have identical skill in answering any particular question put to them, that is, they can prove the same set of theorems. Level of abstraction, on the other hand, refers to the degree of simplification and there is no guarantee that the simpler model can prove all theorems provable by the more complex model. Taking a fire regime simulation model as an example, simplifying entails one of five operations:

- i Ignoring some processes entirely (e.g. herbivory and livestock grazing)
- ii Ignoring some aspects of a process (e.g. terrain effects on wind);
- iii Limiting the amount of an entity (e.g. making space and/or time discrete);
- iv Limiting the number of states of an attribute of an entity (e.g. reducing species abundance to presence/absence values); and
- v Aggregating disparate entities as one (e.g. an organism is an aggregation of organs).

In the field of artificial intelligence, these abstraction operators have formal names: domain hiding, co-domain hiding, domain reduction, co-domain reduction and aggregation respectively (Zucker, 2003). Time and space are continuous and choosing to make either of these domains discrete is domain reduction. Due to the subjective nature of abstraction, there can be no formal way to decide what is the appropriate level of abstraction needed to correctly capture system be-

haviour. However, three approaches have been suggested that may assist (Gignoux *et al.*, 2011):

- i Reduce empiricism by compliance with standard protocols (Grimm *et al.*, 2006, 2010; Gignoux *et al.*, 2011);
- ii Explicitly design scaling-up methods (Barnes and Roderick 2004; Boulain *et al.* 2007); and
- iii Employ modelling tools to allow easy comparison of abstraction decisions (Amouroux *et al.*, 2009; Lacy *et al.*, 2013).

Following these suggestions respectively, in this study:

- i FIREMESH has been documented using the ODD protocol (Overview, Design concepts, Details) (Grimm *et al.*, 2006, 2010) (Appendix 1). In addition, schematic diagrams of the model architecture use the Unified Modelling Language (UML: <http://www.uml.org>) (Rumbaugh *et al.*, 2004);
- ii An approach to scaling has been explored by altering spatial resolution to suit the level of detail required over the spatial extent of simulations (Chapter 4 and introduced in Section 1.4.5 below);
- iii The model has been implemented in a standardised ecological simulation framework. This framework is an implementation of the conceptual model of ecosystems (Gignoux *et al.*, 2011) and it is hoped it may in future complement the ODD protocol. The conceptual design of the model is discussed in Chapter 3 and complies with the ecosystem ontology proposed by Gignoux *et al.* (2011). The framework provides the architecture with which to compare the above abstraction decisions.

1.4.1 *Grounded abstractions*

A grounded abstraction is 'that part of the universe under consideration'. It is the detailed perception of the world (the grounding) upon which we can compare other levels of abstraction with the confidence of objectivity (Zucker, 2003). More formally, abstraction is a reduction of the number of states representable by an abstraction compared to the grounded abstraction. For example, to compare a model working at several different time steps (the abstractions), data of at least the finest time step (the grounded abstraction) must be used unless some form of interpolation is required. However, interpolation introduces states in the abstraction that are not present in the grounded abstraction and so results would be confounded. For example, if half-hourly wind speed and direction data are interpolated to one minute resolution using either a linear or cubic spline method, noticeable exaggera-

tions occur when change is rapid (Figure 1.2). Considering the discontinuous response of fire behaviour to weather variables noted above, these slight exaggerations pose a particular problem for temperature as it introduces fire extinguishment events that are not implied by the original data. Therefore, in the present study, interpolation is avoided in any aspect of the model that is to become an experimental factor (time and space).

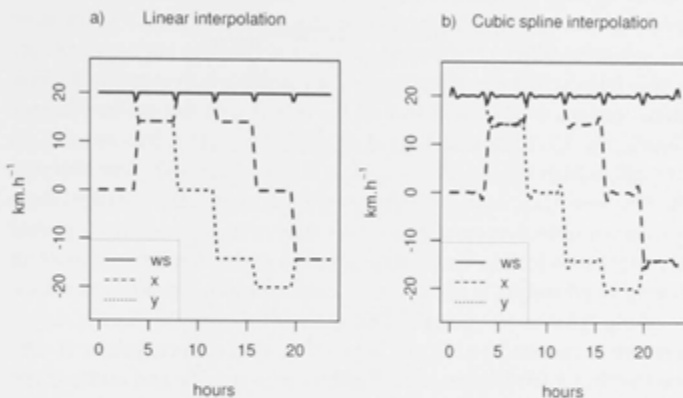


Figure 1.2: The consequences of interpolating wind vectors

Half-hourly wind data interpolated to ten minute values. Interpolation methods are (a) linear and (b) cubic spline. Wind speed and direction are interpolated as wind vectors (x west to east velocity, y south to north velocity). Wind speed is held constant at $20 \text{ km} \cdot \text{h}^{-1}$ and wind direction changes by 45° every 5 hours. Although the wind speed is constant (in the data or grounded abstraction – the five-hourly readings), it does not remain constant in the interpolation (solid line). This is particularly problematic for fire simulation with regard to temperature interpolation when using a cubic spline, as minimum temperatures will be exaggerated. Fire regime simulation models are very sensitive to minimum temperature. Thus the abstraction (10 minute readings) introduces states that are not present in the abstraction upon which this is grounded (the five hour readings)

It follows that, when performing experiments by manipulating a single model, we are comparing various abstractions of the one grounded abstraction. Of course, one can object that the differences so found may only have relevance to this one particular grounded abstraction. Another model will produce different results. Therefore, the model (the grounded abstraction) must be well described with reference to the literature (in this sense a grounded abstraction) so the reader can form a view as to the degree of generality of the findings in the context of their circumstances.

1.4.2 Scale

Abstraction takes place in the context of scale. Each of the processes that comprise *'that part of the universe under consideration'*, that is, an ecosystem or system, can operate at a different scale (Gignoux *et al.*, 2011). This is not always recognized and can lead to confusion in the use of the terms system or ecosystem. All that can be said in defining the term 'system', is that systems have nothing more in common than *'identifiable entities and identifiable connections between them... to say more is to commit the fallacy of misplaced correctness'* (Jordan, 1968, pp. 38–39). It is this fallacy that has possibly led one ecologist to suggest the ecosystem concept is dead and should be *'buried with full military honors'* (O'Neill, 2001). Unlike the concept of a holocoen (Friederichs 1927, in Jax (1998), which Friederichs considered was a *'naturally delimited part of the biosphere'* (Jax, 1998, p 188), the ecosystem of Tansley (1935) does not have an objective existence but is observer-dependent (Gignoux *et al.*, 2011) as is Jorden's system. We could go further and say that an observer need not be taken literally, but is simply the scale at which something (plants or animals) interact with the world (Levin, 1992). Therefore it cannot be said, as Figure 1.3, that an ecosystem is contained within a landscape; to do so is to over-specify and commit the fallacy cited above. Tansley's concept of the ecosystem (Tansley, 1935) is scale-independent (Gignoux *et al.* 2011) until an observer identifies a particular ecosystem; until then the concept does not have an objective boundary as suggested by Friedericks (1927). Changes in spatial or temporal extent over which observations are made will lead to different importance rankings of system drivers (Wiens, 1989). Changes in resolution, on the other hand, can lead to the emergence of patterns not apparent at other resolutions (e.g. Düben and Korn 2014; Schiemann *et al.* 2014). In landscape fire simulation models, for example, persistent long-term patterns of fire severity may not be apparent below some resolutions simply because slope, which increases intensity for fires burning uphill, approaches zero as resolution becomes coarser.

When a list of entities and their connections are identified as an ecosystem (a forest, a soil layer, fire propagation and so forth), each of these entities will have an associated scale for the observer. Note that an ecosystem is a particular type of system. Jordon writes of a taxonomy of systems with a distinction made between static and functioning systems (Jordan, 1968). An ecosystem must clearly function in some way, that is, operate over time. Each identified entity functions at some scale and these scales need not be the same. Therefore any given instance of an ecosystem (list of identifiable functioning entities and identifiable, and possibly changing relationships) is potentially a multi-scale object (Gignoux *et al.*, 2011) and so too are models that represent these systems. This is common practice. FIREMESH, for ex-

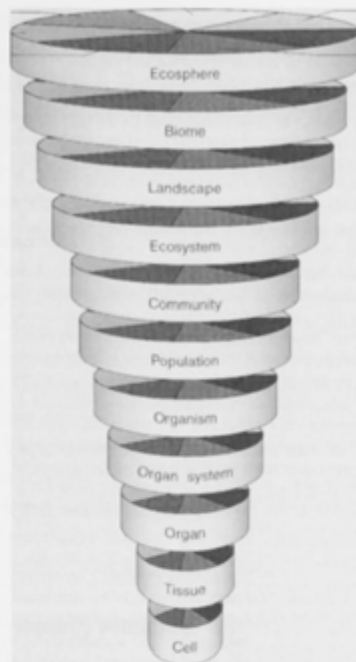


Figure 1.3: Graphic depicting a nested hierarchy of ecological entities
 From this image it could be mistakenly thought that landscapes contain ecosystems in the same way as organisms contain organs (from Odum and Barrett, 1971).

ample, has processes that change in years (litter inputs and decay), days (soil moisture), hours (fire propagation steps) and seconds (ignitions). Likewise the model can have processes that operate from millimeters (soil moisture balance) to square meters (surface litter process) and 1,000's of km^2 (fire propagation).

1.4.3 Physical-biological duality

Tansley conceives of the ecosystem as a combination of physical and biotic elements (Tansley, 1935). However, biotic elements can be viewed as both physical (canopy interception of rainfall) or biotic (canopy growth and seed production) and if Tansley's ecosystem is not over-specified, it can encompass these two aspects of the one thing (Gignoux *et al.*, 2011). This too is common practice in models of ecosystems. The biotic component of FIREMESH is vegetation. This is simply represented as a model of litter input and decay rates (Olsen, 1963): a physical perspective of a biotic component. Other landscape fire succession models represent vegetation from a biotic perspective (e.g. Pausas

and Ramos, 2006; and the LAMOS model in Keane *et al.*, 2013a, used the cohort-based vegetation model of Moore and Noble, 1990 that employ parameters relevant to the vital attributes of plant function types Noble and Slatyer, 1980).

1.4.4 *Landscapes*

A landscape fire succession model is an ecosystem model. An ecosystem model need not be explicitly spatial, but the addition of the term 'landscape' does imply that spatial relations between entities in the system being modelled are important. Lepczyk *et al.* (2008) defines a landscape as a spatially explicit ecosystem, but in common usage not all spatially explicit ecosystem models are landscape models. The purpose in using the term 'landscape' to distinguish this class of model from other models of fire and vegetation interactions seems two-fold: to suggest intuitively the scale at which we (humans) experience the world and at the same time to distinguish these fire models from others which do not explicitly employ spatial relations to simulate fire regimes (Krawchuk *et al.*, 2009; Thonicke *et al.*, 2010; McCarthy *et al.*, 2002; Moreno and Chuvieco, 2013).

However, the term 'landscape' is still not consistently applied. For example, the models listed by Keane *et al.* (2004) as landscape fire succession models also include models such as MCFIRE (Lenihan *et al.*, 1998) which are a set of point-models that do not include spatial interactions between those points. Other authors suggest the term 'landscape' should only be used where spatial relations are viewed as central to the behaviour of the system (Allen and Hoekstra, 1992).

1.4.5 *Spatial representation: Models of space*

Besides spatio-temporal resolution, this study also examines aspects of the way in which space is represented. Time and space differ in their number of dimensions. Because space has more than one dimension, the way points in space are connected (topology) is an attribute of space that can be abstracted in some way.

As noted, fire models such as FARSITE (Finney, 2004) and PROMETHEUS (Tymstra *et al.*, 2010) represent the fire front as a vector of discrete points. However, they differ from other fire simulators in that they attempt to maintain a constant number of points on the fire perimeter as the perimeter changes. This implies that the spatial connectedness of the model is dynamic, as paths from one point to the next are determined with the primary aim of creating more or fewer perimeter points to maintain the polygon segment lengths at some specified resolution. On the other hand, with raster models of space, the neighbourhood relations (distance, angle and slope) are discrete, explicit and unvarying regardless of whether the relations are reg-

ular as in a raster grid (Hengl, 2006) or in fact irregular, as is the case with a Triangulated Irregular Network (TIN) (Heil and Brych, 1978; Peucker *et al.*, 1978). The number of neighbours to a point in space can have implications for the responsiveness of simulated fire spread to weather and terrain (Feunekes, 1991; Johnston *et al.*, 2008; Trunfio *et al.*, 2011; Boer *et al.*, 2011). Studies of percolation in lattices (Plotnick and Gardner, 1993) have identified percolation thresholds: a threshold where the probability of system spanning events (e.g. simulated fires) changes rapidly with the proportion of sites that are connected. In a model, these thresholds depend on the number of neighbours between locations and the frequency of such events is often described as having a power-law distribution producing scale-free patterns in landscapes (Bak *et al.*, 1987). The implication is that the long-tailed distribution of fire sizes typically observed is an emergent property of self-organized criticality. However, Boer *et al.* (2008) and Boer *et al.* (2011) question this and make the case that this observation contains an implicit assumption about the neighbourhood invariance in these models. That is, scale-free pattern formation arises only because the number of neighbours, regardless of how many there are, is fixed. In fire simulators with a fixed topology, the number of neighbours actually represents a maximum rather than a fixed number of neighbours. The realized number of neighbours varies with the weather, fuel and terrain, and thus effects of self-organized criticality do not necessarily apply. If the model included propagation by ember transport (fire spotting), the number of neighbours would be larger again. Boer *et al.* (2008) have shown that it is the long-tailed distribution of extreme fire weather that principally determines the long-tailed distribution of fire sizes rather than some intrinsic property of self-organized criticality.

Typically, landscape fire regime simulation models use a raster grid as their model of the spatial domain because such a design is efficient and this class of model, as already noted, must run over relatively large spatial and temporal extents given the size and frequency of fires in many systems. Raster grids have a topology of four orthogonally adjoining neighbours (von Neumann neighbourhood) or optionally all eight neighbours (Moore neighbourhood). Regular lattices with six neighbours have also been used (Davis and Burrows, 1994; Trunfio, 2004). The number of neighbours can be extended to those points beyond the first annulus to have 24 or 48 neighbours (Perera *et al.*, 2008) but this can violate assumptions of scale (Johnston *et al.*, 2008).

Another model (Johnston *et al.*, 2008) uses TINs with a random Poisson-Disk distribution of vertices (McCool and Fiume, 1992), in effect, a closest-packing arrangement of the area represented by each vertex somewhat similar to a honeycomb. When vertices, arranged in this way, are connected with a Delaunay triangulation (Delaunay,

1934; De Berg *et al.*, 2000) (no crossing edges), an arrangement with, on average, six neighbours to each vertex is produced (Figure 1.4). The distribution of vertices can vary in order to increase resolution in

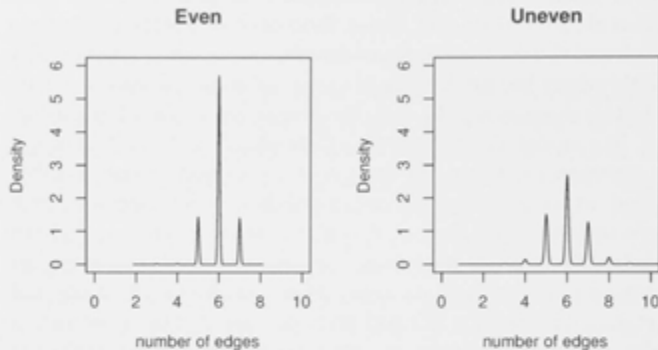


Figure 1.4: Density distribution of the number of neighbours to a vertex with an even and uneven distribution of vertices

The uneven distribution attempts an optimal placement of vertices to increase resolution where rates of change in the terrain are greatest. Methods for creating these meshes are discussed in Chapter 4.

regions where the landscape may have more variability and where the model may require finer resolution to function correctly (Figure 1.5). This has the potential to make the degree of model error attributable to resolution, constant over its spatial extent but will also have the effect of flattening the distribution of the number of neighbours to each vertex (Figure 1.4). Methods for producing these arrangements are discussed in Chapter 4. Using a variable resolution mesh is an approach used in many fields, including seismology (Braun *et al.*, 1995), General Circulation Models (Zarzycki *et al.*, 2014; Düben and Korn, 2014), fluid dynamics (Anderson *et al.*, 2005) and astronomy (Cautun and van de Weygaert 2011 after Schaap 2007). While errors arising in estimates of area burnt from the number of neighbours has been noted, to my knowledge no research has been done to examine whether this is important for landscape fire regime simulation models when ranked with their response to typical experimental treatments. The use of TINs for fire modelling has been pioneered by Johnston *et al.* (2008). I am not aware of any attempts to use variable local point densities to optimize the use of space in a fire model nor any research on how any of these decisions may affect the importance of factors that influence the generation of synthetic fire regimes. It follows that there are three separate questions contained within Hypothesis 2. The first two ask if the relative importance of the drivers of fire by simulation modelling is insensitive to:

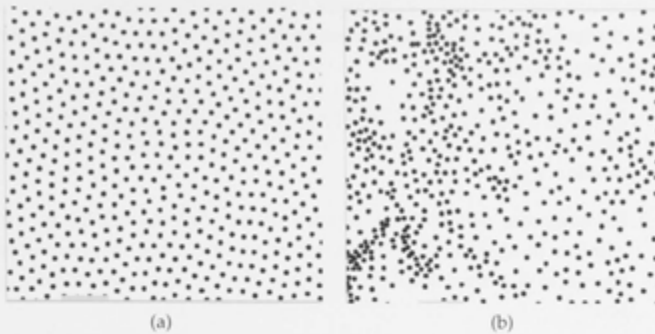


Figure 1.5: Two maps showing an even (Poisson-Disk) distribution (a) and uneven distribution (b) of vertices

The uneven distribution attempts an optimal placement of vertices to increase resolution where rates of change in the terrain are greatest. Methods for creating these arrangements are discussed in Chapter 4. See also Figure 3.1

- i The number of neighbours connecting points (vertices) within the model's the spatial extent;
- ii The regularity / irregularity of disposition of locations in space, that is, a regular grid or a triangulated irregular network with a Poisson-Disk distribution of vertices;

The last questions asks if:

- iii Landscape fire simulation models can be made less sensitive to changes in spatial resolution by some optimal placement of vertices within a complex terrain.

1.5 APPROACH OF THIS STUDY

Fire plays a key role in ecosystem dynamics and its impact on environmental, social and economic assets is increasingly a critical area of research. Estimating the relative importance of the drivers of fire behaviour is an essential first step in understanding how fire effects interact with the social and ecological environment as that environment itself undergoes change. Fire propagates as a contagious process and simulation offers an approach to capture this important behaviour explicitly. However, simulation requires the introduction of nuisance parameters and given the non-linearity of many aspects of fire behaviour, the level of abstraction entailed by the choice of these parameters may challenge previous findings of fire regime landscape simulation models. This, to the best of my knowledge, has not been tested and is the core work of this thesis.

There are four formal hypotheses for this study addressing issues of spatio-temporal resolution and spatial representation in fire-regime simulation modelling:

- i Ranking the relative importance of the drivers of fire by simulation modelling is insensitive to a wide range of spatio-temporal resolutions;
- ii Ranking the relative importance of the drivers of fire by simulation modelling is insensitive to the number of neighbours connecting points (vertices) within the model's spatial extent;
- iii Ranking the relative importance of the drivers of fire by simulation modelling is insensitive to the regularity / irregularity of disposition of locations in space; and,
- iv Landscape fire simulation models can be made less sensitive to changes in spatial resolution by some optimal placement of vertices within a complex terrain.

The hypotheses are tested by adapting a well-established, peer-reviewed fire regime simulation model (FIRESCAPE: Cary and Banks 2000) that has been widely used to estimate the relative importance of many of the factors affecting fire regimes. This model is extensively modified to isolate just those aspects of the model's sensitivity to resolution and discrete geometries that are unavoidable or intrinsic to the choice of these nuisance parameters. The modified model (FIRE-MESH) is used to test the hypotheses above, using published experimental treatments that can stand as yardsticks by which formal estimates of the importance of resolution and discrete geometries (nuisance parameters) can be made. 'Importance' is determined with reference to three of the attributes of fire regimes: frequency, intensity and seasonality.

As noted in Section 1.4.1 concerning a grounded theory of abstraction, the findings in this thesis may only have relevance to the particular model and data set used to test these two hypotheses but in a less formal sense, the abstraction upon which the model is grounded is the literature in this field. To assist in estimating the generality of these findings, the data and model, together with modifications to address the hypotheses of this study, are described in chapters two and three. In Chapter four, the consequences in making time and space discrete are examined in detail and a method proposed whereby model sensitivity to spatial resolution may be minimized. In Chapter five (Verification), the model is tested to confirm that the specifications detailed on Chapter three (and Appendix 1) are correct. In Chapter six (Validation), the model and data are tested to confirm that they are an appropriate choice with which to address the hypotheses of this study. Hypothesis (i), which addresses spatial and

temporal resolution is tested in Chapter seven. The hypotheses addressing questions of discrete geometries are tested in Chapter eight. Chapter nine provides a synthesis of the study and discusses some further directions in modelling studies where the focus is on understanding system behaviour in the context of levels of abstraction.

DATA REQUIREMENTS: TERRAIN, VEGETATION, WEATHER AND REPLICATION

2.1 OVERVIEW OF THE MODEL'S DATA REQUIREMENTS

FIREMESH (see Chapter 3 and Appendix 1 for a full model description) is based on FIRESCAPE (Cary, 1998; Cary and Banks, 2000; McCarthy *et al.*, 2002). The original purpose of FIRESCAPE was to explore variation in spatial patterns of fire regimes and the distribution of plant species that may arise from these patterns. FIRESCAPE was developed in the mid-1990s and much has changed in computer technology and fire science since that time, in particular new methods for estimating rates of fire spread arising from Project Vesta (Gould *et al.*, 2007; Cheney *et al.*, 2012). At its core are the equations derived by Noble *et al.* (1980) based on McArthur's Mk 5 Forest Fire Danger Meter (FFDM) (McArthur, 1973) (see: Appendix Section A.7). The FFDM has been the most widely used method in Australia to calculate forest fire danger indices (FFDI) though it may be replaced for the estimation of fire behaviour by field guides informed by Project Vesta. The parameters for the FFDM are air temperature, humidity, wind speed, soil dryness and the amount and time of the last rainfall event. With the addition of slope and the weight of fine surface litter, the forward rate of spread of the head fire can be calculated. This then, is an empirical one-dimensional model of fire spread upon which FIRESCAPE is based. The only additional input required to model fires in two dimensions is wind direction.

FIRESCAPE has been used in many studies (Cary and Banks, 2000; McCarthy *et al.*, 2002; Keane *et al.*, 2003; King *et al.*, 2008a,b; Cary *et al.*, 2006, 2009; King *et al.*, 2011, 2012; Bradstock *et al.*, 2012; Keane *et al.*, 2013a) and is designed specifically for the forests of SE Australia, the same region in which many of the observations were made to develop the empirical relationships between weather, fuel and terrain that underlie predictions made using the FFDM. The terrain, vegetation and weather used in the present study are very similar to those used in developing FIRESCAPE. This, along with its published record and purpose, make FIRESCAPE an appropriate choice for modification to suit the aims of this work.

The average inter-fire interval (IFI) derived from maps of fire extents (Courtesy: P. Zylstra 2011) for NSW portion of the Australian Alps is 50 years. This value would likely have high uncertainty as the available data spans only about twice the IFI and of course does not include pre-European fire regimes. For example, considering the

larger region of the Southern Alps from the Victorian border to the northern extent of the ACT, two fires, in 1939 and 2003, contribute 70% of the area burnt in the last 90 years. Within the 2,500 km² study region (Figure 2.1) the 2003 fires alone contribute 77% of area burnt over the years 1985–2010. Fire sizes of 10 ha are the most frequent and within the long-tail distribution typical of fire sizes there is a pronounced higher frequency between 103 and 104 hectares (Figure 2.2). Nevertheless, the 50 year IFI from this limited data set accords with estimates by Pryor (1939); Shugart and Noble (1981); Anon (1973) and is used to calibrate simulations in this study.

The number of recorded fires between 1985 and 2009 within the study region is six per annum. Fifty ignitions have been recorded between 1983 and 1996 of which 30% have been attributed to lightning, approximately one per year (NSW National Parks Southern Fire Data). All lightning initiated fires occurred in summer.

2.2 TERRAIN AND VEGETATION

A mountainous region of comparatively complex terrain (in Australian terms) has been chosen for this study to explore any consequences spatial resolution may have for fire regime generation. The area is 2,500 km² of the Brindabella Ranges, encompassing the southern half of the Australian Capital Territory (latitude 35.79–35.45° S, longitude 148.77–149.15° E (Figure 2.1). Elevations range from 560 to 1,910 metres with a mean elevation of 1,189 metres above sea level. Eighty per cent of slopes are less than 20° (see Section 5.7 for the implications of this) and east and west aspects predominate (Figure 2.3). The digital elevation model (DEM) used in this study has a cell area of 0.04 hectares. It was created using ANUDEM version 5.3 (Hutchinson, 2007) based on contour and stream flow vectors from the NSW Department of Lands, corrected for errors by John Stein (ANU).

Under the Interim Biogeographic Regionalization of Australia classification (Anon, 2012), the study region is characterized by the South-East Highlands (SEH) and Australian Alps (AUA) sub-regions. The vegetation cover is predominantly dry sclerophyll forests with shrubby-/grassy understorey at lower elevations and wet sclerophyll forest at higher elevations (Keith, 2004). The highest elevations are often covered by sub-alpine woodland.

This area is a subset of the 9,000 km² area used in developing FIRESCAPE (Cary, 1998) (Figure 2.1). A smaller extent was necessary because, at times, finer resolutions are required for the simulation experiments. For example, at a resolution of 0.25 hectares, one million points are required and beyond this, simulations become impractical with the computer resources available. Edge effects and the scale of fires in this region may limit how small an extent is viable for simulation experiments. However the size of the study area was that adop-

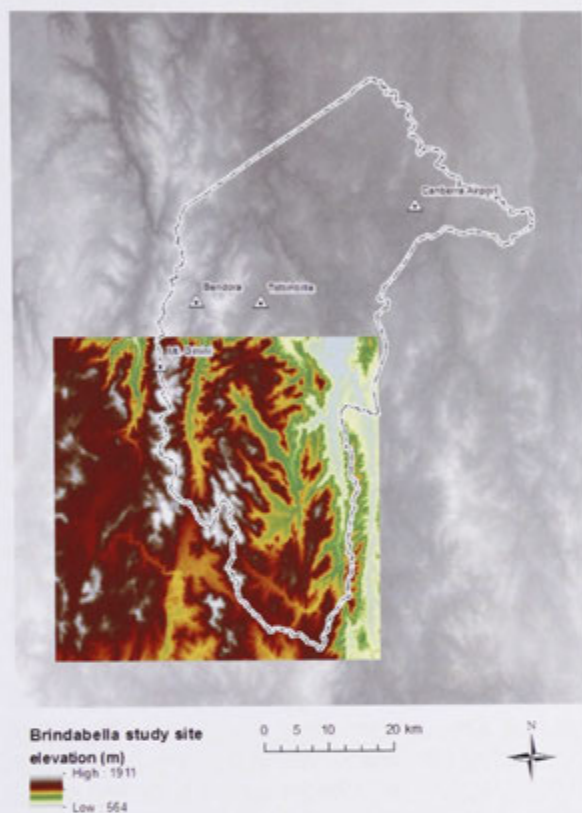


Figure 2.1: The Brindabella Ranges study landscape of 2,500 km² (coloured) is shown against the boundaries of the Australian Capital Territory

The extent of the landscape used in developing FIRESCAPE is shown in grey (approximately 9,000 km²). Weather stations important to the current study are marked: Canberra Airport (Elv.: 577 m, Lat.: -35.31, Lon. 149.2), Bendora (Elv.: 815 m, Lat.: -35.44, Lon.: 148.83), Tidbinbilla (Elv.: 700 m, Lat.: -35.44, Lon.: 148.94) and Mt Ginini (Elv.: 1,760 m, Lat.: -35.53, Lon.: 148.77).

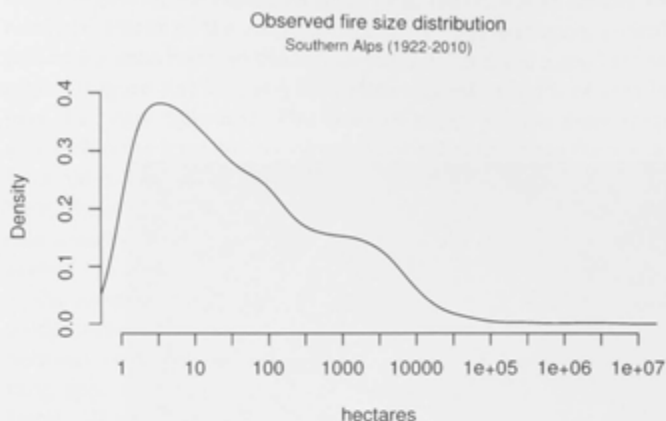


Figure 2.2: Fire size density distribution for the Australian Alps (including the study region) (1922-2010)
(data courtesy: P. Zylstra)

ted for the model comparison studies of Cary *et al.* (2006, 2009) and Keane *et al.* (2013a) which involved a number of landscape fire regime models including FIRESCAPE. The ratio of mean fire size to the extent of the region is about 0.008 and the ratio of recovery to mean fire return interval about 0.3 assuming a recovery time to canopy closure of 15 years (M. Dougherty, pers. comm., 2014). This places the study area in an 'equilibrium' state according to the interpretation of that term by Turner *et al.* (1993).

The fuel maps used are those developed by Cary (1998) for FIRESCAPE (Figure 2.4). These are generated from empirically derived fuel loads of fine surface litter and decomposition rates for five elevation classes (Table 2.1) which form the parameters to the fuel growth equation of Olsen (1963) (Equation 2.1). Equilibrium fuel accumulation levels (X_{SS}) against elevation form approximately a logistic function describing the combined effects on the balance of fuel inputs and decay rates of decreasing temperature and increasing precipitation with elevation.

$$F = X_{SS}(1 - e^{-kt}) \quad (2.1)$$

where:

X_{SS} = equilibrium fuel accumulation level;

k = decomposition constant; and

t = time in years.

(Olsen, 1963)

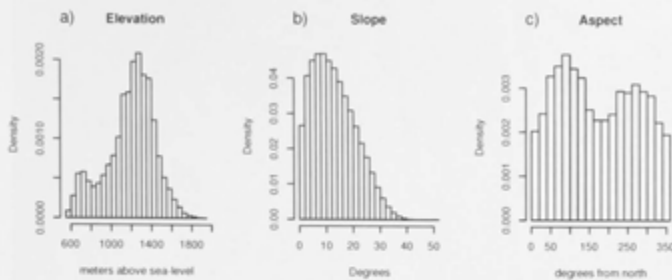


Figure 2.3: Density distributions of elevation, slope and aspect for 2,500 km² of the Brindabella ranges
 Mean elevation is 1,189 m, 80% of slopes are less than 20° and east and west aspects predominate.

Table 2.1: Steady state values (X_{SS} t.ha⁻¹) and litter input rates (L) for surface litter for five elevation classes in the Brindabella study region (from Cary, 1998)

ELEVATION (m)	X_{SS} (t.ha ⁻¹)	L (t.ha ⁻¹ .y ⁻¹)	COVERAGE
≤750	9.64	2.89	7%
≤1,000	9.95	2.98	6%
≤1,250	11.55	3.46	40%
≤1,500	14.67	4.40	40%
>1,500	16.37	4.91	7%

2.3 CLIMATE

The climate is temperate, without a pronounced dry season and with warm summers, classified as cfb under the Koppen-Geiger climate classification system (Peel *et al.*, 2007). Weather data from Canberra Airport (see location in Figure 2.1) shows a slight predominance towards summer rain both during the period of data used for this study (1985-2011) and the long-term records (1939-2014) (Figure 2.5.a). This study is limited to a 26 year span of weather data for reasons described below.

Monthly means of the maximum daily temperatures show a typical continental mid-latitudes profile ranging from 11.5°C in July to 28°C in January. Monthly means of daily minimum temperature are about 0.5°C higher in the 26 year study data than the long-term average data (Figure 2.5.b). Monthly means of daily relative humidity (measured at the time of maximum temperature) range from a maximum in February to a minimum in August while wind speeds achieve their maximum in October and minimum in May. The highest half-hourly wind speed recorded is 70 km.h⁻¹ and only 0.07% of records exceed

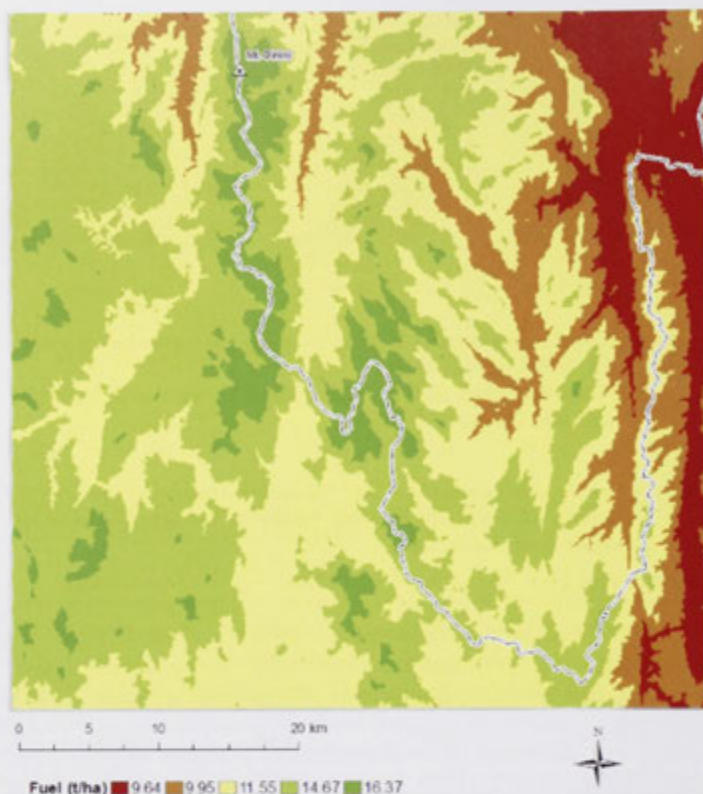


Figure 2.4: Steady state values ($X_{ss} \text{ t.ha}^{-1}$) (fine surface litter) for five elevation classes (Table 2.1) in the Brindabella Ranges after Cary (1998)

Mean elevation is 1,189 m, 80% of slopes are less than 20° and east and west aspects predominate.

50 km.h^{-1} . Monthly mean daily drought factor, calculated using the soil dryness index of Mount (1972), has a maximum in autumn and a minimum in spring (Figure 2.5.e). This follows from the use of different evapo-transpiration tables between spring and autumn to account for the effect of soil temperature inertia on soil dryness (Table A.2). These variables combine to give a clear maximum FFDI in January with an asymmetry towards autumn (Figure 2.5.f).

Wind from the north-west dominates the wind direction. These winds come from the inland, are drier and occur more frequently during summer months. As a consequence, fire runs from the north-west are common (Figure 2.6), cutting diagonally across the predominantly east-west aspect of the Brindabella Ranges (Figure 2.3.c). As noted, one of the topics examined in the present study is spatial represent-

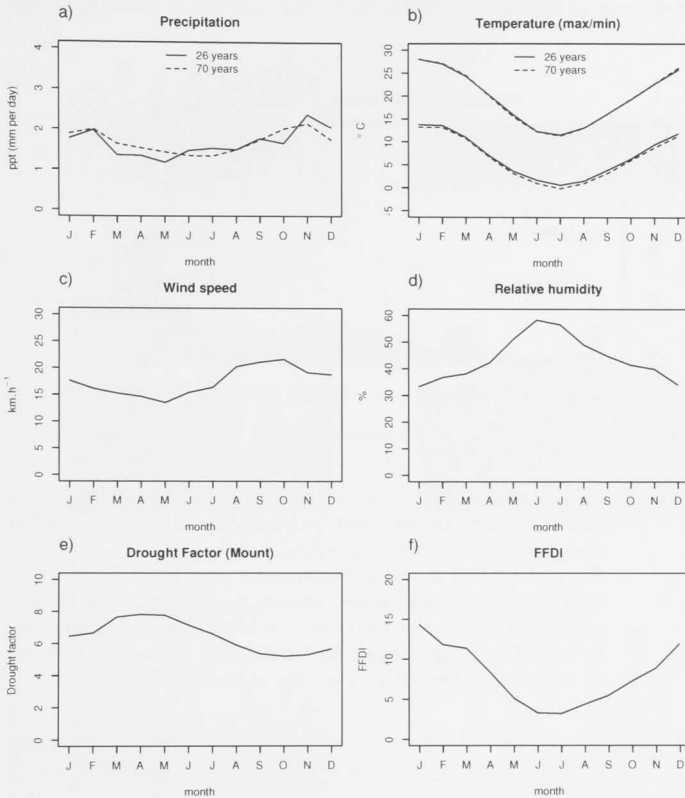


Figure 2.5: Daily values (averaged over the month) of precipitation, temperature, wind speed, relative humidity and drought factor Forest Fire Danger Index are monthly means of 3pm values (McArthur 1973). All data was recorded at Canberra Airport (1985-2011) and (1939-2011) (Elv.: 577 m, Lat. -35.31, Lon. 149.2). Humidity is measured at the time of daily maximum temperature. Drought factor is calculated using the Soil Dryness Index of Mount (1972).

ation. This entails running simulations with various neighbourhood topologies. It is well known that simulating fire spread using a regular eight neighbour configuration produces up to a 50% reduction in rate of spread in directions 22.5 degrees from the eight cardinal and semi-cardinal compass points (Feunekes, 1991). If such an effect is important in the generation of fire patterns from this data, the predominance of fire runs from the NNW may provide a useful test case.

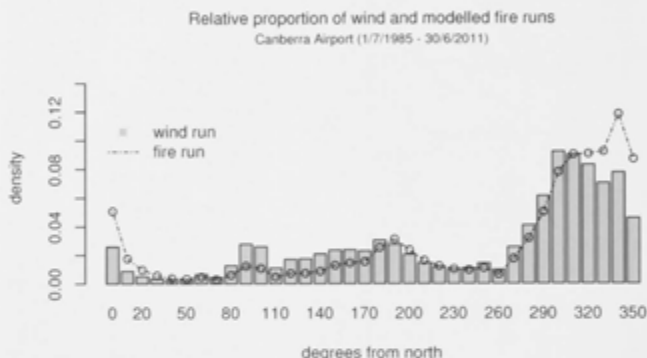


Figure 2.6: Density distribution of wind directions, clockwise from north and fire runs from half-hourly weather data at Canberra Airport (1985-2011) (Elv.: 577 m, Lat. -35.31, Lon. 149.2) Fire runs (circles) are calculated as vector sums (total distance travelled by direction) when fireline intensity is greater than 100 kW.m⁻¹ assuming a surface fuel weight of 12.5 t.ha⁻¹, and using the Mark V Forest Fire Danger Meter (McArthur 1973) and a drought factor calculated using the soil-dryness index of Mount (1972).

Mean daily 3pm FFDI shows considerable inter-annual variability with an increasing trend in FFDI over the 26 year period (Figure 2.7). The model comparison experiments of Cary *et al.* (2006, 2009) and Keane *et al.* (2013a) looked specifically at the relative importance of this weather variability compared to climate and other treatments. Two of these experiments are replicated with FM in Chapter 6 (Validation).

Canberra Airport has the longest record of half-hourly data available within a 50 km radius of the mountainous study region for which FIRESCAPE was developed. Other data is available at coarser resolution but for the purpose of this study, which includes an analysis of temporal resolution, data with a resolution of at least half-hourly readings is necessary.

The data comprises temperature, vapour pressure, wind direction (at 10° resolution) and wind speed at half-hourly intervals. Wind speed is the sustained wind speed averaged over the 10 minutes lead-

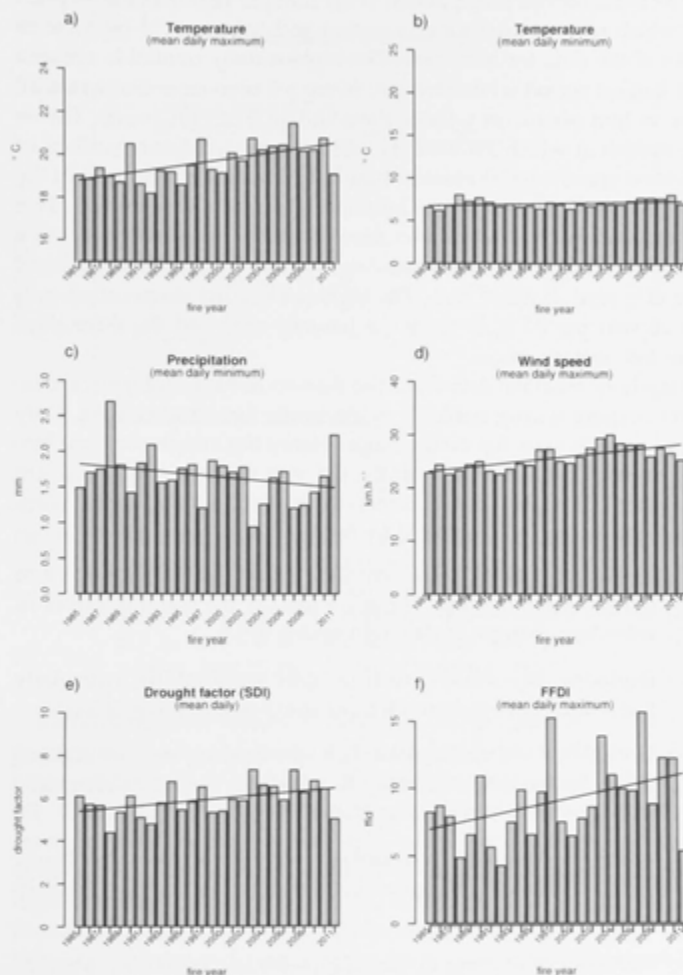


Figure 2.7: Annual average daily values of weather variables recorded at Canberra Airport (1985-2011)

Drought factor is calculated using the soil-dryness index of Mount (1972). Forest Fire Danger Index is determined using the Mark V Forest Fire Danger Meter (McArthur, 1973).

ing up to the time of the observation at 10 metres above ground level (U_{10}). Rainfall, used to drive the soil moisture model, is recorded daily at 9am.

The mean annual precipitation is 647 mm per year over the 70 years for which records exist for this station and 606 mm.y^{-1} over the 26 years of the data for this study. The highest daily rainfall is 126 mm and longest period with a drought factor > 8 is 40 days. Daily rainfall over 10 mm occurs on 5.2% of days and 18% of rain events. This is the rainfall at which FIREMESH will extinguish a fire regardless of the wind speed, temperature or humidity. Thirty eight per cent of the half-hour readings have a maximum wind speed $> 12.5 \text{ km.h}^{-1}$. This is the wind speed at which McCaw *et al.* (2008) consider McArthur's Forest Fire Danger Meter (FFDM) begins to under predict the forward rate of spread of forest fires. The highest recorded temperature over the 26 year period is 40°C on 1st January 2007 and the three days from 6-8 January 2009.

Half-hour weather data from the Bureau of Meteorology for Canberra Airport is only available in electronic format after 1984. Only paper records exist for earlier dates. Hence the simulations are limited to using data starting with the fire year 1st July 1985. There are a number of missing or invalid records, especially in the earlier years. Missing data has been replaced by five methods:

- i Replacing missing values with the nearest value within $1/2$ to 1 hour of the reading. These are usually the result of errors in recording changes in day light saving (9%);
- ii Replacing any missing 6am or 3pm temperatures with daily minimum and maximum temperatures respectively (0.002%);
- iii Using a splined surface based on surrounding weather stations (ANU Spline data: Courtesy K. King) for any remaining 6am and 3pm temperatures (0.002%);
- iv Using the diurnal down-scaling method of Cary and Banks (2000) to replace any remaining temperature, vapour pressure and wind data (2%);
- v Manually examining outliers (approximately 0.004%). Most of these errors were due to the columns of wind direction and speed being transposed.

2.3.1 Extrapolating to other elevations

Empirically derived lapse rates for temperature and precipitation were calculated by comparison with data from nearby weather stations (Figure 2.1). Temperature lapse rates were obtained using three hour data for the same 420 days for both Canberra Airport and the automatic weather station at Mt Ginini (Lat.: 35.53°S , Lon.: 148.77°E , Elev.:

1,760 m) approximately 46 km to the south-west (Figure 2.1). Lapse rates varied between $-0.008^{\circ}\text{C}\cdot\text{m}^{-1}$ at 15:00 to $-0.003^{\circ}\text{C}\cdot\text{m}^{-1}$ at 6:00 hours (Figure 2.8).

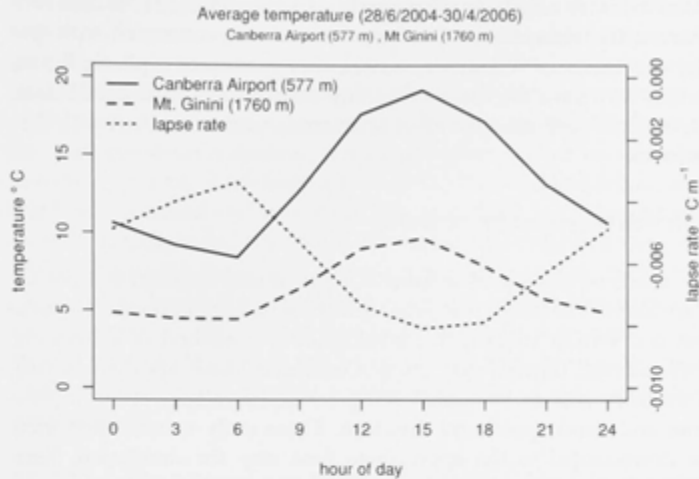


Figure 2.8: The mean of 420 days of three-hourly temperature readings at Canberra Airport and Mt Ginini

The dotted line is the 3 hourly temperature lapse rate ($^{\circ}\text{C}\cdot\text{m}^{-1}$) derived from temperature differences between Canberra Airport (Elev.: 577 m, Lat.: -35.31 , Lon.: 149.2) (solid line) and Mt Ginini (Elev.: 1,760 m, Lat.: -35.53 , Lon.: 148.77) (dashed line).

Records from Mt Ginini were also used to calculate changes in precipitation with elevation. The correspondence of dry/wet days between Canberra Airport and Mt Ginini was found to be 74% where Mt Ginini had a little over twice (2.06 times) as much total precipitation as Canberra Airport over the 9 years from 2004–2013. Stations at Bendora (Elev.: 815 m) and Tidbinbilla (Elev.: 700 m) (Figure 2.1) had higher correspondence with rainfall events at Canberra Airport but their lower elevations make extrapolation less reliable. A simple lapse rate was then derived from a ratio of total precipitation between Mt Ginini and Canberra Airport. The domain of its application was limited to elevations within the range of Canberra Airport (Elev.: 577 m) and Mt Ginini (Elev.: 1,760 m). The mean daily drought factor, using the method of Mount (1972), for Canberra Airport over the 26 years from 1985 to 2011 is 5.9, while the estimated drought factor at Mt Ginini is 3.7.

2.4 REPLICATION OF INPUT DATA

Ideally, simulation experiments using weather and terrain should be performed with replicates of both these data to avoid drawing conclusions that may only have relevance to particular instances of data sets. Because the experiments in the present study are concerned with spatial and temporal resolution, a necessary quality of replicated data is that they have the same variability across scale as observed data. Methods of replicating weather and terrain were examined with this in mind.

2.4.1 *Stochastic weather replication*

As noted, replication of weather has previously been carried out by Cary and Banks (2000) using the method of Richardson (1981, Richardson and Wright 1984) with the addition of a method of generating daily rainfall (Hutchinson 1995). Combined, these approaches produce daily outputs of rainfall, temperature (max/min), vapour pressure and wind speed and direction. These daily values must then be down-scaled to the appropriate time step for simulation. Temperature was down-scaled by combining trigonometric functions to achieve a slow cooling between times of maximum to minimum temperature and a more rapid transition from minimum to maximum. Wind speed and direction were down-scaled by calculating an hourly multiplier of the daily average wind speed expressed as west-east and south-north vectors. The average wind speed was increased in down-scaling, to account for the fact that average wind speed is considerably less than maximum wind speed determined from other observations. Vapour pressure is similarly down-scaled using a multiplier based on average change in vapour pressure over the diurnal cycle. The method was re-implemented as stand-alone Java application, transcribed from the original source code and a test performed to determine if the synthetic weather generated in this manner is suitable for testing sensitivity of the fire model to temporal resolution in order to address Hypothesis (i).

METHOD Ten replicates of 26 years of synthetic weather data were generated and compared to actual data from Canberra Airport. The original parameters for the weather generator were derived from 16 years of daily rainfall data (1978-1993) and 11 years of other daily weather data (1978-1988) from the CSIRO weather station at Ginninderra. The Ginninderra station lies approximately 10 km NW of Canberra Airport and at the same elevation. Rather than re-parameterize the generator with data from Canberra Airport, the original parameters were left intact. There is no provision either in the Richardson method or the down-scaling methods to address the issue of multi-

scale variability. Therefore, the purpose of this test is to determine if this absence of multi-scale variability is a concern when examining the sensitivity of a simulation model to temporal resolution. Furthermore, the test is not one that seeks to determine if the overall mean readings are the same as the source data. Such a test would be tautological as the parameters to the generator are those same mean values and this has already been verified by Cary (1998). The half-hourly synthetic data (GIN) and half-hourly hourly data from Canberra Airport (1985-2011) (CAN) were examined at half and three hour time steps. For each consecutive reading, if the consequent fireline intensity (assuming 12.5 t.ha^{-1} for fuel) was $> 100 \text{ kW.m}^{-1}$, the distance travelled was summed and recorded. This provides a set of contiguous periods of sustainable fire (fire runs) measured as distance travelled. The fire runs were squared to provide a nominal value for area burnt (AB), that is, longer runs should be of greater relative importance. If the difference in AB between half and three hour time steps is of a similar magnitude, then it can be concluded that down-scaled synthetic weather would provide a suitable method of data replication for this study.

RESULT The nominal area burnt (AB) for the CAN data increased by 8% between half and three hour time step analysis, while AB for the synthetic GIN data decreased by 7%. As the results show a different sign, this method of replication is considered unsuitable to the aims of this study. A likely explanation is that conditions that terminate a fire run (fireline intensity $< 100 \text{ kW.m}^{-1}$) are more variable in the CAN data than the GIN and are skipped at coarser resolution. A separate analysis of the sums of the difference in FFDI between successive readings in the observed data, shows they are about twice that of the synthetic data. Therefore, the method of weather replication for fire simulations as implemented here, requires some additional research to provide more realistic methods of down-scaling to create a comparable degree of variability between readings. Researching such methods is beyond the scope of this study and therefore, for the formal hypothesis testing, observed rather than synthetic data will be used.

2.4.2 Stochastic terrain replication

Methods to replicate landscapes were also investigated, beginning with the mid-point displacement algorithm of Saupe (1991). This is the most recent of similar methods beginning with Miller (1986). The mid-point displacement algorithm operates on square lattices. If n is the width of the square, a smaller square can be obtained by taking the mid-point of each side of the $n.n$ square which will then have resolution $n/\sqrt{2}$ and be orientated at 45° to the first square. If mid-

points of this second square are again obtained, resolution will be $n/2$ but with the same orientation as the first $n \times n$ square. Thus resolution (r) will increase at each iteration by $1/\sqrt{2}$ and there will be $\log_2(n-1)$ iterations. Within each iteration, displacements at resolutions of $r/\sqrt{2}$ and $r/2$ are made. It follows that $n-1$ must be a power of 2. The elevation at each of the mid-points is the mean of the four corners of the previous square with variance r^{2H} times the variance (σ^2) at the previous r , where H modifies the fractal dimension: which is equal to $3-H$. That is, at each change in resolution i :

$$\sigma^2 = \sigma_{i-1}^2 0.5^{0.5H} \quad (2.2)$$

Rather than using Equation 2.2, the variance at each iteration can be replaced with variance derived from a digital elevation model at each of these resolutions to give a vector of standard deviations across scales. It is important to capture changes in roughness with scale as this will affect the sensitivity of fire simulations to spatial resolution just as variability between weather readings was an important consideration for the synthetic weather data. As the method is stochastic, each run produces different but statistically related landscapes in terms of the variance in neighbouring elevations across scales.

METHOD Multi-scale standard deviations were derived from a 20 metre cell resolution digital elevation model (DEM) of the Brindabella study site (Figure 2.1) by iterating over the DEM using the algorithm of Saupe (1991) described above. The vector of standard deviations so obtained were used instead of Equation 2.2 to generate a landscape with the same multi-scale fractal dimensions as the Brindabella Ranges. These standard deviations show a relatively rougher terrain at scales of 2–5 km than at 20–35 km compared to Equation 2.2 (Figure 2.9).

RESULTS While the mid-point displacement algorithm produced similar distributions of elevation and slope, it was unable to produce plausible mountain ranges but rather generates sets of isolated peaks with un-drained hollows (Figure 2.10). This follows from the fact that such a statistical approach cannot capture knowledge of processes that build and erode mountain ranges. This is indicated by the distribution of aspects (Figure 2.11) which are almost uniform compared to the bi-modal distribution of the real landscape, a reflection of the predominance of north-south valleys.

A landscape with fragmented aspects such as produced here will create unrealistic patterns of fire regimes. For example, Cary (1998) hypothesized the existence of *ignition neighbourhoods* which can be understood by analogy to watersheds. Fire spreads in a reverse manner to that of water flow - water flows downhill, fire generally spreads fastest uphill (McArthur, 1967). Just as a catchment concentrates wa-

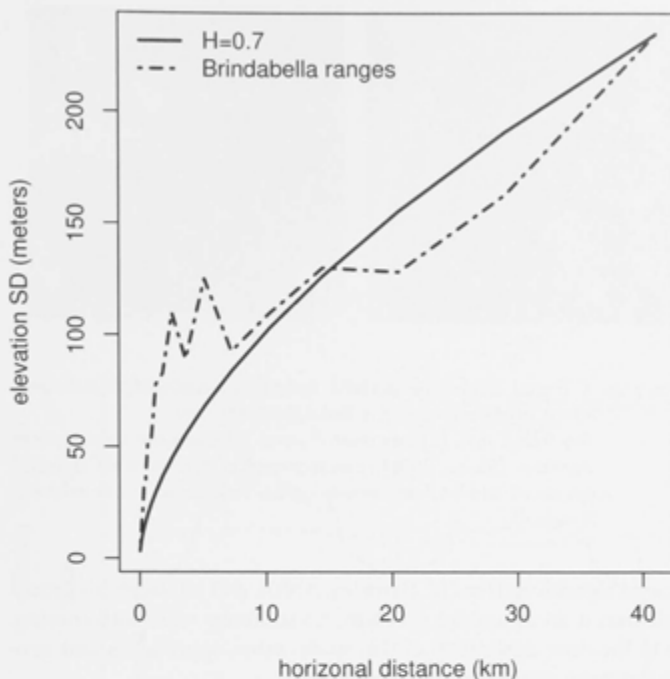


Figure 2.9: Multi-scale standard deviations in elevation for the Brindabella digital elevation model (Figure 2.1) compared to a fractal function (Equation 2.2) (Saupe, 1991).

ter into lakes and streams, so too can landscape formations concentrate fire frequency in some areas, based on a location's ignition 'catchment', or as termed by Cary, 'ignition neighbourhood'. The role of fire in determining realized niches in vegetation dynamics was a key purpose behind the development of landscape fire regime models. Because the mid-point displacement algorithm will not produce realistic fire regime patterns in this regard, it is considered unsuitable for the purpose of this study.

Many other researchers in the field of computer graphics have attempted to address the issue of non-coherent catchment formation (see for example Teoh 2009; G  nevaux *et al.* 2013) using various methods to define river mouths (exit points from the map) and ridge lines. Because the purpose of these synthetic landscapes is an aesthetic one (computer games etc.), assessment of their worth is subjective. However, to achieve true replication some objective method is required to map information from some real case study (a grounded abstraction) and as such begs the question as to what attributes of the landscape are to be replicated. Discussions were initiated with an expert

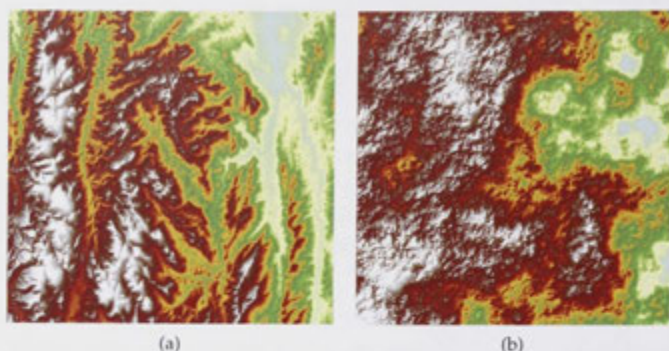


Figure 2.10: A fractal landscape derived from multi-scale standard deviations in elevations of the Brindabella Ranges

The fractal map (b) was created using the mid-point displacement algorithm (Saupe, 1991), parameterized with multi-scale standard deviations derived from semivariogram analysis of the Brindabella Ranges.

in fractal algorithms (Prof M. Barnsley, ANU), and although his group considered it an important problem, no solutions were forthcoming. Due to the time constraints of this study, other approaches that generate drainage systems were not pursued.

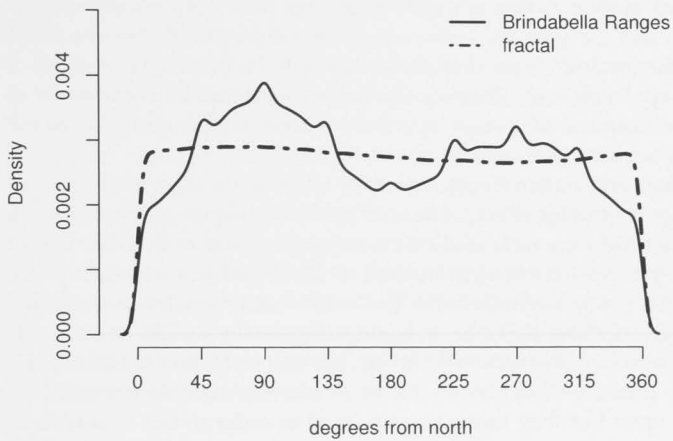


Figure 2.11: Density distributions of aspect for observed and synthetic landscapes

Density distributions of aspect for an area of 2,500 km² of the Brindabella ranges ACT (black line) and a fractal landscape generated using the mid-point displacement method of Saupe (1991) (dotted line).

2.5 MATCHING AVAILABLE DATA TO MODEL REQUIREMENTS

The design of simulation models is constrained by data and computer resources. The scale implied by the purpose of the model and the scale at which environmental data is collected are often a mismatch (Stein *et al.*, 2001) requiring either data aggregation or disaggregation¹.

For a given model, data aggregation is necessary when computer resources are limiting while disaggregation, requiring a model for the purpose of down-scaling, is needed when data is the limiting factor. Because disaggregation requires an additional model, additional states are introduced into the abstraction which are not present in the abstraction on which this is grounded (Section 1.4.1, Zucker 2003). It follows that any differences that arise between the abstraction and the grounded abstraction cannot necessarily be attributed to the level of abstraction per se, but may be due to the method of interpolation itself. Therefore, to avoid interpolation, experiments in this study use time steps which are whole number multiples of the weather data (half-hourly).

Bian and Butler (1999) note that, while there is general acknowledgement of the effects of various methods of aggregation, there has been little systematic evaluation, suggesting that researchers in fact use the most convenient method at hand and not necessarily one with a strong scientific basis. The authors distinguish between *inherent* errors, those that arise in aggregating data to match the demands of the model, and *operational* errors, the way resolution in and of itself may produce model errors. These decisions are not always commented upon but they must be considered in order to not to confound operational errors with inherent errors when resolution itself is an experimental treatment. The distinction between inherent and operational errors can at times be overlooked. Elevation data is almost universally in the form of a raster grid. If the spatial representation in a fire model is an irregular grid (Johnston *et al.*, 2008), a method of mapping from the regular grid to the irregular mesh must be proposed. Bian and Butler examine three methods: mean, median and centroid. The method chosen by Johnston *et al.* (2008) is simply to take the nearest value in the underlying gridded data to the vertex of the irregular grid. As the parameter values of a vertex, one of which is elevation, represent mean values for its surrounding area, this is in effect, the centroid method. Compared to mean and median methods, the centroid method does not reduce variance between values as quickly as the mean and median methods. However, due to spatial auto-correlations in the underlying data, unpredictable changes can

¹ Note the term 'aggregation' used here is not used in the same sense as that used in abstraction theory (Zucker, 2003) discussed in the previous chapter. Data aggregation is domain reduction whereas aggregation in abstraction theory refers to collecting disparate elements as one entity

occur using the centroid method as data is increasingly aggregated (Bian and Butler, 1999). The mean and median methods on the other hand, show greater predictability with aggregation but the variance in the original data declines as resolution becomes coarser.

The same issue arises in reporting a model's state variables at different resolutions. For example, if it takes four time steps for a simulated fire front to cross a location at a particular resolution, how should fireline intensity be recorded at that location as there are many, one for each direction of spread, times the number of time steps the front was within the location? If the maximum fireline intensity in direction at the time of ignition is recorded, this is equivalent to the centroid method. Taking the maximum fireline intensity in any direction (which is constrained by the number of neighbours to each vertex) accounts for the intensity at which the majority of the location is likely to have been burnt.

Again this issue arises for temporal data. If we have data at half hour intervals, how should this be aggregated to, say, three hour intervals? If the average of half-hour readings is used for the three hour values then variance will approach zero as resolution approaches the size of the temporal extent. The trade-offs between the three choices available (mean, median and centroid) mean it is impossible to entirely isolate inherent and operational errors. To examine all three approaches in the many experiments that follow is beyond the scope of this study. However, because this study entails analysis across resolutions, a consistent approach must be taken and the centroid method appears to be both the most practical and the best method to preserve variance between locations as resolution.

2.6 CONCLUDING REMARKS

In summary, terrain cannot be replicated in a manner that satisfies the requirements of replication (plausible patterns of mountain ranges with comparable distributions of aspects) and must remain to topic of further research. Replication of weather data requires addition of down-scaling methods which, while they may be suitable for some applications, do not appear suitable for the current study due to the lack of variability between readings at half-hourly time steps. Replicating terrain and down-scaled weather data to preserve multi-scale variability is, in my view, a valuable area of research that could supply important methods for landscapes simulation studies. However, for this study, the single weather stream and single mountainous landscape described above are used in the present study unless otherwise indicated.

FIREMESH: ITS ORIGINS IN FIRESCAPE AND SUBSEQUENT MODIFICATIONS

3.1 OVERVIEW

The modification of FIRESCAPE used in this thesis is named FIREMESH (FM), because the use of a mesh (or lattice) to represent space is the most visible way in which it differs from FIRESCAPE (Cary and Banks, 2000). This and other differences between FM and FIRESCAPE are discussed in this chapter. The full technical description of FM can be found in Appendix 1, and is described using the Overview, Design concepts, Details (ODD) protocol (Grimm *et al.*, 2006, 2010). Within the ODD, FM is also described in terms of the Ecosystem Ontology of Gignoux *et al.* (2011).

The purpose in using a mesh is twofold:

- i To provide precision in estimating errors due to time step and spatial resolution (Hypothesis (i)) in order to focus (to the maximum extent possible) on just those errors which can be considered operational rather than inherent (Chapter 2, Bian and Butler 1999); and
- ii To allow various configurations of the number of neighbours to a site (Hypothesis 2 i) and ways of arranging those sites in space (hypotheses (ii) and (iii)).

3.2 MODEL

FM, for the most part, uses the same elliptical fire spread model as FIRESCAPE. Differences in this respect are minor but detailed below. As noted, it uses McArthur's Mark V Forest Fire Danger Meter (FFDM) (McArthur, 1973) expressed as equations (Noble *et al.*, 1980) (see Appendix 1), but includes an important (but optional) modification to the rate of spread calculations informed by Project Vesta (Gould *et al.*, 2007; McCaw *et al.*, 2008), as noted below. It uses the same drought factor calculations as FIRESCAPE derived from the soil dryness index (SDI) of Mount (1972). This entails a modification to the drought factor equation of Noble *et al.* (1980) which, being based on the Keetch-Byram drought index (KBDI) (Keetch and Byram, 1968), requires refitting the SDI (Equation A.2). As already mentioned, the dynamics and parameterization of fuel accumulation and decay are those of FIRESCAPE based on the model of Olsen (1963) (Figure 2.4).

3.2.1 Model assumptions

FIRESCAPE has been described in Cary (1998), Cary and Banks (2000) and McCarthy *et al.* (2002). The model assumptions have been noted in these publications and are repeated here for convenience.

- i The vegetation model used in the experiments that follow assumes a uniform vegetation type (Eucalypt forests) (Cary and Banks, 2000). For example, vegetation will not transition from forest to shrub or grassland as a consequence of changed fire regimes and, in the absence of fire, once vegetation has reached its climax state, equivalent to reaching the equilibrium fuel load in this model, no further change occurs. Only fine forest litter fuels are considered when determining fire velocity and no model is proposed as to how fuel structures such as the fuel structure classes defined by Project Vesta (Gould *et al.*, 2007) or the Australian Fuel Classifications (Gould and Cruz, 2012), may change over time. Nevertheless, fuel dynamics are not uniform, but vary in their fuel accumulation and decay rates in five elevation classes (Table 2.1). If simulations are required to run over longer temporal extents than the available data, the data are simply recycled. Therefore, fire regimes produced by simulations of 1,000 years for example, are a measure of the quasi-equilibrium state of the system.
- ii FIRESCAPE has previously been used with both anthropogenic (Bradstock *et al.*, 2012) and natural sources of ignition (Cary, 1998; Cary and Banks, 2000; McCarthy *et al.*, 2002; Cary *et al.*, 2006, 2009; Keane *et al.*, 2013a). FM uses only ignitions from lightning strike as sources of ignition and their spatial and temporal variation is not a treatment in any experiments in this study. This is accords with the original version of FIRESCAPE (Cary, 1998). Lightning ignitions vary in time and space according to temperature and elevation residuals or anomalies. The temperature residual is the difference between daily maximum temperature and the monthly mean. The probability of lightning is based on three-hourly records of thunder activity at Canberra airport, categorized as probabilities for thunder on wet or dry days. The elevation residual is the difference in elevation at the micro-scale (20 m) and the macro-scale (3,700 m) resolutions in six elevation classes. The probability of lightning strike in these elevation classes is based on data from McRae (1992).
- iii Readings from a single weather station are used to drive the model and thus values for effects of elevation require extrapolation as discussed in Chapter 2. This might at first appear a contradiction to the observations in Chapter 1 about introducing

additional models between a grounding and an abstraction. As used here, the grounded abstraction is the extrapolated weather.

- iv The effect of topography on wind speed and direction is not addressed in this study. Software such as WindNinja (Forthofer and Butler, 2007) can determine wind fields given a base station and a digital elevation model (DEM). A method could be devised to develop lookup tables for classes of direction and speed for a given DEM, but the computational overhead would not allow simulations to be completed in the time available for this project. However, WindNinja does not include wind momentum in determining wind fields, and therefore cannot account for effects such as wind channelling and other discontinuous effects of wind in mountainous landscapes enumerated by Sharples (2009).
- v Effect of aspect, which may produce fire regimes that differ between wetter and drier aspects, is also not modelled. While aspect will change fuel moisture, it will also change vegetation and fuel accumulation rates (Geiger *et al.* 2009 in Sharples 2009). Therefore to include aspect, many concerns must be addressed simultaneously that may both increase fuel loads (more growth) and decrease fuel availability (high moisture content, increased decomposition rates).
- vi As noted above, FIRESCAPE models fire spread based upon empirically derived rates of spread under various conditions of weather, slope and the weight of fine forest litter fuels as embodied in the FFDM. In addition, FIREMESH has an optional modification to the rate of spread based on the findings of McCaw *et al.* (2008) (Section 3.2.9). Other processes, such as the effect of convection plumes (buoyancy) (Raupach, 1990) on the developing fire front, could be envisioned. However, this would confound these empirically derived measures of fire velocity and are therefore not included in the model formulation.
- vii Finally, spotting by lofted embers (the setting of fires downwind by firebrands) is a process that was not included in FIRESCAPE and is discussed more fully below.

3.2.2 Weather data

The weather data supplied to FIRESCAPE are essentially daily values of maximum and minimum temperature, vapour pressure, precipitation and wind (speed and direction). Wind, temperature and vapour pressure are interpolated to finer resolutions by a number of means described in Chapter 2. FM, on the other hand, reads a weather file

directly. Any methods required to down-scale from this data to finer resolutions are a separate concern and external to the model.

3.2.3 *Models of space*

The model of space implemented in FM is a mesh, that is, a spatially explicit graph comprising a set of vertices connected by directed edges rather than a raster grid as used in all previous versions of FIRESCAPE (Figure A.1). Fire propagates along edges between vertices and the position of the fire front along the edge is recorded as a continuous variable. Thus the extent of the fire perimeter is recorded precisely at any one moment in time. The mesh is a directed graph allowing edges to burn from both ends. Each vertex in the mesh represents a point in three dimensions and is always in one of three states: *unburnt*, *burning* or *burnt* (Figure A.5). The time of the last fire is also recorded by a vertex and from this and its elevation, the current weight of fine surface litter can be determined. Rate-of-spread calculations use the spatial data (elevation and fuel) of the nearest vertex.

The graph construct allows both regular vertex positions and neighbour relations such as the eight-neighbourhood mesh implicit in the raster grid used by FIRESCAPE, as well as irregular ones such as a Triangular Irregular Network (TIN) (Figure 3.1). FM, unlike FIRESCAPE, measures distance between vertices to accommodate the difference that arises from projecting the mesh onto a DEM. This affects only the calculations of the position of the fire front along edges, that is, the progress of the simulated fire. Area burnt outputs from the model are re-projected onto a flat plane as it is assumed that while field work that has led to estimates of the rate of spread on a slope do so relative to the distance travelled parallel to the slope, area burnt is estimated from maps, un-projected with regard to elevations. The area difference for the Brindabella DEM is 1.97%. Tests with FM show a difference in area burnt estimates of 8% with and without considerations of projection.

As the position of the fire front along an edge is a continuous variable, its position is more independent of resolution than if burnt vertices were simply counted. This makes it possible to perform experiments with spatial resolution as a treatment while minimizing the confounding effect resolution may have on the measurement of area burnt. That is, following Bian and Butler (1999), this is an attempt to isolate *inherent* data errors from *operational* errors of the model.

3.2.4 *Models of time*

The model of time is an event-driven one as once FM is initialized, no other calculations are required at regular intervals other than events

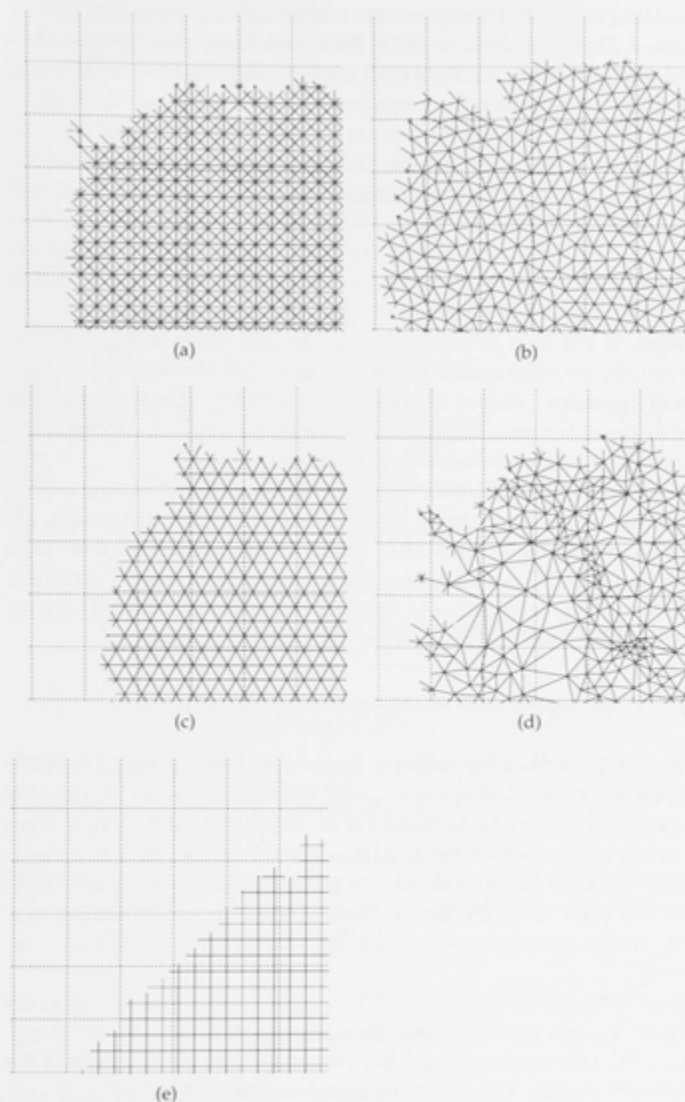


Figure 3.1: A simulated fire burning on five different mesh configurations in otherwise identical conditions

The five mesh configurations used in this study are (a) regular eight neighbour (c) regular six neighbour and (e) regular four neighbour meshes. Mesh (b) is a Triangular Irregular Network (TIN) with evenly distributed (Poisson-Disk) vertices having six neighbours on average. The angle of the edges have a uniform random distribution with respect to the coordinate system (after Johnston *et al.* 2008). Mesh (d) is also a TIN but with an uneven distribution of vertices. The purpose in having an uneven distribution of vertices is to concentrate vertices in regions where rates of change in fire behaviour may be greatest.

indicating when the fireline reaches a new vertex or a weather data is updated. Daily soil dryness index (SDI) and drought factor are calculated as the weather data are read during initialization and an array of values is maintained for a number of elevation classes depending on the elevation range of the terrain (20, 100 meter elevation classes).

FM is implemented within the 3Worlds simulator. The architecture of 3Worlds accords with the conceptual model of ecosystem described in Gignoux *et al.* (2011). At the time of writing, it has not been documented elsewhere. The design and implementation of event-driven time models has been added to the simulator by the author of this study (figures A.2, A.3). After an ignition, fire propagates from one location to the next by contagion events and from one moment to the next by weather update events (Figure A.4). This provides a consistent approach between different spatial and temporal resolutions. The distance between vertices in the mesh can vary as can the time between weather update events (Figure 3.2).

FM, as with FIRESCAPE, need only process those locations (vertices) that are in the burning state. When all vertices extinguish, all revert to the unburnt state after details of the fire are logged. This includes the time, area burnt and fireline intensity at which each location was burnt. Approaches to manipulating time and space to create variable time steps and meshes are discussed in Chapter 4.

3.2.5 Projecting one-dimensional fire models to two dimensions

Fire models such as McArthur's Forest Fire Danger Meter (FFMD) (McArthur, 1973), Rothermel's model (Rothermel, 1972), the model proposed by Project Vesta (Gould *et al.*, 2007) and many others (Pastor *et al.*, 2003), predict the head fire rate of spread (R_h) as a function of weather, fuel and slope at a particular place and moment in time. They are one-dimensional models. In order to predict the rate of spread in directions other than R_h , additional information is required.

If a model can be devised to define a fire shape or template in relation to a point on the fireline, then together with R_h , all else being equal, the rate of spread in other directions can be determined by geometric means. Assuming constant conditions, level ground and no wind, a deterministic model of fire spread will necessarily predict equal rates in all directions thus forming a circle. R_h increases with wind speed, elongating the shape along the axis parallel to the wind direction (Rothermel, 1972). Assuming the same conditions but with a constant wind speed and direction, a deterministic model will produce a shape symmetrical about this long axis.

Fire shapes are often assumed to be ellipses (Van Wagner, 1969). Researchers have suggested other shapes including ovoids (Peet, 1967), double ellipses (Albini and Forest, 1976) and rectangles (Green *et al.*,

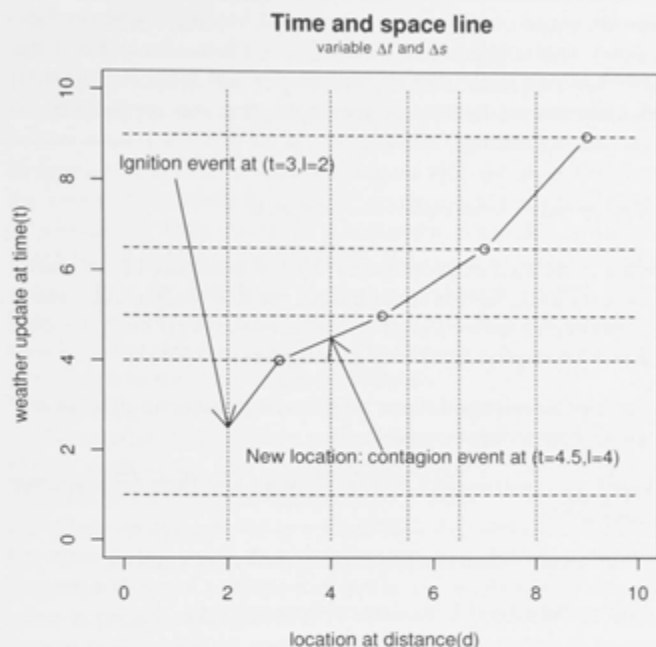


Figure 3.2: Time-space diagram (borrowed from a train timetable schematic) showing irregular time steps and irregular distances (in one dimension) between vertices

The solid line is the position of some point on the fire front moving through these two dimensions. Time steps are marked by horizontal dotted lines. Locations for new spatial data are marked by vertical dotted lines. In this example, ignition takes place at location $l=2$ at time $t=1$. For each time that the fire front crosses a horizontal line, the weather data is updated (a weather update event). For each occasion that the updated fire front reaches a new location, a contagion event occurs to ignite that location. In this manner the fire front's position is recorded in time and space as continuous variables but weather and spatial data is discrete if irregular.

1983a). However, Alexander (1985) considers that though fires may depart from an elliptical shape during the acceleration phase, over time they will attain a shape more closely approximating an ellipse. Apart from the acceleration phase, departures from a regular ellipse may also arise because of fuel distributions (Green, 1983b) and variance in wind direction (Alexander, 1985). Variance in wind direction has been shown to be inversely proportional to wind speed (in Alexander 1985). This suggests that as wind speed increases and fuel distributions become more uniform, fire shapes will more closely align with the elliptical model. However, complicating this approach is the phenomenon of spotting.

3.2.6 *Fire spread by lofted embers and firebrands*

If spotting is defined as propagation by the transport of embers or firebrands, it can be seen as an additional mode of propagation along with radiation and convection determining overall R_h (Koo *et al.*, 2010). Factors that affect propagation by spotting are as follows:

- i Fireline intensity and flame height which increases updraft and allows fires to ignite aerial fuels;
- ii Fuel types such as bark and small twigs and their aerodynamic qualities;
- iii Wind speed to provide forward movement of embers;
- iv Atmospheric conditions that enhance updraft;
- v Ember size;
- vi Fuel (type and moisture content) that determines whether or not incendiaries will ignite surrounding fuel before they themselves extinguish.

These factors can be classified as '*generation, transport, and ignition of fuel at the landing position*' (Koo *et al.*, 2010). A fireline may be thought of probabilistically whereby its location is at the mean of some distribution (A. M. Gill, pers. Comm., 2012). The distribution is the probability that a point at a distance from the mean is currently burning. Therefore, in principle, spotting may span many spatial scales from small sparks to large embers igniting fires many kilometres ahead of the fire but typically classified as simply short or long distance spotting (Gill, 2008). Propagation by spotting is faster than by radiation or convection above some threshold of distance and intensity. The overall velocity of the fire (after coalescing) is the R_h for the main fireline plus the rate of spread of the spot fire. At some scales, wind being drawn towards the main fire will draw spot fires back towards it so it is not necessarily the head rate of the spot fire that is subsumed

in the main fire head rate. Some degree of spotting is inevitably subsumed in empirical measurements of R_h and length-to-breadth ratio (L:B) of the fire footprint. In Project Vesta (Gould *et al.*, 2007), R_h is measured by recording the arrival time of the fire front at markers (fishing line or tags) placed at right angles to the expected direction of spread. If spot fires appear ahead of the main fire front and trigger these markers the recording is deleted from measurements. The probabilistic view of fire front location discussed above, implies that identifying spotting as an independent process depends on the scale of observation. Where is the precise location of the fire front, and at what spatial resolution are spotting events observed? If only the time of ignition, the time of extinguishment and the final fire footprint are known, then while R_h and L:B can be measured, the contribution of spotting to these measures is unknown. Some degree of spotting could be inferred from any barriers the fire may have crossed by reconstructing the fire (Cruz *et al.*, 2012). However, given the coarse level of detail available to researchers developing L:B functions, it is assumed that spotting is included in these empirical equations with due regard to the domain of observations.

If spotting is modelled explicitly in a simulation then, depending on observational scale, other assumptions in the model may be invalidated, such as R_h and L:B. In this study, it is assumed spotting is included in the functions controlling fire growth and shape. Whether to include spotting or not in a simulation experiment will depend on the aims of the study. Investigating the consequences of landscape fragmentation and perhaps fuel treatment, for example, may require some approach that allows fires to jump fuel breaks. Because it is known that the FFDM underestimates R_h for conditions beyond the domain used to develop it, a spotting routine could be added that may account for this underestimation if there is literature available to justify such a model for Australian conditions and it is tractable for fire regime generation. A review of the literature by Koo *et al.* (2010) indicates that while sufficient work has been done to propose a model of ember transport (for example Albin *et al.* 2012), there is insufficient empirical data on ember generation and ignition by firebrands (which can include effects of ember density and feedback from the main convection column) to produce a full model. Another approach taken to modify R_h following Project Vesta is discussed below in Section 3.2.9.

3.2.7 Ellipse properties

Van Wagner (1969) identifies four regions of an ellipse: head, back and two flanks (Figure 3.3). The rate of spread (R) and fireline intensity are highest in the head region (R_h), assumed to be lowest in the back region (R_b) and intermediate in the flanking regions (R_f). An ellipse may be defined as the locus of points whose total distance

from two fixed points (f_1, f_2) is a constant, the two fixed points being the focuses of the ellipse (Figure 3.4). A circle is a special case of an ellipse where the two focuses coincide.

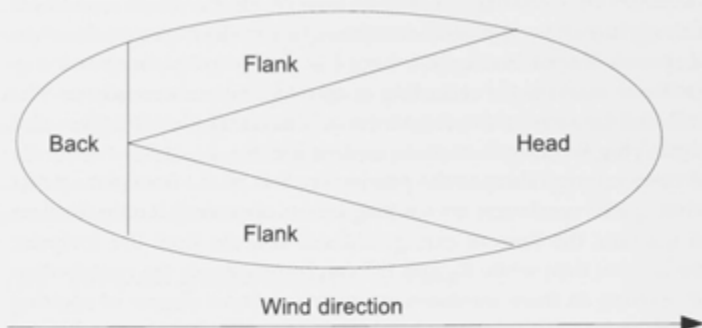


Figure 3.3: Diagram of a simple elliptical fire growth model adapted after Van Wagner (1969)

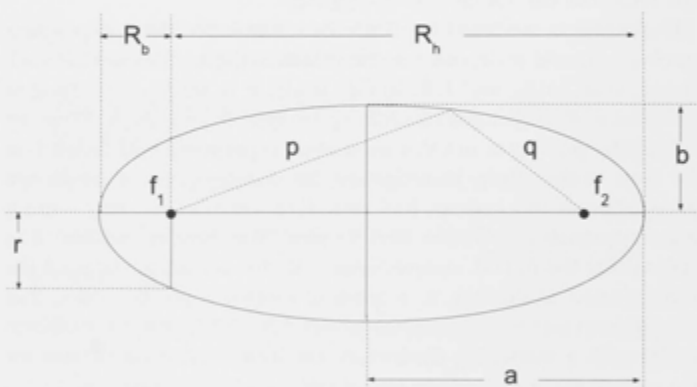


Figure 3.4: Key measures of an ellipse discussed in the text

The length-to-breadth ratio (L:B) is the semi-major axis a , divided by the semi-minor axis b . The head-fire to back-fire ratio (H:B) is the rate of spread of the head-fire (R_h) over the rate of spread of the back-fire (R_b). Note, $R_b + R_h = 2a = p + q$. The measure of ellipse eccentricity (e) is f/a . Distance r is the semi-latus rectum: $r = a(1 - e^2)$.

Two parameters are sufficient to define an ellipse: the lengths of the semi-major and semi-minor axes (a and b in Figure 3.4), alternatively, the longest and shortest distance from one focus to the ellipse perimeter (R_b and R_h in Figure 3.4). Alexander (1985) defines L:B of an ellipse as a/b . H : B is R_h/R_b . The magnitude of the vector p from f_1 to the ellipse perimeter is the rate of spread in that direction. Differences in the ratio of R_h to R_b and the rate of spread of flanking fires

may arise through fuel discontinuity (Green, 1983b). Therefore it can be expected that the relationship between wind speed and L:B will vary with fuel structure requiring different functions for grass (McArthur, 1966), forests and perhaps forests with logging slash (Alexander, 1985; Hirsch, 1996) along with other fuel types such as tussock grass (King *et al.*, 2008b). The geometry of the fuel array will increase L:B in the case where the intensity of R_h is sufficient for the head fire to propagate but insufficient for the flanks and back fire to do likewise.

Alexander (1985) examined 19 north American fires in standing timber to develop an L:B function in terms of wind speed (Figure 3.5):

$$L : B = 1 + 0.0012 \cdot U_{10} \cdot 2.154 \quad \{U_{10} \leq 50 \text{ km.h}^{-1}\} \quad (3.1)$$

where U_{10} = wind speed (km.h^{-1}) in the open at 10 meters above ground level.

Finney (2004) employs a similar exponential function but limits L:B to 8. The Canadian Forest Fire Predication System (CFFPS) (Hirsch, 1996) produced an L:B function based on 35 fires in standing timber forests with and without logging slash:

$$L : B = 1 + 8.729(1 - e^{(-0.03U_{10})^{2.155}}) \quad \{U_{10} \geq 1\} \quad (3.2)$$

Note that in Alexander's study, L:B was found to be higher for forests with logging slash than those without slash at equivalent wind speeds. Equation 3.2, on the other hand, is a fit to fire observations with both fuel types combined.

If the fire is assumed to propagate from the rear focus of an ellipse, then R_h is the magnitude of the longest vector between the focus to the ellipse perimeter and R_b is the shortest. It follows that R_b is inversely proportional to L:B (the ellipse eccentricity) and the relation of L:B to H:B is non-linear (Alexander, 1985). However, Alexander asserts that there is overwhelming evidence to indicate that R_b remains approximately constant and may even increase as wind speed changes (Figure 3.6).

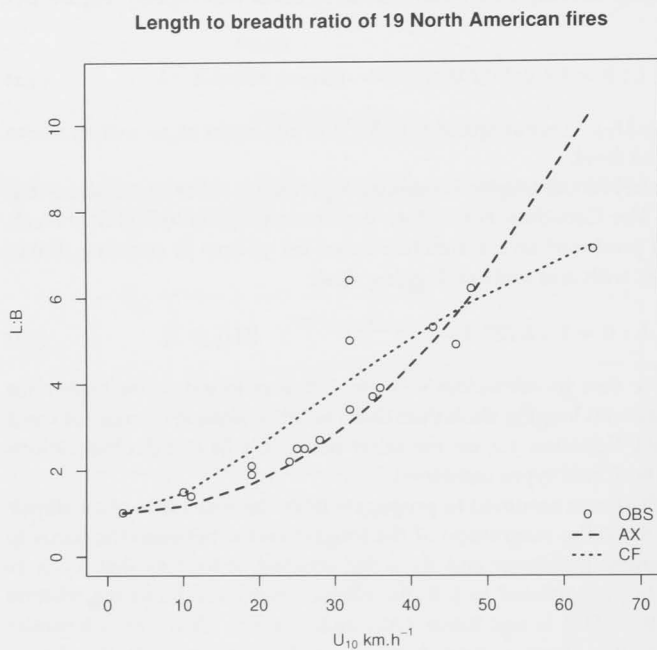


Figure 3.5: Length-to-breadth ratio observations of 19 North American fires in standing timber

AX is the model fitted by Alexander (1985) (Equation 3.1) and CF is the relevant Canadian Forest Fire Predictions System (Hirsch, 1996) (Equation 3.2).

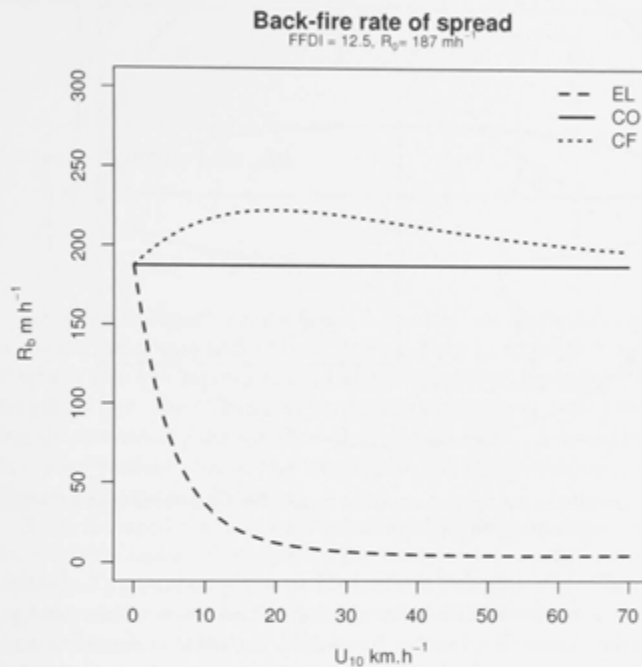


Figure 3.6: Three methods of determining the back-fire rate of spread (R_b)

CO: assumes wind speed is zero for R_b

EL: fire propagates backwards from the ellipse focus. In this case R_b is close to zero at high wind speed.

CF: assumes fire propagates backwards from a point forward of the ellipse using equations from the Canadian Forest Fire Prediction System (Hirsch, 1996)

The Forest Fire Danger Index (FFDI) (McArthur, 1973) is 12.5 producing a rate of spread under no-wind conditions of 187 m h^{-1} .

3.2.8 Implementation in FIRESCAPE

The only way to describe an ellipse, if L:B, R_h and R_b are given, is to assume the point from which the fire propagates to be forward (downwind) of the ellipse focus (Figure 3.7). FIRESCAPE does this

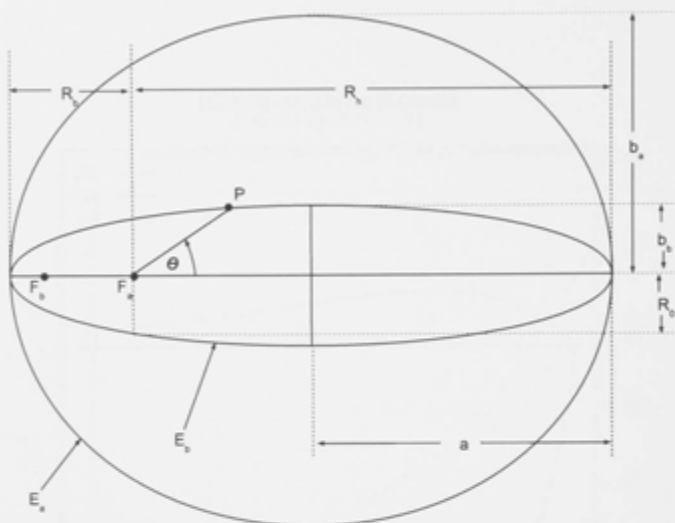


Figure 3.7: Ellipse parameters required to shift the point from which the fire is assumed to propagate

in the following way. L:B is obtained from Equation 3.2. R_b is also obtained from the CFFPS by modifying the effective wind speed to adjust the Forest Fire Danger Index (FFDI) (Noble *et al.*, 1980) and thus the rate of spread (equations 3.3 and 3.4).

$$\text{FFDI}_{\text{BF}} = 1.25.D.e^{((T-H)/30 + 0.0234.U_{10}^{-0.05039.U_{10}})} \quad (3.3)$$

where:

D = drought factor (Cary, 1998);

T = temperature ($^{\circ}\text{C}$);

H = relative humidity; and

U_{10} = wind speed at 10 m above ground level (m.h^{-1})

$$R_b = 0.0012.\text{FFDI}_{\text{BF}}.W \quad (3.4)$$

where:

W = fuel weight (g.m^{-2})

R_b = the rate of spread of the backfire (m.h^{-1})

This is very close to the rate of spread at zero wind speed (Figure 3.6).

R_h is derived from McArthur (Noble *et al.*, 1980). Two ellipses, E_a and E_b , are defined (Figure 3.7). E_a has focus F_a derived from R_h and R_b (Equation 3.5).

$$F_a = (R_h + R_b)/2 - R_b \quad (3.5)$$

E_b has L:B given by Equation 3.2. Both ellipses have the same semi-major axes but differ in the magnitude of their semi-minor axes and thus their focuses.

$$H : B = (L : B + \sqrt{[L : B]^2 - 1}) / (L : B - \sqrt{[L : B]^2 - 1}) \quad (3.6)$$

$$a = R_h/2(1 + 1/[H : B]) \quad (3.7)$$

$$F_b = R_h/2(1 - 1/[H : B]) \quad (3.8)$$

Referring to Figure 3.7, if ellipses E_a and E_b are aligned along their common major axis and a line is defined from F_a at angle θ , to point P where this line intersects E_b , the fire velocity in direction θ is the length of F_aP . The Cartesian coordinates of P may be found by solving simultaneously the equation of the tangent to E_b at P and the line F_aP after Wallace (1993). The length of F_aP is then found by application of Pythagoras's theorem.

If it is assumed that fire propagates from the ellipse focus using L:B from CFFPS and R_h derived from the FFDM, the projected area burnt declines by 50% at 5 km.h⁻¹ (Figure 3.8). There is no evidence to support such a rapid decline in area at low wind speeds. Depending on the frequency of wind speeds > 0 and < 10 km.h⁻¹ during the fire season (30% for the data in this study), for a fire regime model this may produce incorrect fire size distributions. Neither Equation 3.1 nor 3.2 were fitted to fire shapes for wind speeds > 0 and < 10 km.h⁻¹. Therefore the interpolation by the functions in this region of the domain may be an artefact of the fitting. This appears to be the case, particularly for Equation 3.2 (CF in Figure 3.8).

The under-estimation of area burnt at low wind speeds can be ameliorated somewhat by relaxing the assumption that the fire propagates from the ellipse focus and also replacing Equation 3.2 with Equation 3.1. Nevertheless, when we compare the shapes in (Figure 3.9) with those found in the FARSITE manual (Finney, 2004, p 39, plate 2), it is apparent there is a mismatch between R_h and L:B. In short, it would appear that either the FFDM grossly under-estimates R_h as a function of wind speed (McCaw *et al.*, 2008) or the widely used L:B ratios are incorrect.

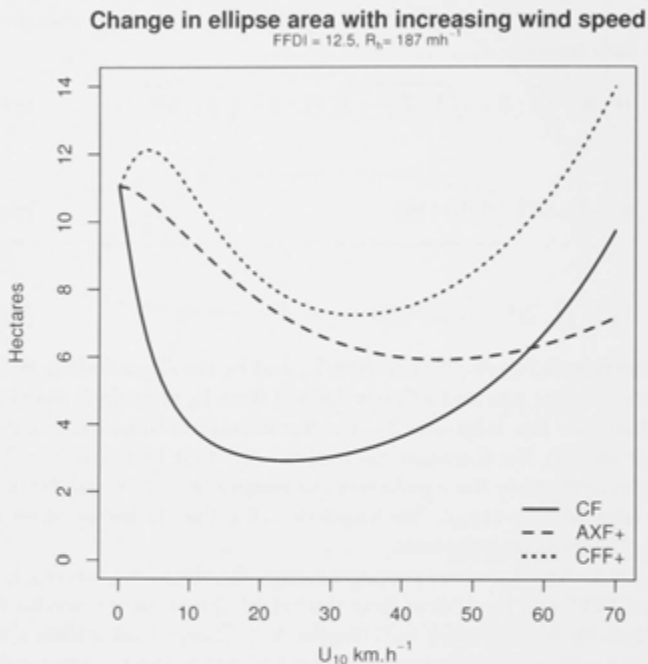


Figure 3.8: Ellipse areas that arise from three different methods of calculating the back-fire rate of spread

CF assumes fire propagates backwards from the ellipse focus and uses a length-to-breadth ratio from the Canadian Forest Fire Prediction System (CFFPS) (Hirsch, 1996) (Equation 3.2).

AXF+ assumes the fire propagates backwards from a point forward of the ellipse focus using a length-to-breadth ratio from Alexander (1985).

CFF+ again assuming fire propagates backward from a point forward of the ellipse focus but using a back-fire rate of spread from the CFFPS (equations 3.3 and 3.4).

The Forest Fire Danger Index (McArthur, 1973) is 12.5 and wind speeds are from 0 to 70 km.h^{-1}

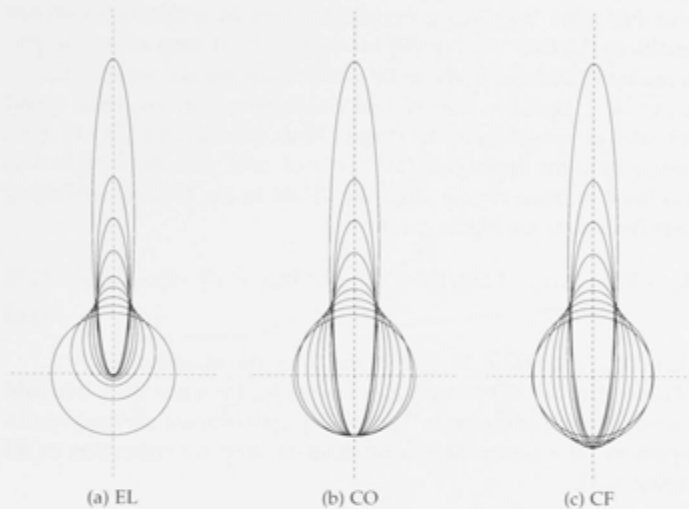


Figure 3.9: Three examples of fire shapes for 9 wind speeds using the FFDM

Wind speeds are 0, 5, 10, 15, 20, 30, 40, 50 and 70 km.h^{-1} using equilibrium rate of spread of the head fire (R_h) from Noble *et al.* (1980) based on the McArthur Forest Fire Danger Meter Mk5 (FFDM) (McArthur, 1973). R_h at zero wind speed is 187 m.h^{-1} . Length-to-breadth ratio (L:B) is from the Canadian Forest Fire Prediction System (Hirsch, 1996) (Equation 3.2).

EL assumes the point of propagation to be the focus of the ellipse with back-fire spread rate (R_b) inversely proportional to wind speed (EL in Figure 3.6).

CO uses a constant (zero wind) R_b and assumes the back-fire propagates from a point forward of the ellipse focus (CO in Figure 3.6).

CF is similar to CO but calculates R_b from the Hirsch (1996) CFFPS adapted for the FFDM using equations 3.3 and 3.4.

The Point of propagation is at the intersection of the dotted lines in each case

3.2.9 Project Vesta

The FFDM is based on observations of 800 prescribed fires under relatively mild conditions and a few observations of unplanned fires under more extreme conditions (McCaw *et al.*, 2008). In contrast, Project Vesta (Gould *et al.*, 2007; Cheney *et al.*, 2012) is a recent fire behaviour experiment conducted in dry eucalypt forests of Western Australia involving more than 100 experimental fires lit under dry summer conditions. McCaw *et al.* (2008) have shown that rates of spread predicted by FFDM are likely to be underestimates for wind speeds $> 12.5 \text{ km.h}^{-1}$. Based on this, and the relationship between wind speed and rates of spread from the Project Vesta nomograms (Gould *et al.*, 2007), a fit to the findings of (McCaw *et al.* 2008 p 21, Figure 1.b) was calculated to more closely align the FFDM to the findings of Project Vesta (Equation 3.9, Figure 3.10).

$$R_V = R_M + (U_{10} - 12.5)/(50 - 12.5)(5.45R_M - 109 - R_M)[U_{10} > 12.5] \quad (3.9)$$

where: R_M is R_h from the FFDM and R_V is the modified R_h .

Given that the FFDM under-estimates R_h by more than two-fold at a wind speed of 50 km.h^{-1} , this very approximate method would appear to be a better alternative than making no correction at all (Figure 3.11).

3.2.10 Implementation in FIREMESH

Ideally, implementing the Vesta equations for R_h (Cheney *et al.*, 2012) would be the preferred alternative to modifying the FFDM with Equation 3.9. However, no method is provided in these equations as how to account for the effect of precipitation on soil moisture and thus the amount of fuel available for combustion as a function of preceding rain events, nor is there a model of fuel development available for the Brindabella Ranges. Therefore, FIREMESH uses the FFDM as used by FIRESCAPE, but with an option to modify R_h by Equation 3.9. This is similar, in principle, to the modification to the rate of spread used by Bradstock *et al.* (2012). The consequences of this are examined in the chapter on validation (Section 5.6).

The FIRESCAPE approach to moving the point of propagation forward of the ellipse focus has been maintained in FIREMESH because it more closely follows research findings (Alexander, 1985; Hirsch, 1996). Of less significance is the choice between equations 3.1 and 3.2 for calculating the length-to-breadth ratio of a fire as a function of wind speed. Equation 3.1 has domain $U_{10} < 50 \text{ km.h}^{-1}$. Equation 3.2 approaches approximately 9.2 at the limit but has a tendency to produce fires that seem intuitively narrow at low wind speeds (Figure 3.8). While wind speeds $> 47 \text{ km.h}^{-1}$ during the fire season for

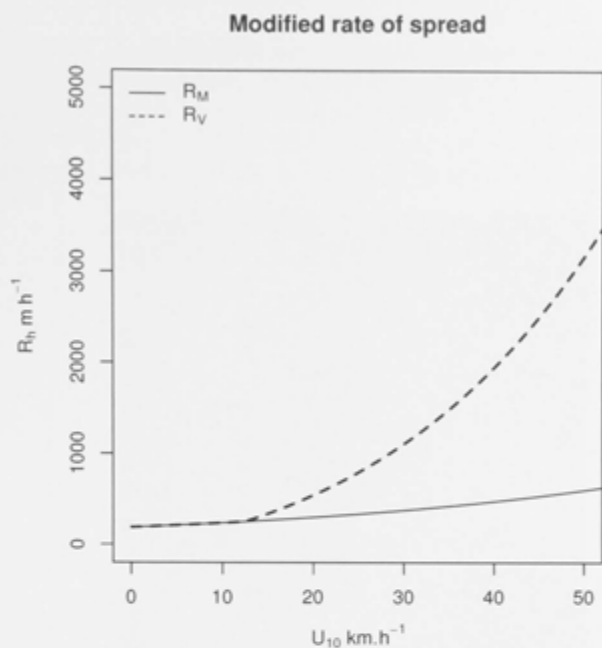


Figure 3.10: Forward rate of spread of the head fire relative to wind speed and its modification after McCaw et al. (2008)

R_M is from the Mark V Forest Fire Danger Meter (FFDM) (McArthur, 1973). R_V is R_M modified using a fit in Equation 3.9.

Canberra (1986-2011) are infrequent, (0.1%), to prevent large if rare errors, FIREMESH uses Equation 3.1 for $U_{10} < 47$ 10 km.h^{-1} (the point of intersection) and Equation 3.2 otherwise.

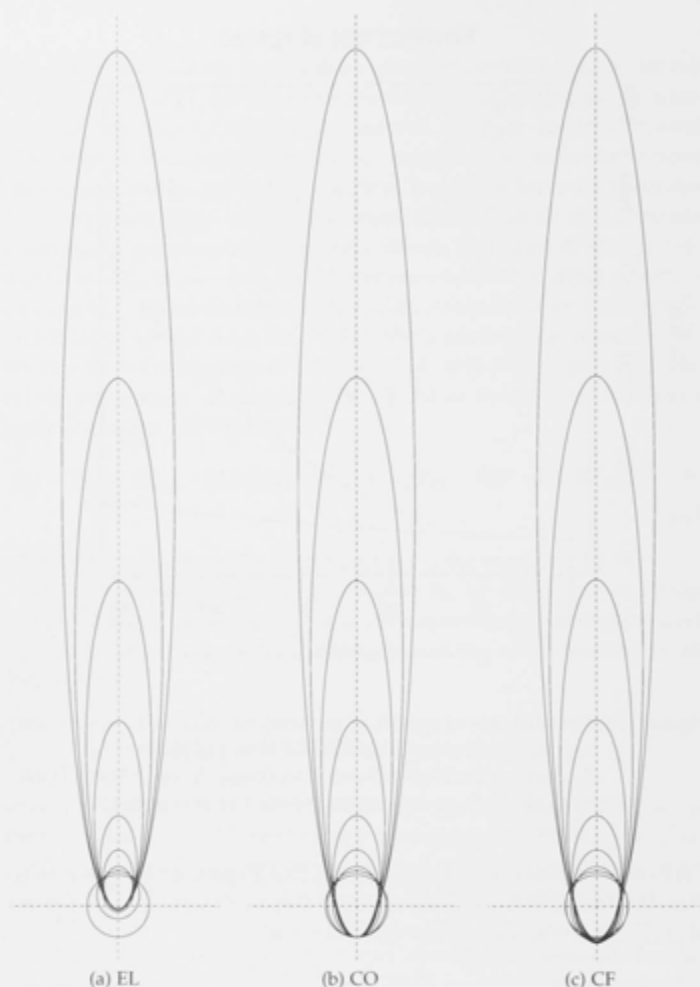


Figure 3.11: Three examples of fire shapes for 9 wind speeds using the modified FFDM

Wind speeds are 0, 5, 10, 15, 20, 30, 40, 50 and 70 km.h^{-1} using equilibrium rate of spread of the head fire (R_h) from Noble *et al.* (1980) based on the McArthur Forest Fire Danger Meter Mk5 (FFDM) (McArthur, 1973). R_h at zero wind speed is 187 m.h^{-1} . Length-to-breadth ratio (L:B) is from the Canadian Forest Fire Prediction System (Hirsch, 1996) (Equation 3.2).

EL assumes the point of propagation to be the focus of the ellipse with back-fire spread rate (R_b) inversely proportional to wind speed (EL in Figure 3.6).

CO uses a constant (zero wind) R_b and assumes the back-fire propagates from a point forward of the ellipse focus (CO in Figure 3.6).

CF is similar to CO but calculates R_b from the Hirsch (1996) CFFPS adapted for the FFDM using equations 3.3 and 3.4.

The Point of propagation is at the intersection of the dotted lines in each case

3.3 CONCLUDING REMARKS

As noted, in FIREMESH, the simulated fire front propagates along edges between vertices and the position of the fire front along these edges is recorded as a continuous variable. Thus the extent of the fire perimeter is recorded precisely at any one moment in time (Figure 3.12). Edges can burn from both ends and therefore fire shapes

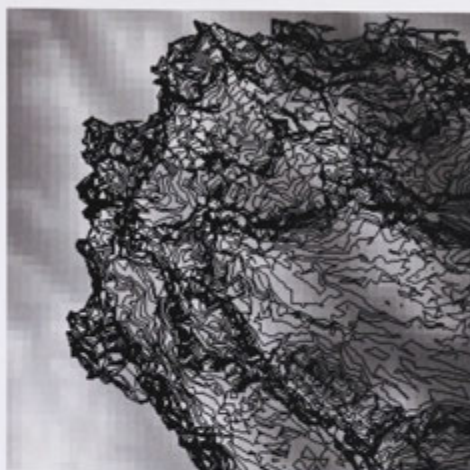


Figure 3.12: Isochrones (lines connecting points on the fireline at equal times) showing the updated position of the fire front at half-hourly intervals

The pattern of densely and sparsely arranged isochrones shows the waxing and waning of fire conditions over the diurnal cycle.

can emerge that leave unburnt islands within main fire perimeter (Figure 3.13). This approach gives the maximum accuracy in fire shapes that is possible within the constraints of discrete geometries. Methods for calculating the area of the final fire footprint are discussed in the next chapter. Fire heterogeneity is quantified as the variability in fireline intensities as discussed in Section 2.5 (Figure 3.14). The rate at which weather data is read (time step) can be any resolution, limited only by the resolution of the input data unless interpolation is used (Figure 3.15).

The resolution at which weather data is read can vary during a simulation. Space can be made discrete with any arrangement of vertices and edges (Figure 3.1, Figure 3.14).



Figure 3.13: Polygons outlining burnt areas, including unburnt islands left behind after the passage of the fire front

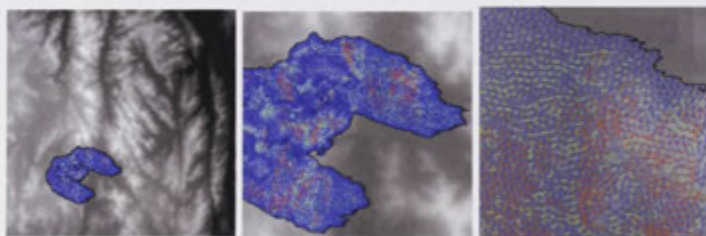


Figure 3.14: Three magnifications of the same simulated fire showing the heterogeneity of conditions over the course of the fire. Colours are indicative of fireline intensity (dark blue: 100 kW.m^{-1} , red: $5,000 \text{ kW.m}^{-1}$). The width of the image on the left is 50 km. The magnification of the right-hand image is sufficient to resolve the one hectare resolution mesh on which the fire is spreading. This mesh is a Delaunay triangulation of a Poisson-Disk distribution of vertices.

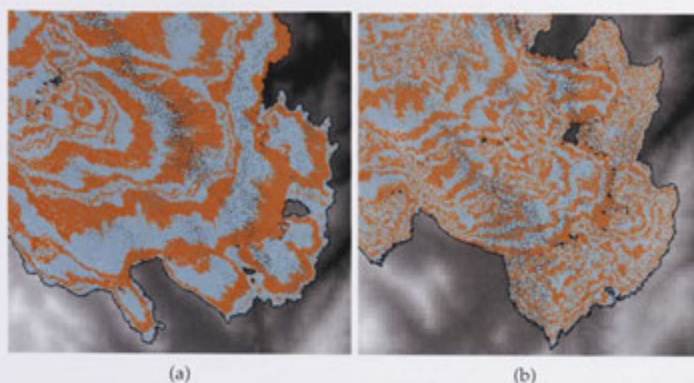


Figure 3.15: Simulated fires burning at two different time steps

The two time steps are (a) one hour and (b) three hours. Alternating colours mark time steps.

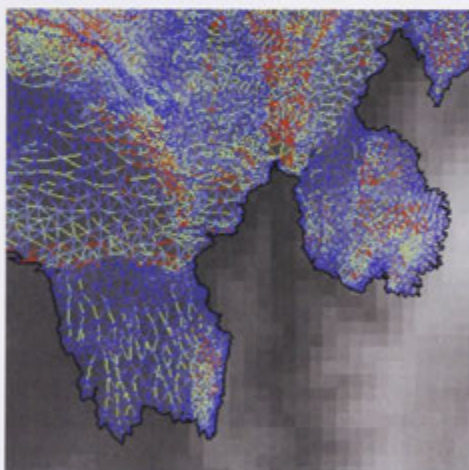


Figure 3.16: A simulated fire spreading over a Delaunay mesh triangulation with an irregular displacement of vertices

The vertices are concentrated around regions where rates of change in the slope of the underlying digital elevation model (DEM) is greatest. The DEM (grey) above is for display purposes only and has a resolution of nine hectares. The DEM that determines the elevation of each vertex is a much finer and has a resolution of 0.04 hectares.

EXAMINING THE OPTIMAL USE OF TEMPORAL AND SPATIAL DATA

4.1 TEMPORAL AND SPATIAL RESOLUTION

Models routinely require parameter recalibration when changing scales or changing some other aspect of the model formulation, to refit the model to observations. If the value of parameters so calibrated are outside plausible limits (those observed in the field if they are real-world parameters) then confidence in the model is reduced. Depending on the model outputs being assessed, it is also quite possible that no parameter presents itself as a candidate for calibration. For example, if changing spatial or temporal resolution were to change mean inter-fire intervals, this could be accounted for by changing ignition rates if that change was still within the bounds of uncertainty for this parameter. However, changing ignition rates will not necessarily modify fire size distributions and the patterns of fire regimes that emerge.

While integrating over time and space with a simulator using regular time steps (Δt) and spatial grain (Δs) may be convenient, the data itself is rarely regular. If Δt and Δs were to vary locally to match the rate of change in the data (as interpreted by the model's equations), then coarser average resolutions would be possible without recalibration. The benefit of this is to reduce the burden of computation rather than to alleviate the need for detailed input data, as the process itself would necessarily be based on the detailed data. In short, as the term is used here, optimization is simply attempting to reduce data redundancy, an abstraction operation of domain reduction on the grounded abstraction of the original data (Zucker, 2003). This is analogous to procedures in numerical integration, where step sizes become smaller as the rate of change in the function increases.

For temporal data, optimization can mean for example: given 26 years of half-hour weather data, how many of those almost 500,000 readings are effectively redundant from the point of view of the model's accuracy? The same question applies to spatial data: how many of the 1 million 1/4 hectare locations in a 2,500 km² extent are likewise redundant? Ideally, the model (using the idea of control theory) would adjust its spatio-temporal resolution on-the-fly to suit changing circumstances (e.g. Hu and Ntaimo, 2006; Anderson *et al.*, 2005). As FM simulates any number of fires simultaneously, it is difficult to see how spatio-temporal resolution could change in a manner to suit all points on the fire perimeters at one time, with their

unique conditions, while at the same time showing improvements in efficiency over simply running at the finest resolution. In this study, the computational burden of temporal resolution can be assumed to be minimal compared with spatial resolution. This is because as Δs increases, the number of points on a fire perimeter increases to the square of resolution. For Δt , on the other hand, the rate of reading weather data is simply linear with temporal resolution. In Big-O notation (Black, 2007), execution time is $O(n)$ with Δt but $O(n^2)$ with Δs . Therefore, reducing redundancy in spatial data offers greater benefit than does reducing redundancy in temporal data.

However, input data can rarely be categorized as solely dependent on just space or time. In reality temperature, humidity, wind, rainfall, soil dryness and fuel vary over both time and space. In FIREMESH, only wind is entirely dependent on time (if not in reality) and slope depends on location and the effect of slope depends on the direction of fire spread.

The objective of the current study is to understand if and how much nuisance parameters, of which spatial and temporal resolution are just two, may affect the estimation of the components of fire regimes by simulation, an area which has not been well studied (Chapter 1). The remainder of this chapter discusses these two aspects of resolution to more closely examine their implications for fire simulation. In addition, opportunities to optimize the use of temporal and spatial data are examined in Section 4.2, with the principle aim of exploring a method to optimize the placement of vertices over complex terrain data (Hypothesis (iii)).

4.1.1 *Temporal resolution*

If the rate of spread of the head fire (R_h) is plotted against time, the area under the curve can be interpreted as the distance an imaginary continuously burning fire would travel in a straight line during a period of observation assuming no slope, a constant fuel load and no change in wind direction (Figure 4.1). In principle, the magnitude of error between a discrete function such as this and a continuous one depends not only on Δt but also the shape of the curve (concave curves produce a greater error than the convex). However, at least in the case of observed weather data, it is unclear if these errors would cancel with increasing Δt given the complex shape of the curve of changes in rate of spread. The difference between the daily fire run length (as calculated by the equations used in FIREMESH) between a 0.5 and 3 hour time step is about 7%, as measured for two days, one in summer and the other in winter (Figure 4.1). The summer day is one where very significant areas were burnt in the Canberra region in January 2003.

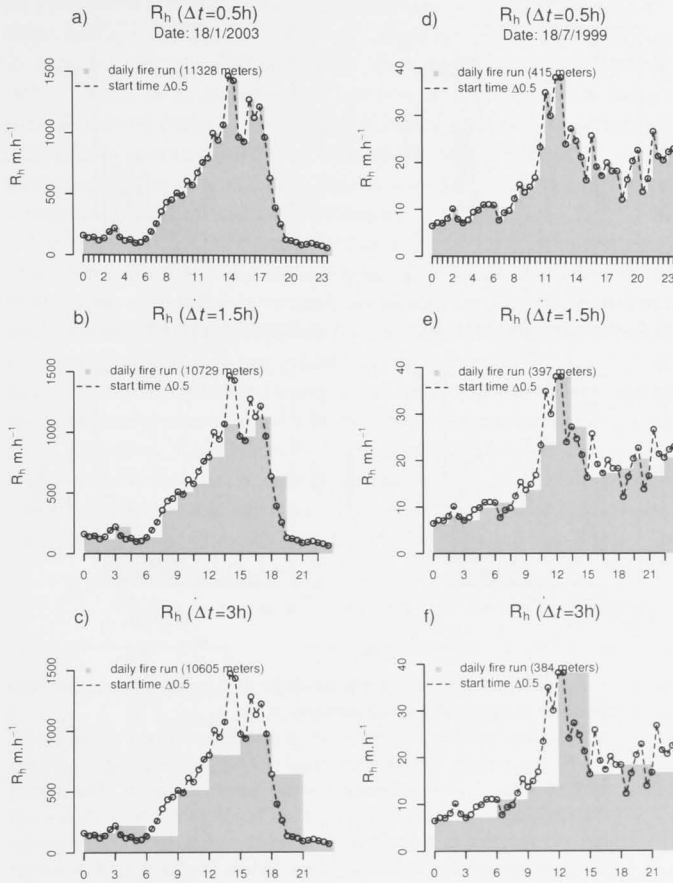


Figure 4.1: Changes in R_h at three different time steps on two days of contrasting fire danger

Half-hourly weather was recorded at Canberra Airport (Chapter 2). R_h is produced by the equations used in FIREMESH, using a fuel load of 12.5 t.ha⁻¹. R_h at 0.5 h time step (dotted line) is superimposed on each chart for easy comparison with coarser resolutions. The legend in each chart shows the distance travelled by fire in a 24-hour period at each resolution (sum of the grey areas).

If the same analysis is performed using accumulated area burnt (Figure 2), the error corrects as FFDI is over or under estimated (Fig-

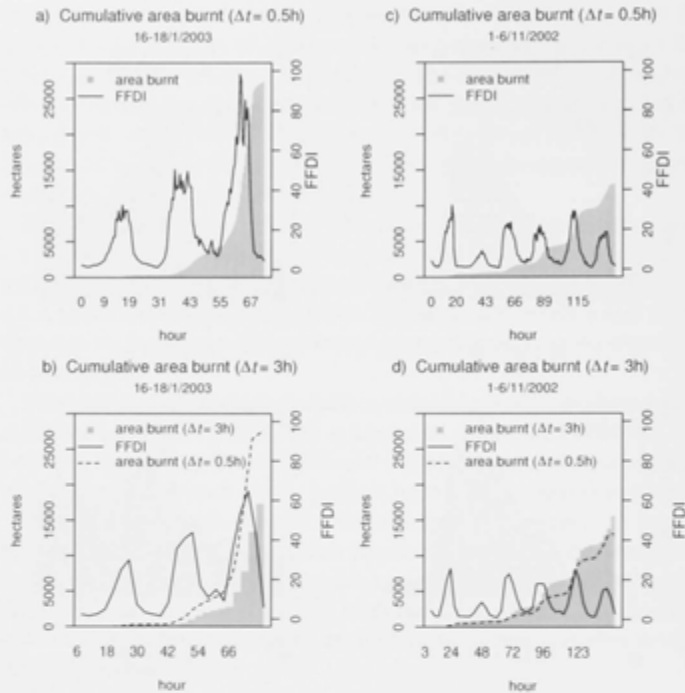


Figure 4.2: Cumulative area burnt for time steps of 0.5 and 3 hours for two periods of contrasting fire danger

Half-hourly weather was recorded at Canberra Airport (Chapter 2). R_h is produced by the equations used in FIREMESH using a fuel load of 12.5 t.ha^{-1} at the elevation of the weather station. The dotted line on each plot (cumulative hectares burnt at 0.5 hour time step) is superimposed over three hour time step plots (b and d) for easy comparison with the finer resolution. Errors for the period in winter cancel (c and d) with resolution, while a large error is apparent for the summer example due to resolution (a and b).

ure 4.2.c and d). However, the sudden rise of FFDI to 100 on the afternoon of the 18th January, 2003 is missed by the simulation using Δt of three hours, resulting in a large under-estimate of the fire size. Calculating the fire run length for the entire weather data (1/7/1985 to 30/6/2011) at a Δt of 0.5 and 3 hours shows there is little difference in the fire run length over this range ($\Delta t = 1.5\text{h} : 0.03\%$, $\Delta t = 3\text{h} : 0.2\%$).

However, the above analyses do not consider fire extinguishment. As Δt increases, the time of extinguishment will occur at increasingly later times. For example, if an line is drawn across Figure 4.1 a, b and c, at say, $R_h = 500$ to represent the threshold above which a fire could

not be controlled, a) can burn between 8:00 and 19:00 (11 hours), b) between 9:00 and 19:00 (10 hours) and c) between 9:00 and 21:00 hours (12 hours). However, this can be misleading. Over the diurnal cycle, ignition times are assumed to have a uniform random distribution in FIREMESH, while extinction times are obviously contingent on there being a fire in the first place. Therefore if we randomly select an ignition time at, say 12:00 hours, then the duration of the burn can only increase as Δt increases. In addition, in some cases this threshold may be missed entirely at coarser resolutions, whereupon the fire will continue to spread until a time of extinguishment is next encountered. Considering the diurnal cycle, this may be some days later leading to a large increase in the final fire footprint.

Nevertheless, rapid change in the weather conditions can lead to large errors in fire simulation (Figure 4.2). Thus an approach to optimize time step using a variable Δt determined by the derivative of the curve might be appropriate. Conversely, resolving the moment of extinguishment is also important, and an approach that minimizes Δt near this threshold at the expense of Δt where conditions are more extreme may prove optimal as well. However, a complicating issue is wind direction. Area burnt by fires under high wind can suddenly increase with changes in wind direction as the fire flank becomes the head fire. Thus some approach that accounts for the changes in the vector of spread (magnitude and direction) is required (Figure 4.3).

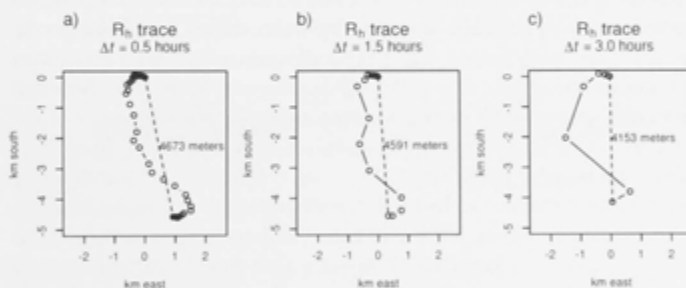


Figure 4.3: Differences in the vector sum of fire spread
Differences in the vector sum of fire spread (speed and direction) for an arbitrary period in the half-hourly weather data recorded at Canberra Airport at three time steps (0.5, 1.5 and 3 hours).

As noted in Chapter 3, points on the (simulated) fire perimeter extinguish when fireline intensity falls below some prescribed value (nominally 83 kW.m^{-1}), the entire fire being extinguished when intensity at all locations falls below this value. Fireline intensity varies not only with the weather data but also with the slope of the terrain and fuel weight and therefore cannot be determined beforehand. To take account of (i) sudden changes in fire danger index, (ii) wind direction and (iii) slight changes in conditions that lead to fire ex-

tinguishment, a simple approach to optimizing time step, based on the rates of change in fire spread vectors, cannot work. Nevertheless, an improvement would be given a range of Δt from some minimum (mn) (the resolution of the input data) and some maximum (mx) (a multiple of mn to avoid interpolation):

$\Delta t = mn$ if maximum intensity $< c_1$ [if close to extinguishing at any elevation]

$\Delta t = mn$ if $(V_t - V_{t+1}) > c_2$ [if a change in velocity]

$\Delta t = mx$ otherwise

where c_1 and c_2 are tuning parameters, V_t is the rate of spread vector at time t , and mn and mx are minimum and maximum Δt respectively.

Note that, the above algorithm is intended to be applied to the data before simulation begins. The values of c_1 and c_2 will determine the total number of time steps used in reading the data set. The mean temporal resolution is the temporal extent of the data set divided by the number of time steps.

4.1.2 *Spatial resolution*

The spatial parameters contributing to rates of spread are fuel, elevation and slope. Slope is overwhelmingly the major spatial parameter contributing to R_h (Figure 4.4). As noted, the centroid method is used in deciding the elevation of a vertex placed over a DEM. The centroid method tends to preserve variation between values as resolution decreases (Bian and Butler, 1999). The difference in fuels, elevations and slopes between a one and nine hectare mesh in this modelled landscape shows slope changes faster as resolution changes (-1.4%, -1.3% and -17% respectively). Furthermore, in FIREMESH, the rate of spread doubles for each 10° of slope. As resolution and the distribution of slopes change, so too will the distribution of fireline intensities and locations where a fire will extinguish at any given time. Thus there will also be a component driving area burnt with changes in intensity and the point at which fires extinguish. For example, the sum of $\Delta s/R_h$ can be interpreted as the time taken by an imaginary continuously burning fire to travel in a straight line moving in one direction. If this is calculated using the equations of fire spread for a transect of mountainous terrain with resolutions of 100, 200 and 300 meters, the time taken to span the transect varies by only between +2 to -4% with no clear trend against Δs (Figure 4.5). Thus from this simple two-dimensional experiment (length and elevation), it would appear that spatial resolution is not a sensitive parameter. However, full simulations in later chapters show this is not the case, demonstrating that interactions with slope and extinguishment must play a role.

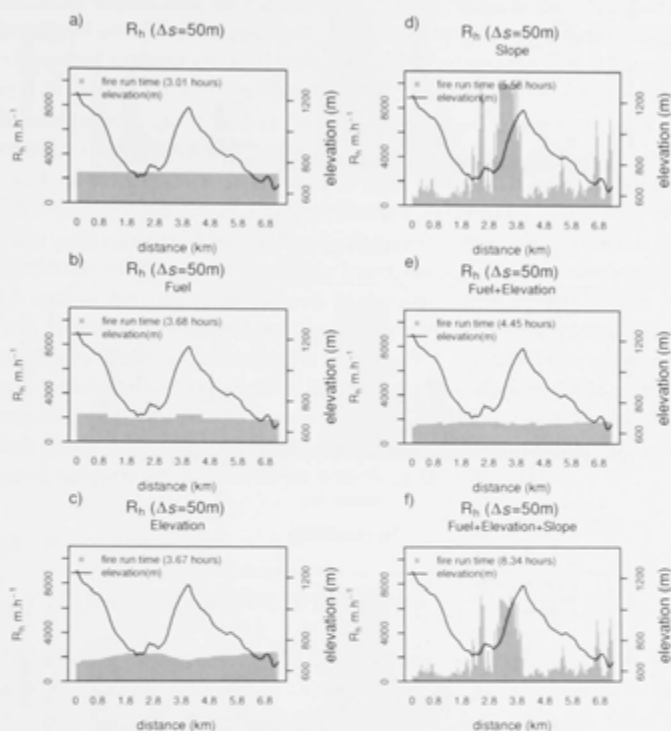


Figure 4.4: A short transect of the study area showing the rate of spread at each location determined by fuel, elevation and slope

The effect of each spatial attribute (fuel, slope and elevation) is shown separately and together). The total time taken to traverse the transect is shown in the legend for each treatment. The rate of spread is based on the Mark V Forest Fire Danger Meter (McArthur, 1973) with modifications informed by Project Vesta (Gould *et al.*, 2007; McCaw *et al.*, 2008). The solid line shows the elevation of the transect. The grey bars are R_h at 50 metre resolution. Fuel loads and temperature lapse rates are those described in Chapter 2.

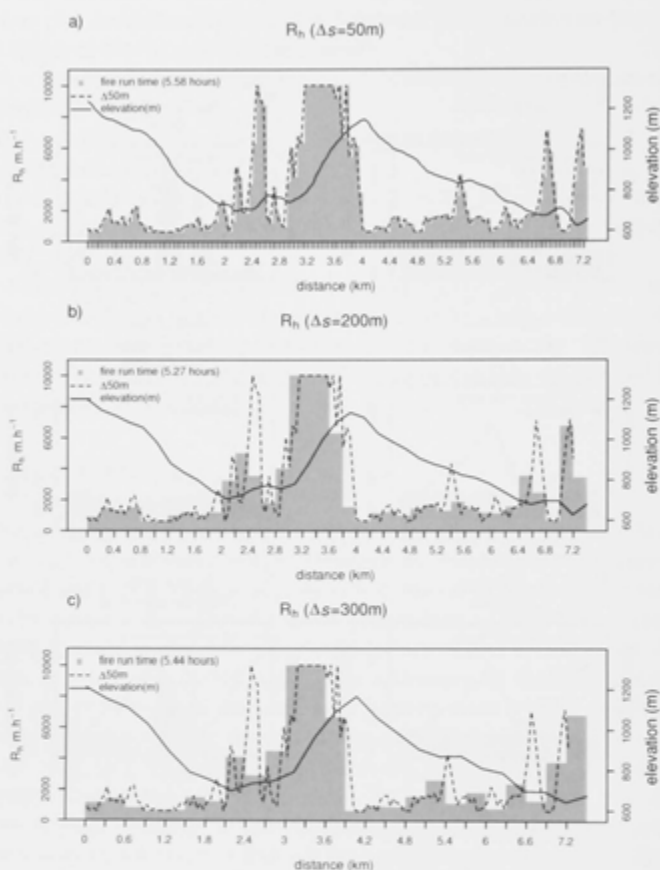


Figure 4.5: A short west-east transect of the study area showing R_h for each location for a fire moving from left to right. R_h is calculated taking account of fuel, elevation and slope factors. The total time taken to traverse this transect at each Δs is shown in the legend for three spatial resolutions. The rate of spread is based on the Mark V Forest Fire Danger Meter (McArthur and Cheney, 1972) with modifications informed by Project Vesta (Gould *et al.*, 2007; McCaw *et al.*, 2008). The solid line shows the elevation of the transect. The dotted line is R_h at 100 m superimposed on charts at the other resolutions for comparison. Fuel loads and temperature lapse rates are those described in Chapter 2.

4.1.3 *Summary of findings*

The examination of Δt above, serves to highlight the importance of capturing moments of synoptic change where sudden changes in wind direction, temperature and humidity can lead to very different outcomes depending on the simulation time step. On the other hand, simulated area burnt is also very sensitive to capturing small changes in weather variables near the point of fire extinguishment. However, as will be shown in later chapters, Δt has only a limited effect on simulation efficiency, and so there appears little reason to pursue an optimization strategy. Within the limits of the data used here (half-hourly data) the finest resolution should be used. If finer resolution data were available, some approach such as outlined above may improve performance. Due to the much greater consequence Δs has for simulation efficiency, on the other hand, an optimization strategy for the spatial domain is developed in the next section. As slope is entirely a spatial parameter, and more strongly affects R_h than does elevation or fuel load, a method is proposed to conserve rate of change in R_h attributable to slope over Δs . The method involves Delaunay triangulation and because this geometry, as used here, produces meshes with predominantly six neighbours (Figure 1.4), the effect of the number of neighbours to a vertex in a mesh is first discussed.

4.2 MESH CREATION

4.2.1 *Definition of equivalent spatial resolutions*

The method of aggregating a DEM to coarser resolutions uses the centroid method (Chapter 2). A spatial extent can be sampled in the field by taking a number of readings of point data; the more samples, the better the coverage but the greater the effort. The same can be said of a mesh, where the number of vertices are the sample. More samples require more computer resources but may show model behaviour at finer resolution which is not apparent at coarser ones. In this study, equivalence in resolution is defined as equivalence in the mean sampling density (the same number of points). The efficiency of the sampling may be changed by altering the local sampling density but the resolutions are equivalent if the mean density over the entire spatial extent is unchanged.

4.2.2 *Regular meshes*

As noted, the number of neighbours to a point in space can have implications for the patterns and behaviours that emerge from spatial simulation models, largely because of the nature of discrete geometries. A regular grid of unit resolution with four Von Neumann

neighbours has a taxicab geometry (Krause, 1973), a system first considered by the mathematician Hermann Minkowski (1864-1909). Modelling fire spread in any system with a discrete number of neighbours means the path of the fire must follow the network of edges. This means the Euclidean distance between two points on the mesh is not necessarily the same as the distance travelled when following along edges. In a four neighbour taxicab system (all four edges are at right angles to each other), the distance between any two neighbours at 45° is 2 units while in Euclidean distance is $\sqrt{2}$ units (Figure 4.6).

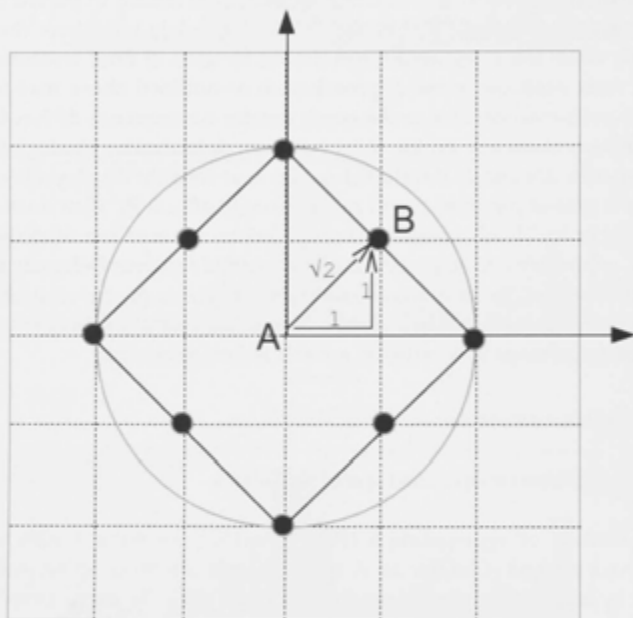


Figure 4.6: A unit grid with four neighbours to each vertex: a taxicab geometric system

The Euclidean distance between A and B is $\sqrt{2}$ units. Within the constraints of the taxicab system (Krause, 1973) the distance is 2. The area of the above circle is $\pi 2^2$ while the area of the taxicab circle is 8.

As the radius of a circle increases in taxicab geometry, the shape manifest is that of a square orientated at 45° to the coordinate system. The area of this square differs from that of a circle by $1 - 2/\pi$ or an error of 36.3% between the fire size implied by the equations of fire spread and that estimated in a system constrained by a four neighbour discrete geometry. Likewise a system with six neighbours will produce hexagons, eight neighbours octagons and so on with each increase in the number of neighbours reducing the error but increasing computational effort. For an octagonal system (eight neighbours)

the error is $1 - 2\sqrt{2}/\pi$ or approximately 10%. More than eight neighbours is possible (Perera *et al.*, 2008) but this requires either mixing resolutions as the additional neighbours are beyond the first annulus, or more complex calculations to obtain intermediate spatial data between the vertex and those beyond the immediate neighbours.

For ellipses, the error varies with the angle of its axis relative to the coordinate system. For an eight-neighbour system, the error is at a maximum at 22.5° , and it follows that the maximum in four and six neighbour systems is 45° and 30° or 90° (depending on orientation) respectively. These differences between the area proposed by the rate of spread model and the actual area manifest through constraints in discrete geometry have been noted and analyzed by Feunekes (1991). The lack of importance of this issue for simulations at larger scales has been speculated by Green *et al.* (1983a). However, to my knowledge no research has focused on examining whether this is significant for performance of fire simulation models in ranking the factors that drive components of fire regimes (Chapter 1).

Many approaches have been taken to overcome the inherent constraints imposed by these geometries while trying to keep the computational burden to a minimum (Markus and Hess, 1990; Miyamoto and Sasaki, 1997; Caballero, 2006; Perera *et al.*, 2008; Johnston *et al.*, 2008; Trunfio *et al.*, 2011; Avolio *et al.*, 2012). The approaches taken by Trunfio *et al.* (2011) and Avolio *et al.* (2012) require a regular grid. If a regular grid is used to vary spatial resolution to accommodate different rates of change in terrain, the resolution can only alter by powers of 2. The approach taken by Johnston *et al.* (2008) and implemented in the *Australis* simulator (unpublished), has the potential to allow resolution to change continuously in response to the rate of change in the terrain, in a sense, the approach taken by finite element analysis in normalizing errors over resolution (Braun *et al.*, 1995; Schaap, 2007; Anderson *et al.*, 2005).

4.2.3 Triangulated Irregular Networks (TIN)

The approach taken by Johnston *et al.* (2008) can be thought of, in the context of the above discussion, as a probabilistic taxicab system where each vertex has, on average, six neighbours and the travel distance in any direction is equal on average, with variance between the travel distances decreasing as distance increases. To generate the mesh, a set of equidistant points are created to sample the DEM – a Poisson-Disk distribution. A Poisson-Disk distribution is one that places points randomly in two or more dimensions but with the constraint that no two points can be closer than some minimum prescribed distance. The angle of the edges between neighbouring points are uniformly random with respect to the coordinate system. Methods for achieving this are discussed below. This results in the differ-

ence between the Euclidean and travel distance between two points being equal, on average, in all directions. This difference can then be accounted for with an empirically derived constant (β) (Equation 4.1).

Two points to note are that firstly, point generation involves some stochasticity. Thus variance in travel distance between any two points will be inversely proportional to the number of vertices traversed (that is inversely proportional to resolution) and replication may be required in some situations. Secondly, for directions of spread $\pm 40^\circ$ ($\pm \alpha$) (Equation 4.1) with respect to the fire heading, a non-linear function of the ellipse eccentricity must be used, calibrated empirically by simulation, to achieve the correct forward rate of spread (Johnston *et al.*, 2008). R_h is the best constrained field observation for fire spread (Johnston *et al.*, 2008) compared with the length-to-breadth ratio (L:B) of the fire footprint. So it is important that the function modifying β within $\pm \alpha$ be such that R_h is correct with respect to these observations.

$$R_{\text{micro}}(\theta) = \begin{cases} \beta \frac{R_0(1 - \cos \theta) + R_h(\cos \theta - \cos \alpha)}{1 - \cos \alpha} & |\theta| < \alpha \\ \beta R_0 & \text{otherwise} \end{cases} \quad (4.1)$$

where:

$$\beta = -0.42/(R_h/R_0)^3 + 0.91/(R_h/R_0)^2 - 0.84/(R_h/R_0) + 0.39$$

R_{micro} is the rate of spread adjusted to account for the difference between the Euclidean distance and the additional distance required to travel on a triangular irregular network (Johnston *et al.*, 2008).

With this approach, the length-to-breadth ratio (L:B) is not prescribed but emerges from the simulation. However, the L:B that emerges can produce unexpected results depending on the particular equations used to estimate rates of spread (see Figure 5.16). As discussed in Chapter 3, the intended fire shape in FIREMESH is that of an ellipse and the purpose in using this irregular form of a discrete geometry is that it has a greater potential to achieve this shape (see Figure 5.14). This presents a problem for the experiments in this work because it is hoped to test the mesh geometry rather than confound the experiment with fire shapes that do not fit the elliptical shapes described previously, particularly the movement of the focus of the ellipse downwind.

In Equation 4.1, R_0 is the rate of spread at zero wind speed (Johnston *et al.*, 2008). Fire shapes can be made to fit the ellipse (E_b), described in Figure 3.7, by setting R_0 to the length of the line from focus F_a to ellipse E_b perpendicular to the semi-major axis (Figure 3.7). However, the back-fire rate of spread (R_b) (the shortest distance between F_a and E_b - Figure 3.7) is not the same as the 'zero wind' rate of spread, which is the definition of R_0 in Equation 4.1 above. To account for this, Equation 4.1 can also be applied for the ellipse region

$\pm(\alpha + 180)$ but substituting R_b for R_h . How well this achieves the desired elliptical shape is examined in Chapter 5 (Verification).

$$R_{\text{micro}}(\theta) = \begin{cases} \beta \frac{R_0(1 - \cos \theta) + R_h(\cos \theta - \cos \alpha)}{1 - \cos \alpha} & |\theta| < \alpha \\ \beta \frac{R_0(1 - \cos \theta) + R_h(\cos \theta - \cos \alpha)}{1 - \cos \alpha} & |\theta| < \alpha + 180 \\ \beta R_0 & \text{otherwise} \end{cases} \quad (4.2)$$

By varying the local density of mesh vertices, we can adapt resolution locally to the rate of change in the spatial data. This may provide an optimal method for managing spatial resolution. However, varying sampling density continuously may also lead to non-random distribution of edge angles, which would introduce fire-shape distortions and invalidate the assumption of uniform random distribution of edge angles that underpins the approach of Johnston *et al.* (2008).

4.2.4 Generating even and uneven density Triangulated Irregular Networks

To achieve an even distribution of points that are independent of the orientation of the coordinate system, and have a very small variance in distance between points, a Poisson-disk distribution algorithm was used by Johnston *et al.* (2008). Two general classes of algorithm exist for this purpose: (i) dart throwing and (ii) relaxation (Lagae and Dutré, 2008). The dart throwing technique adds points by repeated random generation, accepting or rejecting them depending on some minimum allowed distance between points. As available locations become scarcer, the algorithm becomes slower and an arbitrary stopping condition must be used. This makes it impossible to obtain, at the same time, a predetermined number of points and a satisfactorily even distribution. Recall that to assert that two meshes are equivalent in terms of resolution, the number of points must be prescribed. In relaxation methods on the other hand, a fixed number of random locations are created and an algorithm applied to adjusting their position (McCool and Fiume, 1992). However, relaxation algorithms have, until recently, been slow (de Goes *et al.*, 2012). These algorithms were developed in the field of computer graphics and their principal use is for digital half-tone imagery (Ulichney, 1987), that is, rendering images using dots of the same size by varying their local position. A novel application of the Capacity-Constrained Delaunay Triangulation (CDT) (Xu *et al.*, 2011) method has been used in this study which, to date, produces fast and high quality results. A more recent, and possibly superior, algorithm has been created (de Goes *et al.*, 2012) but was published too late to include in this study. The original MatLab source code (available as supplementary information with Xu *et al.* 2011) was re-implemented in Java to allow faster execution time

and larger image processing than is possible with the original implementation.

METHOD Creating a mesh with an even Poisson-Disk distribution is a particular case of creating one with an uneven distribution but derived from a monotone image. CDT works as follows. An image is chosen and a fixed number of points randomly generated within its extent. A TIN is created by application of a Delaunay Triangulation algorithm (Barber *et al.*, 1996). The sum of all pixel values within each triangle is calculated, taking area weighted account of pixels that are not fully contained within the triangle boundary. This is termed the *capacity* of the triangle. The algorithm iterates over the vertex points and adjusts the position of each so that all triangles formed with its immediate neighbours have the same capacity. This repeats until the change in variance of the capacity is below some threshold (Figure 4.7) (for more details see Xu *et al.* 2011). The points

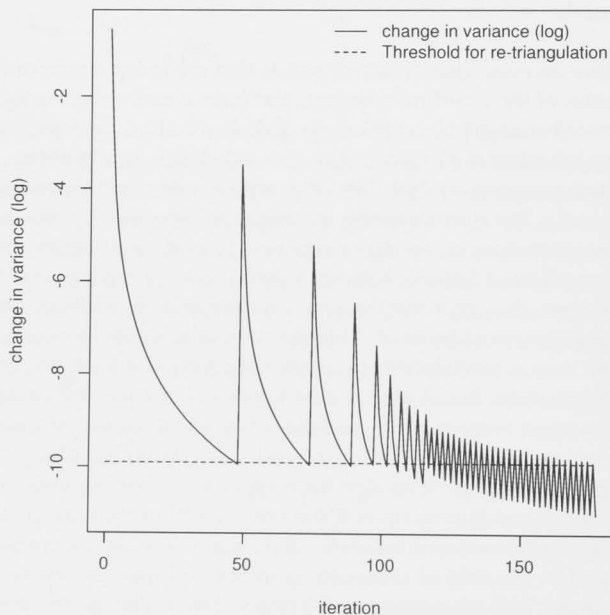


Figure 4.7: Mesh minimum energy produced using the Capacity-Constrained Delaunay Triangulation method (Xu *et al.* 2011) The solid line is the difference in the variance of triangle capacity (the sum of pixel values with each triangle). The dotted line is the threshold where change is sufficiently small as to require re-triangulation. After each re-triangulation, the mesh energy is higher until vertex positions are re-adjusted to minimize capacity variance.

are then re-triangulated and the process repeated until the rate of

change in the variance reaches some minimum: the minimum mesh energy (Anderson *et al.*, 2005). The resulting distribution of points is a half-tone rendering of the original image with point density continuously varying with pixel values (Figure 4.8.b). The final distribution of points is re-triangulated to generate a mesh (Figure 4.8.c). For each such mesh there exists an equivalent Voronoi tessellation, its dual. The area of each Voronoi cell is the area represented by each vertex in the Delaunay triangulation (or mesh). Points within unbounded Voronoi cells (on the perimeter of the spatial domain) are discarded as their area is undefined (Figure 4.8.d). By choosing some spatial attribute relevant to a spatial simulation model, an image can be generated from which a mesh is created that optimizes the sampling of that attribute. The discussion in the previous chapter indicates that the rate of change in R_h with slope is the best attribute to conserve as Δs changes ($\Delta R_h / \Delta s$).

Referring to Figure 4.9, a raster of slopes is created from the DEM using Horn's method (in Burrough *et al.* 1998). From this raster of slopes, a second raster is created using the fire model's response to slope. Finally an image is created from the derivative of this last raster. This is this potential change in rate of spread due to slope. The CDT algorithm is applied to this image (Figure 4.9.d) to produce an optimal placement of vertices in the mesh (Figure 4.10). The area of each vertex is obtained from the equivalent Voronoi mesh (Figure 4.11). As noted, the application of the CDT algorithm without an image (or with a uniform colour) produces a uniform Poisson-Disk distribution.



(a) Original image



(b) Half-tone image



(c) Application of CDT algorithm



(d) Equivalent Voronoi tessellation

Figure 4.8: Sequence of steps in converting a digital image into a Delaunay triangulation and its equivalent Voronoi tessellation
The area of each Voronoi cell (d) is the area represented by each vertex in the Delaunay triangulation (c).

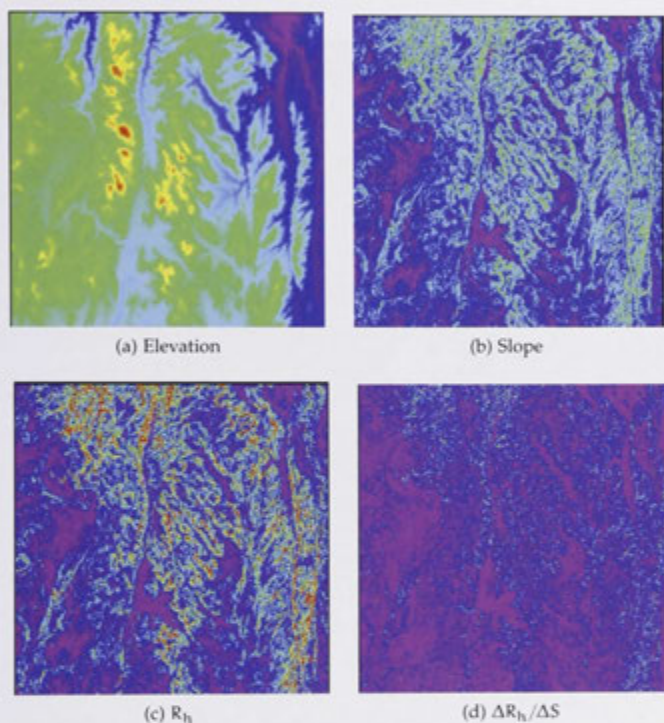


Figure 4.9: Four surfaces depicting the steps involved in creating a surface of the rate of change in the rate of spread of a head fire
(a) Is a DEM of the Brindabella Ranges;
(b) Is the derivative of (a), the maximum slope at each location;
(c) is the change in rate of spread as a function of (b); and
(d) Is the derivative of (c), the rate of change in the rate of spread as a function of slope.

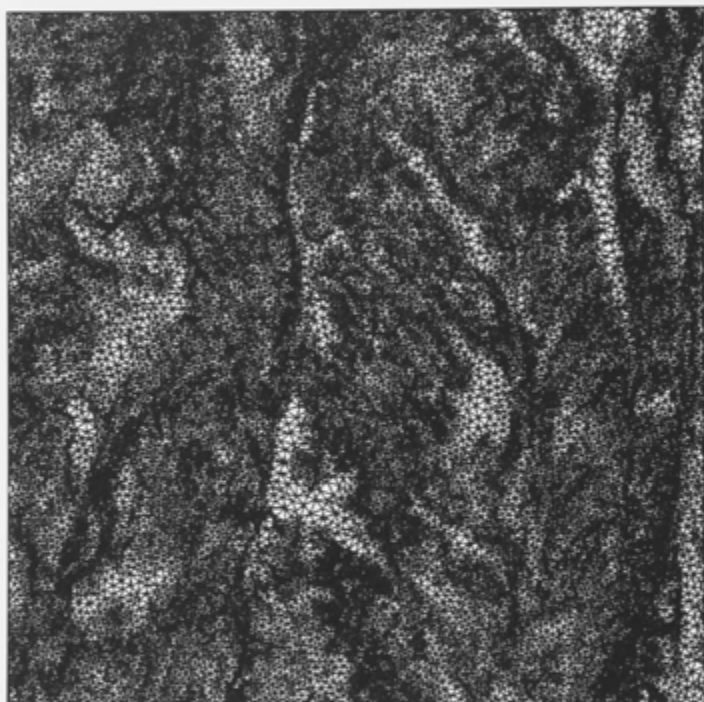


Figure 4.10: A Delaunay triangulation using the Capacity-Constrained Delaunay Triangulation algorithm. The triangulation is based on the image created in Figure 4.9.d). The vertices of this mesh are concentrated in regions where the rate of change in the rate of spread of a fire due to slope is greatest.

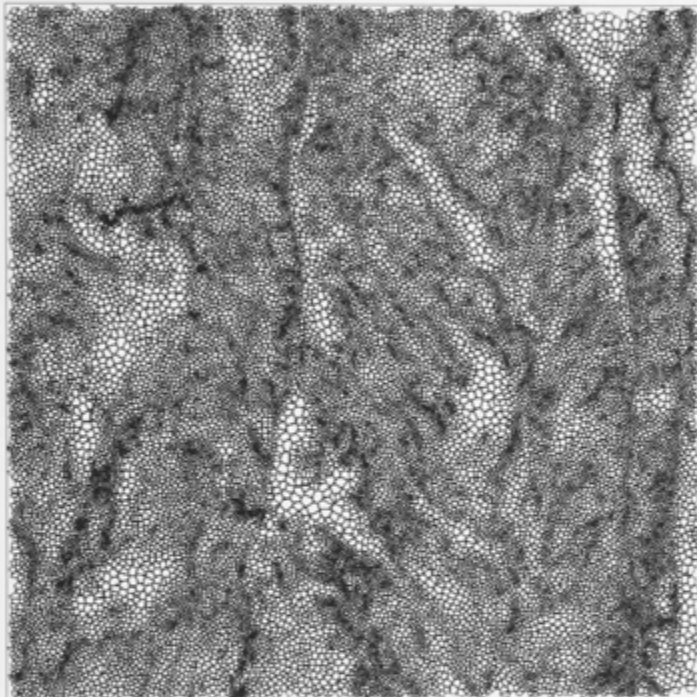


Figure 4.11: A Voronoi tessellation

The area of each cell is the area represented by each vertex in the Delaunay triangulation in Figure 4.10. Unclosed cells on the perimeter are discarded as their area is undefined.

RESULTS The density distribution of $\Delta R_h/\Delta s$ at each vertex in the mesh (Figure 4.12) can be seen to increase, indicating the method has succeeded in sampling space more densely where change is greatest. As noted, for fire to propagate on a mesh with this geometry, without distortion in any one direction, it is important that the distribution of angles between vertices be uniformly distributed. This is the case for an even distribution of points but for the case of varying local vertex densities the distribution of angles shows a small increase in the density of angles near 90 or 270° although this does not appear significant (Figure 4.13). It is assumed this arises because of the dominance of east-west aspects in this landscape (Figure 2.3). It follows that estimated fire velocity in these directions may be slightly greater. Verification tests are performed in the next chapter, to examine if this condition arises in practice.

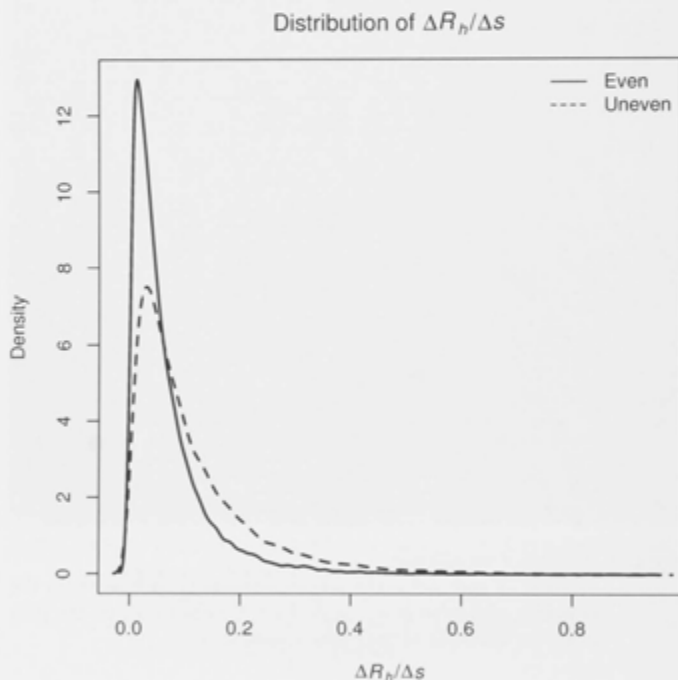


Figure 4.12: Density distribution of $\Delta R_h/\Delta s$

This density distribution shows the distribution of pixel values of Figure 4.9.d at each vertex position for the mesh in Figure 4.10 (dotted line) compared to a mesh with an even disposition of vertices (solid line). The increase in values of high $\Delta R_h/\Delta s$ indicates the Capacity-Constrained Delaunay Triangulation algorithm (Xu *et al.*, 2011) has successfully concentrated vertices around locations where $\Delta R_h/\Delta s$ is greatest.

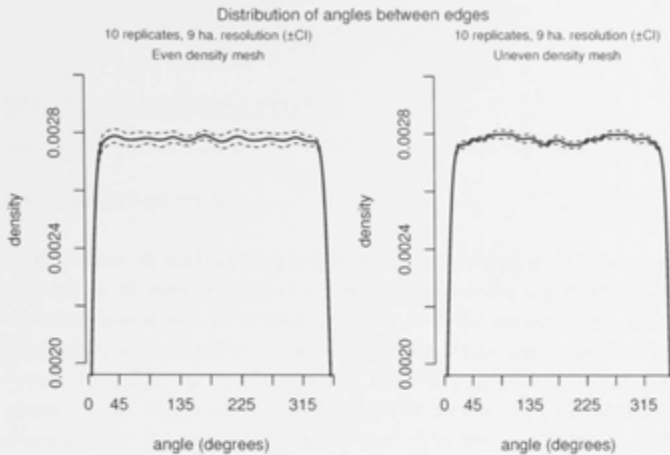


Figure 4.13: Density distribution of angles between neighbouring vertices
Density distribution of angles between neighbouring vertices for an even and uneven triangulated irregular network. Note the distributions must be symmetrical, as each edge between vertices includes its complement.

4.3 CONCLUDING REMARKS

Indications from the above test show that fire simulations are sensitive to both Δt and Δs . The choice of time step affects area burnt estimates by both resolving changes in weather when rates of spread are high and moments of fire extinguishment when rates of spread are low and when wind direction changes. However the benefits of coarse over fine resolution on model execution time are minor and there is little reason to choose a time step coarser than that imposed by the data available.

Spatial resolution on the other hand can provide very significant benefits to performance as will be shown in later chapters. While there may be some bias in the distribution of angles between vertices using the optimized mesh it remains to be established if, in practice, this poses a problem for this approach. This is examined in the next chapter. It also remains to be seen if the mechanisms by which spatial and temporal resolution affect fire simulations will, in fact, alter model estimates of the relative importance of factors determining the components of fire regimes.

5.1 INTRODUCTION

'Verification' is testing that a model implementation is correct with respect to its specifications and is one element in the broader effort of validation which tests that a model is fit for its intended purpose (Rykiel Jr, 1996; Sargent, 2005). These two terms are sometimes confused (Rykiel Jr, 1996). This chapter examines verification through numerous tests designed to confirm that the equations documented produce fires of the size and shape intended by the equations and architecture, even if those simulated fires are incorrect with regard to field observations. As noted, McArthur's Forest Fire Danger Meter (FFDM) (McArthur, 1973) is considered to under-predict rates of spread under more extreme conditions (McCaw *et al.*, 2008). The task of verification is to check these equations have been implemented as specified by the meter, rather than whether the equations lead to under-prediction. This would be a task addressed by validation. In Chapter 6 on validation, the model's performance is examined by comparing its performance to its predecessor.

Validation and verification apply just as much to the materials and methods required for field or glasshouse experiments as they do to the design, development and use of computer models. Verification and validation can never be known with absolute assurance any more than a theory can be proven to be true. Verification can at least be measured by the completeness of the recording of data and methods. Omissions can be noted post hoc. However, validation is more complex and limited by both the conceptual model of the system, which may contain many unrecognized or unrecorded assumptions, and by a paucity of observations with which to evaluate the model.

This is certainly the case with fire regime models because of the large spatial and temporal scales at which they operate and their necessary simplicity compared to the potential complexity of ecological systems at these scales and that of fire and very fine scales. In short, while the terms verification and validation have the ring of a superlative about them, all that can really be done is to take steps to improve our confidence that the materials and methods are as specified (verified) and that they satisfy requirements to the extent that this is testable (validated) before being applied to testing the hypotheses of this study.

5.2 CONSISTENCY ACROSS RESOLUTIONS USING REGULAR MESH CONFIGURATIONS

To examine hypotheses (i) (Section 1.1) and (ii) (Section 1.4.5), it must be established that on flat terrain and under homogeneous conditions, FIREMESH will produce the same fire perimeter regardless of time step, spatial resolution or the number of neighbours to each vertex. At the same time it can be determined whether the distance between the ignition point and the fire perimeter accords with the FFDM in equation form (Noble *et al.*, 1980).

METHOD A trial of 48 simulations were performed using four, six and eight neighbour meshes (N-4, N-6 and N-8). These trials used four time steps (0.5, 1, 2 and 3 hours) and four spatial resolutions (0.25, 1, 4 and 9 ha.). The wind speed was set to zero and the forward rate, derived from the weather and fuel data in Table 5.1 was 197.18 m.h^{-1} . The fire was run for 12 hours and the distance reached by the simulated fire in each of the principal directions (greatest extents) of the three mesh configurations was compared to the predicted distance of 2,366.201 metres. This distance is obtained using equations A.3 and A.4 with the values of temperature, relative humidity, fuel weight and drought factor listed in Table 5.1

RESULTS The fire shapes that emerge agree with the theory of taxicab geometry (Krause, 1973) and the findings of Feunekes (1991) in that all fires reach the circular perimeter and the predicted geometric shapes emerge (Figure 5.1). Small errors were found (differences between expected and simulated distance from the ignition source to the fire perimeter) with the exception of the time step treatment (Table 5.2). All trials produced precisely symmetrical shapes. The same error was found for N-6 meshes between spatial resolutions in all direction (0.007%). A difference between predicted and simulation distance was found for the N-8 mesh between cardinal and inter-cardinal directions (c and i-c columns in Table 5.2). All inter-cardinal directions in N-8 meshes show precisely the same error (-0.002% or 2 cm per kilometre or less than one second in 12 hours) but errors in cardinal directions vary between -0.016% to +0.002% across spatial resolutions. N-4 meshes have identical errors to the cardinal directions as N-8 meshes.

Some of this error may be attributed to the necessity of rounding time to the nearest second (which happens each time fire moves from one location to its neighbour and is thus sensitive to spatial resolution). Rounding time to a discrete value is a condition imposed by the 3Worlds simulator in which this model is embedded. Finer granularity to the micro-second is possible but was not considered warranted.

Table 5.1: FIREMESH equations and parameter values relevant to this chapter

NAME	SYM	UNIT	VALUE	EQUATION
Temperature	T	°C	30	
Vapour pressure	V	kPa	1.2	
Relative humidity	H		28.49	
Soil dryness index	SDI	mm	165	
Days since rain	N	days	30	
Amount of last rainfall	P	mm	2	
Drought factor	D		10	Equation A.2
Wind speed	U_{10}	km.h ⁻¹	0	
Fire Danger Index	F		13.15	Noble <i>et al.</i> (1980)
Fuel weight	W	t.ha ⁻¹	12.5	Table 2.1
Rate of forward spread	R	m.h ⁻¹	197.1	Noble <i>et al.</i> (1980)
Slope	Θ	degrees	0	
Rate of forward spread on slope	R_{Θ}	m.h ⁻¹	197.1	Equation A.6
Heat of combustion	H	kJ.kg ⁻¹	20,000	
Fireline intensity	I	kW.m ⁻¹	1,369	Equation A.14

5.3 CONSISTENCY ACROSS SPATIAL RESOLUTION USING TRIANGULATED IRREGULAR NETWORKS

As with regular meshes, the same independence of simulated fire size from spatial resolution is required of triangular irregular networks (TIN), if FIREMESH is to be applied to Hypotheses (iii) and (iv). As noted, there are two types of TINs used in this study: (i) those with an even distribution of vertices over the spatial extent of the simulations (Figure 5.2.a); and (ii) those where the density of vertices varies with the rate of change in R_h due to slope ($\Delta R_h/\Delta s$) (Figure 5.2.b). Under neutral conditions (Table 5.1), all TINs should produce the same circular fire shape (averaged over replicates) and be a better approximation of a circle than an N-8 mesh. Johnston *et al.* (2008) show that their approach is valid regardless of the resolution. That is, the technique is scale-invariant. The property of scale-invariance is important for two reasons in the present context: (i) because the effect of spatial resolution on generated fire regimes is a treatment in this study; and

Table 5.2: Errors reported between expected and simulated maximum distance travelled

Errors reported between expected and simulated maximum distance travelled (2366.201 metres) for 48 simulations (3 neighbourhood configurations: 4 neighbours (N-4), 6 neighbours (N-6) and 8 neighbours (N-8), 4 temporal resolutions (0.5, 1, 2 and 3 hour time steps) and 4 spatial resolutions (50, 100, 200 and 300 m). No error was found that can be attributed to time step (not shown). Cardinal (card.) and inter-cardinal (inter-card.) errors are shown for N-8. Parameters for the fire spread equations are those in Table 5.1.

		Number of neighbours			
				N-6	N-4
		card.	inter-card.		
Spatial resolution	50m	-0.016%	-0.002%	-0.007%	-0.016%
	100m	-0.015%	-0.002%	-0.007%	-0.015%
	200m	-0.011%	-0.002%	-0.007%	-0.011%
	300m	-0.002%	-0.002%	-0.007%	-0.002%

(ii) because scale-invariance is necessary if a mesh is to be used with continuously varying resolution.

METHOD One hundred and sixty simulations were performed on a flat landscape, comprising 10 mesh replicates, four resolutions (0.25, 1, 4 and 9 hectares) and four fire sizes (6, 12, 18 and 24 hour duration). Constant weather conditions were used as listed in Table 5.1. Temporal resolution has already been shown to have no effect under these conditions and is set at three hours for this experiment. The purpose of testing different fire sizes in addition to spatial resolution is to fully explore the scale-invariance of this type of mesh. Because wind speed is zero, only part (3) of Equation A.15 is relevant ($R_h/R_0 = 1$). All points on the fire perimeter are recorded and the mean and standard deviation of their distance from the point of ignition compared to the theoretical distance (hours $\times R_h$).

RESULTS In Section 4.2.3 it was noted that the distribution of edge angles in the uneven meshes showed a bias towards 90° and 270° . However, examination of 24-hour fires gives no indication that such a bias exists in practice (Figure 5.3). The fire shapes across all resolutions and fire sizes appear very close to the expected circular shape for both even meshes (Figure 5.4) and variable density meshes (Figure 5.5) without distortion in any particular direction for either arrangement. On the other hand, there appears to be an increase in the radii of the patterns as resolution increases, that is, 50 m resolution simulations produce a closer fit to the predicted fire extent



Figure 5.1: Four, six and eight neighbour meshes at three hour time steps and 1 ha. spatial resolution

The simulated fires are run for 12 hours under identical conditions (Table 5.1). Time steps are marked by alternating grey and dark grey bands.

than simulations at 300m resolution. This pattern of results is summarised in figures 5.6 (even meshes) and 5.7 (uneven meshes). There is a 3% decline in fire radius at the 6 hour mark for fires between 50 m and 300 m resolutions on even meshes and a little more (4%) for uneven meshes (Figure 5.7). The maximum radii in any direction for all resolutions and durations reaches, but does not exceed, the predicted radius as intended by Equation 4.2. However, on average, extents are less than the maximum and therefore the area of the fire foot print will always be an under-estimate. The magnitude of this under-estimate decreases as the number of edges traversed increases. Nevertheless, the error in the above tests (<5% at zero wind speed) is less than the theoretical error for N-8 arrangements (10%) and by this test (zero wind speed), a TIN mesh produces a more accurate predication of the area of a simulated fire than does an N-8 mesh, despite TIN meshes having fewer neighbours on average (Figure 1.4). For simulations in complex terrain with varying weather conditions (wind speed > 0), the use of a TIN may well provide more accurate predictions of arrival times than simulations using a regular N-8 mesh depending on the wind direction and speed. However, the stochasticity inherent to this method will inevitably have some scale-dependent error in estimating the area of a fire-footprint unless the method is re-calibrated to given correct fire extent on average.

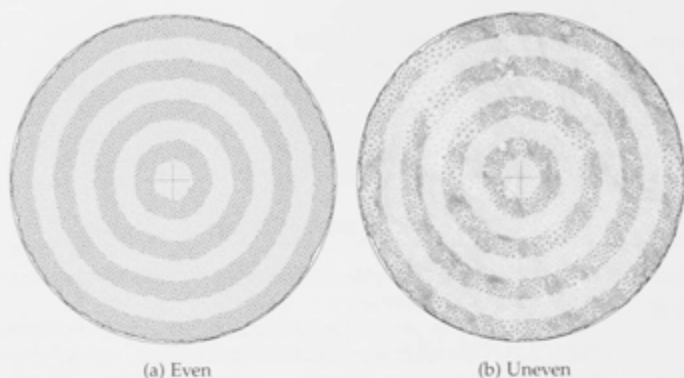


Figure 5.2: Fire spread on triangulated irregular meshes with even and uneven distribution of vertex locations

Time step is three hours indicated by alternating grey and dark grey bands. Weather conditions are listed in Table 5.1.

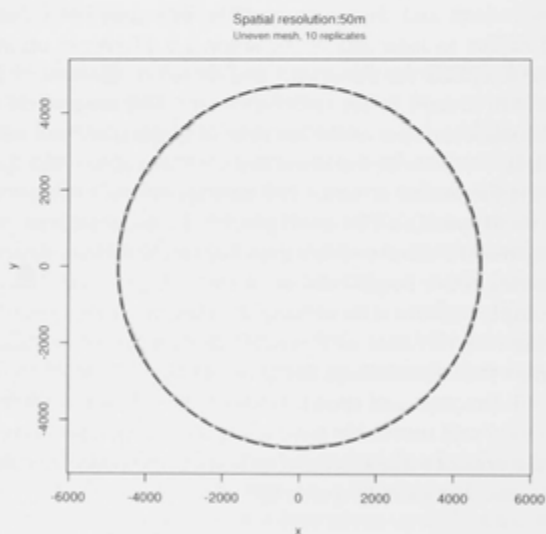


Figure 5.3: Simulated and expected fire perimeter of a 24 hour fires

Fire perimeter of 10 replicate simulations (grey) of a 24 hour fire compared to the expected fire shape (dashed line) on an uneven triangulated irregular mesh with average spatial resolution of 0.25 hectares (equivalent to 50 meter resolution on a regular grid). A constant rate of spread is used as listed in Table 5.1.

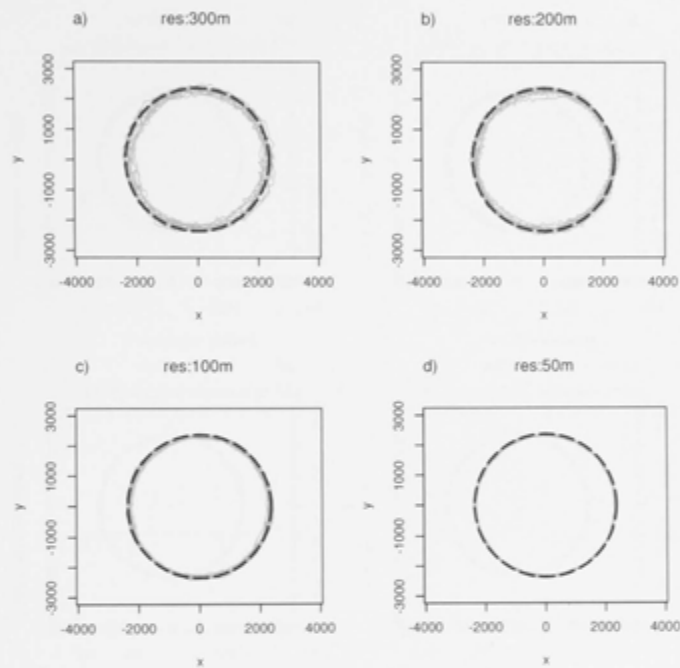


Figure 5-4: Simulated and expected fire perimeters after 6, 12, 18 and 24 hours on a Triangular Irregular Network mesh with an even distribution of vertices
Fire perimeter of 10 replicate simulations (grey) compared to the expected fire shape (dashed line) on an irregular triangulated mesh with an even distribution of vertices. Spatial resolutions were 0.25, 1, 4, and 9 hectares (equivalent to 50, 100, 200 and 300 meter resolution on a regular grid). A constant rate of spread is used as listed in Table 5.1.

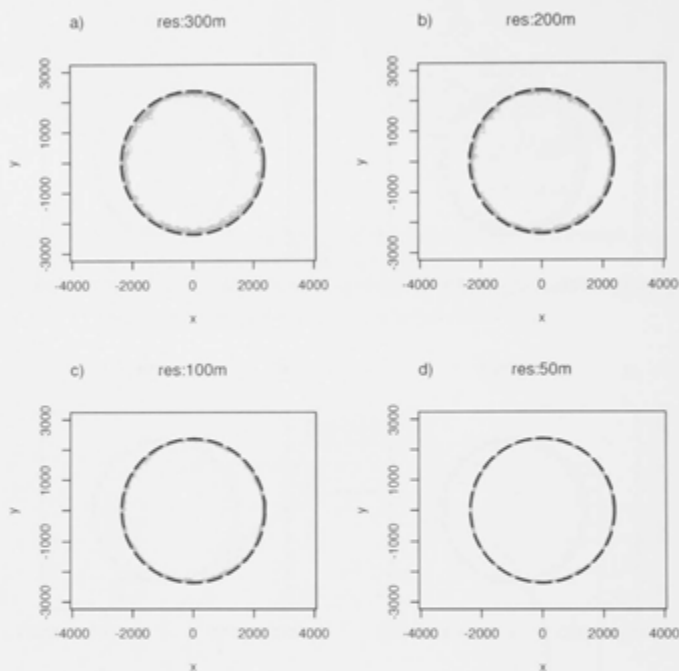


Figure 5.5: Simulated and expected fire perimeters after 6, 12, 18 and 24 hours on a Triangular Irregular Network mesh with an uneven distribution of vertices

Fire perimeter of 10 replicate simulations (grey) compared to the expected fire shape (dashed line) on an irregular triangulated mesh with an even distribution of vertices. Spatial resolutions were 0.25, 1, 4, and 9 hectares (equivalent to 50, 100, 200 and 300 meter resolution on a regular grid). A constant rate of spread is used as listed in Table 5.1.

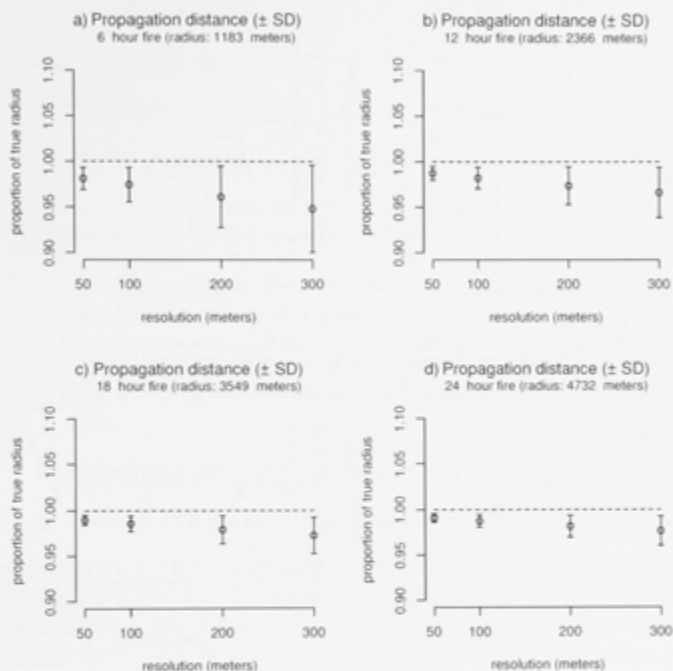


Figure 5.6: Mean and standard deviation of the radii of 10 replicate simulations even distribution of vertices

Mean and standard deviation of the radii of 10 replicate simulations (10 replicate meshes with an even distribution of vertices) of fire durations of (a) 6, (b) 12, (c) 18, and (d) 24 hours. Each fire duration was run at four spatial resolutions (0.25, 1, 2, and 3 hectares). The dotted line shows the expected radius for each fire duration.

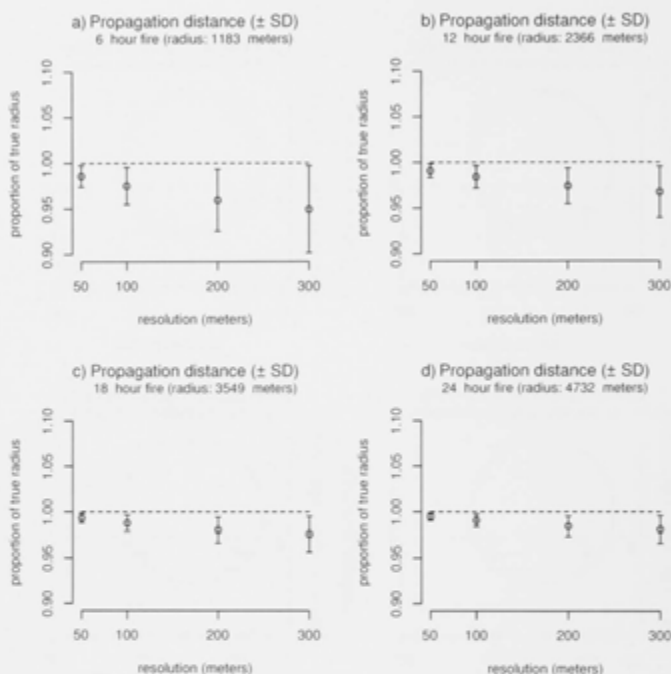


Figure 5.7: Simulated and expected fire perimeters after 6, 12, 18 and 24 hours on a Triangular Irregular Network mesh with an uneven distribution of vertices

Fire perimeter of 10 replicate simulations (grey) compared to the expected fire shape (dashed line) on an irregular triangulated mesh with an even distribution of vertices. Spatial resolutions were 0.25, 1, 4, and 9 hectares (equivalent to 50, 100, 200 and 300 meter resolution on a regular grid). A constant rate of spread is used as listed in Table 5.1.

5.4 MEASURING AREA

For analysis, fire extents must be interpreted as area in a manner that is also independent of resolution and neighbourhood arrangements. Five measures are known at high precision:

- i The area of the landscape;
- ii The area represented by each vertex as calculated from the Voronoi tessellation (Chapter 4);
- iii The total mesh length;
- iv The mesh length within a fire footprint; and
- v The location of each point on the fire perimeter.

From this information, four methods of calculating the area of the fire footprint can be deduced:

- i The proportion of the mesh within a vertex traversed by fire multiplied by the vertex area;
- ii The proportion of the total mesh length traversed by fire to the total landscape mesh length multiplied by the total landscape area;
- iii Including a vertex if $> 50\%$ of its mesh is traversed; and
- iv The area of a polygon surrounding the entire extent of the fire.

Methods (i) and (ii) are not numerically correct (Figure 5.8), while method (iii) has increasing variability inversely proportional to resolution. In the case of method (iv), if the points describing a polygon are ordered consistently (anti-clockwise) then positive values will represent area burnt while negative values will account for unburnt islands. A shortcoming arises when attempting surround an N-8 mesh with a polygon. N-8 meshes are not true tessellations of space. This results in diagonal paths crossing each other leading to ambiguity as to the correct order in which to connect points in the polygon (Figure 5.9).

Special rules were devised to prevent the polygon itself crossing paths but the shape is still relatively convoluted. These rules are not further discussed because this method was not used in the final analysis of area burnt. Polygons surrounding meshes that are true tessellations, that is, meshes that have a dual (Figure 5.10), will not have edges that cross and this ambiguity will not arise. An N-8 mesh can only be constructed without overlapping edges, if vertices are placed at the intersection of the crossing edges, the dual of this mesh being an alternating pattern of octagons and squares (Figure 5.10). These vertices (in the centre of the squares in Figure 5.10) will have only four edges but more importantly, represent a smaller area than vertices

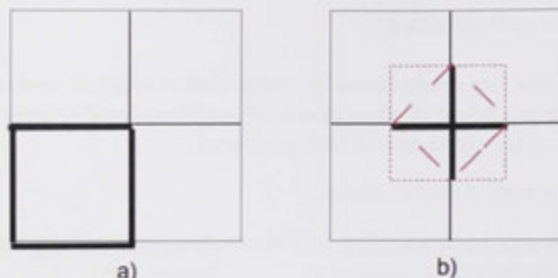


Figure 5.8: Inherent error arising if area is calculated using mesh length traversed

The bold black line indicates the mesh length traversed by a simulated fire. If the area of the entire figure is 4 units, it follows that the intended fire area in both a) the bold black square and b) the red dotted square, is 1 unit. To total length of all edges in a) and b) is 12 units. The area of the central vertex is 1. The area of each vertex on the mid-point of each side is $\frac{1}{2}$ while the area of each corner vertex is $\frac{1}{4}$. Therefore by method:

- i) a) $= 1 \times \frac{1}{2} + \frac{1}{2} \times \frac{2}{3} + \frac{1}{2} \times \frac{2}{3} + \frac{1}{4} = 1\frac{1}{2}$, and b) $= 1$;
- ii) a) $= \frac{4}{12} \times 4 = 1\frac{1}{3}$ and in b) $= \frac{2}{12} = \frac{1}{6}$;
- iii) a) $= 2\frac{1}{3}$ and b) $= 1$; and
- iv) a) $= 1$, and b) $= \frac{1}{2}$.

with eight edges (vertices in the centre of octagons in Figure 5.10). This has not been pursued because to do so would mix scales, as does choosing more than eight neighbours (Perera *et al.*, 2008), and confound the aims of this study.

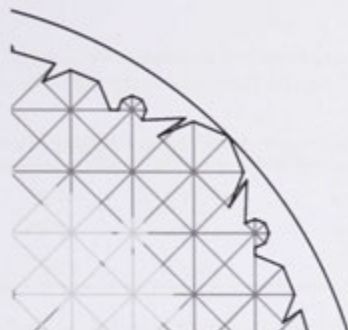


Figure 5.9: Complex polygon surrounding the fire perimeter of an 8 neighbour mesh

Accuracy of the area of the fire footprint increases as either fire size or resolution increases. Ambiguity as to the location of the most likely position of the fire perimeter arises where partially burnt edges overlap.

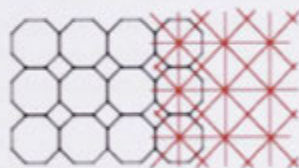


Figure 5.10: A tessellation of space using a combination of octagons and squares (black)

Every tessellation uniquely defines a duel. The duel of this tessellation is a mesh with a combination of 4 and 8 neighbours. This is the only possible way that an N-8 mesh can be modified to prevent edges between vertices from overlapping. However, it follows that the mesh no longer represents locations of equal areas.

Calculating the area of fires simulated on regular 4, 6 and 8 neighbour meshes in the previous experiment shows the areas determined by polygon agrees to within 0.3% in the worst case with the area calculated by geometric means for the radii in Table 5.2 (Table 5.3). The

Table 5.3: Simulated and expected differences for 4, 6 and 8 neighbour geometries of a circular fire (radius 2366.201 metres, area 1758.95 ha.).

NEIGHBOURS	SIMULATED	EXPECTED
N-4	36.4%	36.3%
N-6	17.4%	17.3%
N-8	10.3%	10.0%

error, or difference between predicted and simulated extents, for N-4 meshes was very small, arising from the errors noted in Table 5.2, as the surrounding polygon always has straight edges, unlike N-6 and N-8 meshes (figures 5.11 and 5.12). At particular times, the polygon outlining a N-6 mesh is regular and no measurement error occurs (0.25, 1 and 4 hectare resolution in Figure 5.11). The approximation of the true geometric shape by the surrounding polygon in N-6 and N-8 neighbour arrangements improves as resolution increases. Thus for these meshes there will be a reported reduction in area burnt for between-resolution treatments due to measurement error alone.

Nevertheless, when simulations are performed with a large number of fires there is no systematic difference over resolution between area measured by polygon (method iv) and area measured by the relative proportion of the mesh traversed (method ii) (Figure 5.13). Method (iv) failed at times to correctly mark the perimeter of fires on N-4 meshes (an algorithmic error). As method (ii) is far simpler it is used for the remainder of experiments in the present work and method (iv) is used to visualize fire perimeters for display purposes (e.g. Figure 3.1).

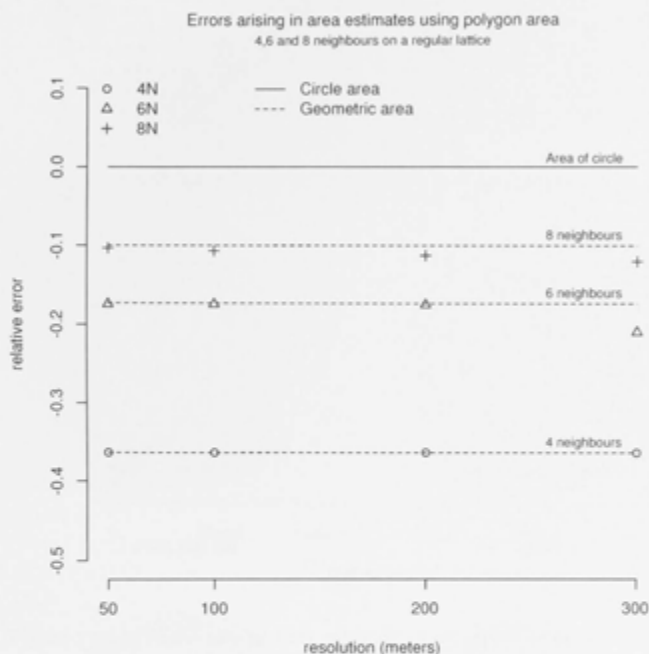


Figure 5.11: Comparison of simulated and expected fire area at four spatial resolutions

Comparison of simulated fire area (symbols) and area calculated by geometric means (dotted lines) at four spatial resolutions (0.25, 1, 4 and 9 hectares). The geometric area is calculated from the maximum extent of the fire in each particular mesh arrangement, that is, the area of a square, hexagon and octagon for 4, 6, and 8 neighbour meshes respectively.

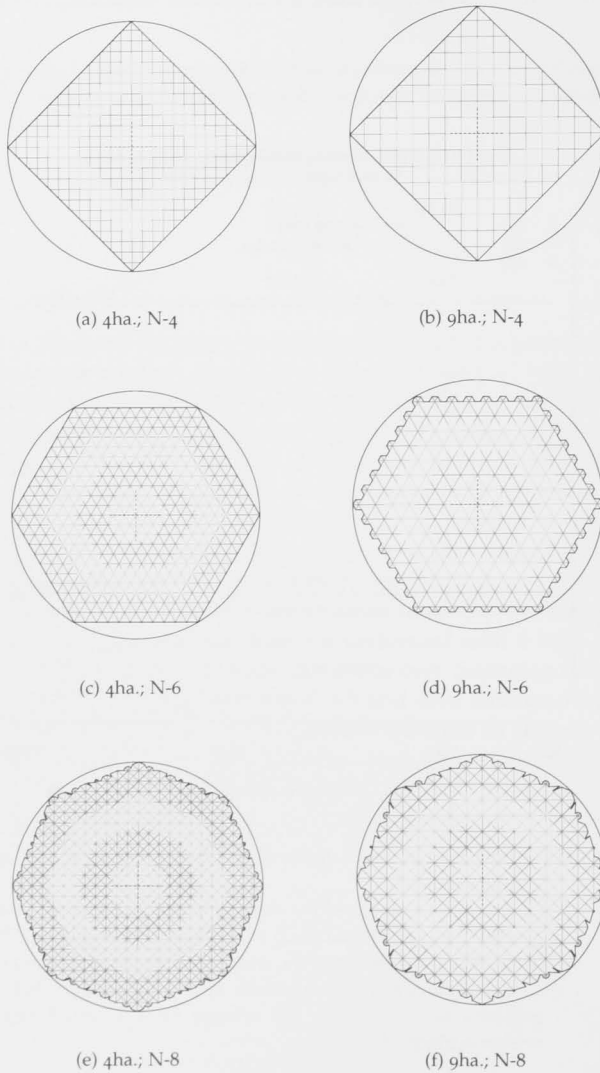


Figure 5.12: Polygons placed around the perimeter of circular fires on 4, 6 and 8 neighbour meshes

On N-4 meshes polygons always have straight edges. On N-6 and N-8 meshes, the regularity varies with the resolution and simulated fire size.

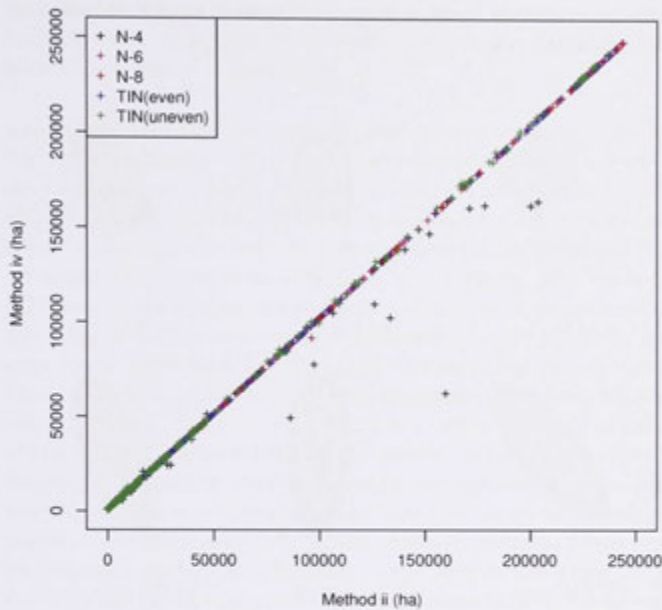


Figure 5.13: Comparison of two methods of calculating area of fire foot prints on five mesh configurations

The mesh configurations are regular 4, 6 and 8 neighbours and irregular triangular networks (even and uneven distribution of vertices). Method (ii) is the proportion of the mesh travelled by fire divided by the total mesh area. Method (iv) is calculated as the area of a polygon surrounding the fire perimeter. There are 5,000 simulations using time steps of 0.5, 1.5 and 3 hours and spatial resolutions of 100, 200 and 300 meters. The outliers are fire areas where the polygon algorithm failed to correctly mark the perimeter of fires on four neighbour meshes and one occasion for a fire on an eight neighbour mesh. As noted in the text, the polygon method was not found to be the preferred method for area measurement and solutions to these algorithmic errors were not pursued.

5.5 WIND DIRECTION

Errors due to the number of neighbours to a vertex noted so far are at a minimum when wind speed is zero. The approximation of an ellipse by 4, 6 and 8 sided polygons will have the greatest error at particular angles (Figure 5.14). While the scale-dependent errors for TINS noted so far have been small (<4%) these errors will be greater as ellipse eccentricity increases because error is amplified in the direction of spread (Equation A.15).

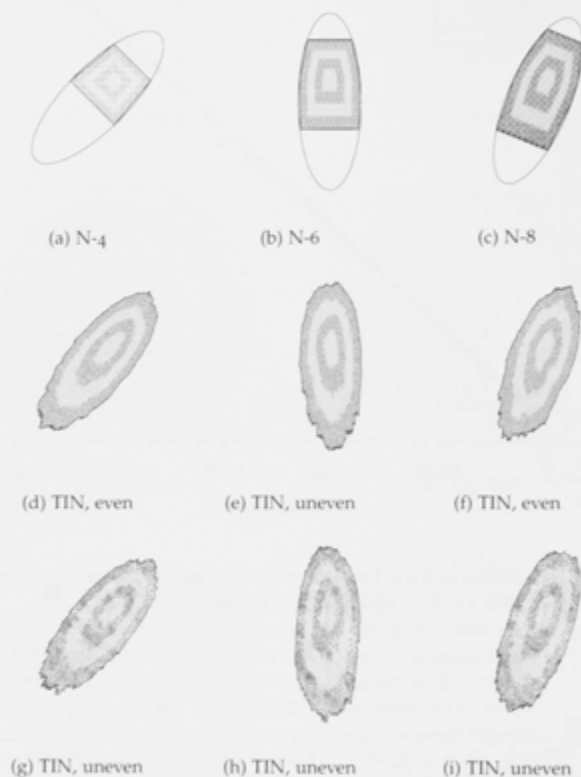


Figure 5.14: Approximations to an elliptical fire shape using meshes with a variety of geometries

These figures demonstrate the worst case fire headings for regular four (N-4), six (N-6) and eight neighbour meshes (N-8). Equivalent ellipses are shown for fire shape on an irregular triangular network mesh with an even and uneven distribution of vertices under otherwise identical conditions. Fire duration is 12 hours with three hour time steps (alternate grey and dark grey bands). Wind speed is 30 km.h^{-1} .

METHOD Simulations were performed with 10 wind directions ($0-90^\circ$), four spatial resolutions (0.25, 1, 4 and 9 hectares) and five mesh configurations (four, six and eight neighbours and a TIN with even and uneven vertex distributions) and 10 replicates of each of the TIN arrangements, totalling 920 simulations. The terrain is again flat and the same weather conditions were those listed in Table 5.1 but with wind speed of 30 km.h^{-1} . The fire is allowed to burn for 12 hours. The theoretical area of an ellipse was compared to the simulated area for each of the nine wind directions. A sample of some of these simulations are shown in Figure 5.14.

RESULTS The difference in estimated area burnt accords with the findings of Feunekes (1991) over this range of angles. N-4 mesh has its maximum error at 45° , N-6 at 60° and 0° and N-8 at 22.5° and 67.5° (Figure 5.15). The difference in measured areas between resolution is substantially less than between mesh configurations for all arrangements on a regular mesh (4, 6, N-8, Figure 5.15.a). While both TIN meshes show a more consistent estimation of ellipse area over the range of angles than regular meshes, they show a greater difference across resolution than do regular meshes (Figure 5.15.b and c). There is a lesser sensitivity to spatial resolution for uneven TINs than even ones. This clearly is not a result of a better sampling of the rate of change in the terrain because the terrain, in this case, is flat. This finding is important when performing experiments using complex terrain, because it will weaken any claim that an uneven mesh is superior to an even mesh solely because the rate of change in terrain has been better sampled. A component of the error in simulated fire area for TINs will be measurement error as discussed above. However, the much greater error over resolution in the case of TINs can only be due to inherent scale-dependence of this mesh arrangement in area estimates as already noted (figures 5.6 and 5.7).

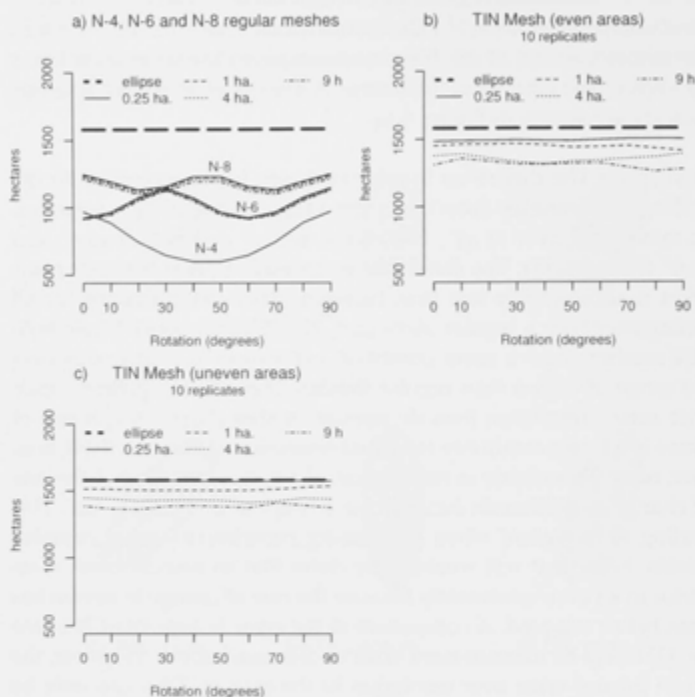


Figure 5.15: Area burnt on a variety of mesh configurations

All simulations use a wind speed of 30 km.h^{-1} and otherwise the same conditions as listed in Table 5.1. The dotted line is the area of an ellipse under these conditions, with length-to-breadth ratio from Alexander (1985). Each simulation was performed at spatial resolutions of 0.25, 1, 4 and 9 hectares for 10 wind directions between 0 and 90° :

- Four, six, and eight neighbour meshes on a regular grid.
- Ten mesh replicates on irregular triangulated network meshes with even distribution of vertices.
- Ten mesh replicates on irregular triangulated network meshes with an uneven distribution of vertices.

All simulations are performed on flat terrain.

5.6 COMPARISON OF METHODS IN DERIVING FIRE SHAPE ON TRIANGULAR IRREGULAR NETWORKS

In simulating fire propagation using the approach of Johnston *et al.* (2008), the length-to-breadth ratio (L:B) of the fire shape is an emergent rather than a prescribed property. The rate of spread in every direction except $\pm\alpha$ (Equation 4.1) is the rate of spread at zero wind speed. The rate of spread for headings within $\pm\alpha$ is determined by a polynomial function of R_h/R_0 , derived empirically to obtain the correct rate of spread in the direction of the wind. At the same time, Johnston *et al.* (2008) define R_0 as the semi-latus rectum of an ellipse, the distance between the ellipse focus and its perimeter perpendicular to its semi-major axis (Figure 3.7). The present formulation of the ellipse of fire spread in placing the focus down-wind of the true ellipse focus (Equation 4.2) and the use of the CFFPS (Hirsch, 1996) to determine the back-fire rate of spread (R_b), means that R_0 in Johnston *et al.* (2008) differs from R_0 as interpreted here (Section 4.2.3). To achieve equivalent R_b it follows that the rate of spread of the back-fire must also be increased for experiments comparing N-8 meshes with TINs. As the zero wind rate of spread is greater than R_0 this will lead to narrower shapes more closely aligning with an ellipse (Figure 5.16).

Despite the large differences between the two approaches in fitting the fire shape to that of an ellipse, the problem lies more with the function relating R_h to wind speed from FFDM as noted by McCaw *et al.* (2008) and the L:B ratios observed in North American fires (Alexander, 1985). If the above simulations are repeated but using the modified R_h from Equation 3.9, the L:B ratios are more similar and closer to the shape of an ellipse apart from the fire breadth at the ignition point (Figure 5.17).

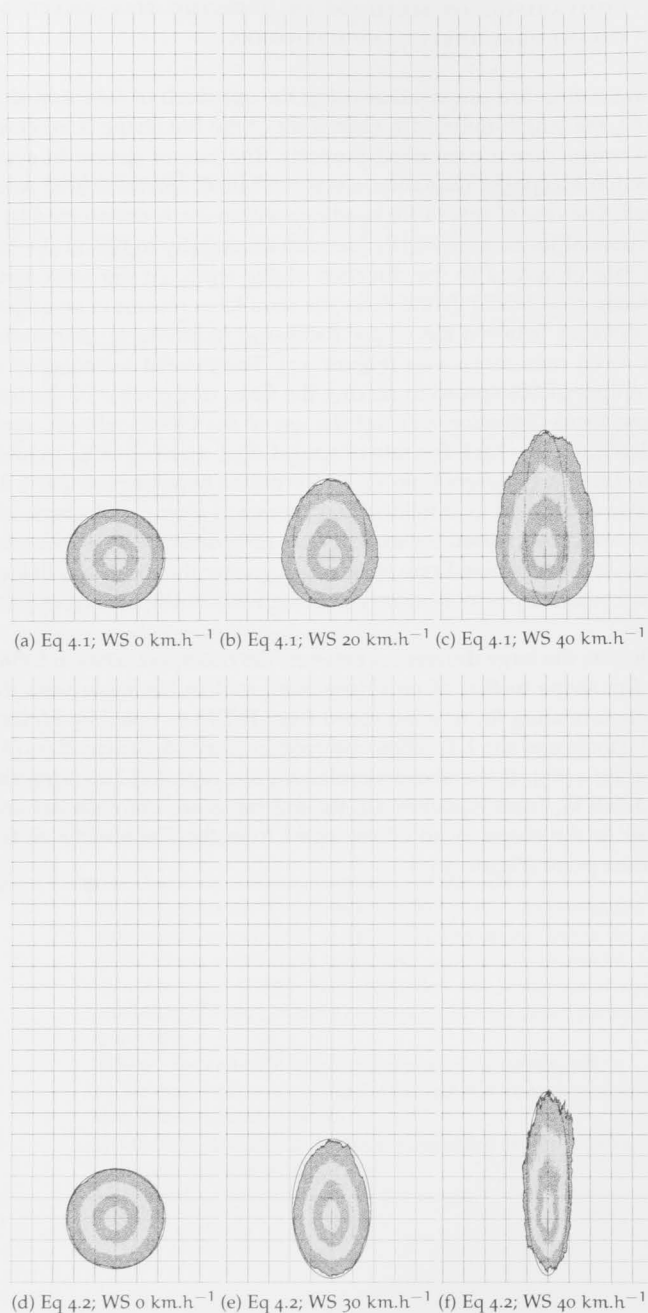


Figure 5.16: Comparison of fire shapes arising on a TIN mesh using the equations R_h from the FFMD

Weather variables are those listed in Table 5.1. The shape of an ellipse under the same conditions (using the L:B of Alexander 1985) is superimposed. Fire duration is 12 hours. The alternating grey and dark grey bands indicate the three hour time steps.

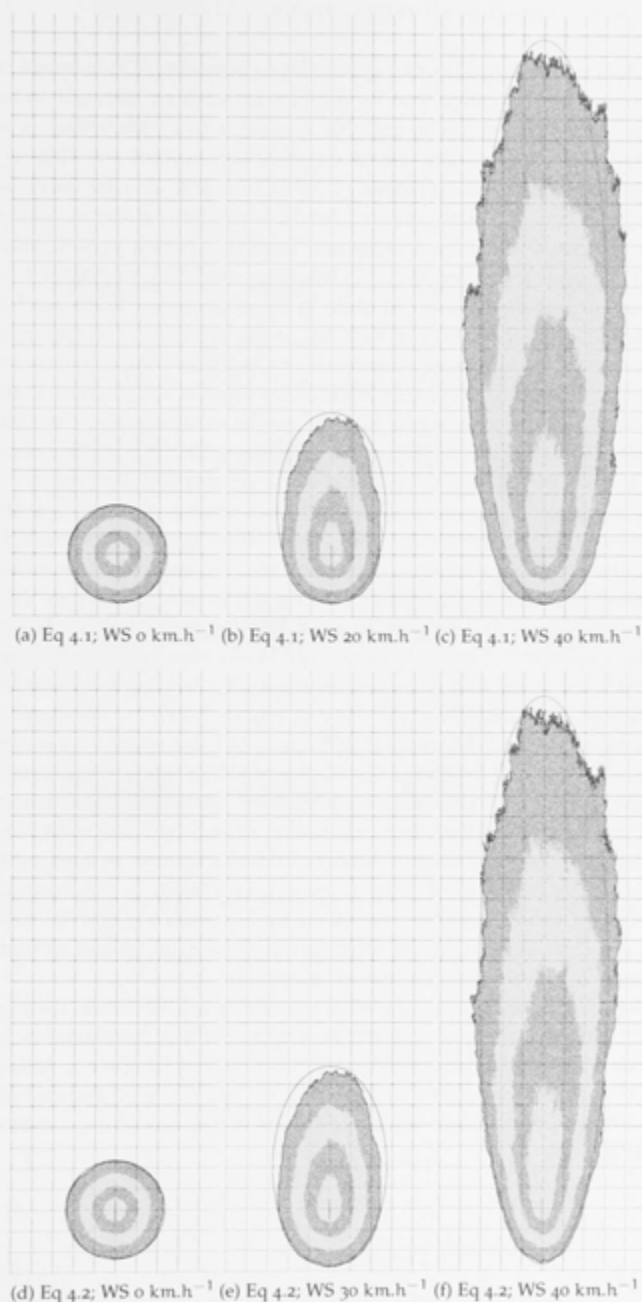


Figure 5.17: Comparison of fire shapes arising on a TIN mesh using the equations R_h from the FFMD, modified according to Equation 3.9. Weather variables are those listed in Table 5.1. The shape of an ellipse under the same conditions (using the L:B of Alexander 1985) is superimposed. Fire duration is 12 hours. The alternating grey and dark grey bands indicate the three hour time steps.

5.7 WIND AND SLOPE INTERACTIONS

The function determining R_h given slope (Equation A.4) is based on McArthur's observation that R_h doubles for each 10° increase in the slope of the terrain up to 20° . No comment from McArthur is recorded that supports the use of this function beyond 20° although it has been validated on slopes of 25° (Cheney et al. 1992, Burrows 1999, Beck 2000 in Catchpole 2002) and Cheney has further suggested that 30° may also be an appropriate limit (P. Cheney, pers. Comm., 2013). However, Catchpole (2002) has suggested that McArthur's observation may be an over estimate in practice as fuel loads tend to decrease with slope. FIRESCAPE limits the application of the equation to slopes $>$ minus 20° . Considering Catchpole's view concerning fuel loads on steep slopes, in FIREMESH slope is constrained to the domain $\pm 20^\circ$ because while the fuel model is effected by elevation (Table 2.1), it does not take account of slope. That is, two concerns are mixed: the behaviour of fire on a slope and the distribution of vegetation over a terrain, and given the vegetation model, it appears prudent to constrain the domain of the slope equation in the light of Catchpole's suggestion (Catchpole, 2002). This results in a foreshortening of elliptical shape of fires on slopes greater than 20° (Figure 5.18). This is more apparent when running the same simulations using a regular N-8 mesh (Figure 5.19). While simulations with equivalent wind speed and slope are approximately symmetrical (top left to bottom right excluding 30° slope of (Figure 5.18), the fire shape is no longer ellipsoid. Sharples (2008) has noted this result in a review of wind, slope and fire interactions. The FARSITE model, for example (Finney, 2004, p 6), uses vector addition to calculate R_h given slope and wind vectors rather than calculating spread by wind speed and then adding the slope effect. The difference can be seen by comparing Figure 5.18 with FARSITE (Finney, 2004, p 41, Plate6). In this example, the rate of spread has been modified by Equation 3.9 derived from McCaw *et al.* (2008) and the relationship of rates of spread to wind speed in Project Vesta (Gould *et al.*, 2007).

Slope is the most sensitive spatial parameter in FIREMESH (Section 4.1.2) and from above discussion, it is apparent that considerable uncertainty surrounds a suitable value. As noted in Chapter 2, 80% of slopes in the study region are less than 20° and the most appropriate modelling choice within the assumptions of the model are a matter of conjecture.

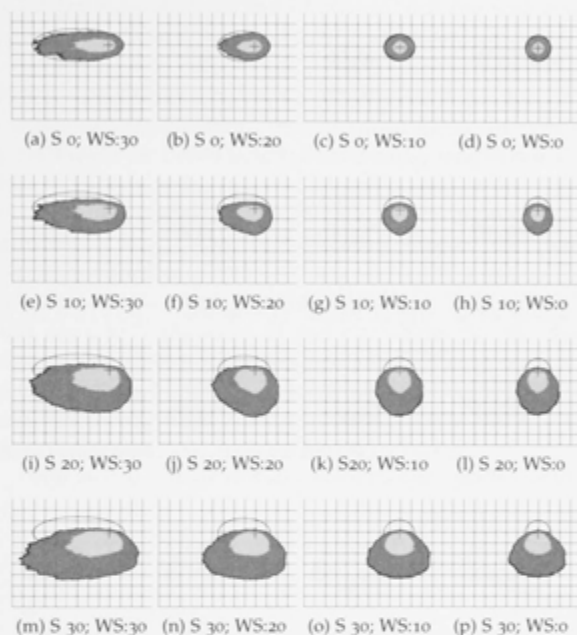


Figure 5.18: Slope and wind speed relationship on a triangulated irregular mesh

In this figure elevation increases down the page. Wind speeds (increasing from right to left) are 0 to 30 km.h⁻¹. Fire conditions are otherwise those of Table 5.1. An ellipse, unaffected by slope but affected by wind speed, is superimposed for comparison and context. The rate of spread is modified by Equation 3.9 derived from McCaw et al. (2008). The alternating grey and dark grey bands indicate the three hour time steps.

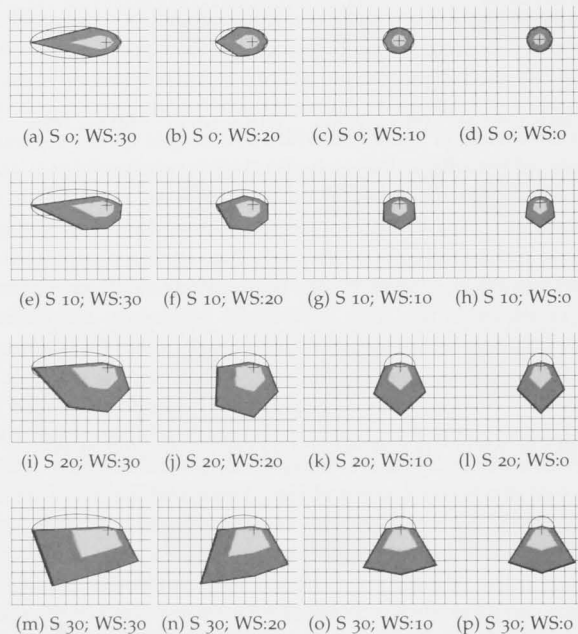


Figure 5.19: Slope and wind speed relationship on a regular N-8 mesh

In this figure elevation increases down the page. Wind speeds (increasing from right to left) are 0 to 30 km.h^{-1} . Fire conditions are otherwise those of Table 5.1. An ellipse, unaffected by slope but affected by wind speed, is superimposed for comparison and context. The rate of spread is modified by Equation 3.9 derived from McCaw *et al.* (2008). The alternating grey and dark grey bands indicate the three hour time steps.

5.8 WIND, SLOPE, ELEVATION AND FUEL

The relative effects of wind, slope, elevation and fuel have been discussed in Chapter 3. Here, their effects are verified by simulating fire spread on a slope with each of the factors tested in turn.

METHOD Twenty simulations were performed to demonstrate independently, and together, each of the three factors influenced by terrain (slope, elevation and fuel) for a six hour fire with a slope of 20° (approx. 35.4%) and the wind direction moving up-slope.

RESULTS The results confirm the discussion in Section 4.1.2 that slope is the strongest spatial determinant of R_{fi} in this model (Figure 5.20). However, the interaction of cooling temperature and increasing fuel loads with elevation approximately cancel. The simulations in this test begin at 18:00 hours at an elevation of 577m, and extinguish at midnight. Despite the fact that they are run under constant weather conditions, different time steps will produce different results because lapse rates vary with time of day from between -0.008 to $-0.002 \text{ deg C.m}^{-1}$ (figures 5.21 and 5.22). Note that the change in elevation over the course of these simulations is 2443 metres, which is considerably larger than the 1,350 elevation range used in later experiments, however, differences in lapse rates are less than if the trial had been performed over daylight hours.

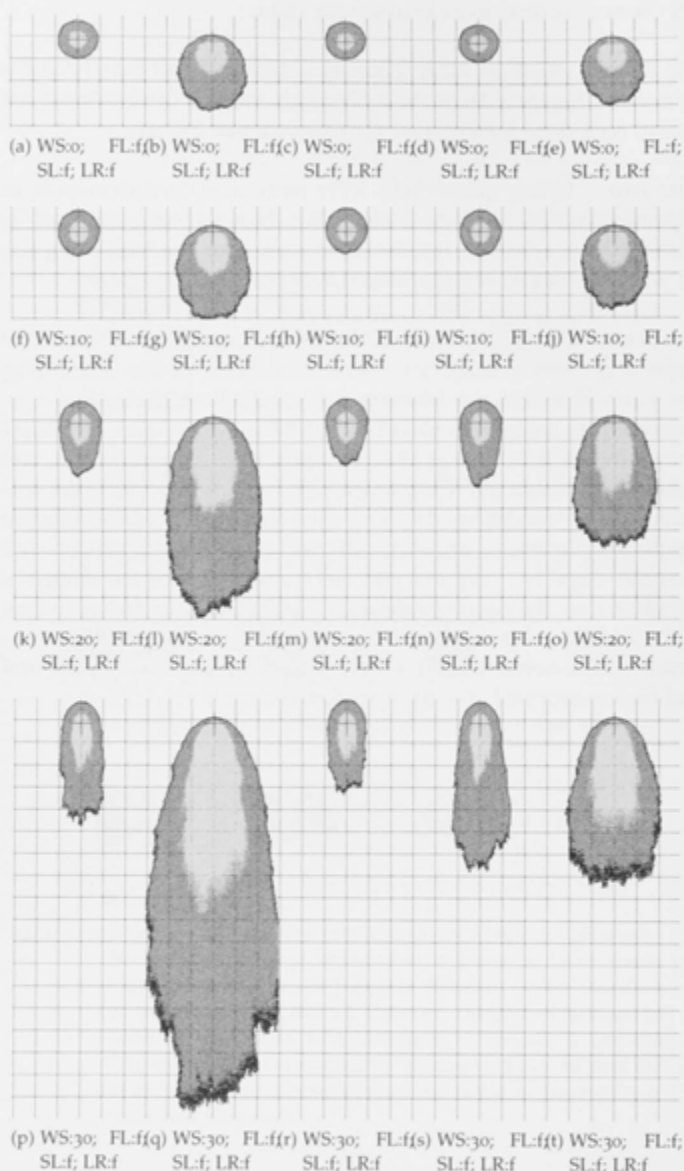


Figure 5.20: Twenty simulations with each of the spatial factors affecting fire spread (slope, elevation and fuel) tested independently and together

The fire duration is six hours, fire burning up-slope with the wind direction (down the page). The slope is 20° (approx. 35.4%) and the grid marks are 1000 metres. The lapse rates are those in Figure 2.8. The ignition time of the fire is 18:00 hours with a 3 hour time step (alternating grey and dark grey bands).

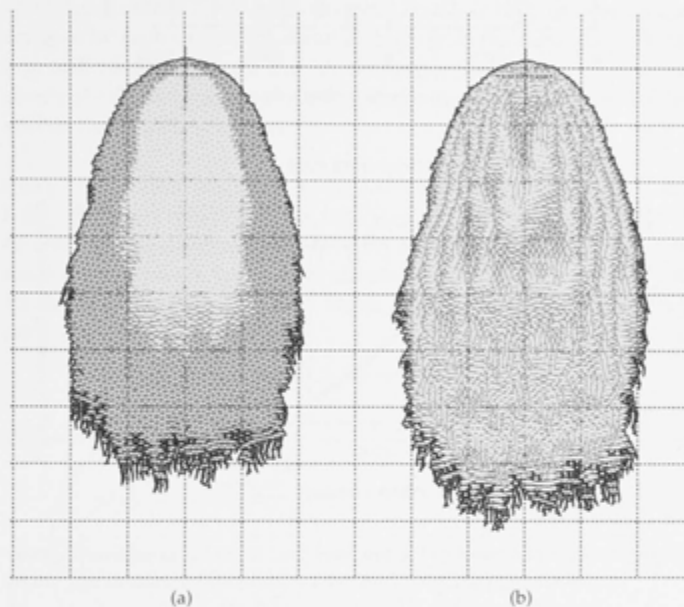


Figure 5.21: Two simulations under constant conditions of slope and wind speed at two different time steps

Slope is 20° , (elevation increasing down the page) and wind speed is 30 km.h^{-1} (moving up slope). Time for (a) is 3 hours and (b) 0.5 hours. Alternating grey and dark grey bands mark the time steps. Ignition time is 18:00 hours at an elevation of 577 AMSL and duration is six hours. Lapse rates are those of Figure 2.8 and fuel loads are those listed in Table 2.1. Grid scale is 1,000 metres.

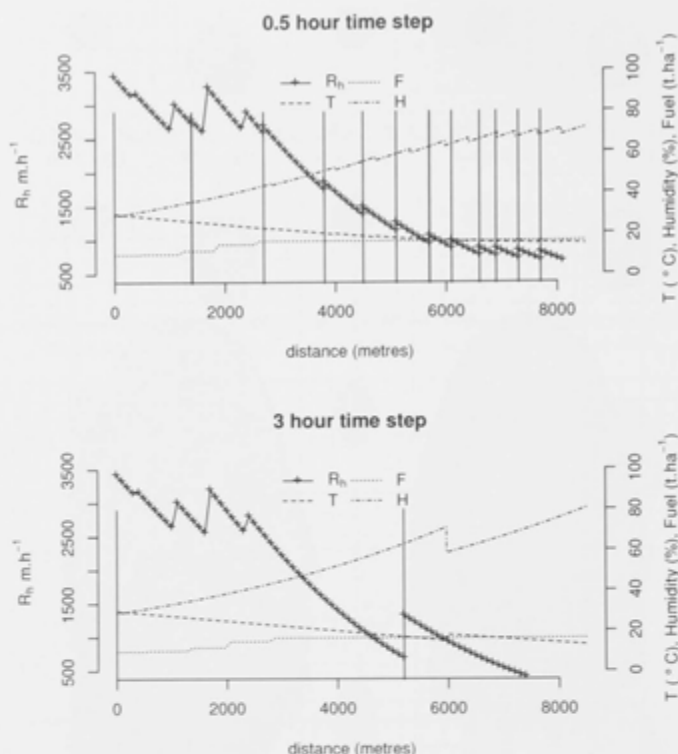


Figure 5.22: Rate of spread of the fire front and its complex interaction over time and space with fuel, temperature and temporal resolution

The two simulations have a constant slope of 20° (elevation increasing during the course of the fire). Wind speed is 30 km.h^{-1} . The simulations are at two time steps (0.5 and 3 hours). Solid line with (+ symbol) is the rate of spread (R_h), dashed line is the temperature (T) (changing with elevation), dotted line is the fuel load (F), and the dot-dash line is the humidity (H) (also changing with elevation). Vapour pressure is constant. Ignition time is 18:00 hours at an elevation of 577 m and duration 6 hours. Lapse rates are those of Figure 2.8 and fuel loads are those listed in Table 2.1. Change in elevation over the duration of the simulated fire is 2,443 metres. The mesh is a one hectare regular mesh. Therefore, elevation values (and thus temperature lapse rates, humidity and fuel) are updated every 100 metres (marked by +). The vertical lines indicate the time step at which weather data is updated. While temperature data in the weather file is constant (30°C), the new weather will have a different lapse rate at this time. It follows that changes in temperature due to elevation, occur at a rate depending on spatial resolution (new elevations), while the value of the lapse rate used will vary with time of day which is updated at the rate of the time step. Note that, as this fire is burning mostly overnight, lapse rates are less than if the simulation had been performed over daylight hours (Figure 2.8).

5.9 TERRAIN PROJECTION

For the reasons discussed in Section 3.2.3, FIREMESH measures the distance between vertices to accommodate the difference that arises from projecting the mesh onto a DEM. This experiment tests that this method is correct.

METHOD Two simulations were performed on a N-4 lattice with zero wind speed on a 30° slope. The effect of slope on the rate of spread calculations has been disabled to allow only geometric concerns to be examined. One simulation projects the mesh onto the terrain and then re-projects that shape onto a flat surface. The second does not take account of the difference between distance on a slope and distance without slope.

RESULTS The change in vertical radius between Figure 5.23.a and b is 317 metres which accords with $\cos(30) \times \text{radius of b}$. This leads to a difference in simulated area burnt on this N-4 mesh of 13.4%. As noted in Chapter 3, full length simulations show approximately an 8% decrease in estimated area burnt using the terrain in Chapter 2, with and without this measure.

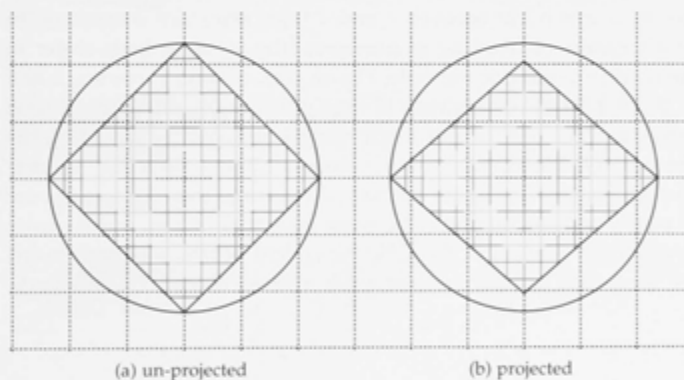


Figure 5.23: Fire shapes arising from projected and un-projected fire travel distances

Both simulations were performed without wind on a 30° slope but, most importantly, slope is not included in the calculation of rates of spread in order to highlight just the geometric issues addressed by this experiment. Elevation increases down the page. The circle (black) is a perfect circle; the limit of the fire extent on a flat plane. Figure (b) shows the expected foreshortening of the fire shape along the vertical axis (the direction of slope) taking account of both the rise and the run. Figure (a) considers only the run distance and extends exactly to the predicted distance indicated by the circle.

5.10 FUEL CHANGE WITH TIME SINCE LAST FIRE

PURPOSE In later chapters, experiments are performed to measure the relative importance of fuel treatments against other factors. This section checks the interaction of fire growth and fuel age given the fuel accumulation equation based on Olsen (1963) used in FIRE-MESH.

METHOD Three hundred and sixty simulations were performed, each with a different wind direction ($0-90^\circ$ in 10° steps) and using 9.64 t.ha^{-1} of fuel (the fuel weight at the elevation of the weather station), 30 km.h^{-1} wind speed (FFDI 26.5) and otherwise the same inputs as Table 5.1. Spatial resolution was varied from one, four and nine hectares. In 30% of the landscape, time since fire was set from between 0-10 years and 20 years in a single random block pattern. For each simulation, the time since fire in each block is the same. The area of each treatment block was 625 hectares. The fire was run for 12 hours under otherwise unchanging conditions (Figure 5.24). Ignition points were chosen not to coincide with treatment blocks.

RESULTS The average area burnt curves are a close fit to the fuel curve indicating the model is operating as designed. The lesser increase in area burnt between 0 and 1 years since fire is assumed to be a measure of blocking of fire spread by younger fuels closer to the ignition point (for example, Figure 5.24, column 1, rows 1, 2 and 3). From informal observation of the simulations, at times, resolution serves to both hinder and foster spread between treatment blocks (for example Figure 5.24, row 1, columns 2 and 3 show fire 'leaking' past to adjacent treatment blocks). On average these effects appear to cancel and the difference between measures of area burnt across resolution is a result of the scale-dependent property already noted for fire spread on irregular triangular network meshes (Figure 5.25).

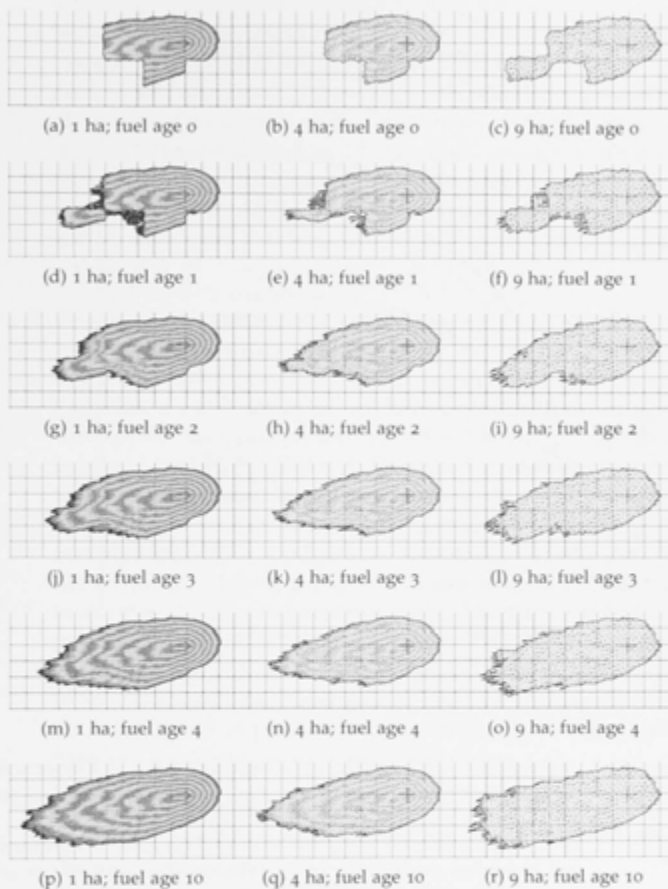


Figure 5.24: A sample of 360 simulations performed under various wind directions and fuel treatment blocks

All 360 simulations were performed under various wind directions, in flat terrain with a random block pattern of square 625 hectare fuel treatments. For each set of simulations, time since fire in each of these blocks as set at 0–10 and 20 years. Only a sub-set of these experiments is shown in this figure with time since fire of 0, 1, 2, 3, 4 and 10 years and one particular wind direction. In this figure, the block patterns for each simulation are the same.).

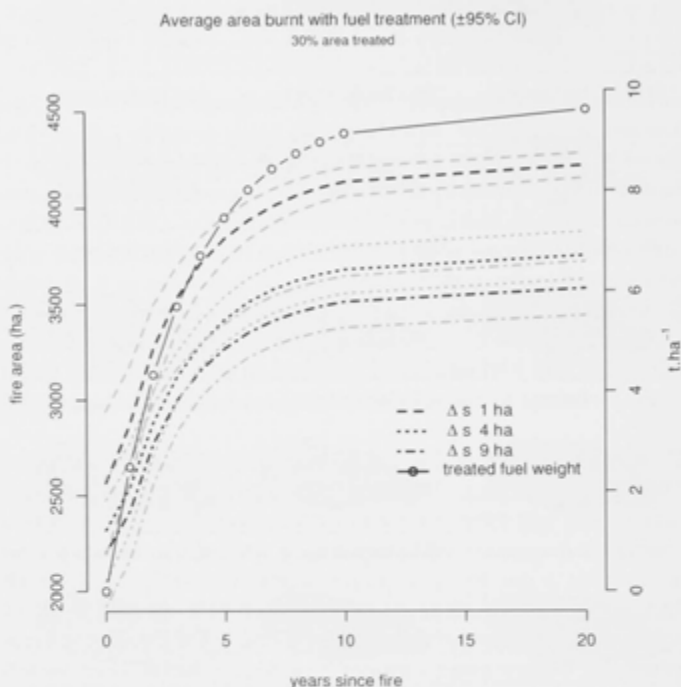


Figure 5.25: Average area burnt and the 95% confidence interval (CI) for 100 random fires under identical condition with wind speed of 30 km.h^{-1} on a triangulated irregular network mesh

Each replicate (dashed lines) combines 10 different wind directions and 10 random meshes with an even (Poisson-Disk) distribution of vertices. The trial was performed at three spatial resolutions (1, 4 and 9 hectares) and a single random map of fuel block treatments (625 ha). Untreated fuel weights were 9.64 t.ha^{-1} . For each map, the fuel treatment was the same for all blocks. Each map had either 0 - 10 and 20 year old fuels. The fuel growth parameters are listed in Table 2.1. Equivalent fuel weights for the fuel ages are 0, 2.5, 4.35, 5.72, 6.74, 7.49, 8.05, 8.46, 8.77 8.99, 9.16 and 9.62 t.ha^{-1} (open circles).

5.11 SUMMARY OF FINDINGS

The purpose of this chapter has been to verify that FIREMESH accords with its specifications.

- i No difference was found between expected and simulated distance travelled by fire for all forms of regular meshes over temporal resolution. Small differences were found for these same meshes over a range of spatial resolutions. However, these errors are at least three orders of magnitude smaller than the differences between simulated fire areas for regular meshes with different number of neighbours. It is the importance of the number of neighbours that is to be tested in Hypothesis (ii) (tables 5.2 and 5.3).
- ii Differences in expected and simulated fire radii for circular fires on triangular irregular network meshes were found. The size of this error varied with the number of vertices within the fire footprint, a combination of resolution and fire size. These errors appear to approach zero as either fire size or resolution increases (figures 5.6 and 5.7). Expressed in area terms Figure 5.6.a shows a decline in measured area of 5% between 100 and 300 meter resolutions and 2% for larger fires (Figure 5.6.d). Assuming FIREMESH produces the long-tailed fire-size distributions typically observed (Figure 2.2) and large fires contribute to the majority of area burnt measures, this error may be unimportant. Experimental results can simply be calibrated by comparison with total area burnt on flat terrain over a suitable range of spatial resolutions. Equation 4.1 (Johnston *et al.*, 2008) could be re-calibrated to produce the correct R_h on average, rather than as a maximum, as appears to be the case.
- iii Extents of simulated fires under various wind directions agree within the expected constraints imposed by discrete geometries (Figure 5.15).
- iv The method of measuring the area of simulated fire has no systematic bias over spatial or temporal resolution or for each mesh configuration (Figure 5.13).
- v The response of fire shapes to wind and slope agrees with the specifications (Figure 5.18)
- vi The shape of fires simulated on irregular triangular network meshes agrees with equations 4.1 and 4.2 (figures 5.16 and 5.17).
- vii The response of fire area to fuel treatments is in agreement with the fuel model used in FIREMESH (figures 5.24 and 5.25)

- viii The response of the model over elevation agrees with its specifications (Figure 5.22).
- ix The change in simulated fire shape on sloping ground agrees with its specifications (Figure 5.23).

MODEL AND DATA VALIDATION

6.1 INTRODUCTION

In the previous chapter, FIREMESH (FM) was tested to verify that its implementation was correct with respect to the documented equations and model architecture. In this chapter, validation experiments are performed to determine if FM is a suitable model with which to address the hypotheses of this work (after Rykiel Jr 1996; Sargent 2005).

This study asks if the inferences about the relative importance of the drivers of fire by an established, validated, widely used and representative model, remain as published under various manipulations of nuisance parameters. For this to stand, it is important that FIREMESH be validated against that model (FIRESCAPE) rather than validating it against observational data. To validate FIREMESH against case studies of observed fire events may, arguably, contribute to establishing the reliability of FIREMESH in its own right. However, this would not contribute to its comparison with an established model, which is the central question – are the results from FIRESCAPE and by implication, similarly constructed models, dependable with regard to temporal and spatial issues?

Validation is an imperfect science. FIREMESH has been *verified* against McArthur's Mark V Fire Danger Metre (FFMD) (Chapter 5). Validation rests not only on comparison of FIREMESH with FIRESCAPE but on the field work from which the FFDM was constructed (800 fires under mild conditions) (McCaw *et al.*, 2008). The FFDM remains the key method of estimating rates of spread in Australian Eucalypt forests. Nevertheless, the FFDM has a significant short coming in estimating rates of spread under severe fire conditions, as has been formally established by McCaw *et al.* (2008). This short-coming has been addressed, as discussed in Chapter 3, by Equation 3.9.

Attempts to validate fire spread models against observations are notoriously difficult. An instructive illustration is the Mt Cook fire used by Johnston *et al.* (2008) as a case study to analyse the behaviour of their fire spread model. Where the model predictions differ from observations, the authors conclude that weather and/or fuel conditions differ in reality from recorded observations. This is inevitable and even if predictions and observations align well, the model may be right for the wrong reasons in this single case. To establish some statistical significance, this process would need to be repeated a large number of times, taking account of varying degrees of inaccuracy

in weather and fuel data and fire suppression activities. Such an approach for this study is neither relevant nor tractable.

As noted, the model used for these tests is based on FIRESCAPE but considerably modified and re-implemented to address the questions posed in Chapter 1. The reason for basing FM on FIRESCAPE is in large part, because FIRESCAPE has been included in published experiments (Cary and Banks, 2000; McCarthy *et al.*, 2002; Keane *et al.*, 2003; Cary *et al.*, 2006; King *et al.*, 2006, 2008a,b; Cary *et al.*, 2009; King *et al.*, 2011, 2012; Bradstock *et al.*, 2012; Keane *et al.*, 2013a), and it is these types of experiments that are the yardstick by which sensitivity of spatio-temporal resolution and spatial representation are measured in this study. Therefore, to validate FM, the revised model and its data must have a comparable level of skill to FIRESCAPE. This is demonstrated in three ways:

- i By comparing broad measures of fire regime metrics with those reported by FIRESCAPE in Cary (1998);
- ii By testing if FM is capable of supporting a particular hypothesis already tested by FIRESCAPE;
- iii By submitting FM to two published fire model comparison experiments in which FIRESCAPE was included (Cary *et al.*, 2006, 2009).

As noted in Chapters 2, 3 and 4, FM differs from FIRESCAPE in a number of ways in both its architecture and in the data to be used in subsequent chapters. The reason for the difference in architecture is to add precision and flexibility to the model's ability to run at any spatio-temporal resolution and with a wide variety of arrangements of space represented as a mesh (Section 3.2.3). The reason for not using the original synthetic weather data used by FIRESCAPE is because this data lacks variability at fine resolution (Section 2.4.1). A fairer test of temporal resolution is to use observed weather data instead. A smaller landscape than that used during FIRESCAPE's development is necessary because of the additional computation burden imposed by the more flexible architecture. This may exacerbate edge effects in the results. Finally, the purpose in choosing a more mountainous subset of the original spatial domain was to maximize any sensitivity the model may have to spatial resolution.

FIREMESH was implemented in Java from the original FIRESCAPE source code in the C language and compared to outputs from printed material and spatial data of inter-fire interval and fireline intensity (courtesy GJ Cary). To the best of my knowledge, FM is equivalent in concept to FIRESCAPE to the extent that this can be concluded from these sources, including the use of an N-8 mesh, but with the following exceptions:

- i Differences in the size and resolution of the digital elevation model (DEM) (Section 2.2);

- ii Differences that arise from the use of a subset of the original spatial extent such as the proportion of mountains and valleys and the distribution of elevations, slopes and proportions of the landscape with various fuel loads (Table 2.1);
- iii A new representation of space as a mesh (Section 3.2.3);
- iv A new event-driven time management architecture (Section 3.2.4);
- v Possible differences in average inter-fire interval between the current mountainous and original more mixed landscape; and
- vi The elevation anomalies used to drive the ignition model are calculated against a higher resolution DEM (Section 3.2.1).

FIRESCAPE has been adapted and used for many research projects over the past 16 years. Each of these projects will have introduced some modifications to the design of the model to suite the purpose of each project. Furthermore, the sources of data from FIRESCAPE against which to validate FIREMESH span more than a decade. Given this and the differences listed above between FIREMESH and data produced by the original version of FIRESCAPE, what is examined here are the higher level behaviours of the two models without an expectation that the results will agree to some fixed number of decimal places.

To validate FM requires separating these differences in data and parameters into three versions of the model. The versions examined in this chapter are: FMF, FMM and FMV. Note, FM is used when referring to all three.

- i FMF (FIREMESH/FIRESCAPE): This is the parameterization that most closely matches the original version of FIRESCAPE with due regard to the exceptions noted above. FMF uses 1,000 years of synthetic weather generated with the same (but re-implemented) stochastic weather generator as FIRESCAPE and the same methods for down-scaling the generated daily weather variables to finer time steps. In addition, the same lapse rates for temperature and precipitation to higher elevations are also used. The algorithm used to generate the temporal and spatial distribution of lightning events was also re-implemented, although some differences may arise following point (vi) above. The domain of application of function to alter rates of spread by slope is the same as that used by FIRESCAPE (-20° to $+50^{\circ}$) (Equation A.6).
- ii FMM (FIREMESH/MCARTHUR): This version uses observed half-hourly weather data (Chapter 2), together with a modification to the model to account for projected burnt area on mountainous terrain (Section 5.9). This change is to remove a source

of error that may confound measurement of the effects of spatial resolution. Slope can be expected to change with spatial resolution. Not accounting for this by the correct measurement of fire spread in three dimensions may mask operational errors with inherent errors. Finally, the domain of application of function to alter rates of spread by slope is $\pm 20^\circ$ (Equation A.6) as discussed (Section 5.7).

- iii FMV (FIREMESH/VESTA): This version is identical to FMM but introduces the modification to the rate of spread to account for the observations of McCaw *et al.* (2008) as noted in Section 3.2.9 and verified in Section 5.6. Note that, the appellation is not intended to imply that this version is an implementation of the equations in Cheney *et al.* (2012). The purpose of FMV is to isolate this important update to the model from differences introduced by FMM.

6.2 VALIDATION

6.2.1 Synthetic and Observed data

In Section 2.4.1, the synthetic weather data was found to have less variability between half-hour readings than the observed data. This follows from the down-scaling methods, particularly for temperature and humidity, due to the smooth curve produced by interpolating between daily maximum and minimum temperatures. The model formulation stipulates that locations on the fireline will stop spreading when intensity falls below 100 kW.m^{-1} and extinguish below 83 kW.m^{-1} . Therefore, the magnitude of the variability between readings can be expected to affect model outcomes.

However, it can also be expected that this statistical approach to weather generation will not reproduce trends in the weather at larger scales, either at the scale of some synoptic systems or capture patterns in the Southern-Oscillation Index (SOI). To account for this, some nested hierarchical approach would be required. Therefore, inter-annual variability will be less than observed weather (see Figure 6.10).

The synthetic data (based on observations over a different time period than the data set used for FMM and FMV), has more humid summers, wetter winters and a lower Fire Danger Index during the fire season (Figure 6.1). These three attributes of the synthetic weather, namely: (i) variability between readings, (ii) variability between years and (iii) the different periods of observations between Canberra Airport and the data used to parameterize the synthetic weather generator, need to be borne in mind when evaluating following tests. For example, it is clear that the seasonality of rainfall is quite different between these two periods. Note that, the purpose of Figure 6.1 is not to examine if the synthetic data is the same as the observed data;

they are based on different periods of observation. Rather it is simply to provide context in the experiments that follow.

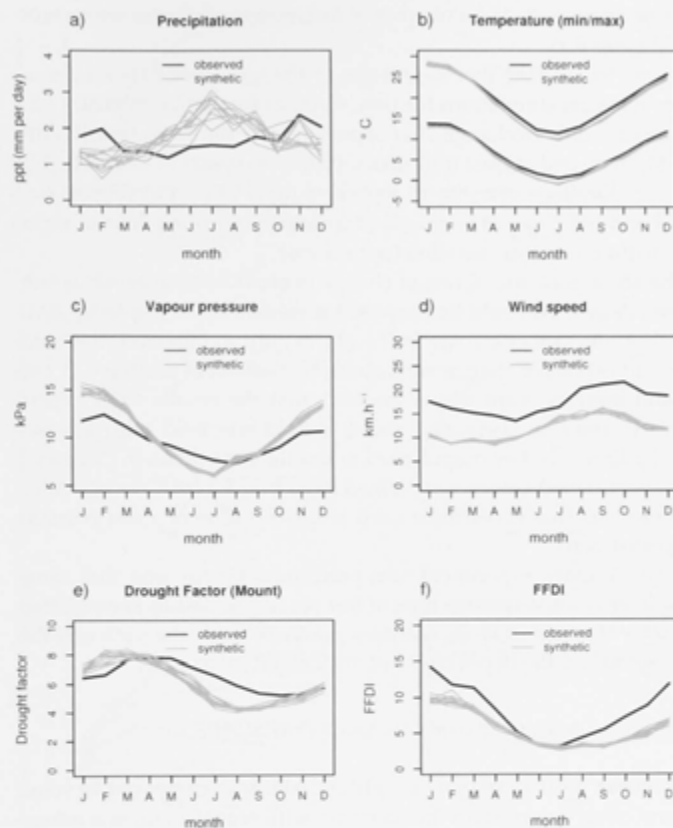


Figure 6.1: Mean monthly weather data for Canberra Airport (1985-2011) (black) and 10 replicates of synthetic weather data (Cary and Banks, 2000) (grey)

6.2.2 Simulation time required for stability of model outputs

FIRESCAPE is a deterministic model except for weather generation (only used in FMF) and the timing and location of lightning events. The initial conditions of a simulation begin with equilibrium fuel loads with a spatial distribution determined by elevation classes (Figure 2.4). For FIRESCAPE, 1,000 years of simulation was found sufficient to ensure stable outputs of fire landscape averages in frequency, intensity and seasonality. In addition, the difference between replic-

ate simulations of this duration was very slight and replication considered unnecessary. To confirm this is the case for FM, ten replicate 1,000 year simulations were performed with both FMF, FMM and FMV and time series of a number of fire regime attributes were recorded (Figure 6.2).

It was found that the magnitude of the 95% confidence interval of the replicate simulations for time series of frequency, intensity and seasonality, did not change after approximately the 800th year (Figure 6). FMF recorded at least four fires within 1,000 years of simulation in 98.5% of locations over the 10 replicates (95% CI 0.03%) (Figure 6.a). FMM and FMV had at least 99% of locations recording four or more fires within the same duration (not shown).

The above measure of rate of change in confidence intervals is subjective. A method could be proposed to decide upon a spin-up time based on the rate of change in the above output. However, this minimum threshold of change would also be somewhat arbitrary. A better and more relevant test is to check that the results from experiments to come in chapters 7 and 8 should still hold with a lesser spin-up time. The key output used to test the hypothesis in Chapter 7 is the partitioned variance explained in ln-transformed average inter-fire interval. That experiment used a spin-up time of 1,000 years as suggested here.

A preliminary experiment was performed by running that same experiment with a spin-up time of 800 years. The results showed that no factor changed in its explanatory power by more the 3.2% and the findings to test the hypothesis are unchanged in any way.

6.2.3 *Broad measures of comparison with FIRESCAPE*

At the time of its development, FIRESCAPE was compared to some general observations from the literature with regard to fireline intensity and the seasonality of forest fires in SE Australia (Walker, 1981; Christensen, 1993; Trevitt, 1994). Modelled fire frequencies were also compared to tree-ring data collected in the Brindabella ranges (Banks *et al.*, 1982). Both FIRESCAPE and FM tune lightning ground strike rates to provide an average landscape wide inter-fire interval (AVIFI) of 50 years based on observations by Pryor (1939) and Shugart and Noble (1981). FIRESCAPE and FMF prescribe a minimum 2 year IFI while FMM and FMV allow a minimum of 1 year before fire can return to a site. Cary and Banks (2000) compared IFI derived from tree-ring data collect by Banks *et al.* (1982) at five locations on the Brindabella Ranges. However, these measures are of limited use in this study. Three of these sites are too close to the edge of the spatial extent to provide a reliable guide. Moreover, as the data from FIRESCAPE was from simulations on larger landscapes, it is entirely unknown how simulated fires entering the region used in this study from outside

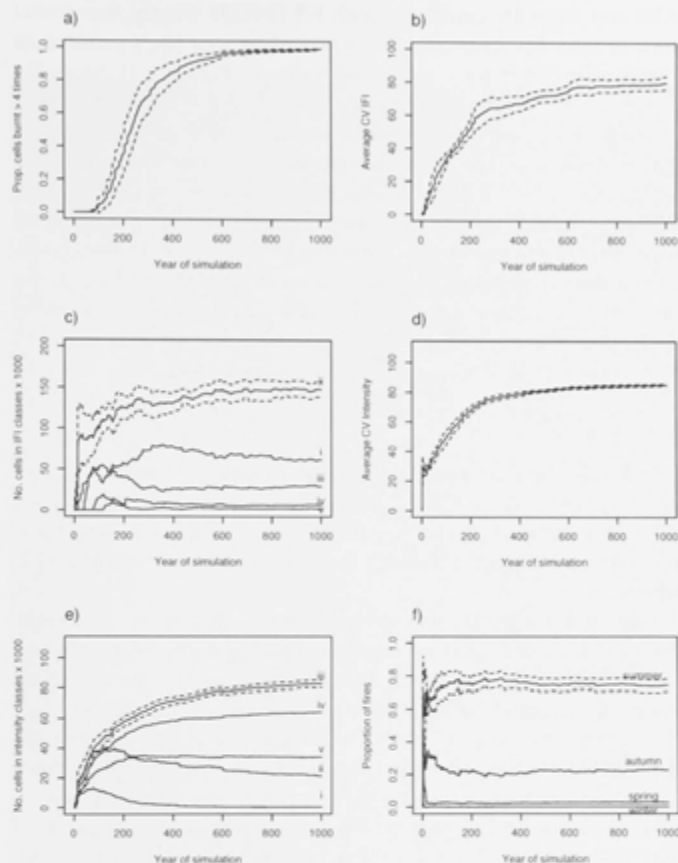


Figure 6.2: Time series (95% CI of 10 replicates) of various measures of frequency, intensity and seasonality for 1,000 year simulations with FIRMESH (FMF)

For clarity, only representative confidence intervals are shown for figures c, e and f. The variables are (after Cary 1998): (a) proportion of cells burnt more than 4 times; (b) landscape average coefficients of variation (CV) for inter-fire interval (IFI) (years); (c) number of cells (x1000) occurring in IFI classes (years) (i = 0–40, ii = 40–80, iii = 80–120, iv = 120–160, v = 160–200); (d) landscape average of coefficients of variation (CV) of fireline intensity (kW.m^{-1}) (for each individual cell); (e) number of cells (x 1000) occurring in fireline intensity classes (kW.m^{-1}) (i = 0–400, ii = 400–800, iii = 800–1200, iv = 1200–1600, v = 1600–2000); and (f) proportion of fires occurring by season for all cells.

may affect fire regime metrics within the study area. Three key spatial and temporal patterns emerge in fire regimes produced by FIRESCAPE and these are compared with FIREMESH. Firstly, the spatial pattern of inter-fire intervals differs according to a site's position in the landscape (ridge tops, slope and valleys) (Figure 6.3). Secondly, for any individual simulated fire, the pattern of fireline intensities is determined by a combination of the change in fire danger over the diurnal cycle, pre-existing patterns of fuel loads from fire history and the interaction of wind direction and slope. However, in FIRESCAPE, over many hundreds of fires, the spatial pattern of fireline intensities closely mirrors that of the slope of the terrain (Figure 6.4). Finally the temporal pattern of area burnt by season is strongly ranked in the order summer, autumn, spring and winter. These patterns and other outputs from FIRESCAPE are compared and discussed in the next three sections for all versions of FIREMESH just described.

6.2.3.1 *Inter-fire interval*

The rank order of inter-fire intervals within four landform classifications was compared for FIRESCAPE and all versions of FIRESMESH. The landform classifications are those produced by the Landform 7 method (Gallant and Dowling, 2003) (Courtesy L. Porfirio and B Mackey).

A map of average IFIs was created from a 1,000 year simulation by FM and a 900 km² portion was extracted for analysis from within the study region to minimise edge effects. A similar data set was extracted the original FIRESCAPE data (courtesy GJ Cary).

Four of the seven Landform 7 classifications are well represented in the study site: ridge top, upper slope, mid slope and upland valley. It was found that the rank order of the IFIs was the same for all version of FM and the data from the original version of FIRESCAPE (Figure 6.5). While magnitudes differ between FIRESCAPE and FMF, it is unknown what affect the larger landscape from which the FIRESCAPE data was excised, would have on the types of fires recorded in the sampled area.

However, FMF, FMM and FMV are directly comparable as these simulations took place under otherwise identical circumstances. The differences in magnitude of IFIs between the three versions of FM are easily understood when it is noted that larger fires will cause inter-fire intervals at a point to regress to the mean, which is set at 50 years. Larger fires from simulations driven by the observed weather data (FMM) (Figure 6.6) can be expected due to the higher FFDI during the fire season (Figure 6.1) and because of the greater inter-annual variability in the observed data (see Figure 6.9). Two additional factors that lessen spatial variability of IFI for FMM and FMV, apart from the different weather (FMM) and rates of spread (FMV), is the limit $\pm 20^\circ$ in the slope equation (Equation A.6) and reduced night-time temper-

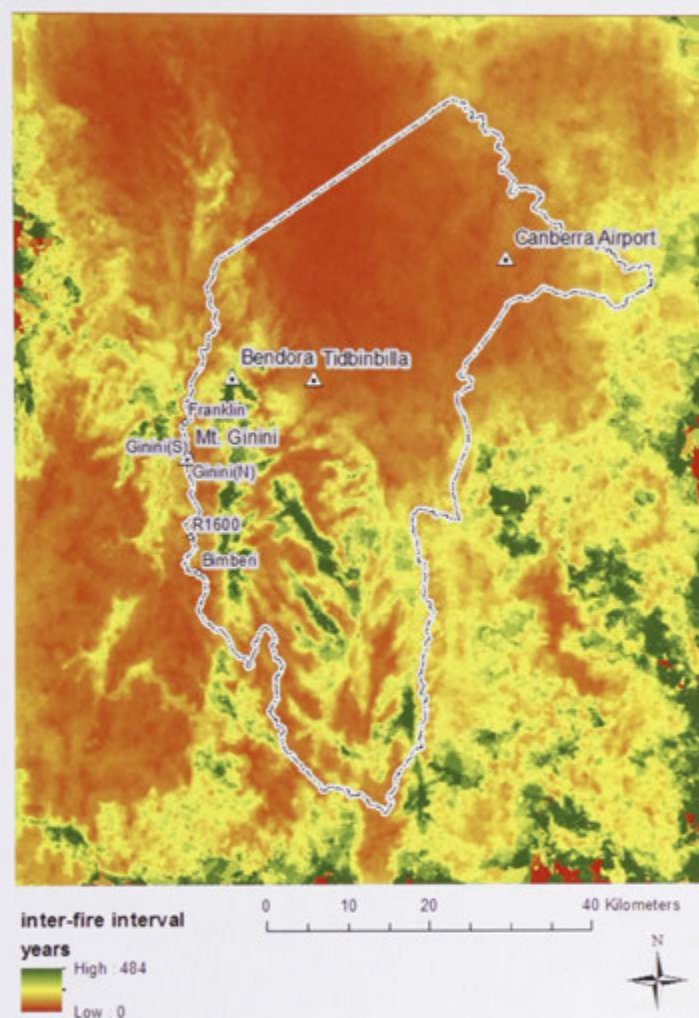


Figure 6.3: Patterns of inter-fire intervals produced by the original version of FIRESCAPE (courtesy GJ Cary)

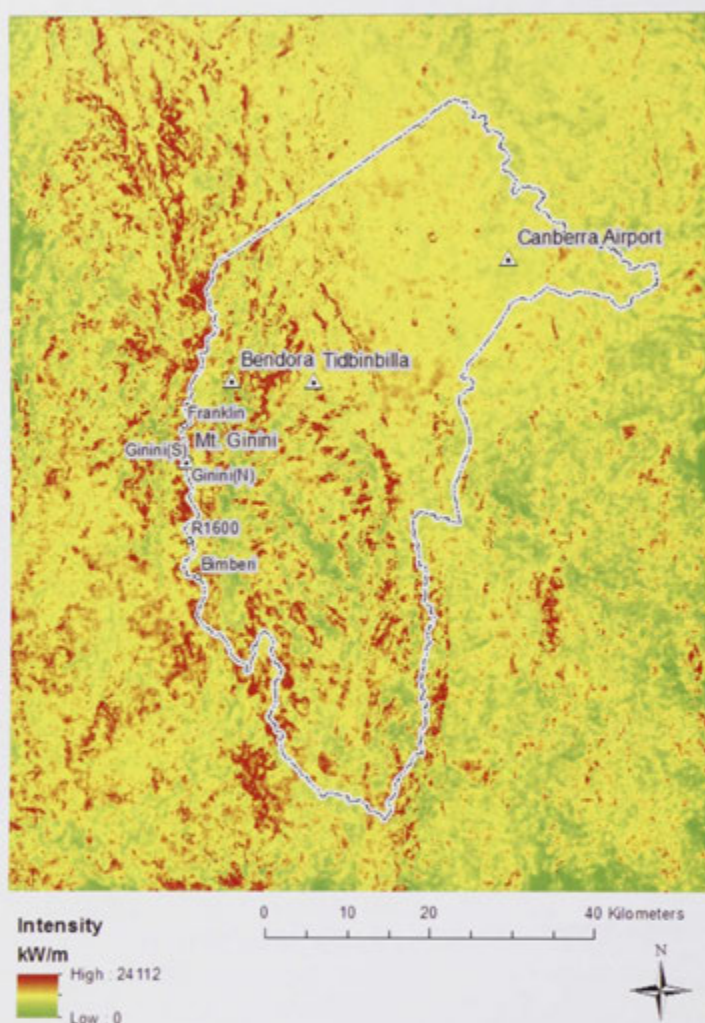


Figure 6.4: Patterns of mean fireline intensity produced by the original version of FIRESCAPE (courtesy GJ Cary)

ature lapse rates (Figure 2.8), which will lead to a proportion of fires failing to extinguish overnight.

The spatial pattern of IFI accords with that of FIRESCAPE in that all versions of FM show the same rank order of IFIs by landform classification. This is the core behaviour that FM must demonstrate for the purposes of the current study.

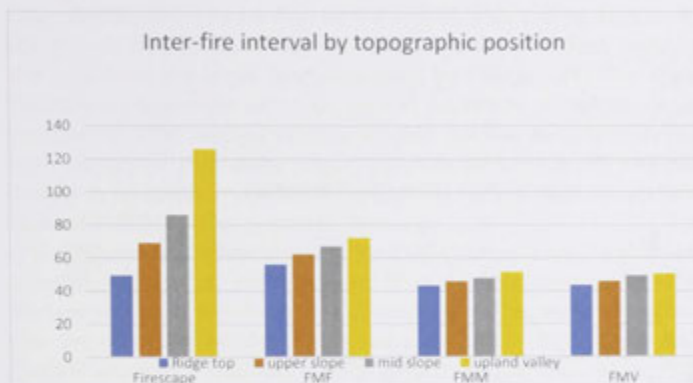


Figure 6.5: Average inter-fire intervals for FIRESCAPE and FIREMESH in four landform classifications
Classification is made using the Landform 7 method (Gallant and Dowling 2003).

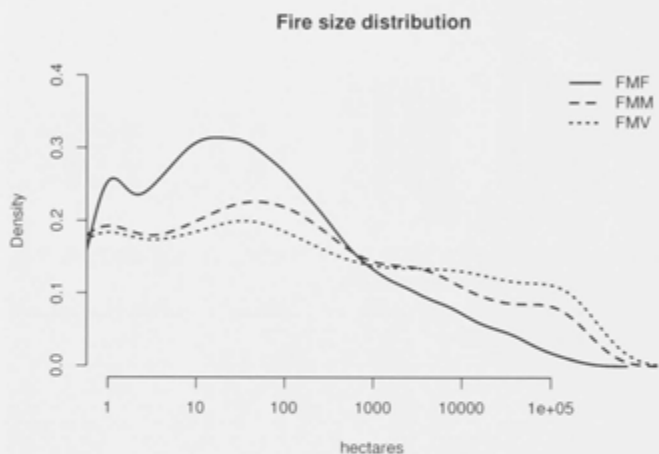


Figure 6.6: Fire size distributions (log scale) for three variants of FIREMESH from 1,000 year simulations

FMF is the version of FIREMESH closest to FIRESCAPE but operating in a subset of the FIRESCAPE landscape. FMM differs in using observed rather than synthetic weather records used by FIRESCAPE and FMF, while FMV includes an additional modifications to rate of spread equation.

6.2.3.2 Intensity

Spatial data of average fireline intensity produced from a 1,000 year simulation by FIRESCAPE (Courtesy GJ Cary) was compared to similar outputs from FMF, FMM and FMV. Data was again extracted for a 900 km² area within the study site to minimise edge effects. The average fireline intensity was classified by slope as a proportion of average fireline intensity for fires on flat terrain. This was to reduce any effect there may be from only particular intensities of fires entering this area from the larger landscape used by FIRESCAPE. The slope classes were limited to 20° as samples of intensities of steeper slopes were few and the average value unreliable. All four models show the same correlation with slope (Figure 6.7). The correlation (r^2) between change in fireline intensity by slope class for FIRESCAPE and all variation of FIREMESH were greater than 0.9.

The maximum fireline intensity for FMF (56,000 kW.m⁻¹) was considerably higher than FMM (22,500 kW.m⁻¹). This is consistent with the restrictions of the domain of equation of slope (Section 5.7) despite the observed weather data producing larger fires (Figure 6.6). Fireline intensity produced by FMV is much greater than either FMF or FMM (111,000 kW.m⁻¹). This follows from modification to rates of spread in this version of FM (Figure 3.10) where rates of spread under high wind speeds (50 km.h⁻¹) can increase by more than twice those predicted by the FFDm (McArthur, 1973; McCaw *et al.*, 2008).

The patterns of intensity produced by FM accord with those of FIRESCAPE in associating areas of high intensity with slope. The spatial correlation between slope and fireline intensity over long simulations is a key property to ensure FM behaves in the same way as FIRESCAPE.

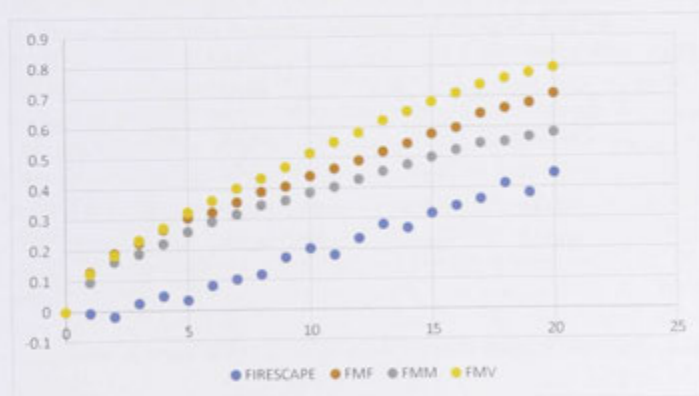


Figure 6.7: Relative change in average fireline intensity by slope class
Slope classes greater than 20° have insufficient samples to provide reliable average fireline intensities (<10).

6.2.3.3 Seasonality

There is considerable spatial variability between replicate runs of FM (not shown) for the patterns of fires occurring by season so little can be concluded from spatial comparison of this seasonal variable with just one instance of the FIRESCAPE data that is available. The same rank order for the seasons across all variants of FM and FIRESCAPE are the same (Table 6.1). The most notable difference is the increased proportion of fires in autumn and a corresponding decrease in spring in FMF compared to FIRESCAPE.

The terrain used by FIRESCAPE (9,000 km²) has a greater proportion of flat terrain than the Brindabella landscape used by FM. However the valleys in the Brindabella Ranges are at a similar elevation to the plains in the ACT. It might be conjectured that any out-of-season fire is more likely to propagate if it is ignited at low elevations. In the Brindabella Ranges, this is most likely a valley and therefore propagation is increased by close proximity to slopes. This effect is enhanced in autumn when soil temperatures are still cooling after summer and fuel moisture is reduced relative to rainfall (Figure 2.5.e). However, in general it is unknown how the larger landscape used by FIRESCAPE may influence seasonality. The core test for this component of the fire regime is that all models record the proportion of area burnt by season in the same rank order.

Table 6.1: Comparison of simulated seasonal proportions of fire occurrence between FIRESCAPE (Cary and Banks 2000) and three variants of FIREMESH (FMF, FMM and FMV) for ten, 1,000 year simulations. FMF is the version of FIREMESH closest to FIRESCAPE but operating in a subset of the FIRESCAPE landscape. FMM differs in using observed rather than synthetic weather records used by FIRESCAPE and FMF, while FMV includes an additional modifications to rate of spread equation.

SEASON	FIRESCAPE	FMF	FMM	FMV
Summer	76%	74%	68%	69%
Autumn	14%	22%	27%	21%
Winter	0.1%	0.3%	0.07%	0.1%
Spring	8.9%	2.8%	6.6%	9.7%

6.2.4 Ignition Neighbourhoods: Model skill in realized niche generation

Validation may also include higher level measures (Rykiel Jr, 1996). This experiment tests whether or not FM can substitute for FIRESCAPE in testing hypotheses in Cary (1997). One of these hypotheses was to examine the role fire may play in restricting the maximum possible species distribution in the environment. This topic was ex-

amined recently by Wood *et al.* (2011) in looking for the existence of fire refugia that might explain differences in community composition in environmentally equivalent locations.

Cary (1997) examined vegetation types and their inter-fire intervals in the Cotter catchment (immediately east of the western border of the ACT (see Figure 2.1), to see if environmental space (elevation, radiation budget and meso-scale elevation) alone was sufficient to explain vegetation patterns in this area. Transformed in various ways, these measures have been found to be good predictors of plant species occurrence (Austin *et al.*, 1990; Moore *et al.*, 1993). In examining differences between potential and realized niche, it was necessary to establish whether or not locations in the same environmental space differed in their fire regimes. Cary hypothesized the existence of ignition neighbourhoods, that is, all else being equal, a site may burn more or less frequently by virtue of its situation within the landscape due to the size of its ignition catchment. For example, as fires burn more readily uphill than down, there is an expectation that valleys will experience a lower fire frequency.

METHOD Only one version of FM is tested here, FMM. This version implements the core architectural differences between FM and FIRESCAPE together with the observed weather data which will be used in subsequent experiments. Three replicate sites in each of three unambiguous situations were chosen (ranges, valleys and plains) to examine the size of their ignition neighbourhoods. A simulation was run for 1,000 years and for each fire reaching these nine locations, the distance from the ignition point to the location was recorded. The distance of the 25th, 50th and 75th percentile was plotted in the same manner as Cary (1997).

RESULTS FMM produced the same rank order of ignition neighbourhoods as reported by FIRESCAPE (Cary, 1997), with plains having the largest and valleys the smallest (Figure 6.8). Beyond this nothing more precise can be claimed as there will inevitably be differences between the precise locations tested by FIRESCAPE and those tested with FM in this more mountainous landscape. As with all modelling studies, significance can change with the number of trials (White *et al.*, 2014). Both the 25th and 50th percentiles appear significant in this test for FMM while the 75th percentile is not significant. As FMM can produce different fire regimes based on the same topographic classification as FIRESCAPE, FMM (with the associated terrain and weather data) can operate with the same level of skill as FIRESCAPE in examining regions where niches may be realized by fire regimes such as those studied by Wood *et al.* (2011).

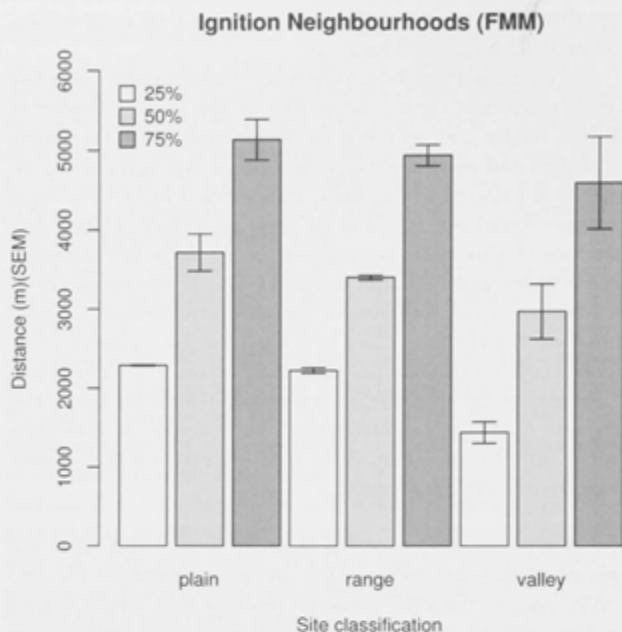


Figure 6.8: Average distances (metres) to the 25th, 50th and 75th percentile of ignition points for three replicates of each site classification, simulated using FMM (observed half-hourly weather data). Site classifications are: plains (sites located on relatively large, flat areas); range (sites located on top of major peaks or ranges); and valley (sites located near the bottom of major valleys). This test was performed using the same methods as Cary (1997).

6.3 REPLICATION OF PUBLISHED EXPERIMENTS

Two further tests of FM were performed to examine higher level function in comparison with FIRESCAPE. FIRESCAPE was used in three peer-reviewed experiments (Cary *et al.*, 2006, 2009; Keane *et al.*, 2013a). The purpose of those experiments was to determine if there was a consensus among a range of independently developed models as to the relative importance of factors affecting the prevalence of fire in the landscape. These studies are the result of more than 13 years of collaboration between fire modellers and other researchers from Europe, USA, Canada and Australia. The first two of these three experiments are repeated here using all versions of FM. This provides an opportunity to compare FM and its weather data, with FIRESCAPE and four other models used in these two experiments.

The original experiments only reported frequency (as annual area burnt) as this was the only output common to all models (Cary *et al.*, 2009). However, the intention of the present study is to look at all three components of a fire regime (except 'fire type') if possible. FIRESCAPE outputs included the proportion of area burnt at fireline intensities $> 3,000 \text{ kW.m}^{-1}$ for the 2009 study, but other than this, there is no data available to give an indication as to how seasonality and intensity might respond to these treatments. Thus while analysing intensity and seasonality in the next two experiments provides no points of comparison with FIRESCAPE (except where noted), it does provide some insight into the response of these variables to these particular treatments, some of which are to be used for hypothesis testing in the next two chapters.

6.3.1 *Sensitivity to variation in terrain, fuel pattern, climate and weather*

Cary *et al.* (2006) compared the sensitivity of five models to variation in terrain, fuel management approach, climate and weather, namely: EMBYR (Hargrove *et al.*, 2000), FIRESCAPE (Cary and Banks, 2000), LANDSUM (Keane *et al.*, 2002), SEM-LAND (Li, 2000) and LAMOS (Lavorel *et al.*, 2000).

6.3.1.1 *Methods*

The five models were run by their authors for 1 simulated year without vegetation dynamics in a standardized four factor experiment. The spatial extent and resolution was 1,000 by 1,000 square cells with a cell width of 50 meters producing a total simulation area of $2,500 \text{ km}^2$. The experimental design is summarized in Table 6.2.

All models used the weather data from the domain of their development (Note that 'model' is not a factor in this experiment). For FIRESCAPE this was 40 years of synthetic weather data produced by the method described in Chapter 2. Following the instructions to modellers, ten years were selected from the full data set that had the same distribution of mean daily temperature and precipitation (Figure 6.9). The same procedure was followed for FMF and similarly, ten years were selected from the 26 years of observed weather for use by FMM and FMV. Note that the observed data has considerably greater variability in average daily temperature and precipitation than the synthetic weather data (Figure 6.10). Ten replicates (randomized fuel maps) were performed for each treatment combination totalling 1,800 one year simulations. FMF, FMM and FMV were subjected to the same experiment using one hour time steps (as used by FIRESCAPE for this experiment) and 50 metre spatial resolution as specified in the instructions to modellers. The fuel loads for all variants of FM in each fuel class were the same as those used by FIRESCAPE (fuel class by 1.6 t.ha^{-1}). Results were analysed in the same manner as Cary

Table 6.2: Experimental design after Cary et al. (2006)

FACTOR	LEVELS	DESCRIPTION
Terrain	Three	<i>Mountainous</i> : 0–2,500m elevation range; 30° maximum slope <i>Rolling</i> : 625–1,875m elevation range; 15° maximum slope <i>Flat</i> : 1,250m elevation; 0° slope
Fuel pattern	Two	<i>Fine</i> : 25 ha. square patches of fuel ages in initial landscape <i>Coarse</i> : 625 ha. square patches of fuel ages in initial landscape
Weather	Ten	10 distinct years of daily weather reflecting observed variability in mean annual temperature and precipitation in observed weather record for each year.
Climate	Three	<i>Observed</i> : Historical climate for each location <i>Warmer/Wetter</i> : Historical +3.6° C; +20 percent precipitation <i>Warmer/Drier</i> : Historical +3.6° C; -20 percent precipitation

et al. (2006) whereby variance explained by each of the factors and their interactions was examined in an analysis of variance (ANOVA). Single factors that explained more the 5% of the variance were noted as important as were factor interactions explaining more than 2.5%. Further details of the experimental design can be found in Cary *et al.* (2006) Reasons for using a lower threshold of importance for factor interactions were not stated in Cary *et al.* (2006), but the same approach is used here for consistency.

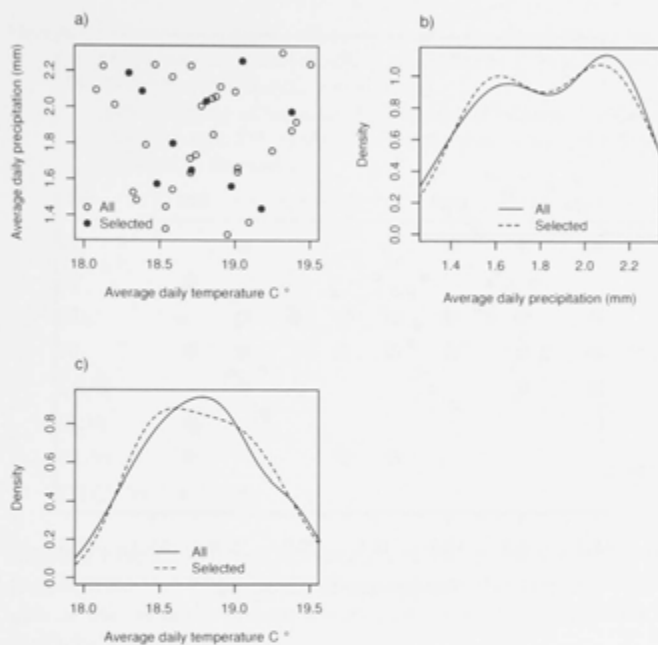


Figure 6.9: Selection of ten weather years

Average daily temperature and precipitation from 40 years of synthetic data created by weather generator (white/black) (Cary 1998). Ten years (black) are the best selection from the 40 years that match the probability density functions for both daily average precipitation (b) and temperature (c).

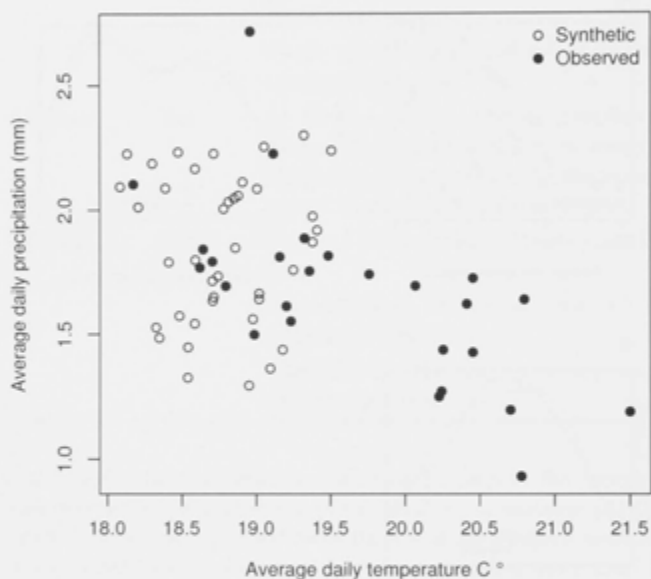


Figure 6.10: Comparison of the daily average temperature and precipitation of 40 years of weather data generated by a synthetic weather generator (Cary 1998) and observed half-hourly data from Canberra Airport (1985-2011)

The weather generator is parameterized with observations from Ginninderra Station (CSIRO) for the years 1977-1993. The observed data has a greater inter-annual variation in these measures than the synthetic data. The Ginninderra and Canberra Airport weather stations are less than 15 km apart and at the same elevation.

6.3.1.2 Results

FIRESCAPE and all versions of FM agree in finding the only important single factors explaining variance in ln-transformed area burnt were CL, W and TR. (Table 6.3). FMM, FMV and FIRESCAPE are also the only models to find the interaction of TR and W important. All models that took part in this experiment found CL important with the exception of EMBYR (Table 6.3). EMBYR also differed from all other models in finding FP important. However, a notable difference

Table 6.3: Experimental factors that were found important (●) in explaining variation in ln-transformed area burnt by FIREMESH and five other models (after Cary et al. 2006)

SOV = Source of variation; EM=Embyr; LA=Lamos; LS=Landsum; SL= Sem-land; FMF, FMM and FMV are three versions of FIREMESH discussed in Section 6.1.

SOV	EM	FS	LA	LS	SL	FMF	FMM	FMV
TR		●				●	●	●
FP	●							
CL		●	●	●	●	●	●	●
W	●	●		●	●	●	●	●
TR.W		●					●	●
FP.W	●							
CL.W	●			●	●			
TR.CL.W		●						

between FIRESCAPE and all versions of FM is the sensitivity of ln-transformed area burnt to CL (Figure 6). For this response variable, 42% of the variance was explained by CL for FIRESCAPE but only 5-11% by FM.

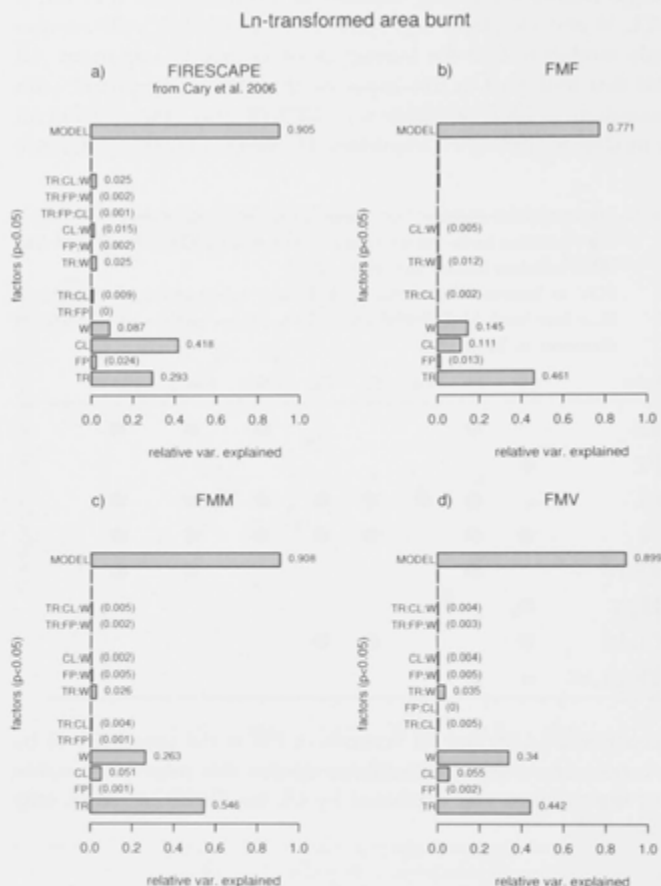


Figure 6.11: Relative Sums of Squares attributed to different sources of variation in the comparison of sensitivity of Ln-transformed area burnt to terrain (TR), fuel pattern (FP), climate (CL) and weather factors (W), and their interactions. Results are shown for FIRESCAPE (a) (from Cary et al. 2006), three configurations of FIREMESH (b) FMF (synthetic weather), (c) FMM (observed weather), and (d) FMV (observed weather with modifications to rates of fire spread). Relative Sums of Squares for factors and factor interactions that are less than 5 and 2.5% respectively, are considered unimportant and shown in brackets. Factors and factor interactions which were not significant ($p < 0.05$), are not shown.

6.3.1.3 Discussion

Models that showed no variance explained in ln-transformed area burnt by terrain (all models except FIRESCAPE and FM), did not incorporate lapse rates in their formulation (Cary *et al.*, 2006). EMBYR for example, was designed to operate in the caldera of Yellowstone National Park where changes in elevation were not sufficient to include in the model design (R. Gardner, pers. comm., 2003). EMBYR also differs from the other models in having a heightened response to fuel patterns as it determines fire spread by a probabilistic state transition matrix between fuel classes, fuel moisture and slope rather than employing a mechanistic model (Cary *et al.*, 2006). In general, model comparison experiments such as this can serve to highlight abstraction choices such as the above, a topic that the ODD protocol (Grimm *et al.*, 2010) and the Ontological approach to ecological models (Gignoux *et al.*, 2011) is designed to facilitate.

However, this experiment highlights a difference in design choice that was not apparent in the model description (Appendix 1). FIRESCAPE has a linkage between ignition rates and climate change that was not incorporated in FM (Figure 6.12.a). FM was designed to hold lightning rates constant over climate treatments. For FIRESCAPE, the greatest change in ln-transformed area burnt occurs between observed and the other two weather treatments (Figure 6.12.b) indicating that it is the increase in temperature that drives the increase in lightning strike rates. FMF and FIRESCAPE have a similar response to terrain when plotted as ln-transformed area burnt against treatment (Figure 6.12.c) but less variance is explained by TR in FIRESCAPE compared to FMF because more variance is partitioned to the CL factor in FIRESCAPE (Figure 6.11).

A second important difference lies in the use of synthetic (FMF) and observed weather data (FMM and FMV). Variance explained in ln-transformed area burnt by weather is 14% for FMF and 26% and 34% for FMM and FMV respectively (Figure 6.11). This may be attributed to; (i) the synthetic data having less inter-annual variability than the observed data (the most likely reason - see Figure 6.10); (ii) methods of down-scaling synthetic weather to hourly readings, in particular the different lapse rates at night (Figure 2.8) and; (iii) less variability between readings in the synthetic compared to the observed weather data (Section 2.4.1).

FMM and FMV are identical in their rank order of variance explained in ln-transformed area burnt across all single factors (Figure 6.11). Despite the large difference in the response of rates-of-spread to wind speed (Figure 3.10), variance explained by weather increases from only 26% (FMM) to 34% (FMV) with a corresponding reduction in the importance of terrain. Alexander and Cruz (2013) have highlighted the uncertainty that surrounds predicting rates of spread under various conditions of terrain, weather and fuel. As noted, the

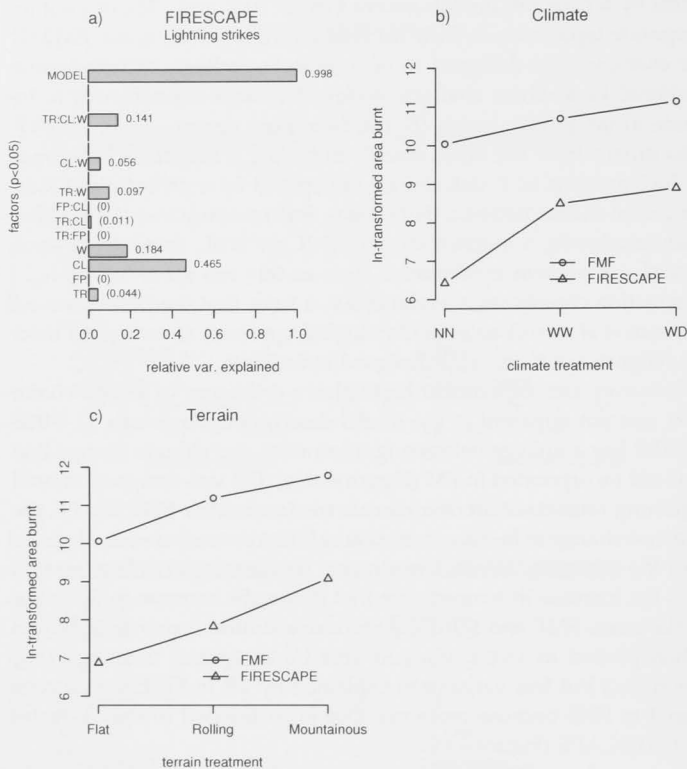


Figure 6.12: Differences and similarities between FIRESCAPE and FIREMESH in determining ignition rates and the response of In-transformed area burnt to climate and terrain treatments

a) Comparison of Relative Sums of Squares attributed to different sources of variation in the comparison of the number of lightning strikes to terrain (TR), fuel pattern (FP), climate (CL) and weather factors (W), and their interactions (original experimental data for FIRESCAPE courtesy GJ. Cary). Relative Sums of Squares for factors and factor interactions that are less than 5 and 2.5% respectively, are considered unimportant and shown in brackets. Factors and factor interactions which were not significant ($p < 0.05$), are not shown.

b) Average In-transformed area burnt for the three levels of Climate treatment for FIRESCAPE and FMF. NN is the observed weather, WW, is warmer-wetter and WD is warmer-drier (see Table 6.4).

c) Average In-transformed area burnt for three levels of Terrain treatment, for FIRESCAPE and FMF. Both FIREMESH and FMF are driven by synthetically generated weather.

reason to include the FMV variant of FIREMESH is to update the model (Section 3.2.9) with the findings of McCaw *et al.* (2008) in relation to the under-predictions of FFDM following Project Vesta (Gould *et al.*, 2007). Over- or under-estimates of rates of spread have critical operational consequences for fire management. However, from this experiment it is clear that the level of uncertainty in rates of spread reported by Alexander and Cruz (2013) does not change the relative importance of the treatments tested here. Estimates of uncertainty are an important consideration in any modelling study, and this low level of sensitivity to rate-of-spread estimates when assessing the relative influence of climate, fuel pattern, terrain and weather variability is an important finding.

The weather years selected for this experiment were chosen based on variance in average annual temperature and precipitation. The difference between FMM and FMV, on the other hand, is their response to wind speed. If it is assumed wind speed is uncorrelated with either temperature or precipitation, then area burnt will be higher for all treatment combinations using FMV (the FP factor explains very little of the variance in ln-transformed area burnt, so little can be concluded from this factor). This difference between FMM and FMV therefore, is a general increase in area burnt by FMV across all factors (Figure 6.13). But how important is this increase compared to changes in area burnt by each of the factors? The original experiment (Cary *et al.*, 2006) did not include the model as a factor, rather, the authors' purpose was to find broadly, what degree of consensus there was between these independently developed models to the experiment factors. However, in the present study, FMV is an abstraction grounded on FMM (Chapter 1) and using 'model' as a factor provides an objective measure of the relative importance of the differences between the models in the context of this experiment. Combining the results from FMM and FMV in a five factor analysis of variance reveals that the choice of model, that is, the difference between these two rates of spread functions, is unimportant (1.1%) when estimating the relative importance of terrain, fuel patterns, climate and weather variability on area-burnt estimates (Figure 6.14).

In summary, FIRESCAPE and FM both identify the same factors as important in determining area burnt in simulated landscapes. The difference in the response of the FM models suggests that choosing observed rather than synthetic weather, makes the use of observed weather data a more appropriate choice for tests in the sensitivity of the model to temporal resolution. Notwithstanding the differences in associating lightning strike rates with climate, these results support the view that FM is suitably constructed to be applied to the questions posed by this study.

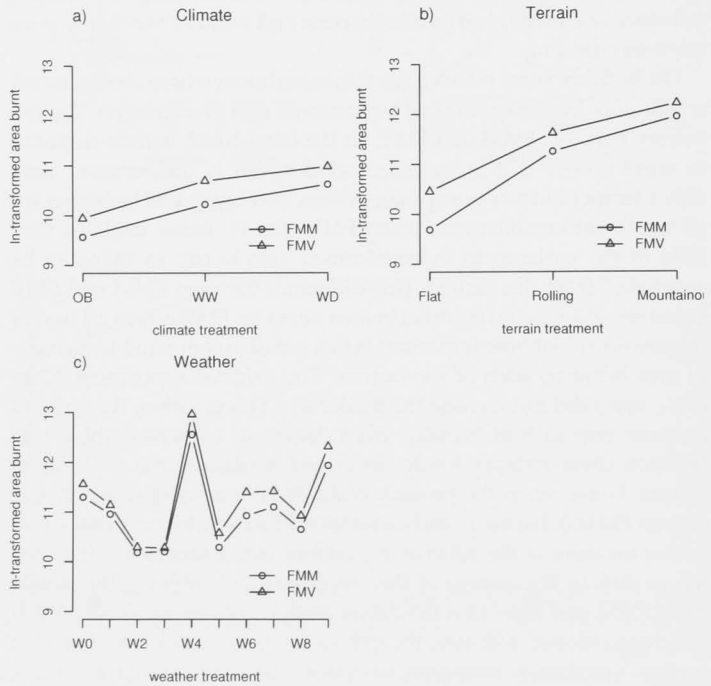


Figure 6.13: Changes in In-transformed area burnt over treatment levels for Climate, Terrain and Weather for two variants of FIREMESH FMM (observed weather), and FMV (observed weather with modifications to rates of fire spread)

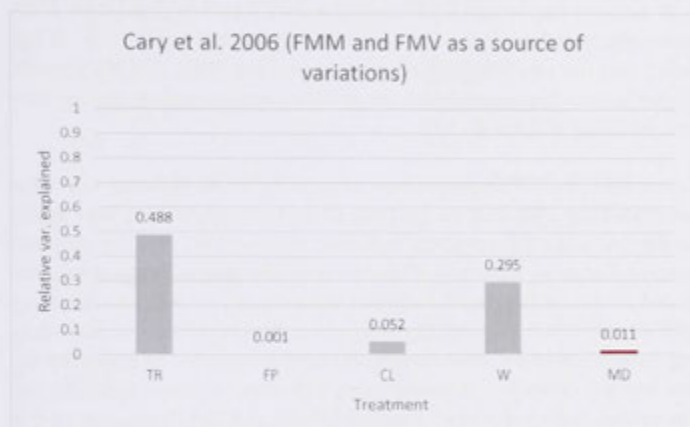


Figure 6.14: Relative Sums of Squares attributed to different sources of variation in the comparison of sensitivity of ln-transformed area burnt to terrain (TR), fuel pattern (FP), climate (CL), weather (W) and model (red bar) (MD) factors and their interactions. The model factor has two levels, FMM and FMV. Factor interactions are minor and not shown.

6.3.1.4 *The sensitivity of other components of fire regimes to the experimental factors*

INTENSITY As noted, no intensity data was published for this experiment. However, analysis of variance in the proportion of area burnt at high intensity (fireline intensity $> 3,000 \text{ kW.m}^{-1}$) (PHINT) produced by FM, reveals that TR and W explain almost all of the variance in PHINT while CL was relatively important for only for the synthetic weather data (FMF 6%) but not for the observed weather data (FMM: 2.5% and FMV: 1.6%) (Figure 6.15). That is, the magnitude of the inter-annual variation in average daily temperature and precipitation (Figure 6.10) is far greater in the observed data than the climate treatment ($\pm 3.6^\circ\text{C}$ temperature and $\pm 20\%$ precipitation).

W is more important for FMM (observed weather data) than FMF (synthetic weather data) and more important again for FMV. It appears that the much higher rates of spread for FMV, and thus much higher intensities overwhelms the effect of terrain with regard to fireline intensity (Figure 6.15.c)

SEASONALITY The proportion of area burnt in summer was also calculated for FM, and an analysis of variance (ANOVA) was again performed with this response variable. Weather (W) was the only important factor in this case (Figure 6.16). The much larger fires produced in dry or hot years increases the proportion of fires extending into autumn (not shown) thus reducing the proportion of fires during summer months. The climate treatment does this to a smaller extent but the effect is not as apparent. The effect is more apparent for the models using observed weather (FMM and FMV) because of the greater inter-annual variability in this data compared to the synthetic data.

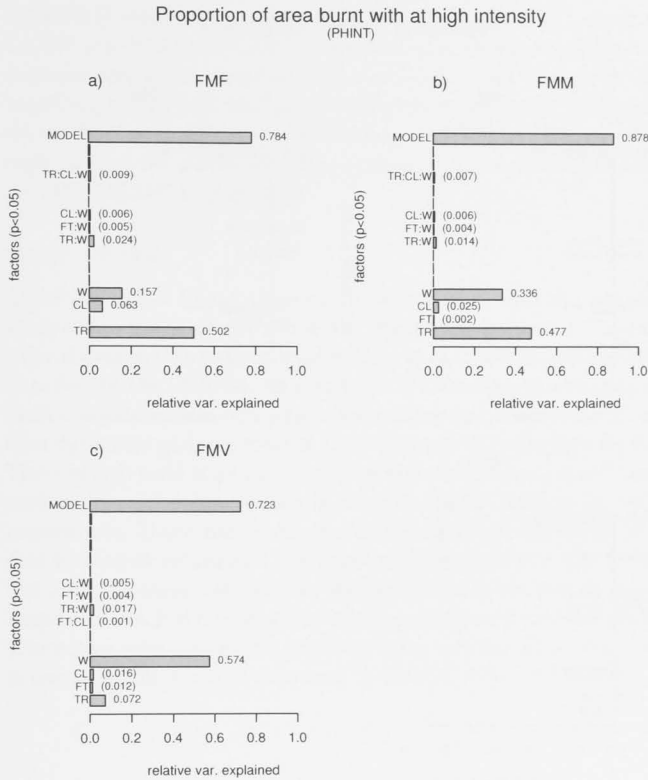


Figure 6.15: Relative Sums of Squares attributed to different sources of variation in the comparison of sensitivity of the proportion of area burnt at fireline intensity $> 3,000 \text{ kW.m}^{-1}$ to terrain (TR), fuel pattern (FP), climate (CL) and weather factors (W), and their interactions. Results are shown for (a) FMF (synthetic weather), (b) FMM (observed weather), and (c) FMV (observed weather with modifications to rates of fire spread). Relative Sums of Squares for factors and factor interactions that are less than 5 and 2.5% respectively, are considered unimportant and shown in brackets. Factors and factor interactions which were not significant ($p < 0.05$), are not shown.

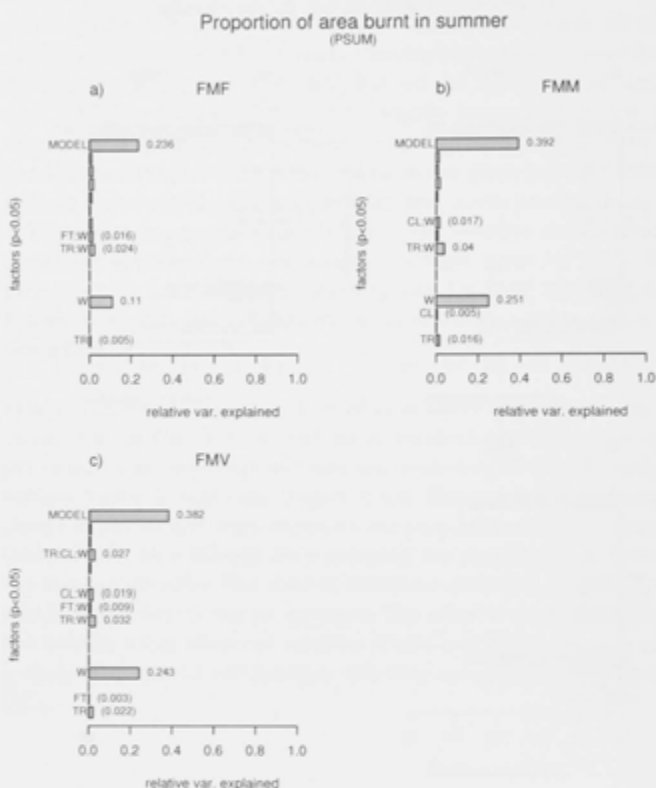


Figure 6.16: Relative Sums of Squares attributed to different sources of variation in the comparison of sensitivity of the proportion of area burnt in summer to terrain (TR), fuel pattern (FP), climate (CL) and weather factors (W), and their interactions. Results are shown for (a) FMF (synthetic weather), (b) FMM (observed weather), and (c) FMV (observed weather with modifications to rates of fire spread). Relative Sums of Squares for factors and factor interactions that are less than 5 and 2.5% respectively, are considered unimportant and shown in brackets. Factors and factor interactions which were not significant ($p < 0.05$), are not shown.




6.3.2 Relative importance of fuel management, ignition management and weather

A second study (Cary *et al.*, 2009) examined the sensitivity of five landscape fire models, namely: FIRESCAPE (Cary and Banks, 2000), LAMOS (Lavorel *et al.*, 2000), LANDSUM (Keane *et al.*, 2002), SEM-LAND, (Li, 2000) and CAFÉ, (Bradstock *et al.*, 1998, 2006) to ignition management effort, weather and a more detailed treatment of fuel involving both a fuel management approach and a fuel management effort. This study was also repeated here with FME, FMM and FMV to explore how the model and data compare with a number of models and FIRESCAPE in particular.

6.3.2.1 Methods

There are again four factors in this experiment and the results are analysed in the same manner as the previous experiment. The experimental design is fully described in Cary *et al.* (2009) and the treatment summarized in Table 6.4. As was the case for the previous experiment, each unique factor combination was run for one year without vegetation dynamics giving a total of 2,400 simulations using five replicates. The low fuel state is 4 t.ha^{-1} and the high fuel state 14 t.ha^{-1} of fine surface litter, the same values as used by FIRESCAPE in the original experiment. These fuel states are considered representative of post-fuel treatment values and late seral-stage respectively. The terrain is flat with the mean elevation of the landscape set to that of the landscape for which the model was developed. Spatial extent is 50 by 50 kilometres with a 50 metre grid size. Time step for all versions of FM is one hour, the same as that used by FIRESCAPE.

Table 6.4: Experimental design after Cary *et al.* (2009)

FACTOR	LEVELS	DESCRIPTION		
Weather	Ten	Ten distinct years of daily weather reflecting observed variability in mean annual temperature and precipitation in observed weather record for each location		
Ignition mngt effort	Four	<i>Zero</i> : 0% ignitions prevented <i>Low</i> : 25% ignitions prevented <i>Mod</i> : 50% ignitions prevented <i>High</i> : 75% ignitions prevented		
Fuel mngt approach	Three	Random (R) treatment	Edge (E) treatment	Buffer (B) treatment
				
Fuel mngt effort	Four	<i>Zero</i> : 0% of landscape treated <i>Low</i> : 10% treated (R); 100 m (B); 50 m (E) <i>Mod</i> : 20% treated (R); 200 m (B); 100 m (E) <i>High</i> : 30% treated (R); 300 m (B); 150 m (E)		

6.3.2.2 Results

In original results for this experiment (Cary *et al.*, 2009), all models report W and IME as the only important factors in variance explained in ln-transformed area burnt, with the exception of CAFE, for which all factor interactions were important (Table 6.5). FIRESCAPE and all versions FM report W and IME as the most important factors and in that order (Figure 6.17). In addition, they report both FMA and FME as significant but unimportant. FIRESCAPE shows a lesser sensitivity to IME than FMF though similar to FMM and FMV (Figure 6.17).

The difference between FMM and FMV is very slight, with W explaining most of the variance (58%, 57% of total variance explained respectively) in ln-transformed area burnt. As noted, both these simulations have a very different response of rates of spread to wind speed (Figure 3.10). The difference between FIRESCAPE and FMF in partitioned variance explained by W is more marked (40% and 30% respectively) and as noted, both these simulations use similar, stochastically generated weather data.

FM is consistent with all the other models that have performed this experiment, with the exception of CAFE, in finding W important for ln-transformed edge area burnt (Table 6.6). In addition, FM agrees with FIRESCAPE in finding only W and IME important in this respect. FMF shows more than a doubling of importance of IME than FIRESCAPE for ln-transformed edge area burnt (16% and 7% respectively) (Figure 6.18). Again there is very little difference between FMM and FMV in this respect.

All variants of FM accord with the published result of FIRESCAPE in finding significance in the random fuel management approach (but at unimportant levels) and no significance for the edge and break approaches.

Table 6.5: Experimental factors that were found important (●) in explaining variation in ln-transformed area burnt by FIREMESH and five other models (after Cary *et al.* 2009)

SOV = Source of variation; CF=Cafe; LA=Lamos; LS=Landsun; SL= Sem-land; FMF, FMM and FMV are three versions of FIREMESH discussed in Section 6.1.

SOV	CF	FS	LA	LS	SL	FMF	FMM	FMV
W	●	●	●	●	●	●	●	●
IME	●	●	●	●	●	●	●	●
FME								
FMA								
FMA.FME.W.IME	●							

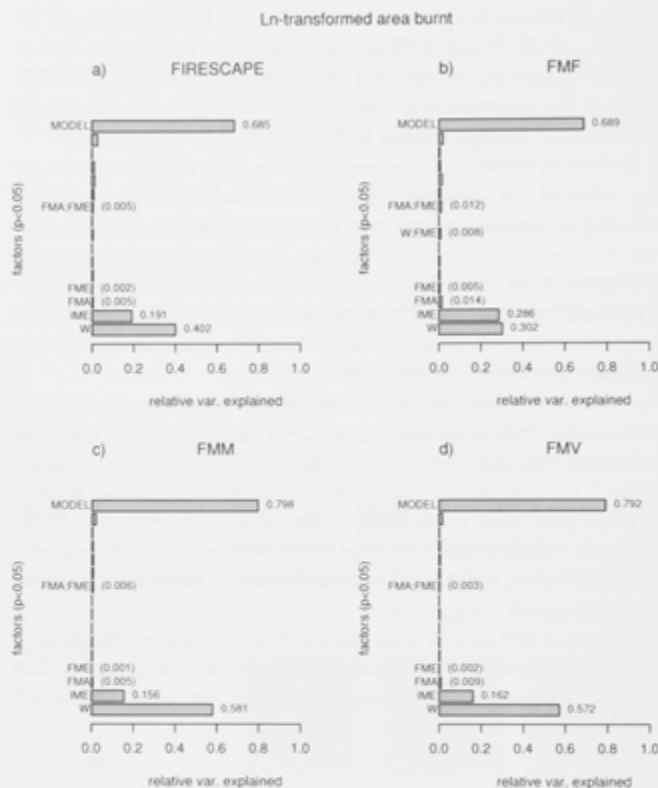


Figure 6.17: Relative Sums of Squares attributed to different sources of variation in the comparison of sensitivity of ln-transformed total area burnt to weather (W), ignition management effort (IME), fuel management effort (FME) and fuel management approach (FMA) and their interactions (after Cary *et al.* 2009). Results are shown for FIRESCAPE (a) (from Cary *et al.* 2009), three configurations of FIREMESH (b) FMF (synthetic weather), (c) FMM (observed weather), and (d) FMV (observed weather with modifications to rates of fire spread). Relative Sums of Squares for factors and factor interactions that are less than 5 and 2.5% respectively, are considered unimportant and shown in brackets. Factors and factor interactions which were not significant ($p < 0.05$), are not shown.

Ln-transformed edge area burnt

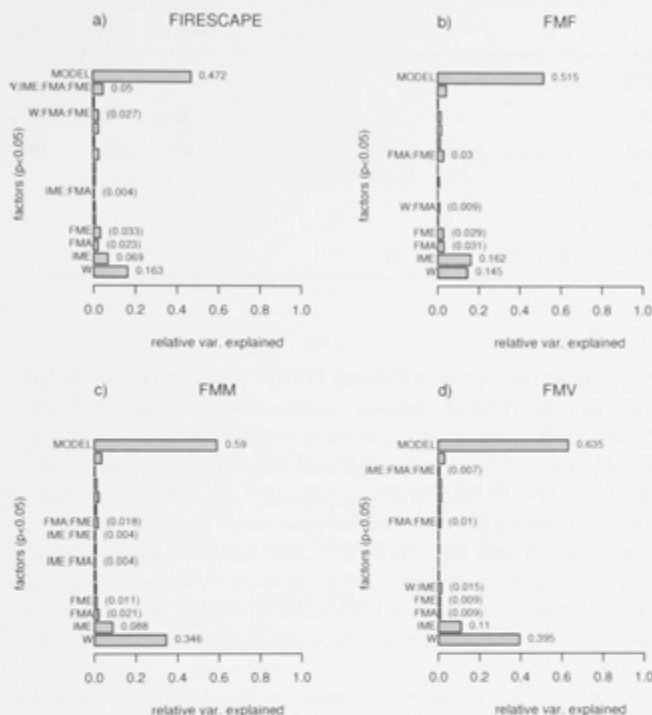


Figure 6.18: Relative Sums of Squares attributed to different sources of variation in the comparison of sensitivity of Ln-transformed total edge area burnt to weather (W), ignition management effort (IME), fuel management effort (FME) and fuel management approach (FMA) and their interactions (after Cary *et al.* 2009). Results are shown for FIRESCAPE (a) (from Cary *et al.* 2009), three configurations of FIREMESH (b) FMF (synthetic weather), (c) FMM (observed weather), and (d) FMV (observed weather with modifications to rates of fire spread) Relative Sums of Squares for factors and factor interactions that are less than 5 and 2.5% respectively, are considered unimportant and shown in brackets. Factors and factor interactions which were not significant ($p < 0.05$), are not shown.

Table 6.6: Experimental factors that were found important (●) in explaining variation in ln-transformed *edge area burnt* by FIREMESH and five other models ((after Cary *et al.* 2009)

SOV = Source of variation; CF=Cafe; LA=Lamos; LS=Landsun; SL= Sem-land; FMF, FMM and FMV are three versions of FIREMESH discussed in Section 6.1. Factors and their interactions are only shown if they explain more than 5 and 2.5% of total variance respectively.

SOV	CF	FS	LA	LS	SL	FMF	FMM	FMV
FMA	●							
W		●	●	●	●	●	●	●
IME	●	●	●			●	●	●
FMA.FME	●							
FMA.W	●							
FMA.FME.W.IME		●						

6.3.2.3 Discussion

There is a consensus between FM and FIRESCAPE as to which factors are important, in terms of variance explained in ln-transformed area burnt, and in the rank order. The most notable difference is the response of both total area burnt and total edge area burnt to ignition management effort (IME) (Figure 6.17, Figure 6.18). The ln-transformed area burnt by treatment level indicates a large drop in area burnt between moderate and high for FIRESCAPE unlike all configurations of FM (Figure 6.19). It is unclear why this is so, however, it does not change the consensus between FIRESCAPE and all versions of FM in finding W and IME the most important factors, and in the same order.

The overall difference in results between FMM and FMV is even less pronounced than the previous experiment. It says that the findings of this and the previous experiment in ranking the relative importance of climate, weather, terrain, fuel pattern, fuel management approach, fuel management effort and ignition management effort to ln-transformed area burnt, are indifferent to the high uncertainty that exists in rate of spread calculations reported by Alexander and Cruz (2013). This is despite the expected larger fire sizes produced by FMV (Figure 6.20). This is not to say that all measures of the generated fire regimes will be unaffected. As can be seen from previous tests in this chapter, increasing rates of spread not only increases intensity but decreases spatial variability of patterns of inter-fire intervals, as a larger proportion of big fires will cause IFIs to regress to the mean. However, from the discussion section of the previous experiment, area burnt is simply increased for all factors by FMV, with very little difference in how variance is apportioned to the experimental factors (Figure 6.13).

In this experiment, however, although the FMA and FME were unimportant, there is some indication that fuel treatments (FME and FMA) are less significant when modelled rates of spread are higher (FMV) as might be expected. It is this treatment where it might be expected that differences in rate of spread would be most telling. Another experimental design such as Finney (2001) would likely show a larger effect of rate of spread estimates. However, experiments treating more than 30% of the landscape with blocks of a fixed size and shape as was done in Finney (2001) are of limited practical significance for broad-scale fuel reduction efforts.

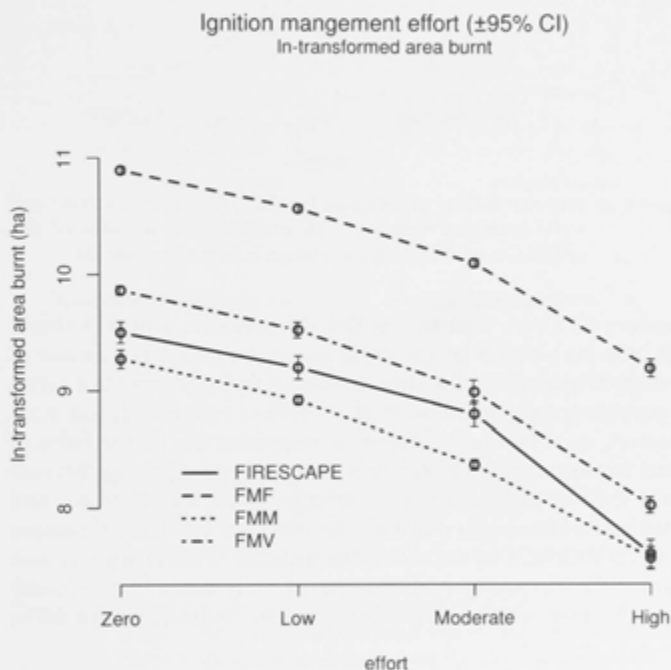


Figure 6.19: Ln-transformed area burnt (ha) for four levels of ignition management effort (0%, 25%, 50% and 75% reduction in ignitions) for FIRESCAPE (Cary et al. 2009), FMF (synthetic weather), FMM (observed weather) and FMV (observed weather with modifications to rates of fire spread)

6.3.2.4 The sensitivity of other components of fire regimes to the experimental factors

INTENSITY AND SEASONALITY Unlike the previous experiment, data for the proportion of area burnt at high intensity (fireline intensities $> 3,000 \text{ kW.m}^{-1}$) (PHINT) was available for FIRESCAPE

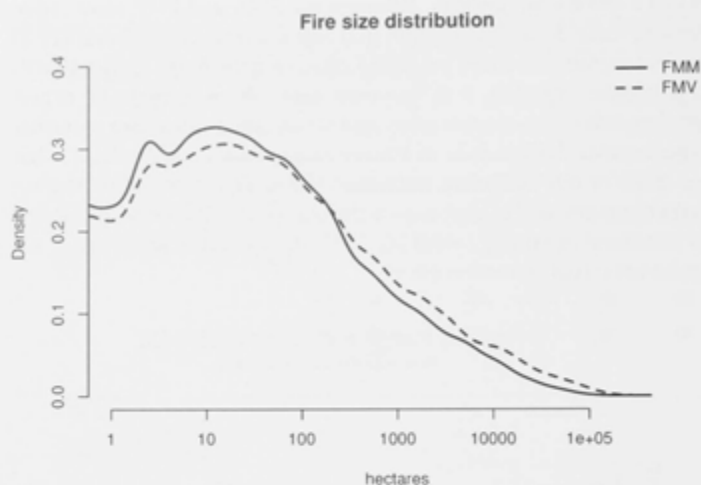


Figure 6.20: Fire-size density distribution for FMM (observed weather) and FMV (observed weather with modifications to rates of fire spread) summed for all factors and replicates combined

(courtesy GJ Cary). Reanalysing this data together with FM shows that only the weather factor (W) is explanatory for this measure of intensity (Figure 6.21). Similarly, weather is the only important factor in explaining the proportion of area burnt in summer (Figure 6.22). However, there is a contradiction in measuring the effectiveness of a fuel treatment through measures of intensity in this way, because where the fuel treatment is 100% effective there will be no fire and therefore no intensity to measure. Therefore the least biased measure of a fuel treatment under these circumstance is the change in area burnt. In later experiments in the present study, mean fireline intensity of all fires is used as a response variable to ameliorate this problem.

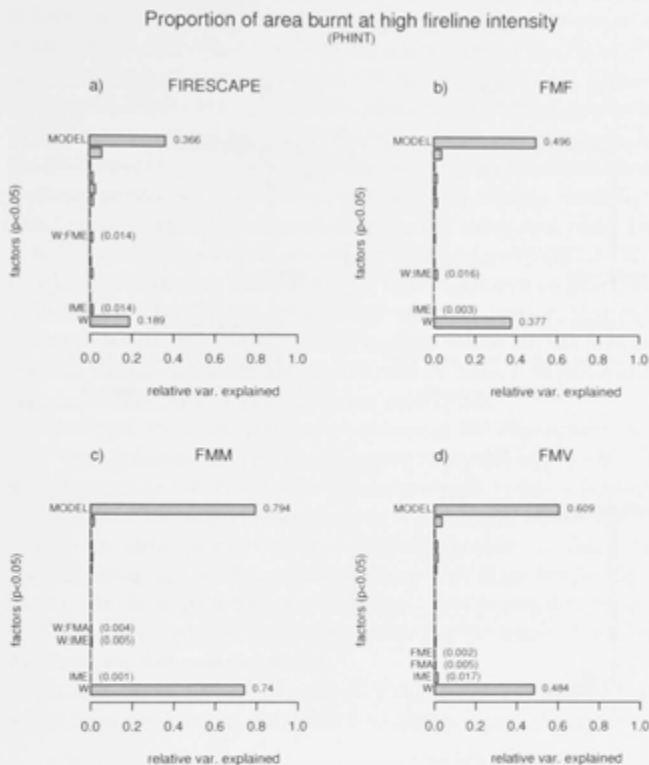


Figure 6.21: Relative Sums of Squares attributed to different sources of variation in the comparison of sensitivity of the proportion of area burnt with fireline intensity $> 3,000 \text{ kW.m}^{-1}$ to weather (W), ignition management effort (IME), fuel management effort (FME) and fuel management approach (FMA) and their interactions for three configurations of FIREMESH

The three versions of FIREMESH are (b) FMF (synthetic weather), (c) FMM (observed weather), and (d) FMV (observed weather with modifications to rates of fire spread). Relative Sums of Squares for factors and factor interactions that are less than 5 and 2.5% respectively, are considered unimportant and shown in brackets. Factors and factor interactions which were not significant ($p < 0.05$), are not shown.

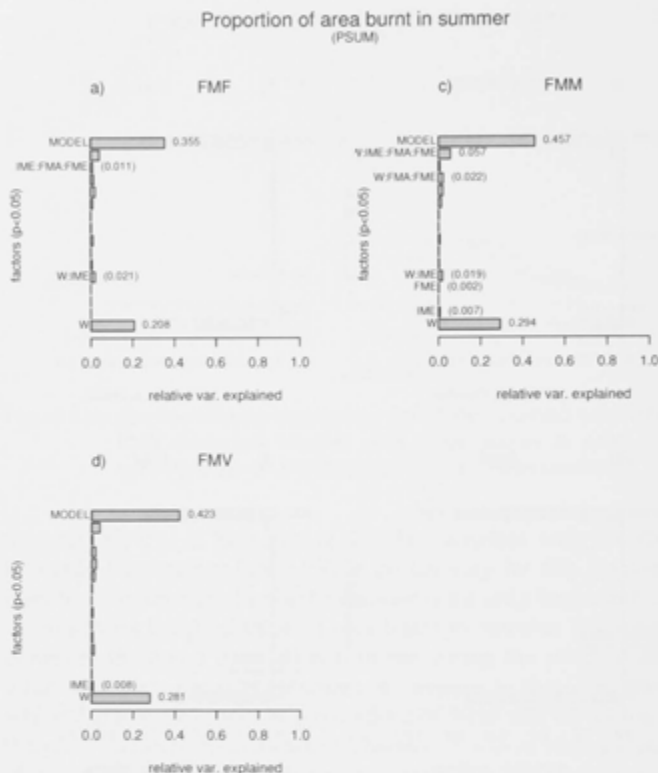


Figure 6.22: Relative Sums of Squares attributed to different sources of variation in the comparison of sensitivity of the proportion of area burnt in summer to weather (W), ignition management effort (IME), fuel management effort (FME) and fuel management approach (FMA) and their interactions for three configurations of FIREMESH

The three versions of FIREMESH are (b) FMF (synthetic weather), (c) FMM (observed weather), and (d) FMV (observed weather with modifications to rates of fire spread). Relative Sums of Squares for factors and factor interactions that are less than 5 and 2.5% respectively, are considered unimportant and shown in brackets. Factors and factor interactions which were not significant ($p < 0.05$), are not shown.

6.4 SUMMARY OF FINDINGS

All variants of FM produce spatial patterns of inter-fire intervals and intensity around the same topographic features (ridges, slopes and valleys) as does FIRESCAPE. Differences for the most part can be explained by model choices such as the rate of spread equations (FMV), restrictions on response to slope (FMM and FMV) and differences between synthetic and observed weather data and their extrapolation to higher elevations (FMF and FMM). Nevertheless, there is a consensus between all versions of FIRESMESH and FIRESCAPE in the patterns generated in inter-fire intervals and fireline intensity. Seasonal proportion of fire occurrence show the same rank order for the seasons across all versions of FM as that found by FIRESCAPE, with summer and autumn contributing to more than 90% of area burnt.

FMM (FIRESMESH using observed weather data) is also capable of the same discrimination of fire regimes based on the size of the ignition neighbourhoods for sites located in valleys, slopes and ridge tops as FIRESCAPE, and in the same rank order.

FM found the same factors important in the experiment of Cary *et al.* (2006) (while noting the difference in model approach to lightning frequency and climate) and the same rank order of importance of factors in the experiment of Cary *et al.* (2009). These two experiments are directly relevant to this study as three of those experimental factors are used as yardsticks by which to test the thesis hypotheses. On these grounds, the validation tests performed above support the view that FM is an appropriate tool to apply to the experiments in the following chapters.

The sensitivity of seven factors to variation in ln-transformed area burnt were explored in the above two experiments. These were:

- i Weather (W)
- ii Climate (CL)
- iii Fuel pattern (FP)
- iv Terrain (TR)
- v Ignition management effort (IME)
- vi Fuel management effort (FME)
- vii Fuel management approach (FMA)

Of these seven experimental factors, only two (W and TR) had an effect on intensity (expressed as a proportion of area burnt with a fireline intensity $> 3,000\text{ kW.m}^{-1}$) and only one (W) had an effect on seasonality (expressed as the proportion of area burnt in summer). Experiments in the next two chapters must introduce additional experimental factors, namely temporal grain (TG) and spatial grain (SG)

together with various forms of spatial representation (SR). Comparing these additional factors to all seven of the above treatments would be too unwieldy and a choice must be made as to which factors are to be used, against which to rank the importance of TG, SG and SR. To be manageable, the experiments that follow are limited to five factors, two of which are TG, SG or SR, leaving three to choose from the above seven. To test frequency, intensity and seasonality would require TR, W and one other - say FME, because this is central to fire management although arguably, so too is IME. Both W and TR are powerful drivers of fire regimes as measured by FIRESCAPE and FM. Therefore, a more sensitive test would be to use treatments involving CL, FME (using one fuel management approach) and IME. This is the choice made in this study and other choices must remain a topic for further research. However, as CL, FME and IME have little or no effect on intensity and seasonality, it means the formal tests of the hypotheses of this study can only be meaningfully tested against fire frequency. Fire frequency is arguably the most important component of fire regimes because it is a measure of the total amount of fire in the system, a primary contribution to measures of risk to environmental, social and built assets. Nevertheless, differences that arise in measures of intensity and seasonality are noted and explained where appropriate.

RELATIVE IMPORTANCE OF SPATIO-TEMPORAL RESOLUTION

7.1 INTRODUCTION

In the next two chapters, four simulation experiments are performed to directly test the hypotheses of this study. In this chapter, the first of these hypotheses is addressed. The aim of this experiment is to ascertain if the relative importance of experimental treatments in published fire modelling studies remain unchanged over a wide range of temporal and spatial resolutions (Section 1.1).

7.2 FACTORS COMMON TO ALL EXPERIMENTS

All experiments in this and the next chapter share three factors in common: (i) climate (CL), (ii) ignition management effort (IME), and (iii) fuel management effort (FME). The CL and IME treatments are the same as those used by Cary *et al.* (2006, 2009) respectively. Both these experimental treatments were tested in Chapter 6 in validation tests and any differences between FIRESCAPE and FIREMESH reported. The third factor, FME, is adapted from Cary *et al.* (2009) and Bradstock *et al.* (2012). These three factors are used as exemplars or yardsticks, against which to compare the importance of the model's abstractions of space and time. In short, to test how important is spatio-temporal resolution in an operational context.

CLIMATE (CL) The three levels of climate treatment were those used by (Cary *et al.*, 2006): observed (OB), warmer and wetter (WW) and warmer and drier (WD). OB is the unaltered observed weather-data. WW adds 3.6 °C to each temperature reading and increases daily precipitation by 20%, 3.6 °C being the mid-point of the IPCC (2001) projected global temperature increase of between 1.4 and 5.8 °C. WD adds the same 3.6 °C and reduces precipitation by 20%. By way of context, this is the same decrease in rainfall as that measured for early winter rainfall in the southwest corner of Australia during the latter half of the 1970s (Timbal *et al.*, 2006). Vapour pressures in the input data were adjusted to ensure that changes in temperature did not affect humidity (Figure 7.1). This approach is the same as that used by FIRESCAPE in the original experiments.

IGNITION MANAGEMENT EFFORT (IME) This factor was used in Chapter 6 (Validation) and is more fully described in Cary *et al.* (2009).

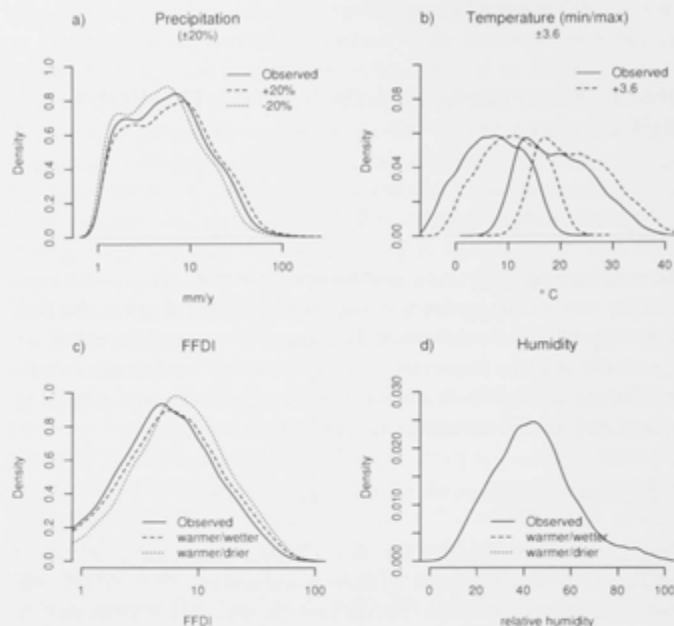


Figure 7.1: Density distributions of precipitation, minimum and maximum temperature and the resulting Forest Fire Danger Index (McArthur, 1973)

A value of 3.6°C is added to the observed temperature and precipitation is altered by $\pm 20\%$. Vapour pressure in the input data is modified to preserve humidity at observed values. Note that Figure (a) has a log scale.

In general its intent is to include any action that leads to a reduction in fire ignitions such as rapid initial attack together with education and other infrastructure programs that reduce ignitions from anthropogenic sources (Cary *et al.*, 2009). This factor models initial attack success, with the above broad definition, by reducing the number of ignition attempts by 0, 37.5 and 75%.

FUEL MANAGEMENT EFFORT (FME) This factor is adapted from Cary *et al.* (2009) and Bradstock *et al.* (2012). Cary *et al.* (2009) examined three approaches to fuel management (Section 6.3.1). Only the random approach is applicable here because both the edge and buffer treatments depend on spatial resolution for their levels of effort. The random approach must also be adapted to operate in this experiment which simulates the effect of fuel treatment in the context of an emerging fire regime over time. The experimental design of Cary *et al.* (2009) did not involve vegetation dynamics.

The maximum area treated by Cary *et al.* (2009) using the random approach was 30%. This is not a per annum rate, but rather a snapshot in time. Interpreting this as an annual rate would lead to unrealistically high treatment levels for a dynamic vegetation model (as is being used here) as almost the whole landscape would have fuel ages no more than three years old at any one time. In this experiment, and those in Chapter 8, up to 30% of the landscape is treated in a five year period with a minimum fire return interval of five years. That is, up to 6% of the landscape is treated per annum. This is equivalent to the treatment in Bradstock *et al.* (2012) where 20% of the landscape was scheduled for treatment every year but only 6% could be realized on average because of constraints on block arrangements and the minimum fire return interval in that study.

Block sizes are 625 ha., the same as those used in Cary *et al.* (2009). Cary *et al.* (2006) showed a relative insensitivity to block size so treatments with finer block sizes were not tested. The random approach represents an attempt to modify the prevalence of fire by reducing fuels in the wider landscape rather than fuel reduction close to assets or to form strategic barriers (Finney, 2001; Bradstock *et al.*, 2012).

In practice, the simplicity of the algorithm employed (random block locations) and the small block sizes compared to Bradstock *et al.* (2012), means that the realized treatment level was within 0.01% of that attempted. For example, if 6% was the proposed fuel reduction level and in the previous five years only 6% of the landscape has been left unburnt, the whole of the remaining 6% was be treated.

An additional consideration was the fuel load remaining after treatment. Planned fires differ from unplanned fires in the time and nature of ignitions (Heemstra, 2007). Planned fires are lit during cooler periods with a higher density of ignitions. While the average fuel load measured at a location may have been substantially reduced, the within-patch variability (patchiness) will affect the ability of subsequent fires to span the site under various weather conditions (Heemstra, 2007). Heemstra (2007) found in a study of 7 planned and 4 unplanned fires that the planned fires burnt on average 62% of the area within the fire perimeter while the unplanned fires burnt of average 86%. Note that, these findings apply to prescribed burning at locations fairly remote from built assets (as is the case with the random treatment) and the area treated is larger and less intensively treated than would be the case for areas in close proximity to buildings. Given the range of fuel loads in this study of between 9.6 to 16.2 t.ha⁻¹, (with a mean value of 12.1 t.ha⁻¹) the values of 4 to 14 t.ha⁻¹ used by Cary (Cary *et al.*, 2009) and the observation of Heemstra (2007) that more than half of the treatment area remains effectively untreated, a value of 5 t.ha⁻¹ for the 'low' fuel state was chosen for this factor. McArthur's Mk 5 Forest Fire Danger Meter (McArthur, 1973) indicates this will carry a fire if the Forest Fire Danger Index is

greater than five. It could be supposed that the algorithm should treat older fuels in preference to younger fuels. However, this will cause an enhanced edge effect because fuel on the edges of the map is usually the oldest and would be chosen in preference.

In general, this treatment was intended to be simple and transparent and did test management approaches as was done by Cary *et al.* (2009) and Bradstock *et al.* (2012). All fuel treatments take place simultaneously in mid-winter. There are three treatments levels: 0%, 3% and 6% of the landscape treated annually with 625 ha. block sizes at locations randomly selected every year and a minimum fire return interval of five years (Figure 7.2).

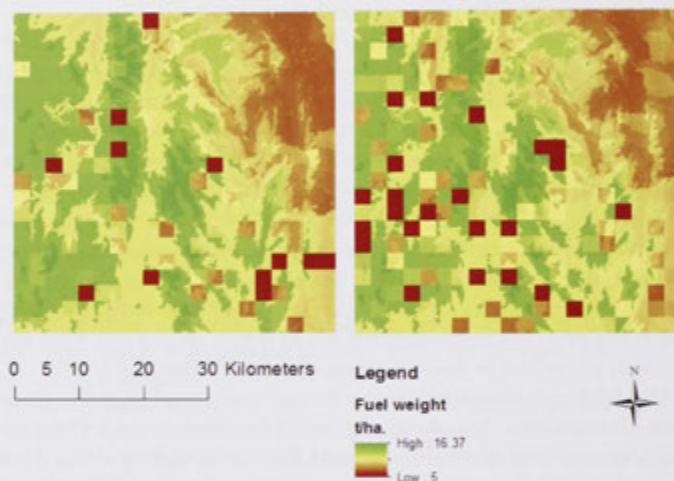


Figure 7.2: Examples of random 625 ha. block fuel treatments

On the left, 3% of the landscape is treated annually. In this example, a recent unplanned fire in the top right-hand quadrant, has prevented treatment in this area concentrating treatment to the remaining quadrants. On the right, 6% of the landscape is treated annually. The fading pattern of treatments from previous years are visible as fuel loads increase over time. 30% of the landscape is treated within any 5 year period.

7.3 DATA ANALYSIS

The fire regime components of frequency, intensity and seasonality were analysed by variance explained (r^2) determined by three fully factorial ANOVAs using the base library of R (R core team 2014). The studies of Cary *et al.* (2006, 2009) were single year experiments and results analyzed in terms of total area burnt. As noted, the experiments in this chapter use vegetation dynamics and average inter-fire

interval (AVIFI) (the inverse of average annual area burnt) is a more appropriate measure in these circumstances (Equation 7.1).

$$\text{AVIFI} = A_s \cdot Y / A_b \quad (7.1)$$

where:

A_s = simulation area;

Y = years of simulation; and

A_b = total area burnt.

AVIFI requires log transformation to satisfy assumptions of normality of residuals in such analysis (Figure 7.3). Intensity was measured as the average of all fireline intensities at every location in the landscape (AVINT) while seasonality was measured as the proportion of area burnt in summer over the whole simulation (PSUM).

It is important to emphasize that variance explained by each of the factors and their interactions is analysed in proportional terms in order to focus on the magnitude of effects rather than statistical significance (p-values) (Section 1.1, White *et al.* 2014).

Each of the four experiments had a different number of factors. In the four-factor experiments of Cary *et al.* (2006, 2009) and Keane *et al.* (2013a), factors and their interactions that explained more than 5% and 2.5% of the variance respectively, were considered important. For the purpose of comparison, these arbitrary thresholds were scaled to 6.67 and 3.3 % for 3 factor analysis and 3.75 and 1.88% for 5 factor analysis for single factor and factor interactions respectively. Note that results are analysed considering only unplanned fires unless otherwise indicated.

Baseline ignition rates for all experiments are calibrated to give a 50 year average inter- fire-interval at one hectare resolution and three hour time step on an eight neighbour regular mesh. Each unique combination of factors had a unique set of random ignitions (unique random number seed), with the distribution of ignitions in time and space determined by the ignition model (Chapter 3). Five replicates of each factor combination were performed with ignition times and locations varying between replicates. All simulations were 1,000 years in duration. The terrain, fuel accumulation model and observed weather were those described in Chapter 2. The option to include the modifications to the R_h informed by Project Vesta as described in Chapter 3, was enabled.

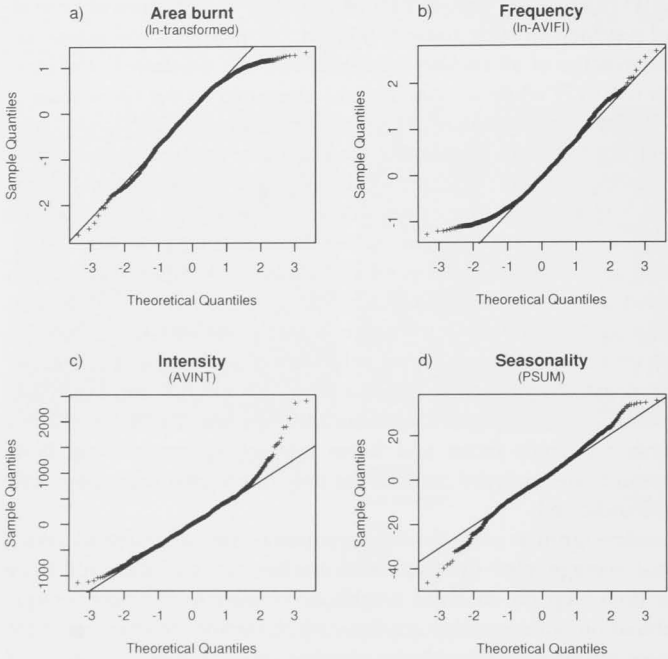


Figure 7.3: Distribution of the residuals of key measures of FIREMESH model outputs

The distribution of residuals of (a) ln-transformed area burnt and (b) its reciprocal, ln- transformed average inter-fire interval (ln-AVIFI). Average fireline intensity (c) (AVINT) and (d) the average for all locations of the proportion of fires occurring during summer (PSUM) do not require transformation.

7.4 TESTING SPATIAL AND TEMPORAL RESOLUTION

Hypothesis (i): Ranking the relative importance of the drivers of fire by simulation modelling is insensitive to a wide range of spatio-temporal resolutions


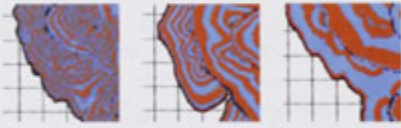
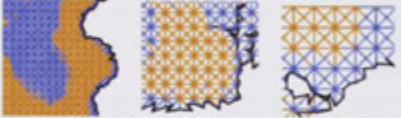
7.4.1 Methods

To accept or reject this hypothesis, FIREMESH was used in a multi-factorial experiment using five factors: (i) climate, (ii) ignition management effort, (iii) fuel management effort, (iv) spatial resolution and (v) temporal resolution. Factors (i)-(iii) have been described above.

SPATIAL RESOLUTION (SG) Past experiments with FIRESCAPE have used either 0.25 (Cary *et al.*, 2006, 2009; Keane *et al.*, 2013a) or one hectare spatial resolution (Cary and Banks, 2000). From the validation tests in Chapter 4, it appears there is no practical benefit in performing these experiments at resolutions finer than one hectare and incurring a very considerable cost in simulation time. Consequently there were three levels for this treatment: one, four and nine hectares using only a regular eight-neighbour mesh. Keane *et al.* (2004) has classed models in this range as mid-scale models. The method of aggregating elevations at each resolution was the centroid method (Bian and Butler, 1999).

TEMPORAL RESOLUTION (TG) Three levels of temporal resolution were used: 0.5, 1.5 and 3 hourly time steps. Half-hour is the resolution of the input data and three hours is the time step used by FIRESCAPE during its development. The aggregation of data to coarser resolutions uses the nearest reading or centroid method (Bian and Butler 1999) and no interpolation between readings was required. To gauge the importance of spatial and temporal resolution, model results were analysed both with and without spatial and temporal resolution as a factor. That is, had simulations been performed with any of the nine combinations of temporal and spatial resolution, would important differences have arisen? The experimental factors and their levels of treatment are summarized in Table 7.1.

Table 7.1: Experimental design for a factorial experiment to measure the importance of spatio-temporal resolution against published experimental factors in fire regime simulation modelling

FACTOR	LEVELS	DESCRIPTION
Climate	Three	<i>Observed</i> : Historical climate <i>Warmer/Wetter</i> : Historical +3.6°C; +20% precipitation <i>Warmer/Drier</i> : Historical +3.6°C; -20% precipitation
Ignition mngt effort	Three	<i>Zero</i> : 0% ignitions prevented <i>Mod</i> : 35.7% ignitions prevented <i>High</i> : 75% ignitions prevented
Fuel mngt effort	Three	Zero% p.a. 3% p.a. 6% p.a. treatment treatment treatment
		
Temporal resolution	Three	0.5 hour 1.5 hour 3 hour 
Spatial resolution	Three	One ha. Four ha. 9 ha. 

7.4.2 Results

As expected from the previous discussion (sections 6.3.1.4 and 6.3.2.4), the total variance explained by all factors and their interactions was far greater for ln-AVIFI (91%) compared to 59 and 30% for AVINT and PSUM respectively (Figure 7.4). Therefore, AVINT and PSUM will be less informative response variables of the importance of the experimental treatments.

FREQUENCY (LN-AVIFI) The relative importance of variance explained in ln-AVIFI by spatial grain (SG) and temporal grain (TG) was unimportant ($< 3.75\%$) compared to the other treatments of IME (55%), CL (28%), and FME (2.5%) (Figure 7.4.a). Within resolution analysis of ln-AVIFI shows the rank order of relative variance explained by all important factors remained unchanged for all nine combinations of spatial and temporal resolution (Figure 7.5). Variance explained by IME changed between resolutions by 9% , CL at most by 7% and FME was always unimportant ($< 6.67\%$).

The change in AVIFI (untransformed) over treatment levels was monotonic for all factors and with an approximately linear response to both SG, TG and FME, and a non-linear response to IME (Figure 7.6.a). Variability in AVIFI increased significantly for IME because this treatment was effectively removing samples from a long-tailed distribution of fire sizes. CL was a categorical treatment so linearity was not relevant. AVIFI decreased as TG became coarser and increased as SG became coarser.

INTENSITY (AVINT) Variance explained in average fireline intensity kW.m^{-1} (AVINT), showed TG (21%), SG (6%) and FME (4%) to be the only important single factors (Figure 7.4.b), as expected from the discussion in section 6.3.1.4 and 6.3.2.4. The response of AVINT to CL was unimportant while IME showed no significance ($p < 0.05$) over the five replicates. AVINT increased as spatial resolution became coarser and the reverse was the case for temporal resolution (Figure 7.4.b).

SEASONALITY (PSUM) Variance explained in the proportion of unplanned fires that occur in summer (PSUM) showed importance only for CL (7%) with only 30% of variance explained by all factors and their interactions (Figure 7.4.c). Differences across treatment levels in PSUM showed the observed weather (OB) had a higher proportion burnt in summer than the other climate treatment levels (Figure 7.6.c). The proportion of area burnt in autumn and spring (not shown) was the reverse of this, with higher proportions for the warmer-wetter (WW) and warmer-drier treatments (WD).

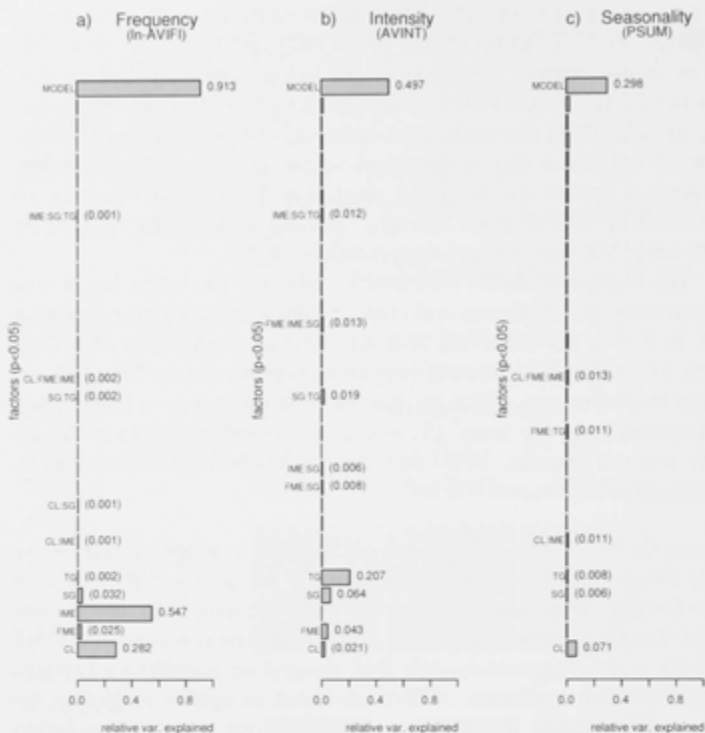


Figure 7.4: Relative Sums of Squares attributed to different sources of variation in the comparison of sensitivity of (a) ln-transformed average inter-fire interval (ln-AVIFI), (b) average fireline intensity (AVINT) and (c) the proportion of area burnt in summer (PSUM). Sources of variation are: climate (CL), fuel management effort (FME), ignition management effort (IME), spatial grain (SG) and temporal grain (TG). Relative Sums of Squares and their interactions are shown in brackets if they are significant ($p < 0.05$) but explain less than 3.75% and 1.88% respectively. Factors and interaction which are not significant are left blank.

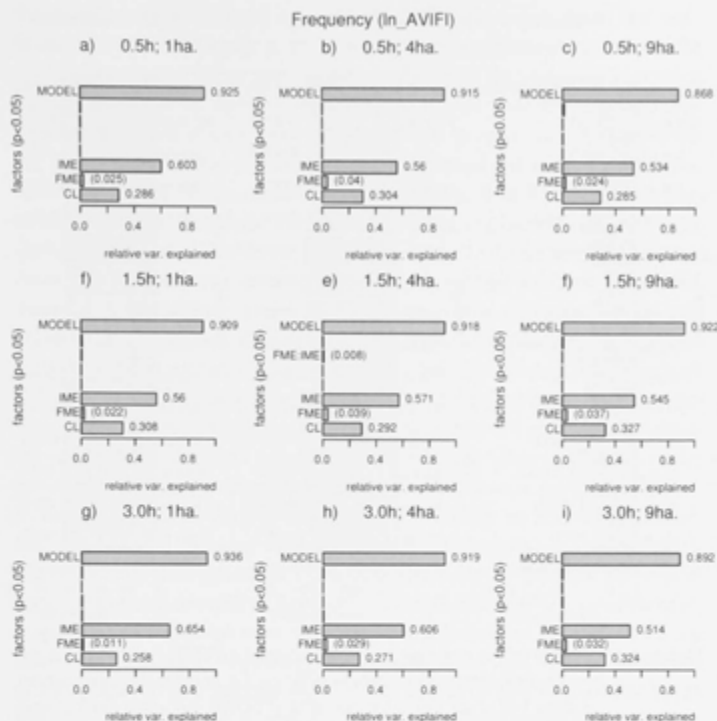


Figure 7.5: Relative Sums of Squares attributed to different sources of variation in the comparison of sensitivity of ln-transformed average inter-fire interval (ln-AVIFI)

Sources of variation are: climate (CL), fuel management effort (FME) and ignition management effort (IME). Relative Sums of Squares and their interactions are shown in brackets if they are significant ($p<0.05$) but explain less than 6.67% and 3.33% respectively. Factors and interaction which are not significant are left blank. Each of (a) to (i) is a separate analysis for each unique combination of temporal resolution (1, 1.5 and 3 hours) and spatial resolution (1, 4 and 9 ha.) resolution.

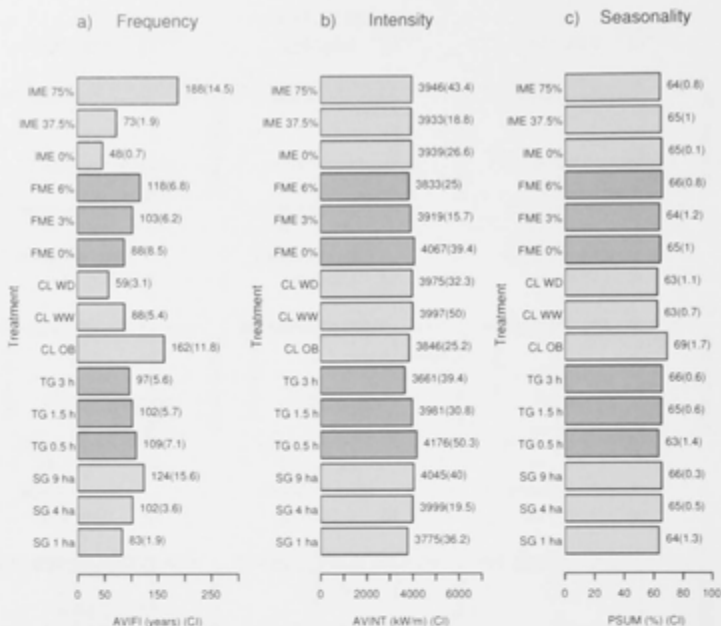


Figure 7.6: Change in (a) average inter-fire interval (AVIFI) (years), (b) average fireline intensity (AVINT) (kW.m^{-1}), and (c) the proportion of area burnt in summer months (PSUM) for each factor and each level of treatment

Experimental factors are spatial grain (SG), temporal grain (TG), climate (CL), fuel management effort (FME) and ignition management effort (IME).

7.4.3 Discussion

Three factors (CL, IME and FME) were chosen for this experiment to set the operational context in which to assess the importance of spatio-temporal resolution. The major response variable for these three factors was $\ln\text{-AVIFI}$. The total of relative variance explained by these three factors combined was 85%. For $\ln\text{-AVIFI}$, the rank order of partitioned variance explained by each of the treatments, CL, FME and IME, remains unchanged across unique combinations of temporal and spatial resolution (Figure 7.5), and on these grounds there is no evidence to suggest Hypothesis (i) should be rejected, that is, the results indicate the ranking of factors was insensitive to spatial and temporal resolution. As measured here, spatio-temporal resolution was relatively unimportant compared to these treatments, and, for example, if other spatio-temporal resolutions had been used by FIRESCAPE in Cary *et al.* (2006, 2009) and Keane *et al.* (2013a), it is most likely that

the results would remain as published. Furthermore, from the verification tests in Chapter 5, it is hoped a more general claim can be made. The aim of those tests was to isolate just those errors that arise from the choice of spatio-temporal resolution that are unavoidable (operational), no matter how the simulator is constructed. Therefore, the claim here is that if simulators are constructed with a consistent management of those domains, these results will hold. This is particularly so for temporal resolution, which explained only 0.2% of the variance in ln-AVIFI. Weather plays a central role in determining inter-fire intervals (or area burnt) (Flannigan and Wotton, 2001) and the lack of sensitivity demonstrated here to the choice of resolution of this data indicates that fire-regime simulation models can afford to be far less particular in this regard, when examining the principal drivers of fire frequency. Insensitivity to spatial resolution in particular, means these models may be able to trade off spatial resolution for other more detailed processes which might otherwise be thought too computationally intensive. For example, there is growing interest in the dynamics of disturbance interactions such as insect attack and fire, storms and fire and drought-fire relationships (Seidl *et al.*, 2011). There is also new research exploring the role of disturbance in patterns of genetic diversity (Banks *et al.*, 2013). FIREMESH, operating at a spatial resolution of nine hectares and a temporal resolution of 0.5 hours, for example, can integrate forcing data and spatial parameters to produce fire regime patterns at a rate of approximately $3,000 \text{ km}^2 \cdot \text{s}^{-1}$ on a desktop computer, four of five fold faster than at a one hectare resolution. This makes FIREMESH and similarly constructed models operating at coarse resolution a practical alternative to using 'cookie cutter' models (a fire model producing a predefined fire footprint) when coupled to other landscape processes such as patterns of genetic diversity (Banks *et al.*, 2013).

A considerable body of work has been done over the past two decades in examining key drivers of fire frequency and much of this work has been done using simulation modelling (Keane *et al.*, 2004). The sensitivity of model results to spatio-temporal resolution is a question that has not been addressed in an operational context for these models and this experiment provides some quantitative support for the robustness of that work. It will always be the case that the detail required of a model necessarily depends on the questions asked of it. For example, spatio-temporal resolution has important consequences for climate models when examining patterns of precipitation (Vanuytrecht *et al.*, 2014), cyclone formation (Zarzycki *et al.*, 2014), hydrological processes (Vereecken *et al.*, 2013; Cornelissen *et al.*, 2014) and simulating single fire events (Jones *et al.*, 2003). For the questions asked of fire regime simulation models however, this experiment finds their results are robust in this regard.

Fire frequency is arguably a primary component of fire regimes as it is a measure of amount of fire in the landscape over a period of observation. However, while TG and SG were unimportant for \ln -AVIFI (and PSUM), TG and SG explained most of the partitioned variance in AVINT (Figure 7.4.b) and experiments using other factors would be required to examine this further.

The IME factor had no effect on intensity, that is, rapid initial suppression of fires did not lead to more intense fires at a later time (Figure 7.6.b). This follows from the fact that, in this landscape, with an average 50 year fire return interval and a fuel accumulation function that returns at least 80% of the fuel within eight years after a fire, the system cannot be considered a fuel limited one.

The effect of the climate treatment on PSUM indicates a lengthening of the fire season with a warmer climate as the proportion of area burnt in summer declines (Figure 7.6.c) but increases in autumn (not shown). As noted (Section 1.3.3), drivers of seasonality are primarily, temporal patterns of rainfall and ignitions, though this experiment indicates that, in forested regions, higher temperatures also effect seasonality by extending the fire season. However, as fuel accumulation, in this model, is not effected by rainfall (apart from a greater amount of fuel being available for combustion during dry periods), it is either the seasonality of the weather conditions or lightning distribution that will determine the seasonality of fire frequencies. The lightning model used in this study is based on a distribution of lightning events driven by seasonal temperature anomalies. By repeating this experiment with a null model of uniform distribution of lightning events, it was found that summer lightning was reduced from 45% to 25% while area burnt is reduced from 70% to 60% for the same season (Figure 7.7). The relative importance of the factors explaining partitioned variance in \ln -AVIFI is almost unchanged when using this null lightning model. Furthermore, when a between-model analysis (combining results of both simulation experiments) is performed, the choice of lightning model was unimportant in explaining partitioned variance in \ln -AVIFI (0.2%) (not shown). This is not to say that patterns of fire regimes will not have changed, but this was not examined.

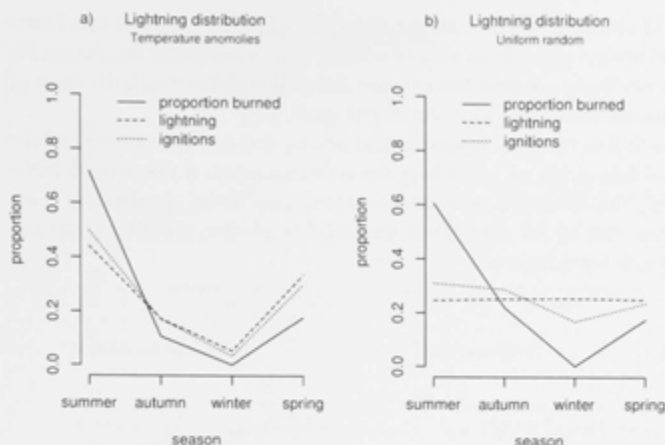


Figure 7.7: Seasonal variation in area burnt that arises from (a) an ignition model driven by temperature anomalies (after Cary 1998) and (b) a null model with a uniform distribution of lightning events

7.4.3.1 Temporal resolution

AVIFI changed by approximately 12% over temporal resolution (97–109 years) for 0.5 and 3 hours respectively, while the number of fires remained unchanged (Figure 7.8). That is, it was an increase in the size of fires that decreased AVIFI as temporal resolution became coarser. Note that, these values are averages over all other treatments and will always exceed the calibrated 50 year IFI because only two factors (CL and TG) lead to a decrease in fire frequency.

To examine TG more closely, additional simulations were performed over a greater range of time steps (0.5–7 hours and 10 replicates) without other treatments. The experiment was performed twice: once using 20,000 year simulations (Figure 7.9.a) and a second with 1,000 year simulations (Figure 7.9.b). The results show a constant increase in area burnt with some particular time steps being outliers (2.5 and 4 hours) (Figure 7.9.b). Reasons for this trend of increasing area burnt are: (i) there is a constant error in exceeding the moment a fire would extinguish proportional to the time step and, (ii) a more variable error as fires fail to extinguish overnight and flare up again in following days. This, more variable source of increasing area burnt, becomes less variable as the sample size (simulation duration) increases (Figure 7.9.a). It might be expected that 2.5 and 4 hour time steps will miss the coolest part of the day in mid-latitude locations though this effect appears to disappear over sufficiently long simulations. It follows that for this temperate mid-latitude climate, time steps should be no more than 3 hours and whole number multiplies of 24 hours to

avoid aliasing effects with the diurnal cycle. The slope of this linear relationship provides a way of scaling across temporal resolution for any similarly constructed fire simulator that determines the time of extinguishment at each time step (Figure 7.9).

With this range of temporal resolution, and assuming much of the error is a result of exceeding the moment when a fire would extinguish, the threshold of extinguishment may be an appropriate parameter with which to calibrate temporal resolution if even coarser resolutions were required.

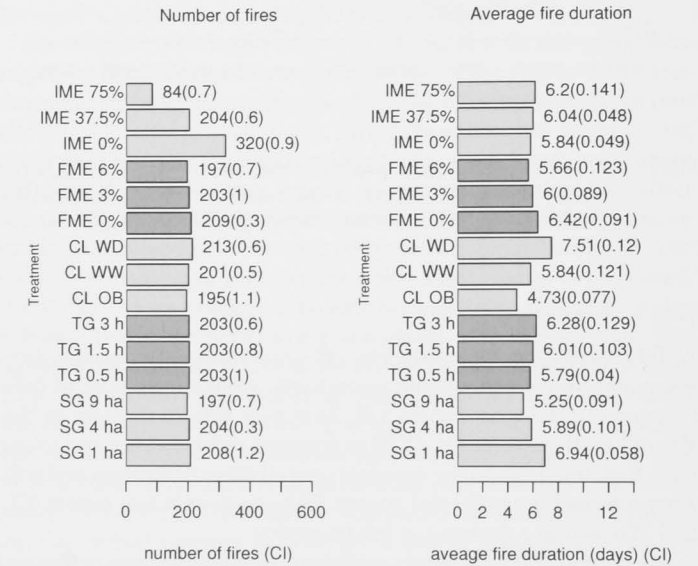


Figure 7.8: Changes in the number of fires (successful ignition per 1,000 years) and the average fire duration (days)
Experimental factors are spatial grain (SG), temporal grain (TG), climate (CL), fuel management effort (FME) and ignition management effort (IME).

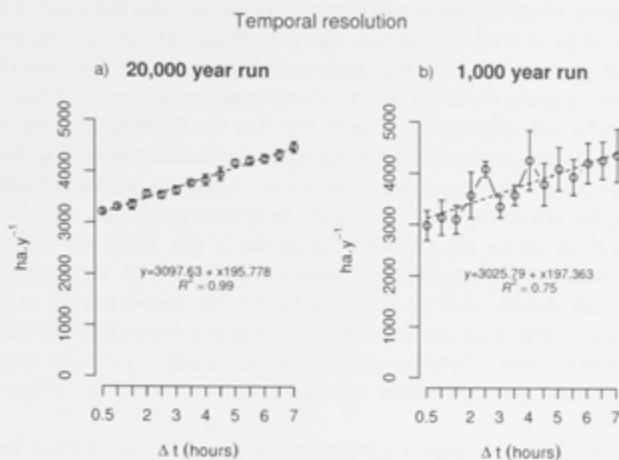


Figure 7.9: Area burnt per annum with time steps ranging from 0.5 to 7 hours (10 replicates) from simulations running for (a) 20,000 years and (b) 1,000 years using 26 years of observed half-hourly weather data (re-cycled every 26 years) in mountainous terrain. Experimental factors are spatial grain (SG), temporal grain (TG), climate (CL), fuel management effort (FME) and ignition management effort (IME).

7.4.3.2 Spatial resolution

AVIFI increases by 49% over spatial resolution (83–124 years for 1 ha and 9 ha respectively) (Figure 7.6.a), because there is both a 5% decline in the number of fires and because fires burn for a shorter time (Figure 7.8). There is an expectation arising from Chapter 4 that area burnt will decline as resolution becomes coarser, because slope must also decline which in turn affects rates of spread. To provide an empirical measure of this relationship, the maximum slope between each site and its neighbour was recorded for each mesh resolution (100–1,000 meters). The change in rate of spread for the 95th percentile of these slopes was calculated at each of those resolutions (Equation A.6). Ten replicate simulations were then performed over this range of resolutions for 1,000 years. As a control, the experiment was repeated using flat terrain (Figure 7.10).

The shape of the curve of area burnt at each resolution was a close match to that of the rate-of-spread for the 95th percentile of slope at that same resolution, suggesting that the geometric relationship between slope and resolution underlies the model's sensitivity in this respect (Figure 7.10). The density distribution of elevations at one and nine hectare resolution shows no discernible difference (not shown).

However, while the sample of elevations may be representative of the population as a whole, because the data is spatial, an aliasing error will arise depending on the cross-scale topographic roughness (the difference in the standard deviation of elevations between locations a particular distances apart) (Figure 2.9). For the DEM used here, this was relatively greater at resolutions up to five kilometres and so there will be slopes that are simply missed as resolution becomes coarser. Thus, the sensitivity of a fire model to spatial resolution almost entirely depends on the range of elevations in the study and the relative scales of topographic roughness and the model. By repeating these simulations and gradually compressing the elevations in the landscape until a flat plain is produced, a non-linear scaling function could be proposed in terms of elevation range that could scale across spatial resolutions. However, this must remain a topic of further research.

It is unclear why there is a slight decline in area burnt on a flat landscape apart from scale errors measured in Chapter 4 (Verification). It may possibly be a result of the constraint imposed by the geometry of the spreading fire by a coarser mesh. To check this, the same simulation was repeated on a flat landscape but using regular meshes with four, six and eight neighbours, however, the result showed no consistent trend so the reason for this remains unclear (Figure 7.11).

7.4.3.3 *Intensity*

The trend in AVINT was inversely proportional to temporal resolution (Figure 7.6.b). As noted, the recorded intensity at which a location burns was the maximum intensity in any direction at the time the location was ignited (whether from lightning or contagion), so in principle, there should be little variation over resolution. If the weather data is sampled at 0.5 and 3 hour intervals and the fireline intensity calculated (assuming a constant fuel load), distributions of intensities recorded at each of these time steps are indistinguishable (not shown). Therefore, the likely explanation for the sensitivity of AVINT to temporal resolution is the increasing proportion of locations ignited near the extinguishment threshold, that is, the area burnt on the fire perimeter during the last time step before extinction. This follows from the observation above that fires inevitably exceed the moment of extinguishment as time step increases.

On the other hand, AVINT is proportional to SG (Figure 7.6.b). That is, as spatial resolution becomes coarser, simulated fires, on average, record a higher intensity. This is an interesting contradiction to the suggestion above, that the decline in fire size is due to the unavoidable reduction in slopes represented in the mesh, as area burnt and intensity are related (Equation A.14). This is not due to some difference in mean elevation as the difference is less than two metres between one and nine hectare resolutions. Fireline intensity is highly sensit-

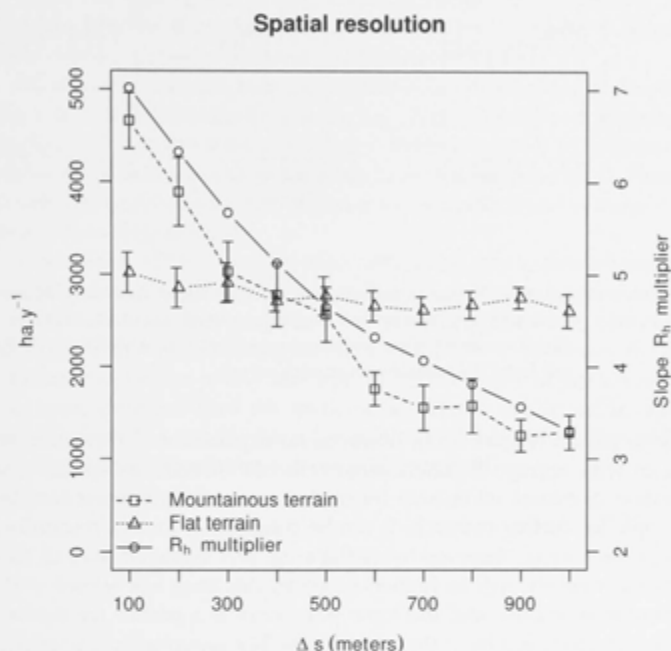


Figure 7.10: Two simulations of 1,000 year duration on flat and mountainous terrain with spatial resolution from 100 to 1,000 metres

The solid line (open circles) is the result of analysis of the mountainous terrain at each of these resolutions and depicts the change in rate of spread due to slope (Equation A.6) based on the slope of the 95th percentile of slopes at each resolution (Right hand axis). By repeating these simulations and gradually compressing the elevations in the landscape until a flat plain is produced, a non-linear scaling function could be proposed in terms of elevation range that could scale across spatial resolutions.

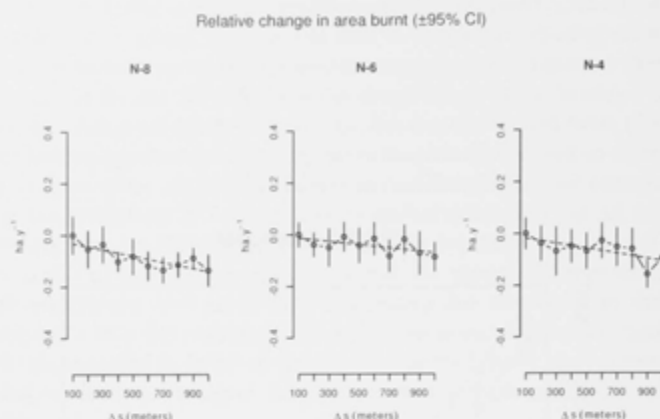


Figure 7.11: Relative change in area burnt for three 1,000 year simulations on flat terrain over spatial resolutions from 100 to 1000 metres. Each experiment is performed on a mesh with eight (N-8), six (N-6) and four (N-4) neighbours to each vertex.

ive to terrain (Figure 6.11), however, no explanation can be offered as to why average fireline intensity should increase as spatial resolution decreases while area burnt decreases and this must remain a topic for further research. It can be conjectured that as resolution becomes coarser, there are fewer flat areas and averaged over all locations, intensity will be higher, however, this does not accord with fires being smaller and the topic must remain a matter for further research as indeed must the issue of whether spatio-temporal resolution is important for measures of fireline intensity relative to typical experimental treatments. As will be shown in the next chapter, other nuisance parameters have a greater effect on estimates of fireline intensity by simulation than do spatial and temporal resolution.

If it can be assumed it is the inverse relationship between slope and spatial resolution that accounts for the sensitivity of AVIFI to SG, the coefficient of slope (Equation A.6) may be the appropriate parameter to calibrate to account for this.

7.4.3.4 Edge effects: The role of spatial extent of model outcomes

The factors that mainly effect unplanned fire size distributions are CL, FME and SG (Figure 7.12). Note, the range of variation in replicate simulations was slight, and can be gauged relative to the treatments in Figure 7.12.f. The magnitude of these factor effects on fire size was constrained by the size of the simulated landscape. This can be seen by the increase in the density distribution of the largest possible

fires in this landscape (0.25 million hectares) (Figure 7.12). Thus, the magnitude of variance explained by factors in this experiment may be reduced by the spatial extent of the simulations, particularly CL and FME (Figure 7.12.a and c), in short, an edge effect. However, the edge effect will suppress the sensitivity of both the CL and FME treatments by constraining the largest fires. Nevertheless, the magnitude of the difference in response of fire frequency between these two treatments is clear. The significance of edge effects is examined more closely in Chapter 8 by replicating an experiment that had a shorter running time over a number of different spatial extents.

SG showed a marked increase in the density distribution of fires at the size of the resolution (1, 4 and 9 ha.) (Figure 7.12.e) and a regular decline in larger fire sizes as resolution became coarser. TG showed a slight increase in fire size as time step increased (Figure 7.12.d). These trends can be seen more clearly over a wider range of spatio-temporal resolutions (Figure 7.13).

Given FIREMESH is capable of recording fire sizes with sub-resolution precision (Chapter 4), the only explanation for this appears to be a conditional one, that is, given a fire can start, it can only continue or extinguish when entering the next location. If it continues, the final fire area can be of any size but those that stop will always have the approximate area of the spatial grain. This is confirmed in later experiments that use meshes of variable resolution where the peak density at mean resolution is more widely spread.

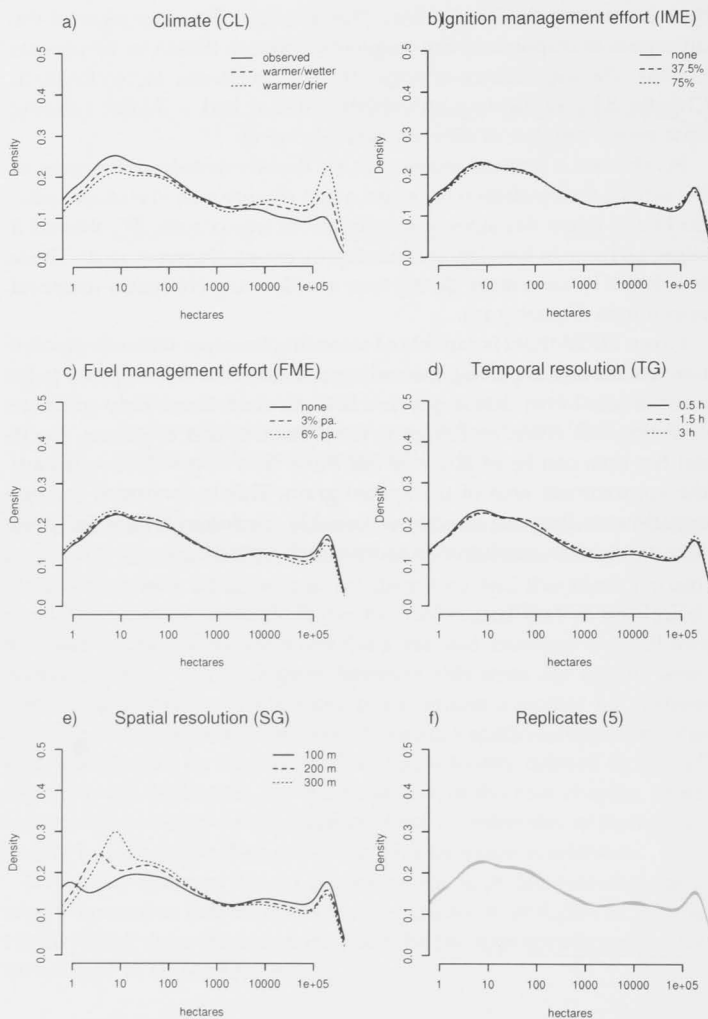


Figure 7.12: Fire size density distributions for each of five treatments and five replicates in experiment 1

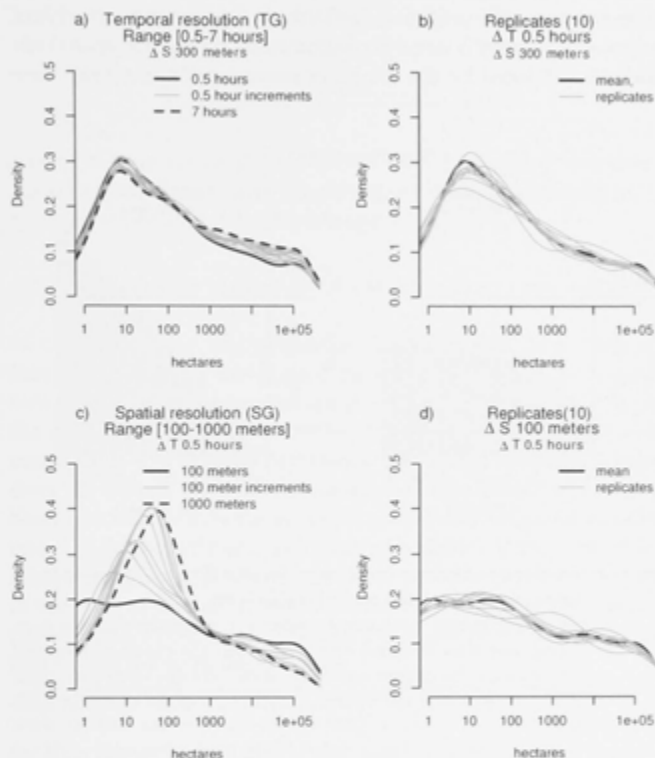


Figure 7.13: Fire size distributions for a wide range of spatial and temporal resolutions (log scale). Temporal resolution was between 0.5–7 hours and spatial resolution between 100–1,000 meters. No other treatments were used. All simulations with varying temporal resolution used a spatial resolution of 9 ha. All simulations with varying spatial resolution used a temporal resolution of 0.5 hours.

7.4.4 Calibration

It was noted above that the coefficient of slope (Equation A.6) may be an appropriate parameter to modify to account for the effect of spatial resolution on model outputs in complex terrain. Similarly, the fireline intensity at which a fire is assumed to self-extinguish may also provide a means of calibration for temporal resolution. In simulation experiments ranging over the scales in these experiments, the choice of temporal resolution is largely constrained by data while spatial resolution is constrained by the computer resources (Figure 7.14). Nev-

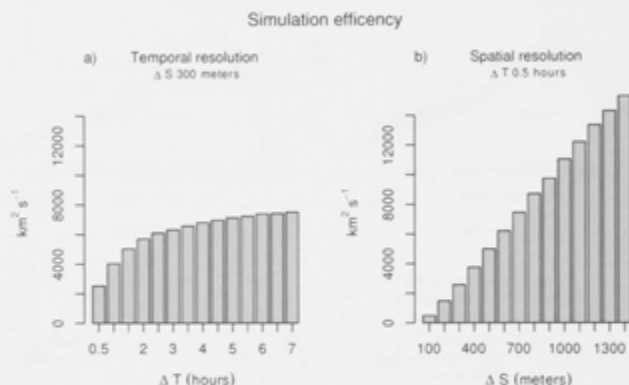


Figure 7.14: Simulation efficiency (area burnt *in silico* ($\text{km}^2 \text{s}^{-1}$)) over a large range of temporal and spatial resolutions

Decreasing spatial resolution provides a much greater gain in computing time than temporal resolution. Thus the choice of temporal resolution can be determined by the data available while the choice of spatial resolution will be limited by the computer resources available.

ertheless, to explore the possibility of calibrating the model for both temporal and spatial resolution, the above experiment (Table 7.1) was repeated having first adjusted the coefficient of slope (Equation A.6) and the threshold of extinguishment (Equation A.7) at three different temporal resolutions, to maintain average fire frequency at a constant value (Table 7.2). The results were analysed in the same fashion as the un-calibrated experiment (Table 7.1).

While the response variable to which the parameters were calibrated (average fire frequency), was no longer sensitive to spatio-temporal resolution at all, as expected, variance in AVINT is almost entirely explained by spatial resolution (not shown). This highlights the problem of calibration to multiple criteria: in the case of fire-regime models, patterns of frequency, intensity and seasonality. Thus optimization

Table 7.2: Calibrated values for the coefficient of Equation A.6 and value of fireline intensity at which a simulated fire extinguishes for three spatial and temporal resolutions
 SG=Spatial resolution; C=exponent (Equation A.6); TG=Temporal resolution; T=Threshold of extinguishment.

SG (HA.)	C	TG (H)	T
1	0.0693	0.5	83
4	0.1	1.5	81
9	0.1272	3.0	84

algorithms are required (such as simulated annealing or genetic algorithms) but these require considerable computer resources for large spatially explicit models (Abdalhaq *et al.*, 2002).

7.5 SUMMARY OF FINDINGS FOR SPATIO-TEMPOAL RESOLUTION

In Chapter 4, any inherent errors in FIREMESH have been noted that may confound the desired measurement of the operational errors that these experiments are designed to expose. In Chapter 5, the suitability of using FIREMESH to address this question has been established. The formal hypothesis that spatio-temporal resolution does not change the relative importance of the drivers of fire has not been rejected. Within the range of spatial and temporal resolutions tested in this experiment, which are reasonable for this class of model (Keane *et al.*, 2004), both are unimportant compared to the magnitude of variance explained in ln-transformed average inter-fire interval by climate, fuel treatment and ignition suppression - three experiments that can be found in the literature.

Modellers make choices in temporal and spatial resolution often without full knowledge of the implications these choices may have for their research (Bian and Butler, 1999). The finding that spatial and temporal resolution are relatively unimportant in this case provides support for the robustness of simulation modelling experiments designed to explore the key determinants of fire frequency. Studies of the sensitivity of individual fire events (Jones *et al.*, 2003; Cui *et al.*, 2008) have noted differences in fire extents due to spatial and temporal resolution, and this too can be demonstrated with FIREMESH (Figure 7.15). This is not uncommon in many fields (see for example Draxler 1987; Zarzycki *et al.* 2014; Vanuytrecht *et al.* 2014). The intensity and longevity of a cyclone may well be better resolved at finer resolutions, and likewise the final the perimeter of a fire may well be better predicted at fine spatial and temporal resolutions (see discussion in Section 4.1). However, what is being asked here is, do these errors accumulate in a systematic fashion that leads different outcomes for

model experiments depending on what may be somewhat arbitrary choices of temporal and spatial resolution made by modellers? This question has not been directly addressed before and this experiment supports the view that these decisions are relatively unimportant in understanding what drives area burnt.

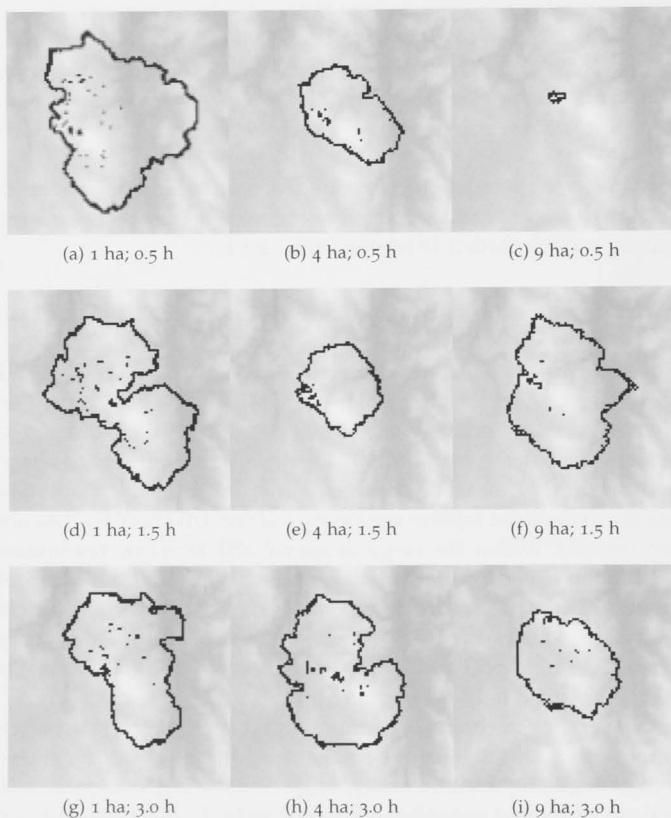


Figure 7.15: Nine simulated fires burning under identical weather, fuel and terrain conditions with different combinations of temporal and spatial resolution

Spatial resolutions (ΔS) are one, four and nine hectares. Temporal resolutions (ΔT) are 0.5, 1.5 and 3 hour time steps. Weather data is from Canberra Airport. Ignition time is 12 midday, 10th January 1991.

At the same time, both spatial and temporal resolution do cause some systematic change in estimated fire frequency. Spatial resolution has a larger effect (in mountainous landscapes) and has very significant consequences for computational effort. However, there appears no simple way of reducing such sensitivity to spatial and tem-

poral resolution through calibration while maintaining the integrity of model outputs of at least fire frequency and intensity.

The factors used in this experiment involving a climate, ignition and fuel treatment, could not provide a formal test of the importance or otherwise of spatial and temporal resolution in estimates of fire intensity or seasonality. This must remain a topic of further research. To test the importance of model resolution on estimates of fireline intensity would require a wider range of experimental treatments involving, for example, exploration of the role of terrain or the inter-annual variability of weather (Section 6.4).

All models are abstractions and a good model should ideally hold over levels of abstraction (Gignoux *et al.*, 2011). This is rarely the case but within the range of the abstraction of space and time as discrete quantities used here, this experiment shows that assertions made by models of this class are robust with regard to this degree of abstraction. Furthermore, if experiments only require flat terrain (e.g. Cary *et al.* 2009), spatial resolution can be considerably coarser again, allowing either more detailed experimental designs, simulation experiments over larger spatial extents or the addition of model processes that explore other system behaviours that may interact with fire.

SPATIAL REPRESENTATION: EXAMINING DIFFERENT FORMS OF DISCRETE SPACE

Three experiments are performed, analysed and discussed in this chapter. These experiments explore the consequences that different forms of spatial representation (apart from spatial resolution) have for the questions typically asked of landscape fire regime simulation models. Because space has more dimensions than time, other issues arise when representing continuous space as discrete points. Firstly, for a spatial model, the points must be connected in some way, that is, the topology of space must be described. In the present study this involves examining the consequences that the number of neighbours to each vertex has for fire regime modelling as defined by Hypothesis (ii) (Section 1.4.5). Secondly, it has been shown that the disposition of vertices over the spatial extent and the consequent angles between them have significant impacts on the shapes of simulated fires (Section 5.6, Johnston *et al.* 2008). This involves describing space as a Delaunay triangulation of vertices with a Poisson-Disk distribution, a particular form of a Triangular Irregular Network (TIN) (Section 4.2.3). The importance or otherwise of this description of space is assessed by addressing Hypothesis (iii) (Section 1.4.5). Other researchers have used TINs, with vertices located unevenly over the spatial extent, to optimize the sampling of space for various purposes from seismology (Braun *et al.*, 1995), fluid dynamics (Anderson *et al.*, 2005), General Circulation Models (Zarzycki *et al.*, 2014; Düben and Korn, 2014) to astronomy (Cautun and van de Weygaert, 2011). Only the latter of these examples uses a prior adapted mesh as is done here (Section 8.3). The others use a mesh that changes resolution dynamically over the course of the simulation. This may not be tractable for fast fire simulations but could be a topic of later research (Hu and Ntamo, 2006). In addition only the first and last examples given above use a mesh created with by Delaunay Triangulation as is done in this study. Sub-division of regular meshes can cause simulation artefacts at the boundaries where resolution changes (Zarzycki *et al.*, 2014) whereas a TIN can vary resolution incrementally. The final experiment in this chapter examines whether or not this technique may be useful in reducing the sensitivity of landscape fire regime models to spatial resolution as described in Section 4.2.5. This experiment (Section 8.3) addresses Hypothesis (vi) (Section 1.4.5).

8.1 HYPOTHESIS (II): RELATIVE IMPORTANCE OF NEIGHBOURHOOD NUMBER

Hypothesis (ii): ranking the relative importance of the drivers of fire by simulation modelling is insensitive to neighbourhood number

8.1.1 Purpose

The purpose of this experiment is ascertain whether the relative importance of the same experimental treatments as employed in the previous experiment (Chapter 7), CL, IME and FME, remain unchanged over a range of neighbourhood arrangements.

8.1.2 Methods



To accept or reject this hypotheses, FIREMESH was used in a multi-factorial experiment using four factors: CL, IME and FME as described in Chapter 7 and neighbourhood number (NN) using a regular mesh employing either four, six or eight edges between vertices. The experimental design and method of analysis are the same as those discussed in Chapter 7 including not calibrating ignition rates to account for the three forms of NN. All treatments use a one hectare mesh and half hour time step. The terrain and weather data used was again that described in Chapter 2. The results were analysed as before: relative variance in \ln -AVIFI, AVINT and PSUM explained (r^2) by each of four factors and their interactions in an ANOVA design as in previous chapters. The experimental factors and treatment levels are summarised in Table 8.1.

8.1.3 Results

Total variance explained by all factors for average fireline intensity (AVINT) and the proportion of area burnt in summer (PSUM) was less than half that explained for \ln -AVIFI (40%, 31% and 93% respectively) (Figure 8.1). As was the case with the previous experiment, AVINT and PSUM were consequently less informative of the importance of the experimental factors than \ln -AVIFI. Variance explained in all three response variables was more similar between N-6 and N-8 arrangements than between N-4 and N-6.

FREQUENCY (\ln -AVIFI) The number of neighbours to a vertex (SR), is the second most important factor in explaining variance in \ln -AVIFI (30%). Both IME (34%) and CL (24%) are important while FME is again unimportant (<5%) (Figure 8.1.a). Within-resolution analysis of \ln -AVIFI showed the rank order of importance of the factors changed across the three levels of NN, with IME becoming more im-

Table 8.1: Experimental design for a factorial experiment to measure the importance of neighbourhood number against published experimental factors in fire regime simulation modelling

FACTOR	LEVELS	DESCRIPTION
Climate	Three	<i>Observed:</i> Historical climate <i>Warmer/Wetter:</i> Historical +3.6°C; +20% precipitation <i>Warmer/Drier:</i> Historical +3.6°C; -20% precipitation
Ignition mngt effort	Three	<i>Zero:</i> 0% ignitions prevented <i>Mod:</i> 35.7% ignitions prevented <i>High:</i> 75% ignitions prevented
Fuel mngt effort	Three	<i>Zero% p.a. treatment</i> <i>Zero% p.a. treatment</i> <i>Zero% p.a. treatment</i>
Neighbourhood Number	Three	
		

portant and CL less so between the N-4 and N-6 arrangements (Figure 8.2). No change in rank order occurred between N-6 and N-8 simulations. Changes in untransformed AVIFI over treatment levels were monotonic and non-linear for all important factors (>5% of variance explained) (Figure 8.3).

INTENSITY (AVINT) Variance explained in the average fireline intensity (AVINT) showed NN to be the most important factor (11%) followed by CL (10%) and FME (6%) (Figure 8.1.b). Values of AVINT show the N-4 neighbour configuration to have the lowest mean intensity (Figure 8.3.b).

SEASONALITY (PSUM) Variance explained in the proportion of unplanned fires that occur in summer (PSUM) showed both CL and NN to be unimportant and the total variance explained by all factors for PSUM was 1/3 that of ln-AVIFI (Figure 8.1.c). It can be assumed that

most of the unexplained variance was due to inter-annual variability in weather (Section 6.3.1.1).

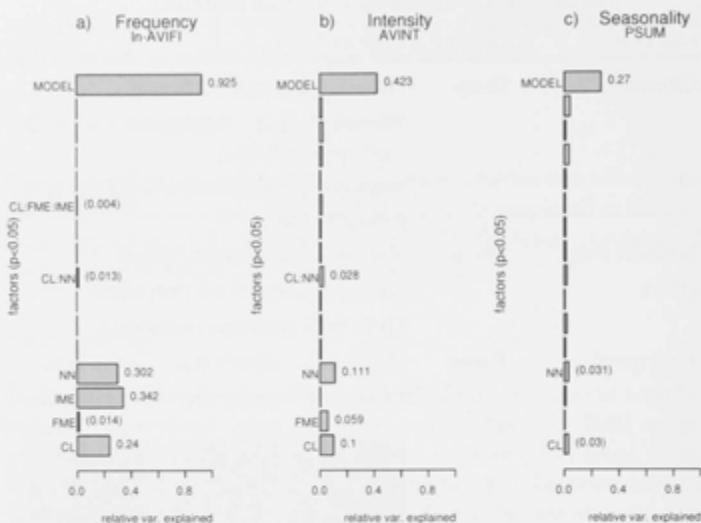


Figure 8.1: Relative Sums of Squares attributed to different sources of variation in the comparison of sensitivity of (a) ln-transformed average inter- fire interval (ln-AVIFI), (b) average fireline intensity (AVINT) and (c) the proportion of area burnt in summer (PSUM). Sources of variation are: climate (CL), fuel management effort (FME), ignition management effort (IME) and spatial representation (SR). Relative Sums of Squares and their interactions are shown in brackets if they are significant ($p < 0.05$) and explain less than 5% and 2.5% respectively. Factors and interaction which are not significant are left blank. Each experiment was run at the same temporal and spatial resolution (0.5 hours and 100 meter cell width respectively).

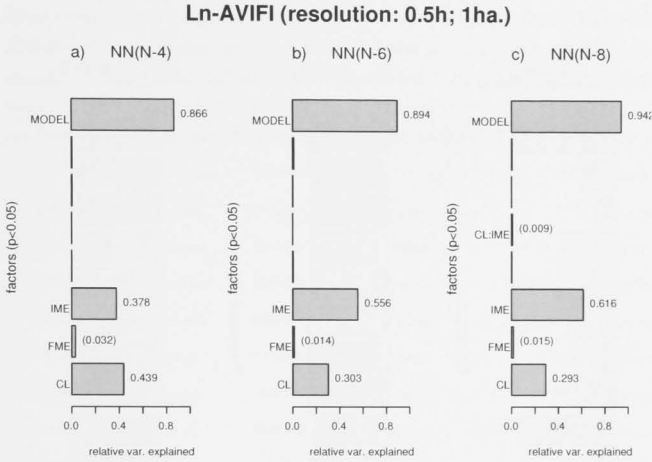


Figure 8.2: Relative Sums of Squares attributed to different sources of variation in the comparison of sensitivity of ln-transformed average inter-fire interval (ln-AVIFI). Sources of variation are: climate (CL), fuel management effort (FME) and ignition management effort (IME), analysed separately for each neighbourhood number. Relative Sums of Squares and their interactions are shown in brackets if they are significant ($p < 0.05$) and explain less than 6.67% and 3.33% respectively. Factors and interaction which are not significant are left blank. Each of (a) to (c) is a separate analysis for each spatial arrangement of number of edges between neighbours: (a) 4 neighbours, (b) 6 neighbours and (c) 8 neighbours. Each experiment was run at the same temporal and spatial resolution (0.5 hours and 100 meter cell width respectively).

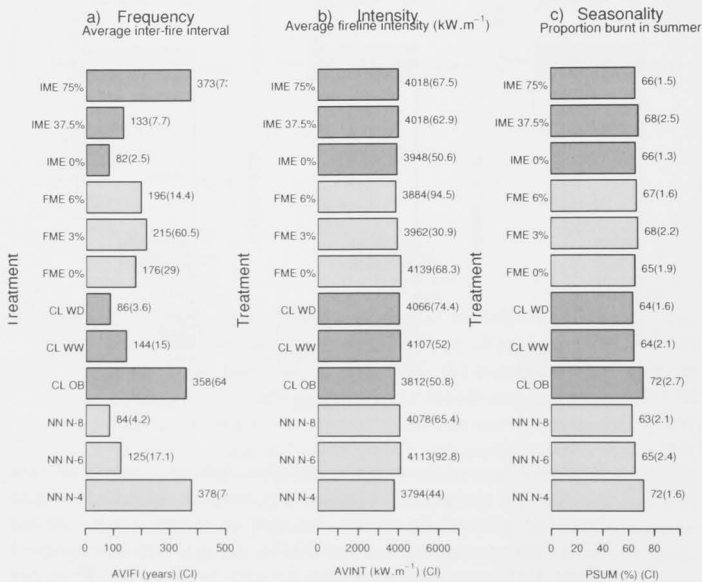


Figure 8.3: Changes over treatment levels in (a) average inter-fire interval (AVIFI) (years), (b) average fireline intensity (kW.m⁻¹) and (c) the proportion of area burnt in summer. Experimental factors are spatial representation (SR) (4, 6 and 8 neighbours), climate (CL), fuel management effort (FME) and ignition management effort (IME).

8.1.4 Discussion

As the rank order of relative variance explained for \ln -AVIFI changed over the levels of the NN treatment, Hypothesis (ii) was therefore rejected (Figure 8.2.a and b). Had this experiment been restricted to N-6 and N-8 representations, on the other hand, the hypotheses would not have been rejected. As meshes with triangular irregular networks have six neighbours on average (Figure 1.4), this is added support for their use (experiments 3 and 4 below) over and above the purpose in over-coming constraints imposed by discrete geometries. In addition, simulation efficiency scales linearly with the number of neighbours, as the work of the simulation is in calculating the rate of spread in each of these directions (Figure 8.4) and therefore, all else being equal, an N-6 mesh may be preferred to an N-8 mesh.

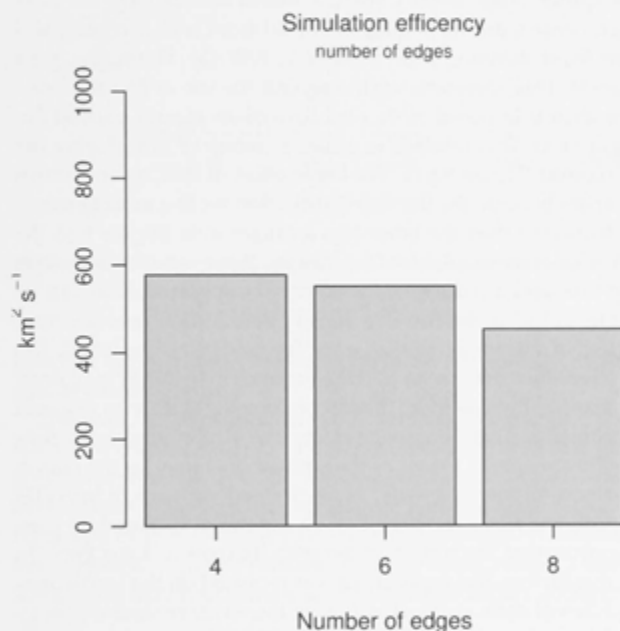


Figure 8.4: Simulation efficiency (area burnt *in silico* $\text{km}^2.\text{s}^{-1}$) with four, six and eight neighbour mesh configurations averaged over all treatments

AVINT was also lower for N-4 (Figure 8.3.b), again because of the constraints imposed on simulated fire spread by such a simplified topology. This follows because fireline intensity is proportional to the rate of spread. The rate of spread in directions other than the wind

direction is less and therefore it can be expected that, for discrete geometries with fewer edges between neighbours, rates of spread and therefore fireline intensities will be lower on average. However, there was little difference between N-8 and N-6 meshes but a large difference between N-4 and the other two arrangements. In large part, this can be attributed to the simple observation that six neighbours is 50% more edges than four and eight neighbours 30% more than six. A second contributing factor may be due to the dominance of wind from the north-west during summer in the Canberra Airport weather data (Figure 2.6), and consequently, most fires will spread to the south-east, a direction that is poorly represented by N-4 meshes. This is not an uncommon situation. Many fire-prone environments have a dominant wind direction during the fire season that does not neatly align with cardinal points of the compass. For example, the Santa Ana winds that drive large fire runs in California come from the NE (Raphael, 2003). In the Canadian Boreal forests, large fire runs most often occur with the passage of a cold front with a consequent change in wind direction from the SW to NW (M. Flannigan, pers. comm., 2014). This, therefore, argues against the use of N-4 meshes.

The constraints imposed by N-4 configurations clearly impede fire sizes (Figure 8.5). This resulted in a concentration of fires during the summer months (Figure 8.3.c). The lesser effect of IME on area burnt possibly arises because the fire size distribution for N-4 arrangements was less truncated than the other two arrangements (Figure 8.5). Because fire sizes were smaller for N-4 meshes, there were fewer system spanning fires and a reduced edge effect was apparent. This can be seen by the 'bulge' in the fire-size density distribution near the maximum extent of the simulated landscape (250,000 ha.) (Figure 8.5). The reduced edge effect may mean that the variance in \ln -AVIFI explained by CL is greater: there is more 'headroom' for the system to respond to the treatments. Therefore, edge effect (the size of simulated fires compared to the spatial extent of the simulations) may be the reason for the reversal of the rank order of partitioned variance in \ln -AVIFI between IME and CL. Note that it was a constraint imposed by computer resources that has restricted the spatial extent to 2,500 km². To examine this further, this experiment was repeated on flat landscapes of three different sizes at the elevation of the weather station providing the observations (Canberra Airport). The range of fire sizes is less on a flat landscapes, where only variability in weather drives fire sizes without the interaction with terrain. A flat landscape was used in order not to confound the results with landscapes that have different proportions of mountains and plains. To achieve a noticeable edge effect the width of the three square landscape sizes chosen were 1024, 512 and 256 twenty metre cells or 419, 105 and 26 km².

The results showed that the sensitivity to the CL, FME and IME experimental factors was proportional to the magnitude of the edge

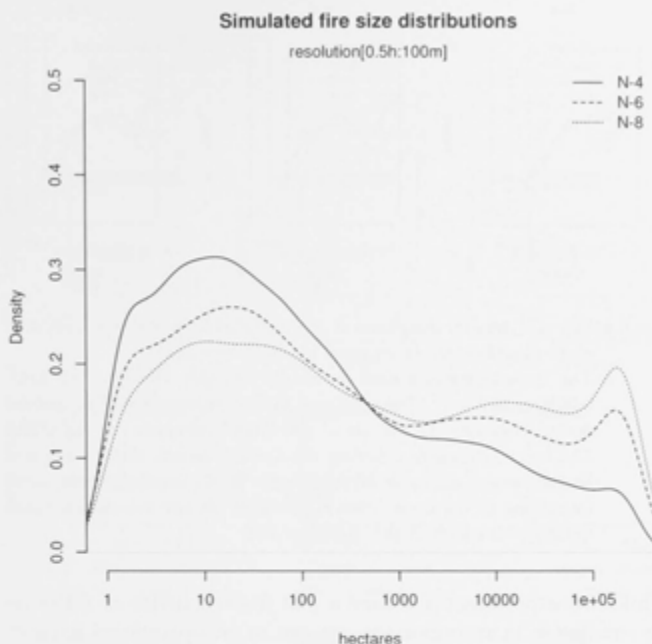


Figure 8.5: Fire size density distribution of simulated fires with four, six and eight neighbours

effect as the N-8 mesh showed a high fire size density at size of the spatial extent (Figure 8.6).

The variance explained in AVIFI for N-4 meshes by CL changed from 21% (Figure 8.6.g) to 13% (Figure 8.6.i) for large and small landscapes respectively. For N-8 meshes, on the other hand, where edge effects were more pronounced (Figure 8.7), the same factor changed from 24% to 4.7%. (Figure 8.7.a and c). Thus while Hypothesis (ii) has been rejected, it can be conjectured that further research using larger landscapes may find otherwise even for this highly constrained geometry.

The less area burnt by N-4 meshes could be accounted for through calibration by increasing the annual ignition rate. Given there have been on average six fires per year in this region over the past 70 years, calibration over this range is not unreasonable but it would not be expected that fire size distributions will change. Furthermore, there is no expectation that calibrating the ignition rate will alter the reversal of the rank order of variance explained in ln- AVIFI by CL across SR treatments.

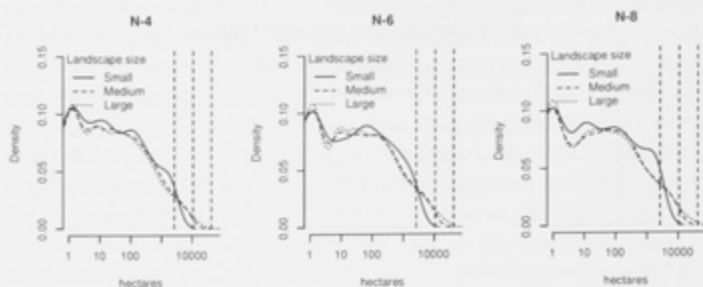


Figure 8.6: Fire size density distribution of simulated fires with four, six and eight neighbours, constrained by landscape size

The three landscapes sizes are small: 26 km², medium: 105 km² and large 419 km². The terrain of all landscapes is flat. The vertical dotted lines indicate the size of the three landscapes (on log scale). The function used to calculate the fire-size density distribution is a kernel density estimator (R core team 2014) which involves some smoothing of the curve. Hence, fire sizes do not appear truncated exactly at the limit of the landscape size.

While this experiment has shown that the sensitivity of a fire regime simulation is an important concern in an operational context, it is only the extreme case of N-4 meshes, less constrained by edge effects in this case, that leads to this conclusion. I am unaware of any fire regime model that uses this arrangement and the difference between the two most common forms (N-6 and N-8) is unimportant. Other modellers, concerned by the constraints of discrete geometries, have implemented models with 24 and 48 edges (BFOLDS: Perera *et al.* 2008) from studies of individual fire events (Cui *et al.*, 2008). However, in an operational context, this experiments indicates these concerns may be unfounded.

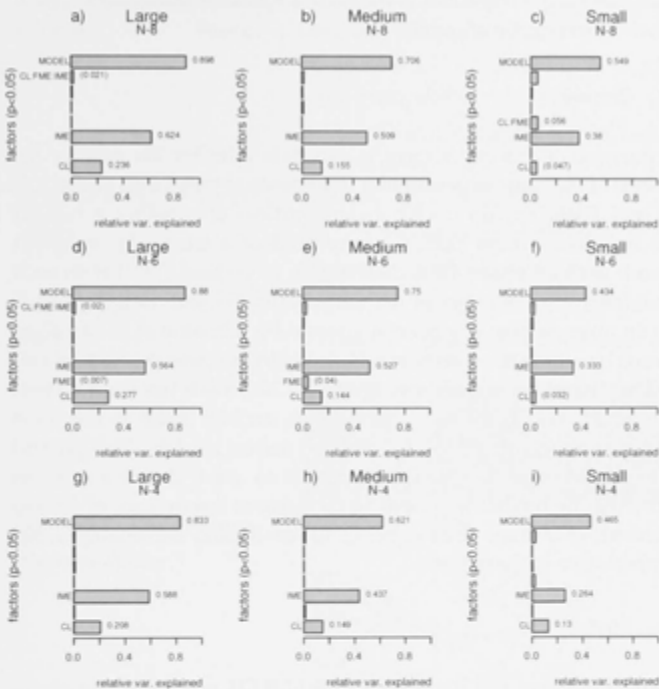


Figure 8.7: Relative Sums of Squares attributed to different sources of variation in the comparison of sensitivity of \ln -transformed average inter-fire interval (\ln -AVIFI). Sources of variation are: climate (CL), fuel management effort (FME) and ignition management effort (IME)

Relative Sums of Squares and their interactions are shown in brackets if they are significant ($p < 0.05$) and explain less than 6.67% and 3.33% respectively. Factors and interaction which are not significant are left blank. Each experiment was run at the same temporal and spatial resolution (0.5 hours and 100 metre cell width respectively). Each chart (a to i) shows these results for each unique combination of landscape size and meshes with four, six and eight neighbours. The variance explained in \ln -AVIFI by each factor is more constrained by landscape size for mesh arrangements that produce larger fires (N=6 and N=8).

8.2 HYPOTHESIS (III): IMPORTANCE OF REGULAR/IRREGULAR SPATIAL REPRESENTATION

Hypothesis (iii): ranking the relative importance of the drivers of fire by simulation modelling is insensitive to the use of a regular or triangular irregular network representation of space

8.2.1 Purpose

The purpose of this experiment is ascertain whether the relative importance of the same experimental treatments as employed above: CL, IME and FME, remain unchanged regardless of whether a regular eight neighbour mesh (REG) is employed or a triangular irregular network with a Poisson-Disk distribution of vertices (TIN) with each vertex having an average of six neighbours (Figure 1.4). As noted, such an arrangement has been suggested by Johnston *et al.* (2008) as a means by which the constraints imposed by discrete geometries can be alleviated in fire simulation. A regular N-8 mesh has been chosen rather than an N-6 mesh as, of the two, an N-8 mesh is the most common arrangement used by fire simulation models. The general question addressed by this experiment is to ask if this is a concern for fire regime models in assessing the relative importance of the determinants of average fire frequency (intensity and seasonality being uninformative in these tests).



8.2.2 Methods

To accept or reject this hypotheses, FIREMESH was used in a multi-factorial experiment using four factors: (i) CL, (ii) IME, (iii) FME, and (iv) either a regular N-8 (REG) or a TIN mesh. This last factor is referred to as SR in this experiment. The experimental design and method of analysis are the same as the previous experiment including not calibrating ignition rates to account for the any difference in area burnt between N-8 and TIN representations (SR). Table 8.2 summarizes the experimental factors and treatment levels. All treatments used a one hectare mesh and half hour time step and the terrain and weather data used was again that described in Chapter 2. The results were analysed as before: relative variance in $\ln\text{-AVIFI}$, AVINT and PSUM explained (r^2) by each factor and their interactions in an ANOVA design.

8.2.3 Results

As with the two previous experiments, AVINT and PSUM were less informative of the importance of the experimental factors than $\ln\text{-AVIFI}$ (41%, 27% and 94% respectively) (Figure 8.8).

Table 8.2: Experimental design for a factorial experiment to measure the importance of sregular/irregular spatial representation against published experimental factors in fire regime simulation modelling

FACTOR	LEVELS	DESCRIPTION
Climate	Three	<i>Observed:</i> Historical climate <i>Warmer/Wetter:</i> Historical +3.6°C; +20% precipitation <i>Warmer/Drier:</i> Historical +3.6°C; -20% precipitation
Ignition mngt effort	Three	<i>Zero:</i> 0% ignitions prevented <i>Mod:</i> 35.7% ignitions prevented <i>High:</i> 75% ignitions prevented
Fuel mngt effort	Three	<i>Zero% p.a. treatment</i> <i>Zero% p.a. treatment</i> <i>Zero% p.a. treatment</i>
Spatial Representation	Three	
		

FREQUENCY (LN-AVIFI) SR and FME were unimportant (< 5%) in explaining partitioned variance in ln-AVIFI, while IME was the most important factor (58%) followed by CL (28%) (Figure 8.8.a), the same order as in previous experiments. When the two forms of spatial representation were analysed separately, there was at most a 1% difference in any of the factors in variance explained and no change in their rank order (Figure 8.9). A higher AVIFI was produced by the TIN representation (less area burnt) than the regular mesh. All other factors showed a monotonic change with treatment level as was the case with the previous experiments (Figure 8.10).

INTENSITY (AVINT) SR and FME were the only important factors in explaining variance in AVINT (21% and 6% respectively). CL was unimportant (2%) (Figure 8.8.b). Changes over treatment levels in AVINT indicate space represented by the TIN mesh produced higher intensities than REG8 mesh (Figure 8.10.b).

SEASONALITY (PSUM) Seasonality showed only the climate treatment was important (8%) (Figure 8.8.c) and that the TIN mesh had a greater proportion of area burnt in summer than the REG mesh (Figure 8.10.c).

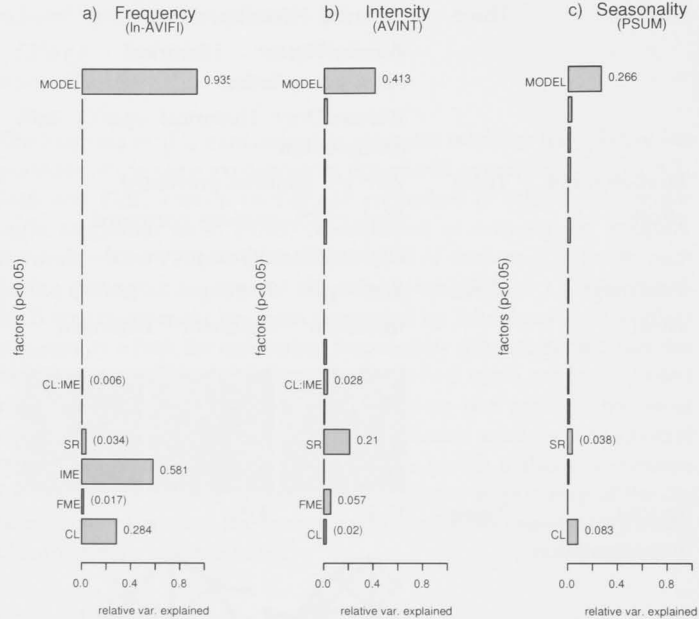


Figure 8.8: Relative Sums of Squares attributed to different sources of variation in the comparison of sensitivity of (a) ln-transformed average inter- fire interval (ln-AVIFI) and (b) average fireline intensity (AVINT). Sources of variation are: climate (CL), fuel management effort (FME), ignition management effort (IME) and spatial representation (SR)

Relative Sums of Squares and their interactions are shown in brackets if they are significant ($p<0.05$) and explain less than 5% and 2.5% respectively. Factors and interaction which are not significant are left blank. Each experiment was run at the same temporal and spatial resolution (0.5 hour and 1 hectare).

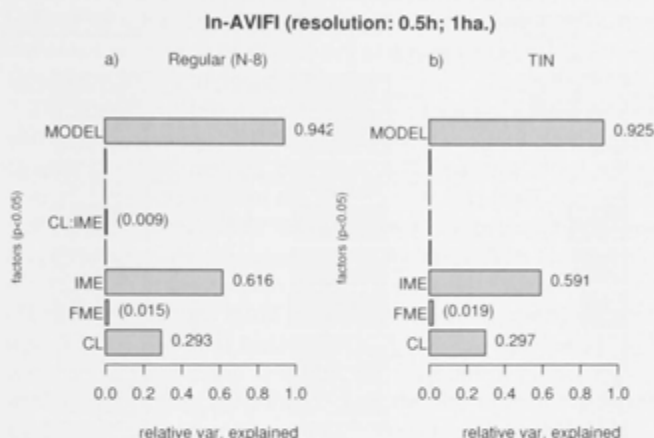


Figure 8.9: Relative Sums of Squares attributed to different sources of variation in the comparison of sensitivity of ln-transformed average inter-fire interval (ln-AVIFI). Sources of variation are: climate (CL), fuel management effort (FME) and ignition management effort (IME)

Relative Sums of Squares and their interactions are shown in brackets if they are significant ($p < 0.05$) and explain less than 6.67% and 3.33% respectively. Factors and interaction which are not significant are left blank. (a) and (b) are separate analyses for two spatial arrangements of (a) a regular 8 neighbourhood arrangement and (b) a Triangulated Irregular Network after Johnston et al. (2008). Each experiment was run at the same temporal and spatial resolution (0.5 hour and 1 hectare).

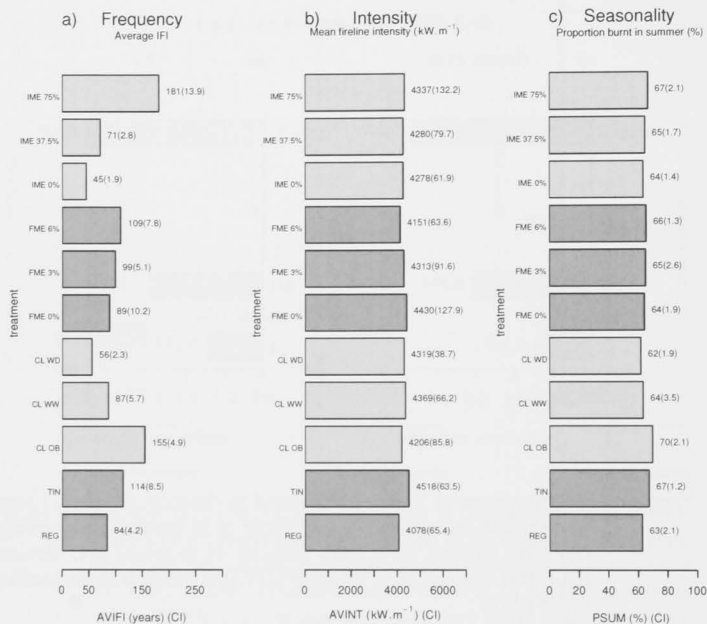


Figure 8.10: Changes over treatment levels in (a) average inter-fire interval (AVIFI) (years), (b) average fireline intensity ($\text{kW} \cdot \text{m}^{-1}$) and (c) the proportion of area burnt in summer (PSUM)

Changes over treatment levels in (a) average inter-fire interval (AVIFI) (years), (b) average fireline intensity ($\text{kW} \cdot \text{m}^{-1}$) and (c) the proportion of area burnt in summer (PSUM)

8.2.4 Discussion

Ln-AVIFI showed little change within SR treatments, and on these grounds, there is no evidence to reject the hypotheses (Figure 8.9). By this measure, the use of the irregular mesh in determining the relative importance of CL, IME, and FME, three important determinants of fire frequency, is unimportant. This finding adds support to the robustness of the results from studies prior to the pioneering work of Johnston *et al.* (2008) and provides further evidence that the constraints imposed by discrete geometries on fire shape, a concern that has led to a considerable body of research, as already noted, does not affect estimation of the drivers of area burnt in the landscape by simulation in any important way.

The fire-size distributions of these two forms of spatial representation indicate that the TIN method produces smaller fires (Figure 8.11). Overall, the TIN method produced 20% less area burnt (averaged over all simulations) than the REG8 mesh. As noted above, the fire size distribution can affect the measures of the proportion of summer fires as the climate treatment pushes the larger fires in the REG simulations into autumn. In principle, simulating fire on a TIN should produce greater area burnt than on a regular eight-neighbour mesh (Figure 5.15). While it has been found that the TIN method will always under-predict the area of a fire footprint in proportion to the number of vertices contained within the fire footprint (Figure 5.6), this under-prediction is an order of magnitude less than that produced by a regular eight-neighbour mesh. Thus the 20% reduction in estimated area burnt using a TIN compared to a regular mesh is surprising. A detailed comparison of the two forms of spatial representation applied to estimating many individual fire events, may provide insights into the reasons for this, however, this must remain a topic for further research.

Despite the insensitivity of Ln-AVIFI to SR, it was the most important factor in determining average fireline intensity (Figure 8.8.b). Note that despite the fact that Equation A.15 produces faster rates of spread (R_{micro}), it is R_{macro} , calculated as $R_{\text{micro}}/(1 + \beta)$, that is used in calculating fireline intensity (Equation A.16). Thus the only reason for the increase in measured fireline intensity is that the average fire spread direction in the data set used for these experiments is captured better with a TIN than with a REG8 mesh despite the fact that a TIN has on average two fewer neighbours than the REG8 mesh.

The better capture of the range of fireline intensity by the TIN configuration and improved efficiency (Figure 7.14) argue for its use over a regular N-8 configuration apart from the justifications for its adoption in Johnston *et al.* (2008). As noted above, simulation efficiency is proportional to the number of neighbours. While the equation to fit simulated rates of spread to observations requires further re-

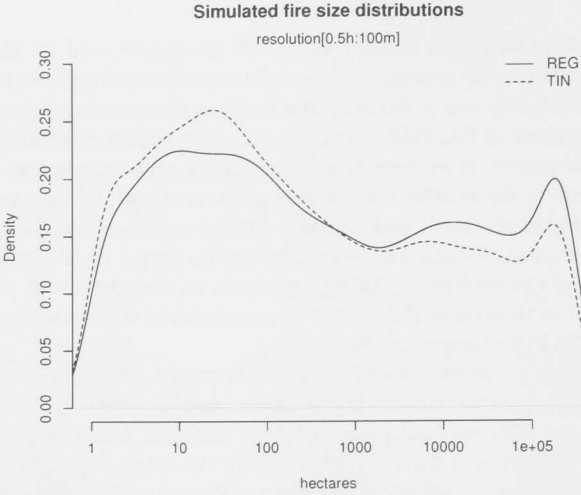


Figure 8.11: Fire size density distributions (log scale) for spatial representations using a regular eight-neighbour mesh (REG) and a mesh composed of a Triangular Irregular Network of vertices with a Poisson-Disk distribution

calibration (Chapter 4), for the purpose to which it has been used here, it is otherwise equivalent to an N-8 regular mesh. What mitigates against its use is the added complexity of the software needed to prepare and run simulations on a mesh compared to a regular raster grid.

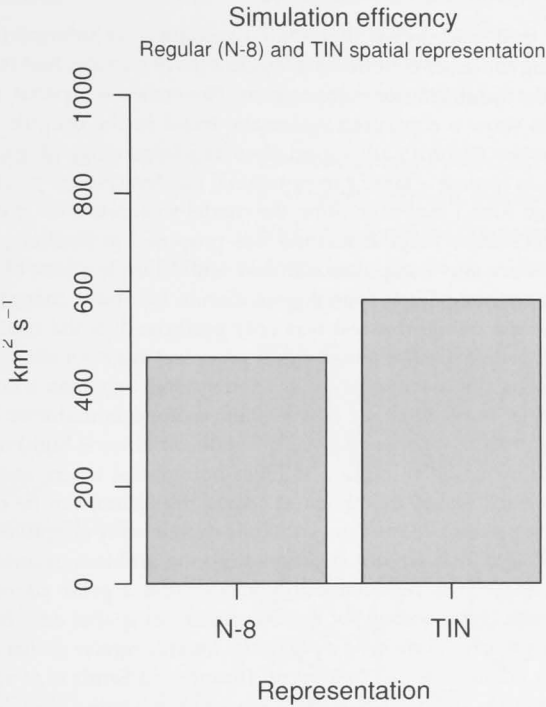


Figure 8.12: The simulation efficiency (area burnt $\text{km}^2.\text{s}^{-1}$ burnt *in silico*) for spatial representations using a regular eight-neighbour mesh (REG) and a mesh composed of a triangular irregular network of vertices with a Poisson-Disk distribution with six neighbours on average

8.3 HYPOTHESIS (IV): OPTIMAL SAMPLING OF SPACE USING A PRIOR ADAPTED MESH

Hypothesis (iv): optimizing the placement of sites to capture rates of change in the terrain can reduce the sensitivity of a fire simulation model to spatial resolution

8.3.1 Purpose

In Chapter 7, it was shown that spatial resolution is unimportant when ranking the other experimental treatments of climate, fuel management effort and ignition suppression. Nevertheless, spatial resolution does show a consistent systematic trend in the outputs for complex terrains (Figure 7.10), especially over a large range of resolutions, and can impose a large computational burden (Figure 7.14). It has also been found that calibrating the model to account for this is problematic (Section 7.4.4). A method was proposed in Section 4.2.3 that may reduce this computational cost while limiting loss of accuracy. The method adjusts spatial resolution to minimize change in R_h due to slope. While this test was only performed in the context of a fire simulator, simulations of other processes may benefit from such an approach. For example, vegetation models that span a large range of environmental space that contain ecotone boundaries (regions where the rate of change in model state variables is high) may benefit from increased resolution at these boundaries where model behaviour, which would be missed at coarse resolution, can be captured by using a prior adapted mesh. While dynamically adaptive approaches to resolution are not appropriate to the problem examined here (Chapter 4), it is reasonable to consider that a prior adapted mesh may take better account of the irregularity in spatial data than a regular approach. *'There is no a priori bias towards regular spatial discretization in nature; it is just convenient'* (Braun and Sambridge 1995 http://rses.anu.edu.au/cadi/NN/HTML_Presentation/Outline.html).



More precisely, the purpose of this experiment is to examine if the slope of the curve describing the response of the fire simulation to spatial resolution (Figure 7.10) can be reduced using a prior adapted mesh. The method for generating a mesh to capture $\Delta R_h / \Delta s$ has been detailed in Section 4.2.3.

8.3.2 Method

Five factors are used in this experiment: the previous experimental factors of (i) CL, (ii) IME, (iii) FME, (iv) spatial resolution (SG) and (vi) spatial representation (SR). SR has two levels: using an even distribution of mesh vertices (TINE) and an uneven distribution of vertices (TINU), fitted to $\Delta R_h / \Delta s$ (Chapter 4). The experimental design is oth-

erwise identical to the three previous experiments and is summarized in Table 8.3.

Table 8.3: Experimental design for a factorial experiment to measure the importance of optimal vertex placement against published experimental factors in fire regime simulation modelling

FACTOR	LEVELS	DESCRIPTION
Climate	Three	<i>Observed</i> : Historical climate <i>Warmer/Wetter</i> : Historical +3.6°C; +20% precipitation <i>Warmer/Drier</i> : Historical +3.6°C; -20% precipitation
Ignition mngt effort	Three	<i>Zero</i> : 0% ignitions prevented <i>Mod</i> : 35.7% ignitions prevented <i>High</i> : 75% ignitions prevented
Fuel mngt effort	Three	<i>Zero% p.a.</i> <i>Zero% p.a.</i> <i>Zero% p.a.</i> treatment treatment treatment
Spatial Representation	Three	
		TIN _E TIN _U 
Temporal resolution	Three	One hectare cell area Four hectare cell area Nine hectare cell area

8.3.3 Results

The slope of the curve describing the response of the fire simulation to spatial resolution was not significantly changed over the spatial domain of this experiment (Figure 8.13) and variance explained by SR in ln-AVIFI was unimportant (< 5%) (Figure 8.14). Furthermore, a within-SR analysis showed no change in the importance of variance explained in ln-AVIFI for any of the factors (Figure 8.15). The reduction in area burnt for simulations on both mesh types between 100

and 300 meter resolution was approximately 35% (Figure 8.13). This is ten-fold greater than the nominal scale-dependent error measured in Chapter 5 of about 3 to 4%. Therefore, this approach to minimizing the effect of spatial resolution on model outputs appears to offer no benefits apart from some indication that variance between replicates was lower for the TIN_U . (Figure 8.13). The simulation efficiency of the two spatial arrangements was identical (not shown).

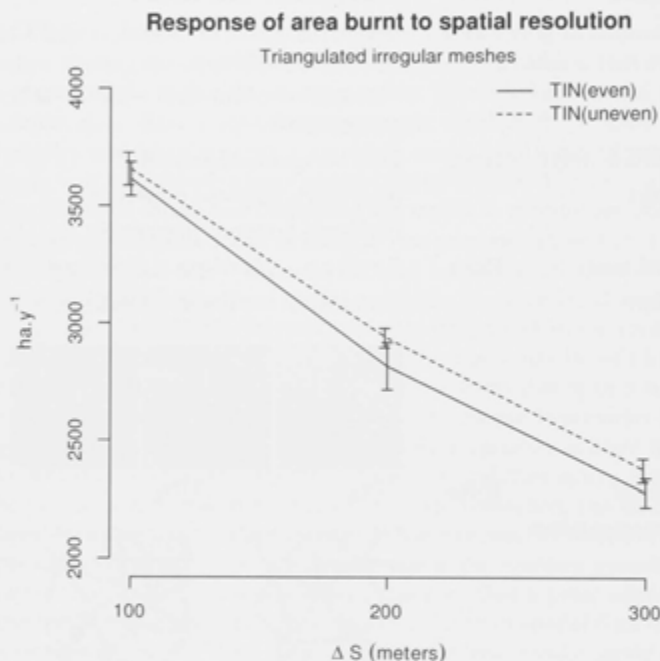


Figure 8.13: Simulated average annual area burnt for two mesh configurations at three spatial resolutions

TIN (even) is a Triangulated Irregular Network (TIN) with a Poisson-Disk distribution of vertices (solid line). TIN (uneven) is also a TIN but with a distribution of vertices that varies to maximize locations where R_h is greatest (dashed line). Each experiment was run at the same temporal and spatial resolution (0.5 hours and 1 hectare respectively).

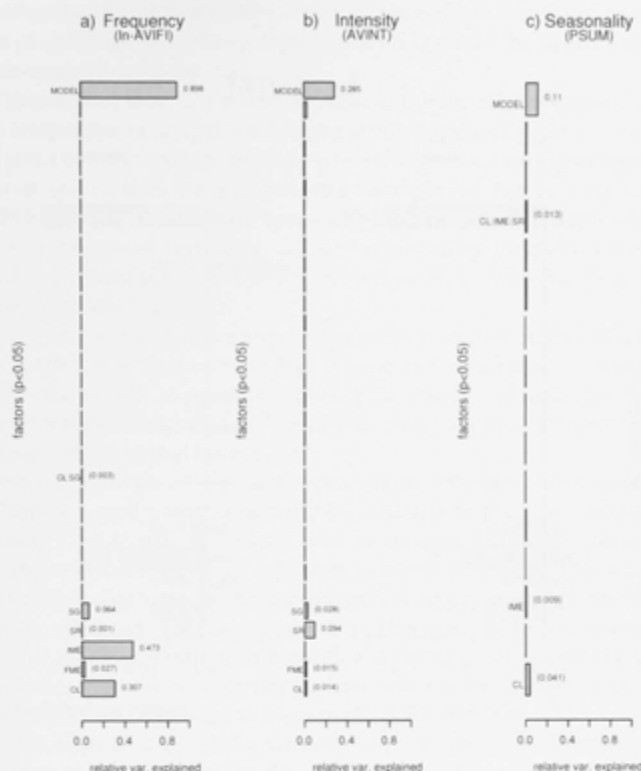


Figure 8.14: Relative Sums of Squares attributed to different sources of variation in the comparison of sensitivity of (a) ln-transformed average inter-fire interval (ln-AVIFI), (b) average fireline intensity (AVINT) and (c) the proportion of area burnt in summer (PSUM)

Sources of variation are: climate (CL), fuel management effort (FME), ignition management effort (IME) and spatial representation (SR). Spatial representation has two levels: TIN (even) is a Tri-angulated Irregular Network (TIN) with a Poisson-Disk distribution of vertices and TIN (uneven), a TIN with a distribution of vertices that varies to maximize locations where $\Delta R_h / \Delta s$ is greatest. Relative Sums of Squares and their interactions are shown in brackets if they are significant ($p < 0.05$) and explain less than 5% and 2.5% respectively. Factors and interaction which are not significant are left blank. Each experiment was run at the same temporal and spatial resolution (0.5 hours and 1 hectare respectively).

In-AVIFI

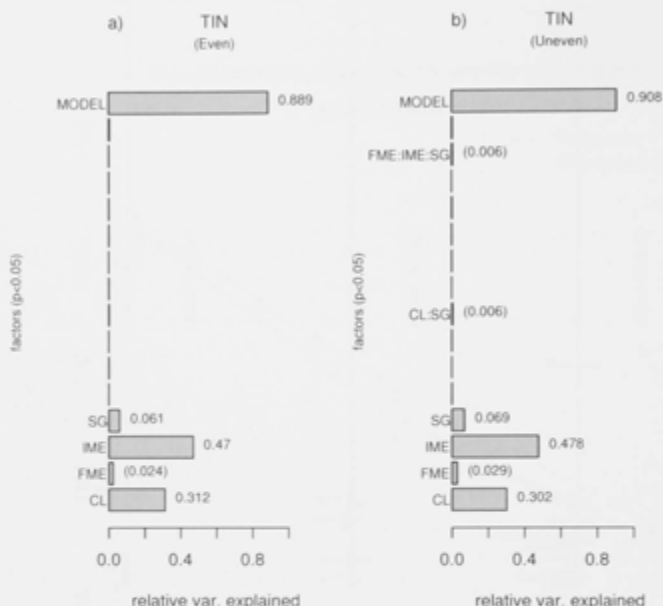


Figure 8.15: Relative Sums of Squares attributed to different sources of variation in the comparison of sensitivity of ln-transformed average inter-fire interval (ln-AVIFI)

Sources of variation are: climate (CL), fuel management effort (FME) and ignition management effort (IME). Relative Sums of Squares and their interactions are shown in brackets if they are significant ($p < 0.05$) and explain less than 6.67% and 3.33% respectively. Factors and interaction which are not significant are left blank. (a) TIN (even) is a Triangulated Irregular Network (TIN) with a Poisson-Disk distribution of vertices. (b) is a TIN with a distribution of vertices that varies to maximize locations where $\Delta R_h / \Delta s$ is greatest. Each experiment was run at the same temporal and spatial resolution (0.5 hours and 1 hectare respectively). s run at the same temporal and spatial resolution (0.5 hours and 1 hectare respectively).

8.3.4 Discussion

This unequivocal result indicates that simulating the complex interaction of spatially and temporally variable data is not suited to optimization of space using a prior adapted mesh. Therefore the hypothesis of this experiment is rejected.

It is assumed that this result is because the model's response to both temporal and spatial resolution cannot be perfectly partitioned into sets of state variables that are wholly dependent on either temporal or spatial data but not both (for example see Figure 5.22). In the face of such variability in space and time, the optimal approach may well be one of regularity, unless the modelling problem is one suited to a dynamically adaptive approach such as Braun *et al.* (1995) or Anderson *et al.* (2005).

There was a noticeable difference in variance between results for both mesh types (Figure 8.13) and it appears the approach has the unexpected benefit of possibly reducing the number of replicates required by these simulations while at the same time imposing no additional computational burden.

There are three parameters in the generation of meshes as described in Chapter 4 that could potentially be adjusted to provide a better outcome. One (contrast) is equivalent to contrast in image production and will limit the range of distances between vertices. This was set to 1 (its maximum) for this experiment. A second is the threshold of mesh minimum energy (Figure 4.7). This was set to the lowest level that was computational practical. With even lower values, there is an increasing risk of a greater uneven distribution of edge angles between meshes (Figure 4.13). Note that it is the uniform random distribution of these angles that guarantees there will not be a systematic distortion in the shape of simulated fires. The third parameter is the maximum allowed slope used to calculate changes in rate of spread and is somewhat equivalent to contrast. It was arbitrarily set to 30° , 10° more than the maximum allowed slope during simulation. The reason for this seemingly contradictory situation is as follows: During simulation, slopes presented to Equation A.6 are constrained within the domain $\pm 20^\circ$ because there is insufficient evidence to support the view that fire velocity will always increase with increasing slope for the reasons discussed in Section 5.7. However, the use of the same equation in mesh generation is in a different context. It is not known at this time, what the realized slope will be because this depends on the random angle between vertices (the edges may lie across the slope). Possibly, in this case, slope should not be limited at all, however this leads to extreme differences between sites as the function is exponential and will produce highly distorted meshes with a very non-uniform distribution of edge angles.

Regardless of this, a new set of meshes were created with no limit placed on the maximum slope. The simulations were run with resolutions from 50 to 1,000 meters, with 10 replicates and no other treatments, however, the results showed no difference from the results above (Figure 8.16).

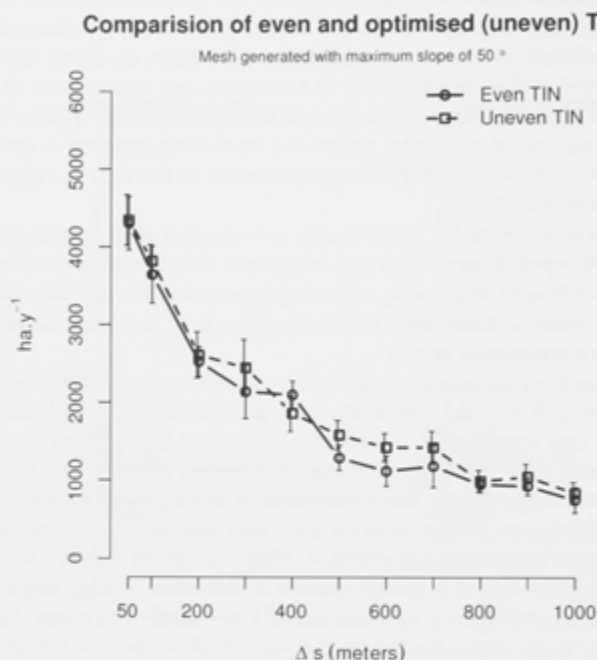


Figure 8.16: Simulated annual area burnt over a large range of spatial resolution comparing a Triangulated Irregular Network (TIN) with a Poisson-Disk distribution of vertices (Even TIN) with a TIN with a distribution of vertices that varies to maximize locations where $\Delta R_h/\Delta s$ is greatest

The mesh for the uneven TIN was produced using the Capacity-Constrained Delaunay algorithm (Xu et al. 2011) with slope unconstrained in the image construction (see text for explanation).

In FIREMESH, slope is entirely a spatial parameter and has no confounding interactions with temporal data. It also strongly influences the rate of spread of a fire and therefore it can be assumed to influence fire size and the total area burnt in a simulation. Spatial resolution has also been found to affect model estimates of average landscape wide fire frequency, even if only to an unimportant degree. Despite this, the application of a method used in other disciplines to vary spatial resolution with a prior adapted mesh, has no effect. The method proposed here may be of use should a model wish to resolve vegetation

boundaries to address other questions. For example, recent research has indicated different vegetation types may pose different levels of risk to built assets (Gibbons *et al.*, 2012). Simulation models designed to investigate this issue would need different empirical models of fire spread for each class of vegetation type. In such a situation, a prior adapted mesh could make a valuable contribution to the model formulation and limit sensitivity to spatial resolution, allowing more efficient simulations at coarse resolutions.

8.4 SUMMARY OF FINDINGS FOR SPATIAL REPRESENTATION

Markus and Hess (1990) proposed one of the first methods for addressing artefacts arising in cellular-automata models due to discrete geometries. The essence of their method in randomizing the location of discrete points in space has been utilized in simulations of lava flow (Miyamoto and Sasaki, 1997), in fire simulations as used here (Johnston *et al.*, 2008) and more recently by Avolio *et al.* (2012). However, apart from the use of N-4 meshes, an arrangement rarely used in fire modelling, any effect these various spatial topologies may have on the emerging shape of simulated fires appears not to have important consequences for identifying the key drivers of average fire frequency.

The method used in this study to overcome the constraints imposed by discrete geometries on fire shape (Johnston *et al.*, 2008) provides an ideal vehicle with which to explore any benefits there may be in using a geometry with variable resolution. As fire growth simulations are discrete approximations of continuous non-linear systems, it might be expected that the spatial resolution will be important (Figure 7.15). The benefit in basing this approach on an Irregular Triangular Network is that it allows resolution to change gradually unlike the sub-division of regular grids where artefacts can arise at resolution boundaries (Zarzycki *et al.*, 2014). However, in most simulations, variable resolution has been used dynamically with adaptive meshes (for example: Braun *et al.* 1995; Anderson *et al.* 2005). While a preliminary investigation has been done with single fire events on an adaptive regular grid (Hu and Ntamo, 2006) it must remain a matter for further research as to whether an adaptive irregular grid could be a tractable approach in simulations of multiple interacting fires over large time frames and spatial extents. The only other research I am aware of that has used a prior adapted mesh is in the field of Astronomy (Cautun and van de Weygaert, 2011) because astronomical observations are essentially unchanging at the scale of observation. The application of the CDT algorithm (Xu *et al.*, 2011) is novel, at least in the context of fire simulation. However, no benefit results and it is assumed that, though slope is an important spatial parameter, its importance is overwhelmed by the interaction of spatial and temporal variables

(Figure 5.22). This method of applying an algorithm from the field of computer graphics to landscape simulations may be of use should a model wish to resolve vegetation boundaries to address other questions, allowing more efficient simulations at coarse resolutions.

The suitability of a model abstraction, such as those examined here, depends on the question being asked of the model. The original purpose of FIRESCAPE, the model from which FIREMESH is derived, was to examine the role of fire in realized niches. For this the spatial patterns of components of the fire regime is important and this has not been examined in this study. With further research, all the different approaches to abstraction of space and time examined by these experiments, could be studied using all the validation tests (and many more) in Chapter 6 including pattern analysis of fire regimes. For example, is an N-4 mesh just as suitable a representation of space to estimate the role fire may play determining species distributions (Chapter 6, Section 6.2.4)? Are the inter-fire intervals as measured by dendrochronological studies (Banks *et al.*, 1982) in the Brindabella Ranges, better represented by a N-4 mesh with a suitably calibrated average fire return interval? All abstractions take place in the context of a defined problem or question (Flint, 2006; Grimm *et al.*, 2006) and the ability to answer these questions quickly and with some objectivity is a subject discussed in the final chapter of this study.

Fireline intensity is also lower for N-4 meshes, an unavoidable consequence of the limited set of directions of fire propagation as noted above. TIN_U captures the widest range of fireline intensities because the mesh is optimized to capture change in rates fire velocity (Figure 8.14.b). While this approach fails to reduce the error in estimates of area burnt that arise because of spatial resolution, the wider range of intensities captured by the method at least indicates it is designed as intended, as fireline intensity is proportional to fire velocity (Equation A.14). Although much uncertainty must surround observations of fireline intensity (Section subsection 1.3.1), depending on the choice of mesh configuration, fireline intensities appear too high in this model. Cruz *et al.* (2012) have estimated an average fireline intensity for periods during the Victorian 2009 fires at $88,000 \text{ kW.m}^{-1}$ assuming a fuel heat content of $18,600 \text{ kW.m}^{-1}$ in dry sclerophyll forests. By contrast, the maximum fireline intensity using N-4, N-6, N-8, TIN_E and TIN_U is 65,000, 120,000, 150,000, 160,000 and 220,000 kW.m^{-1} respectively (but assuming a heat of combustion of 20,000 kW.m^{-1}). Fireline intensity is estimated from the rate of fuel consumption implied by the rate of fire spread (Equation A.14). However, fire spread can also take place through spotting at many scales (Section 3.2.6) and the actual rate of spread is the rate at which these spot fires coalesce. The fuel heat content has possibly been set too high in order to be consistent with FIRESCAPE ($20,000 \text{ kW.m}^{-1}$) (Sullivan, 2007), nonetheless, at such extremes, a real fire would likely spread

with the assistance of spot fires and using Byram's equation (Equation A.14) to infer fireline intensity from the rates of spread generated by the model must have very high uncertainty.

In general, the implication that the severe constraints imposed by discrete geometries on fire shapes (Figure 5.14) does not appear to be crucial when performing simulations with complex weather and terrain data. Understanding what drives area burnt in large landscapes has been a critical area of research in informing land management decision making (Bradstock *et al.*, 2012) and a considerable amount of that work has been done using simulation models that describe space using the same or similar geometries to those tested in this chapter (Davis and Burrows, 1994; Cary and Banks, 2000; Li, 2000; Hargrove *et al.*, 2000; Trunfio, 2004; Johnston *et al.*, 2008; Perera *et al.*, 2008). This chapter has provided some quantitative measure that these details are unimportant when using simulation to estimate area burnt in large landscapes.

SYNTHESIS AND FUTURE DIRECTIONS

9.1 SYNTHESIS

The formal null hypotheses that *ranking the relative importance of the drivers of fire by simulation modelling is insensitive to a wide range of spatio-temporal resolutions* was not rejected by the experiment in Chapter 7. This experiment supports the view that the application of simulation models to assessing the importance of the various determinants of area burnt in the large landscapes, is relatively insensitive to the choice of spatio-temporal resolution. This was tested using treatments of climate, fuel and initial attack, taken from the literature. The key figures to support this are figures 7.4 and 7.5 in Chapter 7. Future work could consider extending the scope of the simulations to determine the point at which this assertion fails, but indications are that it may, in fact, extend to very coarse resolutions depending on the complexity of the terrain.

An additional area of future research is to extend the list of treatments, beyond the three used in this study, to include those that are more informative of fire intensity and seasonality. The design of FIRE-MESH has been such as to isolate operational errors from inherent errors in order that these findings may have more general application than for just this one model. Therefore, the space and time errors reported in this study are unavoidable for any fire simulation model that has: (i) a time step, (ii) a spatial resolution and (iii) a model of space represented by discrete points connected to each other by fixed number of neighbours. Similarly constructed models may have formulations that have additional errors, or errors that cancel or reinforce in some way, but at least the errors reported here appear unavoidable. Other models of space, such as vector models, are not necessarily directly comparable to these results (for example, see Jones *et al.* 2003 though these models are not normally applied to studies of fire regime patterns over large temporal and spatial scales).

Modelled fire seasonality and intensity are both sensitive to the model's spatio-temporal resolution. However, no formal conclusion as to the relative importance of this compared to the effect of climate, fuel management effort or ignition management effort could be established for the simple reason that these treatments do not particularly effect fire seasonality or intensity (Figure 7.4). Apart from the observation that the seasonality of lightning ignitions was not important (Figure 7.7), experiments designed to measure how important spatio-temporal resolution may be in simulation in this regard would be

better addressed by a model of vegetation whose dynamics responds more fully to climate (King *et al.*, 2013; Battlori *et al.*, 2013).

Hypothesis (ii), that *Ranking the relative importance of the drivers of fire by simulation modelling is insensitive to the number of neighbours connecting points (vertices) within the model's spatial extent*. This hypothesis was rejected. The key figure supporting this is Figure 8.2. N-4 meshes greatly under-estimate rates of spread in non-cardinal directions which results in smaller fire sizes and larger average inter-fire intervals overall. Because the size of fires simulated using N-4 meshes are smaller than N-6 or N-8 meshes (Figure 8.5), there will be a lesser edge effect using N-4 meshes compared to N-6 or N-8 meshes for simulations on otherwise identical landscapes. The magnitude of the edge effect serves to lessen the sensitivity of the model to experimental treatments (Figure 8.7). Again, future work could consider extending this experiment to much larger landscapes. For the data used in this study, a four-fold increase may be sufficient (10,000 km²). It can be conjectured that such a study may find the hypothesis should not be rejected, as suggested by Green *et al.* (1983a). However, N-4 meshes are particularly unsuited to estimating fire-size when the predominant wind direction during the fire season comes non-cardinal directions as is the case in SE Australia, California and the boreal forests of Canada and doubtless many other fire-prone regions.

N-4 meshes were included in this treatment to maximise the treatment range. However, as noted, their use is rare and to the best of my knowledge this form has only been used in theoretical studies on percolation thresholds (Plotnick and Gardner, 1993). With each additional facet to fire shapes that result from additional neighbours on regular grids (6, 8, 16, 24 etc.), the relative benefit declines (Section 4.2.2). Therefore, while the formal hypothesis has been rejected, for what is common practice in fire regime simulation modelling, this result provides support for the robustness of work that has been done over the past two decades using N-6 or N-8 meshes. Increasing neighbourhood number 16 or 24 to achieve better approximations of elliptical fire shapes is unlikely to alter the proportionate response of the model to determinants of area burnt.

A considerable amount of discussion and research has taken place over the past 30 years, devoted to overcoming the fire shapes that result from simulating fire in discrete space (Green *et al.*, 1983a; Alexander, 1985; Feunekes, 1991; Caballero, 2006; Johnston *et al.*, 2008; Trunfio *et al.*, 2011; Avolio *et al.*, 2012). The experiment, designed to test Hypothesis (iii) simply asks if this issue is a concern for fire regime simulation modelling. A method of improving fire shapes in discrete geometries was chosen from the literature (Johnston *et al.*, 2008) and compared to the most common way of depicting spatial topologies in fire regime simulation, that of a regular eight-neighbourhood mesh. The result of this experiment found that the choice between these

two models of space was unimportant, that is, Hypothesis (iii) was not rejected. The key figures to support this are figures 8.8 and 8.9. However, the method of Johnston *et al.* (2008) does execute 25% faster than a regular eight-neighbour mesh because each vertex has, on average, only six neighbours (Figure 1.4). This consideration has some importance because fire regime simulations are often used over large spatial and temporal extents and simulation speed can be a limiting factor. This benefit must be weighed against the added complexity in preparing a model with such a mesh (using algorithms similar to Xu *et al.* 2011) rather than a simple regular mesh.

For Hypothesis (iv), that such sensitivity as there is to spatial resolution can be accounted for by either calibration or having a variable spatial resolution, is clearly rejected. The key information to support this finding is Figure 8.13 and the calibration experiment based on parameter values in Table 7.2. Varying spatial resolution to account for the rate of change in the model response to a spatial variable (slope), had little or no effect on model output (Figure 8.13). Finite element analysis is an approach taken in many fields of modelling (Braun *et al.*, 1995; Anderson *et al.*, 2005; Cautun and van de Weygaert, 2011) and it might have reasonably been expected that a prior adapted mesh would be of benefit in this case. However, it appears that the interaction of temporal and spatial data (weather, terrain and fuels) is more complex than might have been expected. Future research, using the algorithm of de Goes *et al.* (2012) rather than that of Xu *et al.* (2011) used in this study, may provide better tool for this research. In addition, other researchers may find benefit in this approach by focusing spatial resolution on boundaries between vegetation types, allowing coarser resolutions overall but maintaining resolution where it is most required by the particular model.

The attempt to calibrate an empirical equation for slope to account for spatial resolution (Table 7.2), while successful for the calibrated output (fire frequency), simply heightened the response of fireline intensity to spatial resolution (Chapter 7). Calibration of any model requires an (often complex) objective function with which to calibrate multiple parameters to multiple outputs (Fonseca *et al.*, 1993). In this study, only one spatial and one temporal parameter were identified (Table 7.2), further research may find other parameters or approaches. Optimization methods such as genetic algorithms (GA) can require considerable computer resources, especially for landscape simulations which are difficult to parallelize (Abdalhaq *et al.*, 2002). However, GA is particularly suited to parallelization, and the increasing availability of computer cloud resources now makes this a viable approach (<http://ssrg.nicta.com.au/projects/cloud/>).

Overall, the constraints imposed by spatial representation appear to manifest themselves most clearly in measures of fireline intensity. Estimated fireline intensity increases with the number of neighbours

(Figure 8.1.b), with the use of a Poisson-Disk distribution of vertices (Figure 8.10.b) and again with a distribution of vertices designed to capture rates of change in the terrain (not shown). However, the variance explained by the other experimental treatments in fireline intensity was insufficient to draw definitive conclusions in this regard, as fuel and climate treatments explained very little of the variance in fireline intensity, and none at all for ignition suppression.

The particulars of this study landscape, (dominated by an east and west aspect (Figure 2.3.c), and weather data (most winds during the fire season come from the NW- Figure 2.6), lend support to the view that studies such as this would be better served using some form of weather and terrain replication. Chapter 2 showed that Richardson's method of stochastic weather generation (Richardson, 1981; Richardson and Wright, 1984) did not account for weather patterns at multiple scales. The lack of realistic patterns of extended periods of drought or high rainfall will necessarily confound experiments that attempt to measure the importance of weather variability against other drivers of fire regimes. Furthermore, this method only produces daily weather variables. Down-scaling this data to half-hourly values poses problems for replicating realistic variability between readings comparable to those of observed data. Fire simulations are sensitive to this fine-scale variability, as determining if a fire will extinguish over night or continue to burn in following days has obvious consequences for estimating fire-size distributions (Figure 6.6) and average fire frequency in the landscape. Synthetic generation of fine-scale weather data that captures realistic multi-scale patterns that appear in observed data is therefore a valuable area of future research in order that findings, such as those in the present study, can have more general application.

The most common method of generating synthetic terrain, the mid-point displacement algorithm (Saupe, 1991), cannot produce landscapes with a realistic distribution of aspects (Figure 2.11). Such synthetic landscapes, with their absence of ridge lines, will produce particular patterns of fire regimes not generally applicable to most study areas. However, this approach does capture multi-scale variability in landscape elevations. Creating replicate landscapes is an area that has not been much commented upon outside the field of computer games, and there is need of such a method for landscape modelling studies, in order to generalise findings beyond the particulars of individual data sets.

An unexpected finding in this study is relative insensitivity of model estimates of the drivers of fire to uncertainty in empirical equations of fire velocity (Figure 6.14, Figure 6.17). This, together with the findings in Chapters 7 and 8, serves to enhance more than a decade's research into the determinants of area burnt in large landscapes (Cary *et al.*, 2006, 2009; Keane *et al.*, 2013a). There has been high uncer-

tainty surrounding McArthur's empirical equations of fire spread, both because they have largely been derived from fires under relatively mild conditions (McCaw *et al.*, 2008) and because of uncertainty about the provenance of the data. This has led to Project Vesta (Gould *et al.*, 2007), a very large undertaking involving more than 100 experimental fires lit under dry summer conditions. The findings of this Project have led to very important insights for operational management. However, it is reassuring that these new estimates of rates of fire spread do not challenge previous research in the primary drivers of area burnt.

This finding also suggests interesting areas of further research. For example, using experimental designs similar to those of chapters 7 and 8, the importance or otherwise of uncertainties surrounding other aspects of model formulation could be examined. As fuel treatments are the most common way of intervening in the dynamics of fire-vegetation systems, understanding the consequences that vegetation dynamics and the structure of the fuel array may have for estimating the relative importance of the drivers of fire could provide some research focus as could a more detailed examination of initial attack success.

An important caveat in using the method to adjust rates of fire velocity to more closely align with the findings of Project Vesta (Figure 3.10, Gould *et al.* 2007; McCaw *et al.* 2008), is that extremely high fireline intensities are produced. This is especially so using the variable resolution mesh (Section 8.3). While this is not of concern for estimates of area burnt or fire frequency (Figure 6.13), for studies focusing on measures of fireline intensity in the landscape, (such as asset loss or fire controllability), inferring intensity from rates of spread using Byram's equation (Equation A.14) will over-estimate intensity unless some model of propagation by lofted embers is included. Including such a process effectively maintains area burnt while at the same time reduces the rate of spread applied to Byram's equations.

As noted in the introduction (Section 1.1), simulation modelling has been an important tool in informing land managers on the relative importance of the key determinants of area burnt in large landscapes. The sensitivity of these research findings to the nuisance parameters examined in the present study has been a 'lurking' unknown. This study supports the view that these models are robust with regard to the particular values of nuisance parameters used in the models providing enhanced value to a considerable body of existing research.

9.2 GENERALITY OF FINDINGS

This thesis has used a single simulation model, weather stream, topography and vegetation pattern. The question then arises as to how general the study findings may be. The core finding of this thesis was

that nuisance parameters are unimportant, within reasonable limits, for simulation models that have: (i) a time step, (ii) a spatial resolution and (iii) a model of space represented by discrete points connected to each other by fixed number of neighbours. As noted, fire growth models with this architecture may have formulations that have additional errors, or errors that cancel or reinforce in some way, but at least the errors reported here, though minor, appear unavoidable. It should be stressed that this applies only to fire frequency or its inverse, average area burnt. While nuisance parameters do affect fireline intensity and possibly seasonality, the relative importance of these effects could not be established in the context of typical experimental treatments, because the treatments used here were not sensitive to these two components of fire regimes.

With regard to fire frequency:

- i Temporal resolution (TG) affects estimates, to a very *unimportant* degree (0.2%), simply by overshooting the moment a fire extinguishes. While model estimates of any single fire event may vary greatly for different time steps, when averaged over many fires, the effect of smoothing the weather data to coarser resolutions had almost no effect. On these grounds, this result must hold for any fire growth model with a time step. The magnitude of this effect is determined to some degree by the fire-size distribution. As the overshoot is constant (on average), the percentage error will be smaller for larger fires. Therefore, in regions where there may be a larger proportion of small fires, the effect of TG on fire frequency will be slightly greater.
- ii Spatial resolution (SG) also affects estimates to a greater, but still *unimportant* degree (3.2%), even in this mountainous landscape. SG had little effect on simulations performed on a flat landscape. Therefore, the effect will become important in more mountainous landscapes with high variability in elevations at fine-scale, that is, relatively young landscapes such as those found in western Americas or New Zealand, compared to the ancient landscapes of Australia. SG may also become important in landscapes with very contrasting fuel mosaics at fine scale, increasingly so for regions where small fires contribute more to the fire-size distributions than those in the present study. However, Cary *et al.* (2006, 2009) found fuel patterns and levels of fuel treatment very unimportant for a range of independently developed models with a wide variety of fuel development sub-models. In general, it is likely that large infrequent fires, burning under extreme conditions, contribute most to measures of area burnt and therefore fire frequency.
- iii For N-6, N-8 and Triangular Irregular Network models of space, the difference in model estimates of fire frequency is very *unim-*

portant. I can think of no conditions under which this would be contradicted for model estimates of the relative importance of the drivers of fire for fire frequency. On the other hand, these choices appear to have a major impact on estimates of average fireline intensity and the shapes of individual fire events but again, these decisions do not affect estimates of driver importance for fire frequency.

9.3 FUTURE DIRECTIONS

The experiments performed in this study have been limited to a small set the many experiments that could be imagined to explore the wider concept of levels of abstraction. When we '*isolate systems for the purpose of study*' (Tansley, 1935), we can never be certain how much, and what level of detail, is required to perform this abstraction for the aims of any given study. Representations of systems can display very different behaviours depending on these details. For example, in passing, a null model of lightning strike distributions in time was compared to the method used in FIRESCAPE and no important difference in model outputs was found (Section 7.4.3). On the other hand, a study of connectivity in food-webs has shown quite a different model response depending on whether or not food-chains are represented in classical linear fashion or more complex networks representing functional diversity at each trophic level (Hulot *et al.*, 2000). This is common in any modelling study and it is the inevitable problem that arises from the subjective nature of abstraction (Gignoux *et al.*, 2011).

One way forward in this sea of subjectivity, is grounded model comparisons. Modelling frameworks have been proposed to do this (Lavorel *et al.*, 2000; Lacy *et al.*, 2013) but they essentially define a framework in which model processes can be swapped only if they adhere to a formal coupling specification. They are in fact a pattern or recipe for a particular class of problem. They are also often inflexible in that the specification of the model is represented as computer source code, where many concerns, apart from the scientific problem that the model is designed to address, are all mixed together in the one representation (i.e. the computer source code). As we discover new insights from models, the original problem changes and agility is central to adapting to the new situation (see Boyd's OODA loop in Higgins and Freedman 2013). Hence the model pattern needs to be captured at an appropriate level and the concerns that must be addressed by the model need to be kept separate to foster this agility. Problems addressed by models also arise in the context of a multi-disciplinary environment. It is the critique of single discipline view of many areas in science that is the motivation behind Lacy's approach to meta-modelling (Lacy *et al.*, 2013).

The approach of Aspect-Orientated Thinking (AOT) (Flint, 2006), addresses the issue of rapidly responding to changed circumstances in a multi-discipline environment, by developing and maintaining a set of independent, domain-specific models. That is, they describe knowledge in that domain but not in context of any particular, yet to be defined, problem. When a particular problem is defined, a specific model then becomes a set of statements that denote required knowledge from each and any of these reusable domain-specific models. When these requirements are made in accordance with a pattern, recipe or archetype, generating the computer source code from these specifications can then be largely automated. In this view, Lacy's meta-model is an archetype, as it describes, rules and patterns which must be followed in order to integrate computer code from various sources. However, as noted, this pattern is captured at the level of source code itself, where many concerns, irrelevant to the problem at hand, are mixed together. In AOT, a model is created to address a specific problem by drawing on knowledge (requirements) from a library of domains from different disciplines that are independent of the problem at hand (ecology, law, computer user-interfaces, code optimization and so forth). Some approaches to multi-disciplinary research assume the way forward is to develop common protocols between disciplines, in short, to enforce standards. Any attempt to enforce cross-discipline standards without first defining the problem that is to be addressed, simply imposes unnecessary constraints on the way in which that discipline chooses to model its own knowledge. However, once a specific problem has been defined, the requirements or knowledge needed from each of those independent domains of knowledge can be identified and captured as a specification of an archetype. This archetype, and the independent domains from which knowledge is drawn, represent intellectual assets that may be reused for, what on the surface may appear to be, quite different problems (Flint, 2006).

One such archetype is in the process of development, an archetype for ecological simulations. This archetype draws on knowledge from two key independent domains: an ontology of ecosystems and a domain describing how models can be distributed over a network. The ecosystem ontology accords with the conceptual view of ecosystems proposed by Gignoux *et al.* (2011) and has been named 3Worlds, as three particular domains arose in author's review of Tansley's concept (Tansley, 1935). The first two of these domains (physics and biology) comes from the observation that it is common practice (and consistent with Tansley's description of the ecosystem), to view ecosystems as having not only physical and biological entities, but that the biological entities themselves can be viewed as either having physical or biological behaviour (Chapter 1). The third domain is scale, and the observation that researchers commonly model ecosystems as

multi-scale objects. An ecosystem is a set of identified processes, each of which may operate at a different scales. I would argue in fact, that this approach has a more general application than just models of ecosystems, but could be applied to any dynamic system. After all, the key attribute that distinguishes biological from physical behaviour is life and death, and in a model this is essentially the dynamic addition and deletion of entities and relationships. It is hoped that the workflow when using the combination of Aspect-Orientated Thinking and an archetype describing 3Worlds simulations may provide researchers with a very rapid and practical way in which appropriate levels of abstraction in models of ecosystems may be compared through simulation (Figure 9.1). Landscape fire simulations, and landscape modelling in general, can be very computationally intensive for two reasons. Firstly, because often large landscapes are required and secondly because the spatial interaction of processes makes them difficult to parallelise. Spatial interactions are a key attribute of landscape models (Section 1.4.4). Exploring levels of abstraction is a way forward in enhancing confidence in model estimates, as has been shown here with regard to nuisance parameters.

The second domain mentioned above, addresses the issue of rapidly responding to questions that arise in studies such as this, where limits are imposed by the available computer resources. Many more questions and areas of investigation could have been pursued in the present study were it not for this limitation. The 3Worlds archetype recognizes this and a specific domain is being finalized to allow simulation experiments to be deployed over a network or to connect to a computer cloud stack to foster more rapid response to changing circumstances as the *'problem situation'* (Checkland, 1981) evolves.

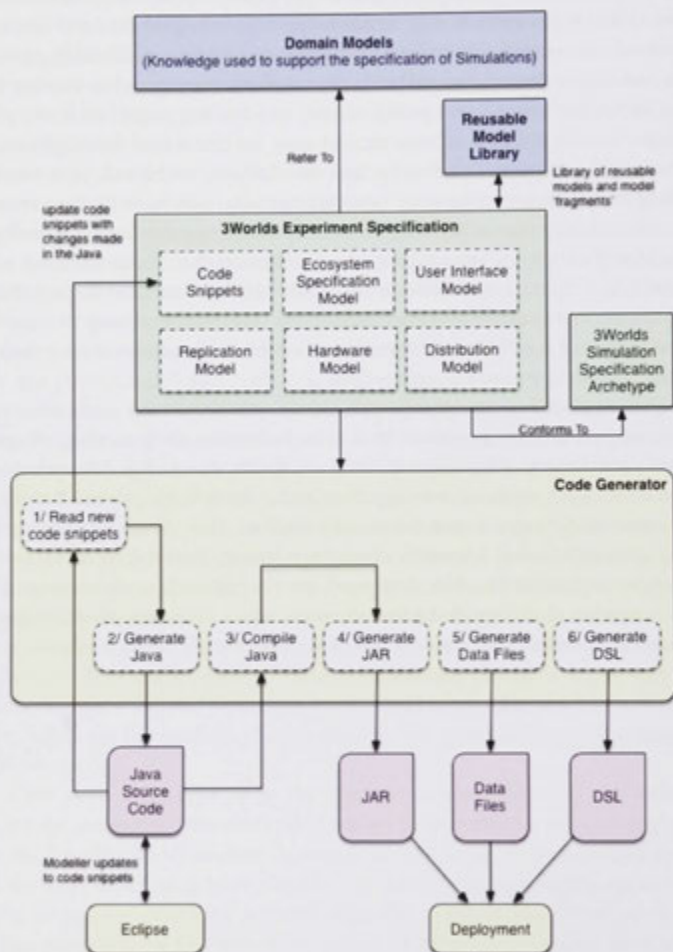


Figure 9.1: Proposed workflow for rapid model development currently under development (courtesy S. Flint)

REFERENCES

- Abdalhaq, B., Cortés, A., Margalef, T. and Luque, E.: 2002, Optimization of fire propagation model inputs: A grand challenge application on metacomputers, Springer, pp. 447–451.
- Abt, K. L., Prestemon, J. P. and Gebert, K. M.: 2009, Wildfire suppression cost forecasts for the us forest service, *Journal of Forestry* **107**(4), 173–178.
- Albini, F. A., Alexander, M. E. and Cruz, M. G.: 2012, A mathematical model for predicting the maximum potential spotting distance from a crown fire, *International Journal of Wildland Fire* **21**(5), 609–627.
- Albini, F. A. and Forest, I.: 1976, *Computer-based models of wildland fire behavior: A users' manual*, USFS Intermountain Forest and Range Experiment Station.
- Alexander, M.: 1985, Estimating the length-to-breadth ratio of elliptical forest fire patterns, *Proceedings of the eighth conference on fire and forest meteorology*, Vol. 29, pp. 85–04.
- Alexander, M. E. and Cruz, M. G.: 2012, Interdependencies between flame length and fireline intensity in predicting crown fire initiation and crown scorch height, *International Journal of Wildland Fire* **21**(2), 95–113.
- Alexander, M. E. and Cruz, M. G.: 2013, Are the applications of wildland fire behaviour models getting ahead of their evaluation again?, *Environmental Modelling & Software* **41**, 65–71.
- Alexander, M. E. et al.: 2000, *Fire behaviour as a factor in forest and rural fire suppression*, New Zealand Forest Research Institute.
- Allen, T. F. and Hoekstra, T. W.: 1992, *Toward a unified ecology: complexity in ecological systems*, Columbia University Press, New York.
- Amiro, B., Stocks, B., Alexander, M., Flannigan, M. and Wotton, B.: 2001, Fire, climate change, carbon and fuel management in the Canadian boreal forest, *International Journal of Wildland Fire* **10**(4), 405–413.
- Amouroux, E., Chu, T.-Q., Boucher, A. and Drogoul, A.: 2009, Gama: an environment for implementing and running spatially explicit multi-agent simulations, Springer, pp. 359–371.

- Anderson, A., Zheng, X. and Cristini, V.: 2005, Adaptive unstructured volume remeshing-i: The method, *Journal of Computational Physics* **208**(2), 616–625.
- Andison, D. W.: 2012, The influence of wildfire boundary delineation on our understanding of burning patterns in the alberta foothills, *Canadian Journal of Forest Research* **42**(7), 1253–1263.
- Anon: 1973, *A Resource and Management Survey of the Cotter River Catchment*, Department of Forestry, The Australian National University: Canberra.
- Anon: 2012, *IBRA 7: Interim Biogeographic Regionalisation for Australia*, Australian Government Department of Sustainability, Environment, Water, Population and Communities.
- Anon: 2013, *Victorian Bushfire Risk Profiles: A foundational framework for strategic bushfire risk assessment*, Department of Environment and Primary Industries, Victorian Government.
- Ashe, B., McAneney, K. and Pitman, A.: 2009, Total cost of fire in australia, *Journal of Risk Research* **12**(2), 121–136.
- Austin, M., Nicholls, A. and Margules, C. R.: 1990, Measurement of the realized qualitative niche: environmental niches of five eucalyptus species, *Ecological monographs* **60**(2), 161–177.
- Avolio, M. V., Di Gregorio, S., Lupiano, V. and Trunfio, G. A.: 2012, Simulation of wildfire spread using cellular automata with randomized local sources, *Cellular Automata*, Springer, pp. 279–288.
- Bak, P., Tang, C., Wiesenfeld, K. et al.: 1987, Self-organized criticality: an explanation of $1/f$ noise., *Physical review letters* **59**(4), 381–384.
- Banks, J., Carson, J. and Nelson, B.: 2000, *DM Nicol, Discrete-Event System Simulation*, Prentice Hall.
- Banks, J. C. et al.: 1982, *The use of dendrochronology in the interpretation of the dynamics of the snow gum forest*, PhD thesis, The Australian National University.
- Banks, S. C., Cary, G. J., Smith, A. L., Davies, I. D., Driscoll, D. A., Gill, A. M., Lindenmayer, D. B. and Peakall, R.: 2013, How does ecological disturbance influence genetic diversity?, *Trends in ecology & evolution* **28**(11), 670–679.
- Barber, C. B., Dobkin, D. P. and Huhdanpaa, H.: 1996, The quickhull algorithm for convex hulls, *ACM Transactions on Mathematical Software (TOMS)* **22**(4), 469–483.

- Barnes, B. and Roderick, M. L.: 2004, An ecological framework linking scales across space and time based on self-thinning, *Theoretical population biology* **66**(2), 113–128.
- Basu, D.: 1977, On the elimination of nuisance parameters, *Journal of the American Statistical Association* **72**(358), 355–366.
- Batllori, E., Parisien, M.-A., Krawchuk, M. A. and Moritz, M. A.: 2013, Climate change-induced shifts in fire for Mediterranean ecosystems, *Global Ecology and Biogeography* **22**(10), 1118–1129.
- Bennetton, J., Cashin, P., Jones, D. and Soligo, J.: 1998, An economic evaluation of bushfire prevention and suppression, *Australian Journal of Agricultural and Resource Economics* **42**(2), 149–175.
- Bian, L. and Butler, R.: 1999, Comparing effects of aggregation methods on statistical and spatial properties of simulated spatial data, *Photogrammetric Engineering and Remote Sensing* **65**, 73–84.
- Black, P. E.: 2007, big-o notation, *Dictionary of Algorithms and Data Structures*.
- Boer, M. M., Johnston, P. and Sadler, R. J.: 2011, Neighbourhood rules make or break spatial scale invariance in a classic model of contagious disturbance, *Ecological Complexity* **8**(4), 347–356.
- Boer, M. M., Sadler, R. J., Bradstock, R. A., Gill, A. M. and Grierson, P. F.: 2008, Spatial scale invariance of southern Australian forest fires mirrors the scaling behaviour of fire-driving weather events, *Landscape Ecology* **23**(8), 899–913.
- Bond, W. J. and Keeley, J. E.: 2005, Fire as a global 'herbivore': the ecology and evolution of flammable ecosystems, *Trends in Ecology & Evolution* **20**(7), 387–394.
- Bose, C., Bryce, R. and Dueck, G.: 2009, Untangling the Prometheus nightmare, *Proceedings of the 18th World IMACS/MODSIM Congress*, pp. 74–80.
- Boulain, N., Simioni, G. and Gignoux, J.: 2007, Changing scale in ecological modelling: a bottom up approach with an individual based vegetation model, *ecological modelling* **203**(3), 257–269.
- Bradstock, R.: 2010, A biogeographic model of fire regimes in Australia: current and future implications, *Global Ecology and Biogeography* **19**(2), 145–158.
- Bradstock, R. A., Cary, G. J., Davies, I., Lindenmayer, D. B., Price, O. F. and Williams, R. J.: 2012, Wildfires, fuel treatment and risk mitigation in Australian eucalypt forests: insights from landscape-scale simulation, *Journal of environmental management* **105**, 66–75.

- Bradstock, R., Bedward, M. and Cohn, J.: 2006, The modelled effects of differing fire management strategies on the conifer *callitris verrucosa* within semi-arid mallee vegetation in australia, *Journal of Applied Ecology* **43**(2), 281–292.
- Bradstock, R., Bedward, M., Gill, A. and Cohn, J.: 2005, Which mosaic? a landscape ecological approach for evaluating interactions between fire regimes, habitat and animals, *Wildlife Research* **32**(5), 409–423.
- Bradstock, R., Bedward, M., Kenny, B. and Scott, J.: 1998, Spatially-explicit simulation of the effect of prescribed burning on fire regimes and plant extinctions in shrublands typical of south-eastern australia, *Biological Conservation* **86**(1), 83–95.
- Braun, J., Sambridge, M. et al.: 1995, A numerical method for solving partial differential equations on highly irregular evolving grids, *Nature* **376**(6542), 655–660.
- Brookhouse, M., Brack, C. and McElhinny, C.: 2010, The distance to structural complement (disco) approach for expressing forest structure described by aerial photograph interpretation data sets, *Forest ecology and management* **260**(7), 1230–1240.
- Burrough, P. A., McDonnell, R., Burrough, P. A. and McDonnell, R.: 1998, *Principles of geographical information systems*, Vol. 333, Oxford university press Oxford.
- Burrows, N.: 1997, Predicting canopy scorch height in jarrah forests, *CALMSCIENCE-COMO- 2*, 267–274.
- Burton, P. J., Parisien, M.-A., Hicke, J. A., Hall, R. J. and Freeburn, J. T.: 2009, Large fires as agents of ecological diversity in the north american boreal forest, *International Journal of Wildland Fire* **17**(6), 754–767.
- Byram, G. M.: 1959, Combustion of forest fuels, *Forest fire: control and use* **1**, 61–89.
- Caballero, D.: 2006, Taxicab geometry: some problems and solutions for square grid-based fire spread simulation, *Forest Ecology and Management* **234**(1), S98.
- Caldararo, N.: 2002, Human ecological intervention and the role of forest fires in human ecology, *Science of The Total Environment* **292**(3), 141 – 165.
URL: <http://www.sciencedirect.com/science/article/pii/S0048969701010671>
- Cary, G.: 1997, Analysis of the effective spatial scale of neighbourhoods with respect to fire regimes in topographically complex landscapes, *Proc. Int. Congr. Model. Simulation* pp. 434–439.

- Cary, G. J.: 1998, *Predicting fire regimes and their ecological effects in spatially complex landscapes*, PhD thesis, The Australian National University.
- Cary, G. J. and Banks, J. C.: 2000, Fire regime sensitivity to global climate change: an Australian perspective, *Advances in Global Change Research: Biomass burning and its inter-relationships with the climate system*. Kluwer Academic Publishers, London, UK .
- Cary, G. J., Flannigan, M. D., Keane, R. E., Bradstock, R. A., Davies, I. D., Lenihan, J. M., Li, C., Logan, K. A. and Parsons, R. A.: 2009, Relative importance of fuel management, ignition management and weather for area burned: evidence from five landscape-fire-succession models, *International Journal of Wildland Fire* **18**(2), 147–156.
- Cary, G. J., Keane, R. E., Gardner, R. H., Lavorel, S., Flannigan, M. D., Davies, I. D., Li, C., Lenihan, J. M., Rupp, T. S. and Mouillot, F.: 2006, Comparison of the sensitivity of landscape-fire-succession models to variation in terrain, fuel pattern, climate and weather, *Landscape ecology* **21**(1), 121–137.
- Catchpole, W.: 2002, Fire properties and burn patterns in heterogeneous landscapes, *Flammable Australia: the fire regimes and biodiversity of a continent* pp. 49–75.
- Cautun, M. C. and van de Weygaert, R.: 2011, The DTFE public software-The Delaunay Tessellation Field Estimator code, *arXiv preprint arXiv:1105.0370* .
- Checkland, P.: 1981, *Systems Thinking, Systems Practice*, J. Wiley, New York.
- Cheney, N., Gould, J. and Catchpole, W. R.: 1998, Prediction of fire spread in grasslands, *International Journal of Wildland Fire* **8**(1), 1–13.
- Cheney, N. P., Gould, J. S., McCaw, W. L. and Anderson, W. R.: 2012, Predicting fire behaviour in dry eucalypt forest in southern australia, *Forest Ecology and Management* **280**, 120–131.
- Christensen, N. L.: 1993, Fire regimes and ecosystem dynamics, *Fire in the environment: The ecological, atmospheric, and climatic importance of vegetation fires* pp. 233–244.
- Clark, T. L., Coen, J. and Latham, D.: 2004, Description of a coupled atmosphere-fire model, *International Journal of Wildland Fire* **13**(1), 49–63.
- Clarke, M. F.: 2008, Catering for the needs of fauna in fire management: science or just wishful thinking?, *Wildlife Research* **35**(5), 385–394.

- Clements, F. E.: 1916, *Plant succession: an analysis of the development of vegetation*, number 242, Carnegie Institution of Washington.
- Cornelissen, T., Diekkrüger, B. and Bogena, H. R.: 2014, Significance of scale and lower boundary condition in the 3d simulation of hydrological processes and soil moisture variability in a forested head-water catchment, *Journal of Hydrology*.
- Cruz, M., Sullivan, A., Gould, J., Sims, N., Bannister, A., Hollis, J. and Hurley, R.: 2012, Anatomy of a catastrophic wildfire: the black saturday kilmore east fire in victoria, australia, *Forest Ecology and Management* **284**, 269–285.
- Cui, W., Perera, A. et al.: 2008, *A study of simulation errors caused by algorithms of forest fire growth models*, number 167, Ontario Forest Research Institute.
- Davis, F. W. and Burrows, D. A.: 1994, Spatial simulation of fire regime in mediterranean-climate landscapes, *The role of fire in Mediterranean-type ecosystems*, Springer, pp. 117–139.
- De Berg, M., Van Kreveld, M., Overmars, M. and Schwarzkopf, O. C.: 2000, *Computational geometry*, Springer.
- de Goes, F., Breeden, K., Ostromoukhov, V. and Desbrun, M.: 2012, Blue noise through optimal transport, *ACM Transactions on Graphics (TOG)* **31**(6), 171.
- Delaunay, B.: 1934, Sur la sphere vide, *Izv. Akad. Nauk SSSR, Otdelenie Matematicheskii i Estestvennyka Nauk* **7**(793-800), 1–2.
- Doerr, S., Shakesby, R., Blake, W.H. and Chafer, C., Humphreys, G. and Wallbrink, P.: 2006, Effects of differing wildfire severities on soil wettability and implications for hydrological response, *Journal of Hydrology* **319**(1–4), 295–311.
URL: <http://www.sciencedirect.com/science/article/pii/S0022169405003677>
- Draxler, R. R.: 1987, Sensitivity of a trajectory model to the spatial and temporal resolution of the meteorological data during captex, *Journal of climate and applied meteorology* **26**(11), 1577–1588.
- Düben, P. D. and Korn, P.: 2014, Atmosphere and ocean modeling on grids of variable resolution—a 2d case study, *Monthly Weather Review* **142**(5), 1997–2017.
- Eberhart, K. E. and Woodard, P. M.: 1987, Distribution of residual vegetation associated with large fires in alberta, *Canadian Journal of Forest Research* **17**(10), 1207–1212.
URL: <http://www.nrcresearchpress.com/doi/abs/10.1139/x87-186>

- Enright, N. and Lamont, B.: 1989, Seed banks, fire season, safe sites and seedling recruitment in five co-occurring banksia species, *The Journal of Ecology* pp. 1111–1122.
- Feller, M.: 1996, The influence of fire severity, not fire intensity, on understory vegetation biomass in british columbia, *Proceedings, 13th Conference on Fire and Forest Meteorology*, pp. 335–348.
- Feunekes, U.: 1991, *Error analysis in fire simulation models*, PhD thesis, University of New Brunswick (Canada).
- Finney, M. A.: 2001, Design of regular landscape fuel treatment patterns for modifying fire growth and behavior, *Forest Science* 47(2), 219–228.
- Finney, M. A.: 2004, *FARSITE, Fire Area Simulator—model development and evaluation*, US Department of Agriculture, Forest Service, Rocky Mountain Research Station.
- Fiorucci, P., Gaetani, F. and Minciardi, R.: 2008, Regional partitioning for wildfire regime characterization, *Journal of Geophysical Research: Earth Surface* 113(1), 1–9.
URL: <http://dx.doi.org/10.1029/2007JF000771>
- Flannigan, M. D., Krawchuk, M. A., de Groot, W. J., Wotton, B. M. and Gowman, L. M.: 2009, Implications of changing climate for global wildland fire, *International Journal of Wildland Fire* 18(5), 483–507.
- Flannigan, M., Stocks, B. J. and Wotton, B.: 2000, Climate change and forest fires, *Science of the total environment* 262(3), 221–229.
- Flannigan, M. and Wotton, B.: 2001, Chapter 10 - climate, weather, and area burned, in E. A. Johnson and K. Miyanishi (eds), *Forest Fires*, Academic Press, San Diego, pp. 351 – 373.
URL: <http://www.sciencedirect.com/science/article/pii/B978012386660850012X>
- Flint, S.: 2006, *Aspect-oriented thinking: an approach to bridging the disciplinary divides*, PhD thesis, Australian National University, Canberra.
- Fonseca, C. M., Fleming, P. J. et al.: 1993, Genetic algorithms for multiobjective optimization: Formulation discussion and generalization., *ICGA*, Vol. 93, pp. 416–423.
- Forthofer, J. and Butler, B.: 2007, Differences in simulated fire spread over Askervein Hill using two advanced wind models and a traditional uniform wind field, Butler BW, Cook W (Compilers)(eds) *The fire environment-innovations, management and policy* pp. 26–30.
- Gallant, J. C. and Dowling, T. I.: 2003, A multiresolution index of valley bottom flatness for mapping depositional areas, *Water Resources Research* 39(12).

- Gammage, B.: 2011, The biggest estate on earth: How aborigines made australia, *Allen & Unwin*.
- Geiger, R., Aron, R. H. and Todhunter, P.: 2009, *The climate near the ground*, Rowman & Littlefield.
- Génevaux, J.-D., Galin, E., Guérin, E., Peytavie, A. and Beneš, B.: 2013, Terrain generation using procedural models based on hydrology, *ACM Trans. Graph.* **32**(4), 143:1–143:13.
URL: <http://doi.acm.org/10.1145/2461912.2461996>
- Gibbons, P., van Bommel, L., Gill, A. M., Cary, G. J., Driscoll, D. A., Bradstock, R. A., Knight, E., Moritz, M. A., Stephens, S. L. and Lindenmayer, D. B.: 2012, Land management practices associated with house loss in wildfires, *PloS one* **7**(1), e29212.
- Gignoux, J., Davies, I., Flint, S. and Zucker, J.-D. e.: 2011, The ecosystem in practice: Interest and problems of an old definition for constructing ecological models, *Ecosystems* **14**(7), 1039–1054. cited By (since 1996) 1.
- Gill, A. M.: 1975, Fire and the Australian flora: a review, *Australian forestry* **38**(1), 4–25.
- Gill, A. M.: 2008, *Underpinnings of fire management for biodiversity conservation in reserves*, Department of Sustainability and Environment: Melbourne.
- Gill, A. M. and Allan, G.: 2008, Large fires, fire effects and the fire-regime concept, *International Journal of Wildland Fire* **17**(6), 688–695.
- Gill, A. M., Allan, G. and Yates, C.: 2003, Fire-created patchiness in Australian savannas, *International Journal of Wildland Fire* **12**(4), 323–331.
- Gill, A. M., Stephens, S. L. and Cary, G. J.: 2013, The worldwide "wild-fire" problem, *Ecological applications* **23**(2), 438–454.
- Gill, A. M. and Zylstra, P.: 2005, Flammability of Australian forests, *Australian forestry* **68**(2), 87–93.
- Gleason, H. A.: 1917, The structure and development of the plant association, *Bulletin of the Torrey Botanical Club* **44**(10), pp. 463–481.
URL: <http://www.jstor.org/stable/2479596>
- Gould, J. and Cruz, M.: 2012, Australian fuel classification: Stage ii. Ecosystem Sciences and Climate Adaption Flagship.
- Gould, J., McCaw, W., Cheney, N., Ellis, P., Knight, I., Sullivan, A. et al.: 2007, Project Vesta: Fire in dry eucalypt forest.

- Green, D. G.: 1983b, Shapes of simulated fires in discrete fuels, *Ecological Modelling* **20**(1), 21–32.
- Green, D., Gill, A. M. and Noble, I.: 1983a, Fire shapes and the adequacy of fire-spread models, *Ecological Modelling* **20**(1), 33–45.
- Grimm, V., Berger, U., Bastiansen, F., Eliassen, S., Ginot, V., Giske, J., Goss-Custard, J., Grand, T., Heinz, S. K., Huse, G. et al.: 2006, A standard protocol for describing individual-based and agent-based models, *Ecological modelling* **198**(1), 115–126.
- Grimm, V., Berger, U., DeAngelis, D. L., Polhill, J. G., Giske, J. and Railsback, S. F.: 2010, The ODD protocol: a review and first update, *Ecological Modelling* **221**(23), 2760–2768.
- Hargrove, W., Gardner, R., Turner, M., Romme, W. and Despain, D.: 2000, Simulating fire patterns in heterogeneous landscapes, *Ecological Modelling* **135**(2), 243–263.
URL: <http://www.sciencedirect.com/science/article/pii/S0304380000003689>
- Heemstra, S.: 2007, *Bush fire patchiness*, PhD thesis, University of Wollongong.
- Heil, R. J. and Brych, S. M.: 1978, An approach for consistent topographic representation of varying terrain, *Proceedings of the Digital Terrain Models (DTM) Symposium*, pp. 397–411.
- Heinselman, M. L.: 1981, Fire intensity and frequency as factors in the distribution and structure of northern ecosystems [Canadian and Alaskan boreal forests, Rocky Mountain subalpine forests, Great Lakes-Acadian forests, includes history, management; Canada; USA], *USDA Forest Service General Technical Report WO*.
- Hengl, T.: 2006, Finding the right pixel size, *Computers & Geosciences* **32**(9), 1283–1298.
- Hennessy, K. J., Lucas, C., Nicholls, J., Bathols, J., Suppiah, R. and Ricketts, J.: 2005, Climate change impacts on fire-weather in south-east Australia.
- Higgins, G. and Freedman, J.: 2013, Improving decision making in crisis, *Journal of business continuity & emergency planning* **7**(1), 65–76.
- Hirsch, K. G.: 1996, *Canadian forest fire behavior prediction (FBP) system: user's guide*, Vol. 7.
- Hu, X. and Ntamo, L.: 2006, Dynamic multi-resolution cellular space modeling for forest fire simulation, *SIMULATION SERIES* **38**(1), 95.
- Hulot, F. D., Lacroix, G., Lescher-Moutoué, F. and Loreau, M.: 2000, Functional diversity governs ecosystem response to nutrient enrichment, *Nature* **405**(6784), 340–344.

- Hutchinson, M.: 2007, Anudem version 5.2, <http://fennerschool.anu.edu.au/publications/software/anudem.php>.
- Jax, K.: 1998, Holocoen and ecosystem—on the origin and historical consequences of two concepts, *Journal of the History of Biology* **31**(1), 113–142.
- Johnston, P., Kelso, J. and Milne, G. J.: 2008, Efficient simulation of wildfire spread on an irregular grid, *International Journal of Wildland Fire* **17**(5), 614–627.
- Jones, C., Dennison, P., Fujioka, F., Weise, D. and Benoit, J.: 2003, Analysis of space/time characteristics of errors in an integrated weather/fire spread simulation, *Proceedings 5th symposium on fire and forest meteorology/2nd international wildland fire ecology and fire management congress. (Orlando, FL) Paper J2.8. (CD-ROM) (American Meteorological Society: Boston, MA)*.
- Jordan, N.: 1968, Some thinking about 'System', in *Systems Thinking: 2. Selected Readings*, Emery, F. E. (ed.), 1981, pp. 15–39.
- Keane, R. E., Cary, G. J., Davies, I. D., Flannigan, M. D., Gardner, R. H., Lavorel, S., Lenihan, J. M., Li, C. and Rupp, T. S.: 2004, A classification of landscape fire succession models: spatial simulations of fire and vegetation dynamics, *Ecological Modelling* **179**(1), 3–27.
- Keane, R. E., Cary, G. J., Flannigan, M. D., Parsons, R. A., Davies, I. D., King, K. J., Li, C., Bradstock, R. A. and Gill, M.: 2013a, Exploring the role of fire, succession, climate, and weather on landscape dynamics using comparative modeling, *Ecological Modelling* **266**, 172–186.
- Keane, R. E., Cary, G. J. and Parsons, R.: 2003, Using simulation to map fire regimes: an evaluation of approaches, strategies, and limitations, *International Journal of Wildland Fire* **12**(4), 309–322.
- Keane, R. E., Herynk, J. M., Toney, C., Urbanski, S. P., Lutes, D. C. and Ottmar, R. D.: 2013b, Evaluating the performance and mapping of three fuel classification systems using Forest Inventory and Analysis surface fuel measurements, *Forest Ecology and Management* **305**, 248–263.
- Keane, R. E., Morgan, P. and Running, S. W.: 1996, Fire-bgc: A mechanistic ecological process model for simulating fire succession on coniferous forest landscapes of the northern rocky mountains. forest service research paper, *Technical report*, Forest Service, Ogden, UT (United States). Intermountain Research Station.
- Keane, R. E., Parsons, R. A. and Hessburg, P. F.: 2002, Estimating historical range and variation of landscape patch dynamics: limitations of the simulation approach, *Ecological Modelling* **151**(1), 29–49.

- Keeley, J. E.: 2009, Fire intensity, fire severity and burn severity: a brief review and suggested usage, *International Journal of Wildland Fire* **18**(1), 116–126.
- Keeley, J. E., Pausas, J. G., Rundel, P. W., Bond, W. J. and Bradstock, R. A.: 2011, Fire as an evolutionary pressure shaping plant traits, *Trends in Plant Science* **16**(8), 406–411.
URL: <http://www.sciencedirect.com/science/article/pii/S1360138511000835>
- Keetch, J. J. and Byram, G. M.: 1968, *A drought index for forest fire control*, US Department of Agriculture, Forest Service, Southeastern Forest Experiment Station.
- Keith, D. A.: 2004, *Ocean shores to desert dunes: the native vegetation of New South Wales and the ACT*, Department of Environment and Conservation (NSW).
- Keith, D. A., Williams, J. E. and Woinarski, J. C.: 2002, Fire management and biodiversity conservation: key approaches and principles. in 'Flammable Australia: the fire regimes and biodiversity of a continent'. (Eds RA Bradstock, JE Williams, AM Gill), pp. 401–428.
- King, K. J.: 2004, *Simulating the effects of anthropogenic burning on patterns of biodiversity*, PhD thesis, Australian National University.
- King, K. J., Bradstock, R. A., Cary, G. J., Chapman, J. and Marsden-Smedley, J. B.: 2008b, The relative importance of fine-scale fuel mosaics on reducing fire risk in south-west Tasmania, Australia, *International Journal of Wildland Fire* **17**(3), 421–430.
- King, K. J., Cary, G. J., Bradstock, R. A., Chapman, J., Pyrke, A. and Marsden-Smedley, J. B.: 2006, Simulation of prescribed burning strategies in south-west Tasmania, Australia: effects on unplanned fires, fire regimes, and ecological management values, *International Journal of Wildland Fire* **15**(4), 527–540.
- King, K. J., Cary, G. J., Bradstock, R. A. and Marsden-Smedley, J. B.: 2013, Contrasting fire responses to climate and management: insights from two Australian ecosystems, *Global change biology* **19**(4), 1223–1235.
- King, K. J., Cary, G. J., Gill, A. M. and Moore, A. D.: 2012, Implications of changing climate and atmospheric CO₂ for grassland fire in south-east Australia: insights using the GRAZPLAN grassland simulation model, *International Journal of Wildland Fire* **21**(6), 695–708.
- King, K. J., de Ligt, R. M. and Cary, G. J.: 2011, Fire and carbon dynamics under climate change in south-eastern Australia: insights from FullCAM and FIRESCAPE modelling, *International Journal of Wildland Fire* **20**(4), 563–577.

- King, K., Marsden-Smedley, J., Cary, G., Allan, G., Bradstock, R. and Gill, M.: 2008a, Modelling fire dynamics in the West MacDonnell Range area, *Technical report*, Desert Knowledge CRC Working paper 20.
- Koo, E., Pagni, P. J., Weise, D. R. and Woycheese, J. P.: 2010, Firebrands and spotting ignition in large-scale fires, *International Journal of Wildland Fire* **19**(7), 818–843.
- Koutsias, N., Xanthopoulos, G., Founda, D., Xystrakis, F., Nioti, F., Pleniou, M., Mallinis, G. and Arianoutsou, M.: 2013, On the relationships between forest fires and weather conditions in Greece from long-term national observations (1894–2010), *International Journal of Wildland Fire* **22**(4), 493–507.
- Krause, E. F.: 1973, Taxicab geometry, *The Mathematics Teacher* pp. 695–706.
- Krawchuk, M. A., Moritz, M. A., Parisien, M.-A., Van Dorn, J. and Hayhoe, K.: 2009, Global pyrogeography: the current and future distribution of wildfire, *PLoS One* **4**(4), e5102.
- Krebs, P., Pezzatti, G., Mazzoleni, S., Talbot, L. and Conedera, M.: 2010, Fire regime: history and definition of a key concept in disturbance ecology, *Theory in Biosciences* **129**(1), 53–69.
URL: <http://dx.doi.org/10.1007/s12064-010-0082-z>
- Kuleshov, Y., de Hoedt, G., Wright, W. and Brewster, A.: 2002, Thunderstorm distribution and frequency in Australia, *Aust. Met. Mag* **51**, 145–54.
- Lacy, R. C., Miller, P. S., Nyhus, P. J., Pollak, J., Raboy, B. E. and Zeigler, S. L.: 2013, Metamodels for transdisciplinary analysis of wildlife population dynamics, *PloS one* **8**(12), e84211.
- Lagae, A. and Dutré, P.: 2008, A comparison of methods for generating Poisson disk distributions, *Computer Graphics Forum*, Vol. 27, Wiley Online Library, pp. 114–129.
- Lavorel, S., Davies, I. D. and Noble, I. R.: 2000, LAMOS: a landscape modelling shell, *Landscape Fire Modeling—Challenges and Opportunities*, Natural Resources Canada, Canadian Forest Service, Victoria, British Columbia.
- Leavesley, A. J., Cary, G. J., Edwards, G. P. and Gill, A. M.: 2010, The effect of fire on birds of mulga woodland in arid central Australia, *International journal of wildland fire* **19**(7), 949–960.
- Lenihan, J. M., Daly, C., Bachelet, D. and Neilson, R. P.: 1998, Simulating broad-scale fire severity in a dynamic global vegetation model, *Northwest Science* **72**(4), 91–101.

- Lepczyk, C. A., Lortie, C. J. and Anderson, L. J.: 2008, An ontology for landscapes, *ecological complexity* 5(3), 272–279.
- Levin, S. A.: 1992, The problem of pattern and scale in ecology: the Robert H. MacArthur award lecture, *Ecology* 73(6), 1943–1967.
- Li, C.: 2000, Reconstruction of natural fire regimes through ecological modelling, *Ecological Modelling* 134(2), 129–144.
- Linn, R., Reisner, J., Colman, J. J. and Winterkamp, J.: 2002, Studying wildfire behavior using FIRETEC, *International journal of wildland fire* 11(4), 233–246.
- Lucas, C. et al.: 2007, *Bushfire weather in Southeast Australia: recent trends and projected climate change impacts*, Citeseer.
- Luke, R. and McArthur, A.: 1978, *Bushfires in Australia*, CSIRO Division of Forest Research, Australian Government Publishing Service, Canberra.
- Mann, C. C.: 2000, The End of Moores Law, *Technology Review* 103(3), 42–48.
- Markus, M. and Hess, B.: 1990, Isotropic cellular automaton for modelling excitable media, *Nature* 347(6288), 56–58.
- Matthews, S., Sullivan, A. L., Watson, P. and Williams, R. J.: 2012, Climate change, fuel and fire behaviour in a eucalypt forest, *Global Change Biology* 18(10), 3212–3223.
URL: <http://dx.doi.org/10.1111/j.1365-2486.2012.02768.x>
- McArthur, A. and Cheney, N.: 1972, Source notes on forest fire control, *Unpublished report. Forest Research Institute, Australian Forest and Timber Bureau, Canberra*.
- McArthur, A. G.: 1966, *Weather and grassland fire behaviour*, Forestry and Timber Bureau, Department of national Development, Commonwealth of Australia.
- McArthur, A. G.: 1967, *Fire behaviour in eucalypt forests*, Commonwealth of Australia Forestry and Timber Bureau Leaflet No.107, Canberra.
- McArthur, A. G.: 1973, *Forest Fire Danger Meter Mark V*.
- McBride, J. R.: 1983, Analysis of tree rings and fire scars to establish fire history, 3.
- McCarthy, G.: 2003, *Drought Factor (fine fuel consumption) prediction from field measurement of Fine Fuel Moisture Content*, Forest Science Centre. Dep. of Sustainability and Environment.

- McCarthy, M., Cary, G., Bradstock, R., Williams, J., Gill, A. *et al.*: 2002, Fire regimes in landscapes: models and realities., *Flammable Australia: the fire regimes and biodiversity of a continent* pp. 76–93.
- McCaw, W., Gould, J. and Cheney, N.: 2008, Existing fire behaviour models under-predict the rate of spread of summer fires in open jarrah (*Eucalyptus marginata*) forest, *Australian Forestry* **71**(1), 16–26.
- McCool, M. and Fiume, E.: 1992, Hierarchical Poisson disk sampling distributions, *Proceedings of the conference on Graphics interface*, Vol. 92, pp. 94–105.
- McRae, R. H.: 1992, Prediction of areas prone to lightning ignition, *International Journal of Wildland Fire* **2**(3), 123–130.
- Miller, G. S.: 1986, The definition and rendering of terrain maps, *ACM SIGGRAPH Computer Graphics*, Vol. 20, ACM, pp. 39–48.
- Milne, M., Clayton, H., Dovers, S. and Cary, G. J.: 2014, Evaluating benefits and costs of wildland fires: critical review and future applications, *Environmental Hazards* **13**(2), 114–132.
- Miyamoto, H. and Sasaki, S.: 1997, Simulating lava flows by an improved cellular automata method, *Computers & Geosciences* **23**(3), 283–292.
- Mladenoff, D. J. and He, H. S.: 1999, Design, behavior and application of LANDIS, an object-oriented model of forest landscape disturbance and succession, *Spatial modeling of forest landscape change: approaches and applications*. Cambridge University Press, Cambridge, UK pp. 125–162.
- Moore, A. D. and Noble, I. R.: 1990, An individualistic model of vegetation stand dynamics, *Journal of Environmental Management* **31**(1), 61–81.
- Moore, I. D., Norton, T. W. and Williams, J. E.: 1993, Modelling environmental heterogeneity in forested landscapes, *Journal of Hydrology* **150**(2), 717–747.
- Moore, P., Gill, A. and Kohnert, R.: 1995, Quantifying bushfires for ecology using two electronic devices and biological indicators, *CALM Science Supplement* **4**, 83–88.
- Moreno, M. V. and Chuvieco, E.: 2013, Characterising fire regimes in Spain from fire statistics, *International Journal of Wildland Fire* **22**(3), 296–305.
- Mount, A.: 1972, *The derivation and testing of a soil dryness index using run-off data*, Forestry Commission, Tasmania.

- Noble, I., Gill, A. and Bary, G.: 1980, McArthur's fire-danger meters expressed as equations, *Australian Journal of Ecology* **5**(2), 201–203.
- Noble, I. R. and Slatyer, R.: 1980, The use of vital attributes to predict successional changes in plant communities subject to recurrent disturbances, **43**, 5–21.
- Noble, J. C.: 1997, *Delicate and Noxious Scrub*, CSIRO.
- Noonan-Wright, E. K., Opperman, T. S., Finney, M. A., Zimmerman, G. T., Seli, R. C., Elenz, L. M., Calkin, D. E. and Fiedler, J. R.: 2011, Developing the US wildland fire decision support system, *Journal of Combustion* **2011**.
- Odion, D. C. and Hanson, C. T.: 2008, Fire severity in the Sierra Nevada revisited: conclusions robust to further analysis, *Ecosystems* **11**(1), 12–15.
- Odum, E. P. and Barrett, G. W.: 1971, *Fundamentals of ecology*, Saunders Philadelphia.
- Olsen, J.: 1963, Energy storage and the balance of producers and consumers in ecological systems, *Ecology* **44**, 322–32.
- Olson, D. M., Dinerstein, E., Wikramanayake, E. D., Burgess, N. D., Powell, G. V., Underwood, E. C., D'amico, J. A., Itoua, I., Strand, H. E., Morrison, J. C. et al.: 2001, Terrestrial Ecoregions of the world: A new map of life on earth: A new global map of terrestrial ecoregions provides an innovative tool for conserving biodiversity, *BioScience* **51**(11), 933–938.
- O'Neill, R. V.: 2001, Is it time to bury the ecosystem concept?(With full military honors, of course!), *Ecology* **82**(12), 3275–3284.
- Opperman, T., Gould, J., Finney, M. and Tymstra, C.: 2006, Applying fire spread simulators in New Zealand and Australia: Results from an international seminar, *Fuels Management—How to Measure Success. USDA Forest Service, Rocky Mountain Research Station, Fort Collins, CO. Proceedings RMRS-P-41* pp. 201–212.
- Parr, C. L. and Andersen, A. N.: 2006, Patch mosaic burning for biodiversity conservation: a critique of the pyrodiversity paradigm, *Conservation Biology* **20**(6), 1610–1619.
- Pastor, E., Zarate, L., Planas, E. and Arnaldos, J.: 2003, Mathematical models and calculation systems for the study of wildland fire behaviour, *Progress in Energy and Combustion Science* **29**(2), 139–153.
- Pausas, J. G.: 1999, Response of plant functional types to changes in the fire regime in Mediterranean ecosystems: a simulation approach, *Journal of Vegetation Science* **10**(5), 717–722.

- Pausas, J. G., Alessio, G. A., Moreira, B. and Corcobado, G.: 2012, Fires enhance flammability in *Ulex parviflorus*, *New Phytologist* **193**(1), 18–23.
- Pausas, J. G. and Fernández-Muñoz, S.: 2012, Fire regime changes in the Western Mediterranean Basin: from fuel-limited to drought-driven fire regime, *Climatic change* **110**(1–2), 215–226.
- Pausas, J. G. and Ramos, J. I.: 2006, Landscape analysis and simulation shell (Lass), *Environmental Modelling & Software* **21**(5), 629–639.
URL: <http://www.sciencedirect.com/science/article/pii/S1364815204003263>
- Peel, M. C., Finlayson, B. L. and McMahon, T. A.: 2007, Updated world map of the köppen-geiger climate classification., *Hydrology & Earth System Sciences Discussions* **4**(2).
- Peet, G.: 1967, The shape of mild fires in Jarrah forest, *Australian Forestry* **31**(2), 121–127.
- Perera, A. H. and Cui, W.: 2010, Emulating natural disturbances as a forest management goal: lessons from fire regime simulations, *Forest ecology and management* **259**(7), 1328–1337.
- Perera, A. H., Ouellette, M., WenBin, C., Drescher, M., Boychuk, D. et al.: 2008, *BFOLDS 1.0: a spatial simulation model for exploring large scale fire regimes and succession in boreal forest landscapes.*, number 152, Ontario Forest Research Institute.
- Peucker, T. K., Fowler, R. J., Little, J. J. and Mark, D. M.: 1978, The triangulated irregular network, *Amer. Soc. Photogrammetry Proc. Digital Terrain Models Symposium*, Vol. 516, p. 532.
- Pickett, S. T. and White, P.: 1985, *The ecology of natural disturbance and patch dynamics*, Academic press.
- Plotnick, R. E. and Gardner, R. H.: 1993, Lattices and landscapes, *Lectures on mathematics in the life sciences* **23**, 129–156.
- Price, C. and Rind, D.: 1994, Possible implications of global climate change on global lightning distributions and frequencies, *Journal of Geophysical Research: Atmospheres* (1984–2012) **99**(D5), 10823–10831.
- Pryor, L.: 1939, The bush fire problem in the Australian Capital Territory, *Australian Forestry* **4**, 33–8.
- Raphael, M.: 2003, The Santa Ana winds of California, *Earth Interactions* **7**(8), 1–13.
- Raupach, M.: 1990, Similarity analysis of the interaction of bushfire plumes with ambient winds, *Mathematical and Computer Modelling* **13**(12), 113–121.
URL: <http://www.sciencedirect.com/science/article/pii/089571779090105V>

- Richards, G. P. and Evans, D. M.: 2004, Development of a carbon accounting model (FullCAM Vers. 1.0) for the Australian continent, *Australian Forestry* **67**(4), 277–283.
- Richardson, C. W.: 1981, Stochastic simulation of daily precipitation, temperature, and solar radiation, *Water Resources Research* **17**(1), 182–190.
- Richardson, C. W. and Wright, D. A.: 1984, WGEN: A model for generating daily weather variables, *ARS*.
- Rodríguez y Silva, F. and González-Cabán, A.: 2010, 'sinami': a tool for the economic evaluation of forest fire management programs in mediterranean ecosystems, *International journal of wildland fire* **19**(7), 927–936.
- Rothermel, R. C.: 1972, *A mathematical model for predicting fire spread in wildland fuels*, USFS.
- Rumbaugh, J., Jacobson, I. and Booch, G.: 2004, *The Unified Modeling Language Reference Manual*, Pearson Higher Education.
- Rummer, B.: 2008, Assessing the cost of fuel reduction treatments: a critical review, *Forest Policy and Economics* **10**(6), 355–362.
- Russell-Smith, J., Yates, C. P., Whitehead, P. J., Smith, R., Craig, R., Allan, G. E., Thackway, R., Frakes, I., Cridland, S., Meyer, M. C. et al.: 2007, Bushfires 'down under': patterns and implications of contemporary Australian landscape burning, *International Journal of Wildland Fire* **16**(4), 361–377.
- Rykiel Jr, E. J.: 1996, Testing ecological models: the meaning of validation, *Ecological modelling* **90**(3), 229–244.
- Sargent, R. G.: 2005, Verification and validation of simulation models, *Proceedings of the 37th conference on Winter simulation*, WSC '05, Winter Simulation Conference, pp. 130–143.
- Saupe, D.: 1991, Random fractals in image synthesis, *Fractals and chaos*, Springer, pp. 89–118.
- Schaap, W. E.: 2007, *The Delaunay tessellation field estimator*, PhD thesis, Ph. D. thesis, Groningen University.
- Scheller, R. M., Spencer, W. D., Rustigian-Romsos, H., Syphard, A. D., Ward, B. C. and Strittholt, J. R.: 2011, Using stochastic simulation to evaluate competing risks of wildfires and fuels management on an isolated forest carnivore, *Landscape Ecology* **26**(10), 1491–1504.
- Schiemann, R., Demory, M.-E., Mizielinski, M. S., Roberts, M. J., Shafrey, L. C., Strachan, J. and Vidale, P. L.: 2014, The sensitivity of the tropical circulation and maritime continent precipitation to climate model resolution, *Climate Dynamics* **42**(9–10), 2455–2468.

- Seidl, R., Fernandes, P. M., Fonseca, T. F., Gillet, F., Jönsson, A. M., Merganičová, K., Netherer, S., Arpacı, A., Bontemps, J.-D., Bugmann, H. *et al.*: 2011, Modelling natural disturbances in forest ecosystems: a review, *Ecological Modelling* **222**(4), 903–924.
- Sharples, J. J.: 2008, Review of formal methodologies for wind-slope correction of wildfire rate of spread, *International Journal of Wildland Fire* **17**(2), 179–193.
- Sharples, J. J.: 2009, An overview of mountain meteorological effects relevant to fire behaviour and bushfire risk, *International Journal of Wildland Fire* **18**(7), 737–754.
- Short, J. and Smith, A.: 1994, Mammal decline and recovery in Australia, *Journal of Mammalogy* pp. 288–297.
- Shugart, H. H. and Noble, I. R.: 1981, A computer model of succession and fire response of the high-altitude Eucalyptus forest of the Brindabella Range, Australian Capital Territory, *Australian Journal of Ecology* **6**(2), 149–164.
URL: <http://dx.doi.org/10.1111/j.1442-9993.1981.tb01286.x>
- Slocum, M. G., Platt, W. J., Beckage, B., Panko, B. and Lushine, J. B.: 2007, Decoupling natural and anthropogenic fire regimes: a case study in Everglades National Park, Florida, *Natural Areas Journal* **27**(1), 41–55.
- Sousa, F., Dos Reis, R. and Pereira, J.: 2012, Simulation of surface fire fronts using <i>firelib</i> and GPUs, *Environmental Modelling & Software* **38**, 167–177.
- Specht, R.: 1970, Vegetation in the Australian environment.(ed. gw leeper.) pp. 44–67.
- Spies, T. A., Lindenmayer, D. B., Gill, A. M., Stephens, S. L. and Agee, J. K.: 2012, Challenges and a checklist for biodiversity conservation in fire-prone forests: Perspectives from the Pacific Northwest of usa and Southeastern Australia, *Biological Conservation* **145**(1), 5–14.
- Stein, A., Riley, J. and Halberg, N.: 2001, Issues of scale for environmental indicators, *Agriculture, ecosystems & environment* **87**(2), 215–232.
- Stephens, S. L., Weise, D. R., Fry, D. L., Keiffer, R. J., Dawson, J., Koo, E., Potts, J., Pagni, P. J. *et al.*: 2008, Measuring the rate of spread of chaparral prescribed fires in northern California, *Fire Ecology* **4**(1), 74–86.
- Sturtevant, B. R., Scheller, R. M., Miranda, B. R., Shinneman, D. and Syphard, A.: 2009, Simulating dynamic and mixed-severity fire regimes: a process-based fire extension for LANDIS-II, *Ecological Modelling* **220**(23), 3380–3393.

- Sullivan, A. L.: 2007, *Competitive thermokinetics and non-linear bushfire behaviour*, PhD thesis, College of Science, Australian National University.
- Sullivan, A. L.: 2009a, Wildland surface fire spread modelling, 1990–2007. 1: Physical and quasi-physical models, *International Journal of Wildland Fire* **18**(4), 349–368.
- Sullivan, A. L.: 2009b, Wildland surface fire spread modelling, 1990–2007. 2: Empirical and quasi-empirical models, *International Journal of Wildland Fire* **18**(4), 369–386.
- Sullivan, A. L.: 2009c, Wildland surface fire spread modelling, 1990–2007. 3: Simulation and mathematical analogue models, *International Journal of Wildland Fire* **18**(4), 387–403.
- Swetnam, T. W. et al.: 1993, Fire history and climate change in giant sequoia groves, *Science(Washington)* **262**(5135), 885–889.
- Syphard, A. D., Scheller, R. M., Ward, B. C., Spencer, W. D. and Strittholt, J. R.: 2011, Simulating landscape-scale effects of fuels treatments in the Sierra Nevada, California, usa, *International Journal of Wildland Fire* **20**(3), 364–383.
- Tansley, A. G.: 1935, The use and abuse of vegetational concepts and terms, *Ecology* **16**(3), 284–307.
- Teoh, S. T.: 2009, Riverland: an efficient procedural modeling system for creating realistic-looking terrains, *Advances in Visual Computing*, Springer, pp. 468–479.
- Thompson, M. P. and Calkin, D. E.: 2011, Uncertainty and risk in wildland fire management: A review, *Journal of Environmental Management* **92**(8), 1895 – 1909.
URL: <http://www.sciencedirect.com/science/article/pii/S0301479711000818>
- Thonicke, K., Spessa, A., Prentice, I., Harrison, S., Dong, L. and Carmona-Moreno, C.: 2010, The influence of vegetation, fire spread and fire behaviour on biomass burning and trace gas emissions: results from a process-based model., *Biogeosciences* **7**(6).
- Thonicke, K., Venevsky, S., Sitch, S. and Cramer, W.: 2001, The role of fire disturbance for global vegetation dynamics: coupling fire into a Dynamic Global Vegetation Model, *Global Ecology and Biogeography* **10**(6), 661–677.
- Timbal, B., Arblaster, J. M. and Power, S.: 2006, Attribution of the late-twentieth-century rainfall decline in southwest Australia., *Journal of Climate* **19**(10).

- Tolhurst, K., Shields, B. and Chong, D.: 2008, Phoenix: development and application of a bushfire risk management tool, *Australian Journal of Emergency Management, The* **23**(4), 47.
- Trevitt, C.: 1994, Developing a national bushfire strategy, *Search* **25**, 126–127.
- Trunfio, G. A.: 2004, Predicting wildfire spreading through a hexagonal cellular automata model, *Cellular Automata*, Springer, pp. 385–394.
- Trunfio, G. A., D'Ambrosio, D., Rongo, R., Spataro, W. and Di Gregorio, S.: 2011, A new algorithm for simulating wildfire spread through cellular automata, *ACM Transactions on Modeling and Computer Simulation (TOMACS)* **22**(1), 6.
- Turner, M. G., Romme, W. H., Gardner, R. H., O'Neill, R. V. and Kratz, T. K.: 1993, A revised concept of landscape equilibrium: disturbance and stability on scaled landscapes, *Landscape Ecology* **8**(3), 213–227.
- Tymstra, C., Bryce, R., Wotton, B., Taylor, S. and Armitage, O.: 2010, *Development and structure of Prometheus: the Canadian wildland fire growth simulation model*, Northern Forestry Centre.
- Tymstra, C., Flannigan, M. D., Armitage, O. B. and Logan, K.: 2007, Impact of climate change on area burned in Alberta's boreal forest, *International Journal of Wildland Fire* **16**(2), 153–160.
- Ulichney, R.: 1987, *Digital halftoning*, MIT press.
- Van Wagner, C. E.: 1969, A simple fire-growth model, *The Forestry Chronicle* **45**(2), 103–104.
- Van Wagendonk, J. W.: 1996, Use of a deterministic fire growth model to test fuel treatments, *Sierra Nevada ecosystem project, final report to congress*, Vol. 2, pp. 1155–1166.
- Van Wilgen, B.: 1986, A simple relationship for estimating the intensity of fires in natural vegetation., *S. AFR. J. BOT./S.-AFR. TYDSKR. PLANTKD.* **52**(4), 384–385.
- Vannière, B., Colombaroli, D., Chapron, E., Leroux, A., Tinner, W. and Magny, M.: 2008, Climate versus human-driven fire regimes in Mediterranean landscapes: the holocene record of Lago dell'Accesa (Tuscany, Italy), *Quaternary Science Reviews* **27**(11–12), 1181–1196.
- Vanuytrecht, E., Raes, D., Willems, P. and Semenov, M. A.: 2014, Comparing climate change impacts on cereals based on cmip3 and eu-ensembles climate scenarios, *Agricultural and Forest Meteorology* **195**, 12–23.

- Vereecken, H., Huisman, J., Pachepsky, Y., Montzka, C., van der Kruk, J., Bogen, H., Weihermüller, L., Herbst, M., Martinez, G. and Vanderborght, J.: 2013, On the spatio-temporal dynamics of soil moisture at the field scale, *Journal of Hydrology*.
- Walker, J.: 1981, Fuel dynamics in Australian vegetation, *Fire and the Australian biota* pp. 101–127.
- Wallace, G.: 1993, A numerical fire simulation-model, *International Journal of Wildland Fire* 3(2), 111–116.
- Wein, R. W.: 1981, Characteristics and suppression of fires in organic terrain in Australia, *Australian Forestry* 44(3), 162–169.
- Whelan, R., Dickman, C. and EF, S.: 2002, Critical life cycles of plants and animals: developing a process-based understanding of population changes in fire-prone landscapes. in *Flammable Australia: the fire regimes and biodiversity of a continent*. (Eds RA Bradstock, JE Williams, AM Gill), pp. 94–124.
- White, J. W., Rassweiler, A., Samhouri, J. F., Stier, A. C. and White, C.: 2014, Ecologists should not use statistical significance tests to interpret simulation model results, *Oikos* 123(4), 385–388.
URL: <http://dx.doi.org/10.1111/j.1600-0706.2013.01073.x>
- Whittaker, R. H.: 1953, A consideration of climax theory: the climax as a population and pattern, *Ecological monographs* 23(1), 41–78.
- Wiens, J. A.: 1989, Spatial scaling in ecology, *Functional ecology* 3(4), 385–397.
- Williams, R., Gill, A. and Moore, P.: 1998, Seasonal changes in fire behaviour in a tropical savanna in northern Australia, *International Journal of Wildland Fire* 8(4), 227–239.
- Wood, S. W., Murphy, B. P. and Bowman, D. M.: 2011, Firescape ecology: how topography determines the contrasting distribution of fire and rain forest in the south-west of the Tasmanian Wilderness World Heritage Area, *Journal of Biogeography* 38(9), 1807–1820.
- Wright, B. R. and Clarke, P. J.: 2007, Fire regime (recency, interval and season) changes the composition of spinifex (*Triodia* spp.)-dominated desert dunes, *Australian Journal of Botany* 55(7), 709–724.
- Xu, Y., Liu, L., Gotsman, C. and Gortler, S. J.: 2011, Capacity-constrained Delaunay triangulation for point distributions, *Computers & Graphics* 35(3), 510–516.
- Zarzycki, C. M., Jablonowski, C. and Taylor, M. A.: 2014, Using variable-resolution meshes to model tropical cyclones in the Community Atmosphere Model, *Monthly Weather Review* 142(3), 1221–1239.

Zucker, J.-D.: 2003, A grounded theory of abstraction in artificial intelligence, *Philosophical Transactions of the Royal Society B: Biological Sciences* **358**(1435), 1293–1309.

Zylstra, P.: 2006, *Fire history of the Australian Alps: Prehistory to 2003*, Department of the Environment and Water Resources.

FIREMESH: OVERVIEW, DESIGN CONCEPTS AND DETAILS

This model description follows the ODD (Overview, Design concepts, Details) protocol for describing individual- and agent-based models (Grimm et al. 2006, 2010). In what follows, references to elements in UML diagrams (see Box A.1) are shown in mono-spaced font.

Box A.1 Interpreting UML class, object sequence and state diagrams (Unified Modeling Language www.uml.org)

UML class and object diagrams list a model's entities, relationships and their multiplicity. As used here, a single line indicates a *has* relationship. A line with an arrow indicates a specialization of a class and can be read as an *is a* relationship. For example a *car has* doors and *is a* vehicle. Phrases can be associated with the relationship and sentences constructed with the entity name and the multiplicity. For example, *a Car is a type of Vehicle that has 4 Wheels*. The entities in object diagrams are instances of classes, in the same sense that a plant is an instance of a species. For example FIREMESH is an instance of a Model, noted as `FIREMESH:Model`. A sequence diagram shows a lifeline (dotted line) of an object through time. The object's state is updated in response to a message (horizontal arrow). Time is read from top to bottom. A state diagram shows the possible states an object can have and the events that cause transitions between them.

A.1 PURPOSE

The purpose of Landscape Fire Regime simulation models is to produce spatially auto-correlated patterns of fire regimes, where fire regimes are defined as the history of fire frequency, intensity and seasonality at a point (Gill 1975). An additional purpose, specific to FIREMESH, is to test the sensitivity of the drivers of these patterns (climate, weather, vegetation, ignition patterns, management interventions, terrain and so forth) to spatio-temporal resolution and fundamentally different ways in which space can be represented. FIREMESH is derived from FIRESCAPE (Cary and Banks 2000).

A.2 ENTITIES, STATE VARIABLES, AND SCALES

The entities in FIREMESH are the components of its spatial model, collections of them (`Fireline`, `Fire_footprint` and `Fire_complex`)

and ignition events. The model of space is a mesh, that is, a spatially explicit graph comprising a set of vertices connected by directed edges rather than a raster grid as used in all previous versions of FIRESCAPE (Figure A.1). The three entities of a mesh are *Vertex*, *Edge* and *Direction*, the latter, a class that encapsulates the directional relationship an *Edge* has with the two *Vertices* it connects. A *Vertex* is a location in three dimensions (meters) and has three state variables, *residual_fuel_weight* (t.ha^{-1}), *time_last_burnt*, and *state*, one of {unburnt, burning, burnt}. The *residual_fuel_weight* is the weight of unburnt fuel at *time_last_burnt*.

- i An *Edge* represents the distance (meters) in two and three dimensions between *Vertices*. It has no state variables.
- ii *Direction* (*To* and *From*) has state variable *fireline* which records the distance burnt from a vertex along an edge. The edge may burn from either end.
- iii A *Fireline* (not shown in Figure A.1): a set of *Vertices* with *State*{burning} that have been burnt from a particular lightning strike. The time and location of that ignition is its unique identifier. Note that, two ignition events cannot occur at the same time and location.
- iv A *Fire_footprint* (not shown in Figure A.2.1): a set of vertices with *State*{burnt} which disappears, after details are logged, as soon as the *fireline* is empty.
- v A *fire_complex* is a set of *firelines* that have ignited from different lightning_strike events. For the purpose of observation, it is the area of a fire complex that is recorded. That is, all fires that have burnt, bracketed by periods of no fire.
- vi An ignition event is an entity composed of a time (seconds) and location (*Vertex*). It is contained within *lightning_strike* and *new_location* messages (Figure A.4).

SPATIAL SCALE The spatial resolution of FIREMESH is defined as the spatial extent divided by the number of vertices. The spatial resolutions used in experiments to date have been between 0.25 ha. and 100 ha. with an extent of 250,000 ha. However, these scales depend on some model assumptions. Data from one weather station is used and therefore the spatial extent is limited by how appropriate extrapolations are to the spatial domain chosen. Other model assumptions that may limit the scale of application of the model are listed below. Spatial resolution can vary depending on the disposition of vertices within the spatial domain.

TEMPORAL SCALE The temporal resolution is defined as the rate at which forcing variables (weather) are read by FIREMESH and should be between half an hour and three hours to avoid violating assumptions in the empirical equations for fire spread. The temporal extent is limited by the duration of the forcing data and assumptions of vegetation dynamics. Temporal resolutions can vary, if required, with some measure of the rate of change in the forcing data. Experiments running over longer durations than the forcing data, recycle the data. Thus, with the current vegetation model (Equation A.1), FIREMESH is a pseudo-equilibrium model.

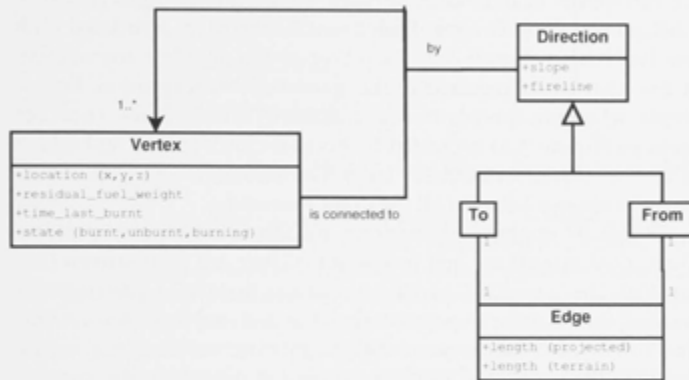


Figure A.1: Class model of a spatially explicit directed mesh

Each Vertex is connected to 1 or more vertices. Each connection is defined by an Edge class. Each Edge has a To and From Direction class. Each Vertex has parameters, location and state variables residual_fuel_weight, time_last_burnt and state. The Edge class has two parameters. Length (projected) is the distance between vertices on a flat plain. Length (terrain) is the distance between two vertices in three dimensions (taking account of the different elevations of the vertices). The Edge class has a directed relationship with two vertices. The Direction class contains the parameter slope and the state variable fireline recording the distance of the fireline along the edge. Thus, an edge can be burnt from either end simultaneously. The fire perimeter is the set of points derived from all vertices that have a fireline > 0 in their To or From classes.

A.3 PROCESS OVERVIEW AND SCHEDULING

The model of time is an event-driven one, as once the model is initialized, no other calculations are required at a regular intervals.

The Simulator manages one or more TimeModels (Figure A.2). A TimeModel simply reports the time of its next advance and the Simulator chooses the earliest. Each TimeModel has one or more Processes associated with it. When the simulator selects a particular

TimeModel, all the associated Processes are executed. On some occasions, two or more TimeModels may be called simultaneously. If such is the case, it may be important to specify the order of execution of simultaneous Processes. This order, if required, is specified in the model's parameter file as a dependency relationship (Figure A.2). If, for example, a lightning_strike occurs at precisely the same time as a weather_update (Figures A.4), the execution of Propagation:Process (Figure A.3) is specified to occur after the lightning strike so that if the vertex does burn, it can join the fireline before propagation takes place. Ignition:Process and Contagion:Process are behaviours of individual vertices while Propagation:Process is a behaviour of the Fireline. Each EventTimeModel is associated with one EventQueue (Figure A.2). Each Process can populate any number of EventQueues as required in the course of their execution. For example, when fire spreads to a neighbouring Vertex, a new_location message (Figure A.4) is created by Propagation:Process and added to the Contagion:EventQueue (A.3). The simulator will then ensure time consistency between all the event processing.

FIREMESH implements four time models of which the IgnitionTimer, ContagionTimer and PropagationTimer are event-driven (Figure A.3). The ScenarioTimer simply ensures that the LightningModel is called first in order to populate Ignitions:EventQueue with events that will be used for the simulation. Lightning_strikes (A.4) are extrinsic to the model and can thus be created initially in this manner. Note that time steps (Weather_update messages) need not be regular. The architecture of FIREMESH allows time steps to be pre-calculated based on the rate of change in the weather variables.

After a fire is initiated by a lightning_strike, if the ignition is successful (defined as a fireline intensity > extinguishment threshold (Section A.7) and vertex state {unburnt}), the vertex moves to the burning state (Figure A.5). Fire spreads from one vertex to the next through new_location messages, that is, when an edge is completely consumed. When all edges of a vertex are consumed by the fire front, the cell moves to the burnt state. When the fireline intensity of all burning vertices falls below the threshold of extinguishment, any partially burnt vertices with more than 50% of edges consumed, move to the burnt state. FIREMESH need only process those locations (vertices) that are in the burning state, that is, the Fireline. If all vertices are extinguished, an extinguishment message is sent (Figure A.4) whereupon all those in a burnt state (the fire footprint) revert to the unburnt state after details of the fire are logged (Figure A.5).

A.4 DESIGN CONCEPTS

Many implicit assumptions are made and often difficult to identify when any model abstraction is made. To assist the reader in identify-

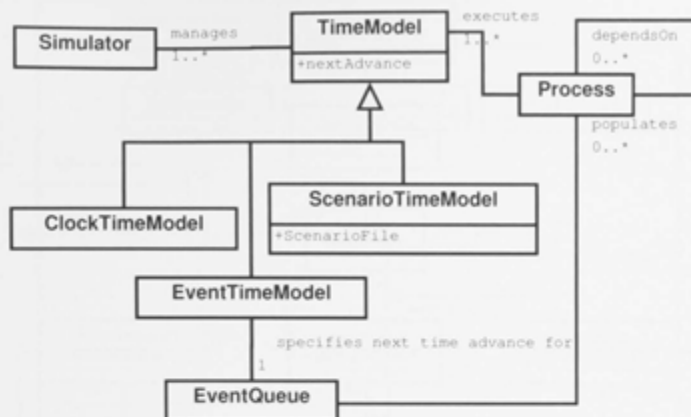


Figure A.2: Classes and relationships in event-driven time model of FIRE-MESH

The Simulator has one or more TimeModels. TimeModels are called in the order of their nextAdvance. TimeModels are associated with 1 or more Processes. These are all executed at the nextAdvance. If the order of execution within a time step is important, this is specified by the dependsOn relationship. An EventTimeModel is a particular type of TimeModel associated with an EventQueue. The EventQueue determines the nextAdvance of a EventTimeModel. Processes populate the EventQueue with events as required.

ing model assumptions, the specification of FIRESMESH is described in terms of the Ontology of Ecosystems (Gignoux et al. 2011) (Figure A.6). The ODD protocol does not appear to directly address this topic under any other heading. FIREMESH, as are all ecosystem models, is a representation of an instance of an ecosystem. The definition of the classes and their relationships noted in Figure A.6 can be found in the public domain (Gignoux et al. 2011, Table 1 and Figure 2). Published sub-models of FIREMESH are noted ((Figure A.6) and discussed in later sections. Main model assumptions are listed below.

- i The vegetation model (Olsen 1963) assumes a climax state exists and the patterns will not change spatially over time. For example, vegetation will not transition from forest to shrub or grassland as a consequence of changed fire regimes and, in the absence of fire, once vegetation has reached its climax state, no further change occurs. Nevertheless, fuel dynamics are not uniform, but vary in their fuel accumulation and decay rates in five elevation classes (the associated spatial representation Figure A.6). If simulations are required to run over longer temporal extents than the available data, the data are simply recycled. Therefore, fire regimes produced by simulations of 1,000 years

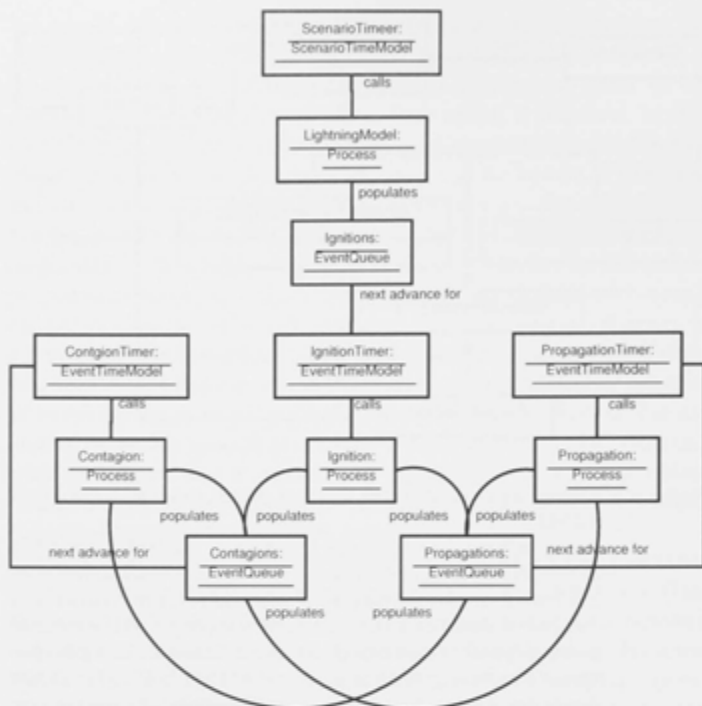


Figure A.3: Objects (instances of classes - Figure A.2) and their relationships in the time model of FIREMESH

The Scenario:ScenarioTimeModel is always called first by the Simulator. The Simulator is not shown for reasons of clarity, but is associated with each of the four TimeModels and calls them in the order of their nextAdvance (Figure A.2). The only task of the Scenario:ScenarioTimeModel is to call LightningModel:Process. This process generates events in time and space that populate Ignitions:EventQueue with the vertex and time of ignition, based on analysis of terrain and weather data anomalies. These ignition events drive the system. When Ignition:Process is executed by IgnitionTimer:TimeModel, the fireline is updated by the distance from the vertex along edges for a period from the moment of ignition until a weather_update (the model's time step). If the fire has not reached a neighbouring vertex during this time, Ignition:Process places a new event in Propagations:EventQueue (if one is not already present) and Propagation:Process will continue to update the position of the fireline for this and any other vertices in the fireline in response to weather_update events (Figure A4). If the spreading fire reaches another vertex before the model's time step is complete, Propagation:Process adds a new_location event (Figure A.4) to Contagions:EventQueue for that vertex scheduled for the appropriate time. Each of the three processes: Ignition, Contagion and Propagation, can populate the Contagion and Propagation event queues.

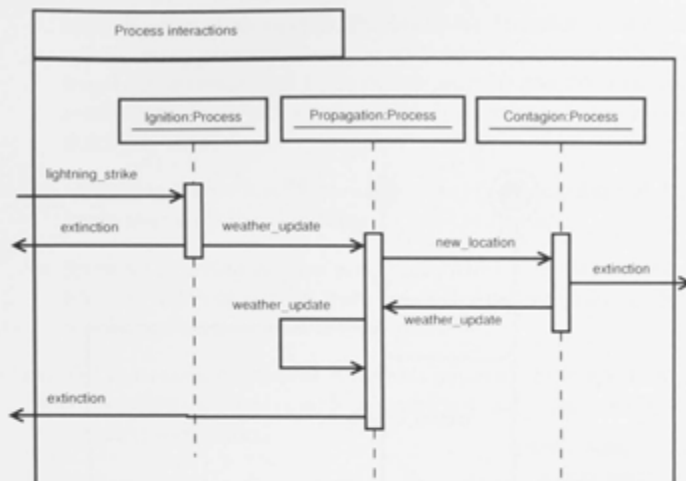


Figure A.4: Sequence diagram for the three implemented processes that operate during simulation

The sequence of events begins with the external input of a lightning_strike event. If fireline intensity is above the smouldering threshold (See end of Section 7, Appendix 1), fire propagates again upon receipt of a weather_update event. The fire perimeter is recalculated for subsequent weather_update events until it reaches a new location (new_location event). This continues until all points on the perimeter have extinguished whereupon details of the fire are logged, all locations revert to the unburnt state, and time jumps forward to the next lightning strike. If a Lightning.Strike or new_location event occurs for a location that is already burning or burnt, the message is ignored (Figure A.5).

for example, are a measures of the quasi-equilibrium state of the system.

- ii Fire ignition is assumed to occur only from lightning: the model does not propose a model of anthropogenic ignitions, which may have implications for spatial patterns of fire regimes.
- iii Readings from a single weather station are used to drive the model and thus values for elevations other than those of the weather station require extrapolation. The validity of these extrapolations will vary with spatial extent.
- iv The effect of topography on wind speed and direction is ignored. These effects are discussed by Shaples (2009).
- v Effect of aspect, which may produce fire regimes that differ between wetter and drier aspects, is ignored. While aspect will change fuel moisture, it will also change vegetation and fuel

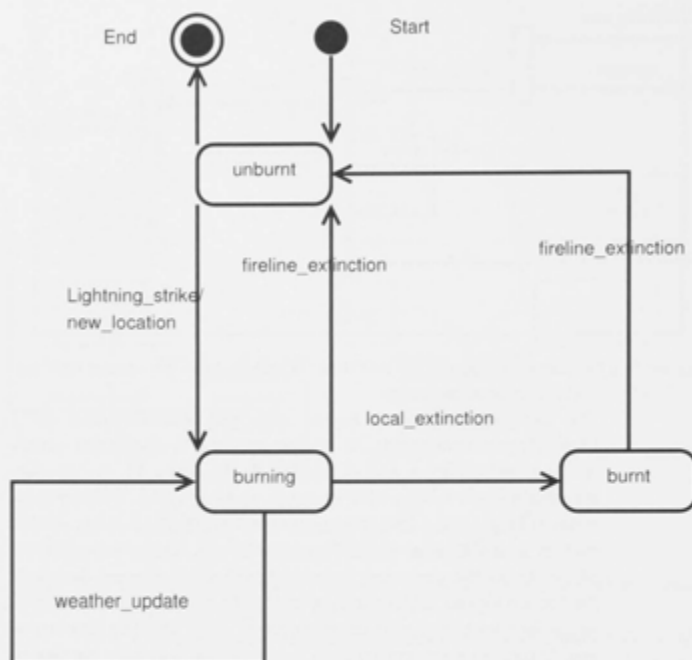


Figure A.5: State transition diagram for a Vertex in FIREMESH

Simulation begins with all vertices in the unburnt state. A **Lightning_strike** or **new_location** event moves the vertex to a burning state. It remains burning with each new **weather_update** event until all edges have been traversed, whereupon it moves to the burnt state (**local_extinction**). When all edges record a fireline intensity < extinguishment threshold, a **fireline_extinction** event occurs. All burnt vertices move to the unburnt state after details of the fire are logged. The details of any vertex that remains in the burning state are logged if the total area burnt is greater than 50% before moving to the unburnt state. The cycle begins again with each **Lightning_strike**. It follows that any lightning_strike or new_location event that reaches a burning or burnt vertex will be ignored. The fireline does not move if the maximum fireline intensity < the smouldering threshold (See end of Section 7, Appendix 1).

- loads (Geiger et al. 1995 in Shaples 2009). Therefore to include aspect, many concerns must be addressed simultaneously that may both increase fuel loads (more growth) and decrease fuel availability (high moisture content and increased decomposition).
- vi Modelling convection plumes (buoyancy) is ignored which has implications for the calculation of rates of spread.
 - vii Spotting by lofted embers is ignored, which may have implications for rates of spread, patterns of fire regimes and ignition neighbourhoods (see Basic Principles).
 - viii The horizontal movement of water is ignored. The evapo-transpiration model (Mount 1972) is entirely empirical and unaffected by vegetation succession.

BASIC PRINCIPLES The basic principle of the model is to expand a one-dimensional model (McArthur 1973) used to predict fire velocity to two dimensions. This model, together with a model of vegetation development, is applied over time to a digital elevation model (DEM) to generate spatial patterns of fire regimes. The modelling formulation is a simulation one, in order to emulate this spatially correlated contagious process. These synthetic fire regimes are used to provide insight in the relative importance of parameters to the one-dimensional model to fire regime attributes of frequency, fireline intensity and seasonality. FIREMESH is designed to test the relative importance of spatial and temporal resolution in simulations compared to the parameters of the one-dimensional model of fire velocity.

The velocity of fire in the direction of the wind is determined from the Mark V Forest Fire Danger Meter (McArthur 1973) expressed as equations (Noble et al. 1980). This meter has been the most widely used method of predicting fire velocity in forest surface litter in eastern Australian. It is based on observations of approximately 800 fires under mostly low fire danger conditions but has been reported to under-estimate velocity under more extreme conditions (McCaw et al. 2008). An option has been included in FIREMESH to adjust the fire velocity as indicated by McCaw et al. (2008) from fire experiments conducted under more extreme conditions (Project Vesta Gould et al. 2007, Cheney et al. 2012).

The transformation of the one-dimensional model to two dimensions is based on the assumption that fires propagate in a manner that produces an elliptical shape (Alexander 1985). These shapes are represented by discrete geometries in many models which are known to under predict the area of a fire compared to an ellipse (Feunekes 1991). FIREMESH is designed to test the importance of this under-prediction compared to the parameters of the one-dimensional model

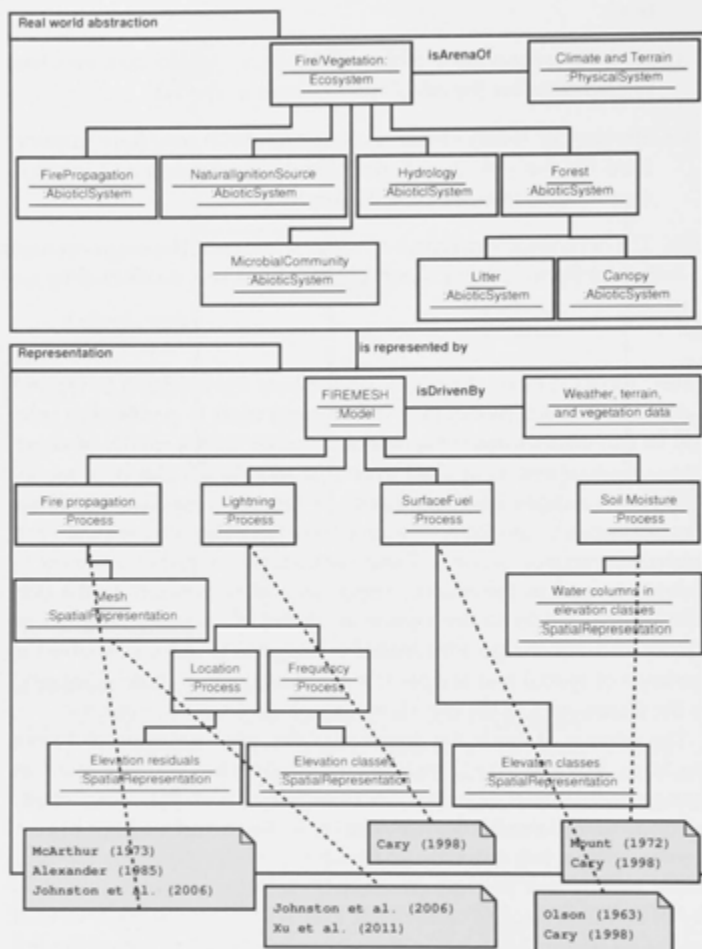


Figure A.6: FIREMESH using the Ecosystem Ontology (Gignoux et al. 2011) showing the conceptual model (top panel) and its representation as the FIREMESH simulation model (bottom panel). Notes (grey) indicate references to each process implementation. The classes of each object above are from Gignoux et al. (2011), Figure 2. Each Process is associated with one SpatialRepresentation.

of fire velocity in terms of the patterns of fire regimes produced by the model. The vegetation model is based on the concept of a climax state, where the state is reset by disturbance (Olsen 1963, Walker 1981).

EMERGENCE What naturally emerges from FIREMESH (and other similar models) is auto-correlated spatial patterns of fire regimes. Fire is a contagious process and a vertex's position among other vertices will play a role in determining its fire regime. This follows from the concept of ignition neighbourhoods (Cary 1998, Wood et al. 2011), together with elevation anomalies that drive ignition locations (Cary 1998, McRae 1992). A location is more likely to burn if it is up slope of a burning neighbour. It is also more likely to be struck by lightning if it has a higher elevation than the mean of elevations in a larger radius, and of course, more likely to burn if its neighbour is burning.

STOCHASTICITY FIREMESH is deterministic with the exception of stochasticity in (i) time and location of lightning ignitions and (ii) the production of Triangular Irregular Network (TIN) meshes. TIN meshes are used to examine the relative importance of constraints imposed by discrete geometries on patterns of fire regimes.

COLLECTIVES The fireline is the only collective entity in FIREMESH that has its own behaviour. As the fireline propagates from time t to $t+1$, the shape of the whole is the sum of each individual propagation and is shown to accord with Huygens Principle (Alexander 1982).

OBSERVATION Outputs take place after each extinguishment of the fireline. These include the time a vertex entered the burnt state, the proportion of the area represented by a vertex that has burnt, and the fireline intensity at which all vertices were ignited.

A.5 INITIALIZATION

At time $t = 0$:

- i the state of each Vertex(residual_fuel_weight, time_last_burnt, state) is (0, 50, unburnt).
- ii A soil dryness index (SDI) has been calculated from the weather data and placed in a lookup table for each elevation class (100 meter classes) for each day within the extent of the weather data. For each day in the weather records, the size and time since the last rain event (days) has been calculated.
- iii The time and location of all lightning strikes have been calculated by the lightning model with a unique random number seed to generate stochasticity.

- iv All vertices have been initialized with x, y and z locations and all `Direction:fireline` is set to zero.

A.6 INPUT DATA

Input data is a set of half-hourly readings of temperature ($^{\circ}\text{C}$), vapour pressure (hPa), wind direction (at 10° resolution from north) and wind speed ($\text{km}\cdot\text{h}^{-1}$). Wind speed is the sustained wind speed averaged over the 10 minutes leading up to the time of the observation at 10 meters above ground level (U_{10}). Daily rainfall is that recorded at 9am.

This input data, sourced from a single weather station, is extrapolated to higher elevations by comparison with a station at a higher elevation. This applies only to temperature and precipitation. The change in precipitation is based on the ratio 2.06:1 for an elevation difference of 1,183 meters. The temperature lapse rate is calculated by comparison with each 3 hour reading over 460 days for the same range in elevation (Figure A.7).

A digital elevation model with a resolution of 20 meters is read to set elevations in each Vertex using the elevation (z) closest to the vertex's x, y location.

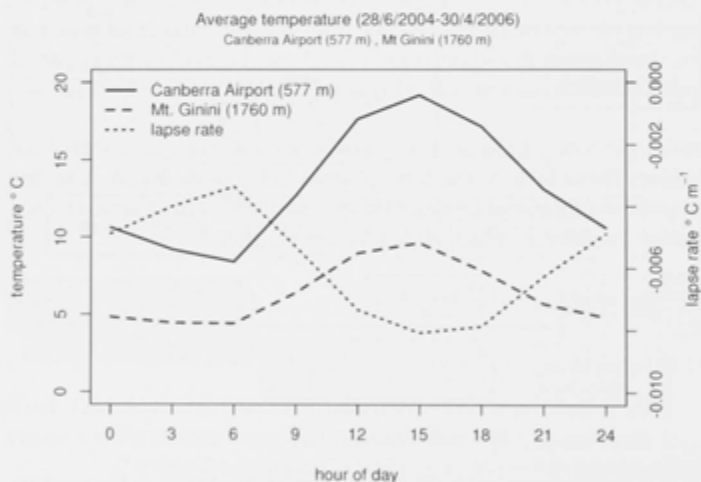


Figure A.7: The mean of 420 days of three-hourly temperature readings at Canberra Airport and Mt Ginini

The dotted line is the 3 hourly temperature lapse rate ($^{\circ}\text{C}\cdot\text{m}^{-1}$) derived from temperature differences between Canberra Airport (Elev.: 577 m, Lat.: -35.31, Lon.: 149.2) (solid line) and Mt Ginini (Elev.: 1760 m, Lat.: -35.53, Lon.: 148.77) (dashed line).

A.7 SUBMODELS

LIGHTNING Lightning Ignition model is described in Cary (1998) and Cary and Banks (2000).

SURFACE FUEL The fuel model is a physical model of litter inputs and decay rates (Olsen 1963) (Equation A.1)

$$F = F_r + (X_{SS} - F_r)[1 - e^{(-L/(X_{SS} - F_r)t}] \quad (A.1)$$

where:

F_r = residual_fuel_weight (t.ha^{-1});

X_{SS} = the fuel weight at steady state (t.ha^{-1});

L = Litter input rate ($\text{t.ha}^{-1}.\text{t}^{-1}$); and

t = time (years).

Parameterization is from observations by Cary (1998) and Walker (1981).

Table A.1: Steady state values ($X_{SS}\text{t.ha}^{-1}$) and litter input rates (L) for surface litter for five elevation classes in the Brindabella study region (from Cary, 1998)

ELEVATION (m)	$X_{SS}(\text{t.ha}^{-1})$	$L (\text{t.ha}^{-1}.\text{y}^{-1})$	COVERAGE
≤ 750	9.64	2.89	7%
$\leq 1,000$	9.95	2.98	6%
$\leq 1,250$	11.55	3.46	40%
$\leq 1,500$	14.67	4.40	40%
$> 1,500$	16.37	4.91	7%

SOIL MOISTURE The soil moisture sub-model is based on the lookup tables of Mount (1972). The tables specify the amount of evapo-transpiration from a 200 mm column of water with 9 temperature and 5 soil water deficit classes (Table A.2). There are two tables, one for spring and a second for autumn, to account for warming and cooling trends in soil temperature. The equation to calculate the drought factor (Noble et al. 1980) has been modified to suit the SDI of Mount (1972) rather than the Keetch-Byram Drought Index (Keetch and Byram 1968) (Equation A.2) and limited to a maximum of 10 as recommended by Sirakoff (1985).

$$D = [0.141 * (SDI + 156) * (N + 1)^{1.5}] / [4.5 * (N + 1)^{1.5} + P - 1] \quad (A.2)$$

where:

D = Drought factor;

SDI = soil dryness index;

P = size of the last rain event (mm); and

N = days since the last rain event.

Table A.2: Evapo-transpiration table for Canberra from Mount (1972) in Soil Dryness Index (0-200mm) and temperature classes

Jun-Jan°C		0	5	10	15	20	25	30	35	40
Feb-May°C		2	7	12	17	22	27	32	37	42
SDI	0+	0.5	1	2	2.5	3	4	5	6	7
	25+	0.5	1	1	1.5	2.5	3	4	5	6
	50+	0	0	0.5	1	2	3	4	4.5	5.5
	140+	0	0	0.5	1	1	1	1.5	1.5	2
	165+	0	0	0	0	0	0.5	0.5	0.5	1

FIRE VELOCITY IN DIRECTION OF THE WIND The fire velocity in the direction of the wind is calculated using the equations for rate of spread of fires in forest surface litter (Noble *et al.* 1980).

$$FFDI = 1.25 \times D \times \left(\frac{T - R_h}{30.0} + 0.0234 \times U_{10} \right) \quad (A.3)$$

where:

FFDI = Forest Fire Danger Index

D = Drought factors (Equation A.2)

T = Temperature (°)

R_h = Relative humidity

U₁₀ = Wind speed

$$R_h = 0.0012 \times FFDI \times W \times 1000 \quad (A.4)$$

where:

R_h = Rate of spread (m.h⁻¹)

W = Fuel weight (t.ha⁻¹)

The option to alter the rate of spread following McCaw *et al.* (2008) is:

$$R_V = R_M + (U_{10} - 12.5) / (50 - 12.5) (5.45 R_M - 109 - R_M) \{U_{10} > 12.5\} \quad (A.5)$$

where:

R_M = rate of spread following Noble *et al.* (1980); and

U₁₀ = wind speed at 10m above ground level.

FIRE VELOCITY ON A SLOPE Noble *et al.* (1980) do not specify the domain of Θ (slope degrees from horizontal). It is limited to $\pm 20^\circ$ in FIREMESH following discussion in Catchpole (2002).

$$R_\Theta = R_h \cdot e^{-0.0693 \cdot S} \quad (\text{A.6})$$

Where S is slope from horizontal in degrees.

FIRE VELOCITY IN DIRECTION Θ ON REGULAR GRIDS Length-to-breadth ratio ($L:B$) of an ellipse that determines rates of spread in any direction:

$$L : B = \begin{cases} 1 + 0.0012 \cdot U_{10}^{2.154} & \{U_{10} \leq 47 \text{ km.h}^{-1}\} \\ 1 + 8.729(1 - e^{(-0.03 \times U_{10})^{2.155}}) & \{\text{otherwise}\} \end{cases} \quad (\text{A.7})$$

Rate of spread of the back fire:

$$\text{FFDI}_{BF} = 1.25 \cdot D \cdot e^{(\frac{T-H}{30} + 0.0234 \cdot U_{10} \times e^{-0.05039 \cdot U_{10}})} \quad (\text{A.8})$$

$$R_b = 0.0012 \cdot \text{FFDI}_{BF} \cdot W \quad (\text{A.9})$$

where:

FFDI_{BF} = Forest fire danger index for the back-fire;

D = drought factor;

T = temperature ($^\circ\text{C}$);

H = relative humidity;

U_{10} = wind speed (km.h^{-1}); and

W = fuel weight (g.m^{-2}).

R_b = rate of spread of back-fire (m.h^{-1}).

To calculate rate of spread in any direction:

With reference to Figure A.8:

$$F_a = (R_h + R_b) / 2 - R_b \quad (\text{A.10})$$

E_b has $L:B$ given by Equation A.5. Both ellipses have the same semi-major axes but differ in the magnitude of their semi-minor axes and thus their focuses.

$$H : B = \frac{(L : B + \sqrt{L : B^2 - 1})}{L : B - \sqrt{L : B^2 - 1}} \quad (\text{A.11})$$

$$a = R_h / 2(1 + 1/H : B) \quad (\text{A.12})$$

$$F_b = R_h / 2(1 - 1/H : B) \quad (\text{A.13})$$

In Figure A.8, if we align E_a and E_b along their common major axis, and define a line from F_a at angle Θ we have point P where this line intersects E_b . The fire velocity in direction Θ is the length of $F_a P$. The Cartesian coordinates of P may be found by solving simultaneously the equations for the tangent of E_b at P and the line $F_a P$ after Wallace (1993). The length of $F_a P$ is then found by application of Pythagoras's theorem.

FIRELINE INTENSITY Fireline intensity (Byram 1959) is a measure of the rate of energy released per unit of fireline length (I) (kW.m^{-1}), a product of the heat of combustion (H) ($20,000 \text{ kJ.kg}^{-1}$), the fuel weight (W) (g.m^{-2}) and the rate of spread of the fire (R) (m.s^{-1}).

$$I = H.W.R \quad (\text{A.14})$$

FIRE VELOCITY IN DIRECTION Θ ON MESHES COMPOSED OF TRIANGULAR IRREGULAR NETWORKS (TIN) The equation to account for the difference between Euclidean and travel distance on an TIN follows Johnston et al. (2006) but with two modifications to align point of ignition within an ellipse to be consistent with the method for regular meshes as just described.

$$R_{\text{micro}}(\theta) = \begin{cases} \beta \frac{R_0 [1 - \cos \theta] + R_h [\cos \theta - \cos \alpha]}{1 - \cos \alpha} & |\theta| < \alpha \\ \beta \frac{R_0 [1 - \cos \theta] + R_h [\cos \theta - \cos \alpha]}{1 - \cos \alpha} & |\theta| < \alpha + 180 \\ \beta R_0 & \text{otherwise} \end{cases} \quad (\text{A.15})$$

where:

$\beta = -0.42/(R_h/R_0)^3 + 0.91/(R_h/R_0)^2 - 0.84/(R_h/R_0) + 0.39$; and $\alpha = 40$.

R_0 is noted in Figure A.8, and differs from R_0 in Johnston et al. (2006) which is equivalent to R_b in Figure A.8.

FIRELINE INTENSITY ON A TRIANGULAR IRREGULAR NETWORK

$$I = H.W.R_{\text{micro}}/(1 + \beta) \quad (\text{A.16})$$

SPREAD AND EXTINGUISHMENT THRESHOLD Fire spread at a vertex halts (smoulders) when the maximum fireline intensity in any direction is less than 100 kW.m^{-1} (Cary and Banks 2000).

A fire has extinguished when no vertex reports a fireline intensity greater than or equal to 83 kW.m^{-1} (Cary and Banks 2000).

A.8 REFERENCES

Alexander, M. (1985), Estimating the length-to-breadth ratio of elliptical forest fire patterns, in *Proceedings of the eighth conference on fire and forest meteorology*, pp. 85-04.

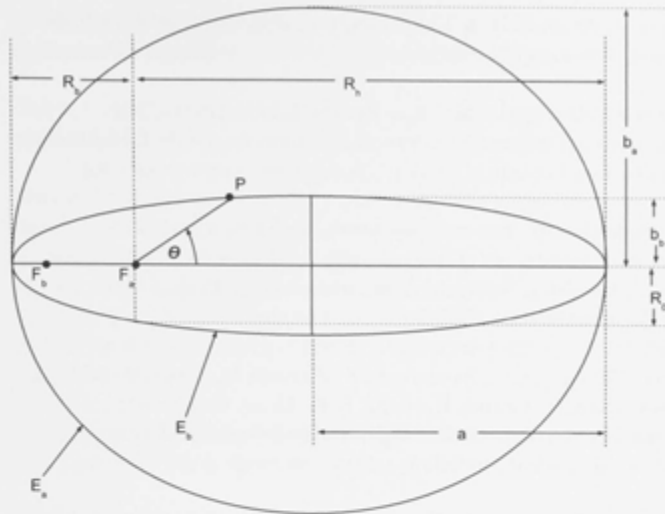


Figure A.8: Ellipse parameters required to shift the point from which the fire is assumed to propagate

Alexander, M. E. (1982), Calculating and interpreting forest fire intensities, *Canadian Journal of Botany* 60(4), 349–357.

Byram, G. M. (1959), Combustion of forest fuels: Forest fire: control and use 1, 61–89.

Cary, G. J. (1998), 'Predicting fire regimes and their ecological effects in spatially complex landscapes'.

Cary, G. J. & Banks, J. C. (2000), Fire regime sensitivity to global climate change: an Australian perspective, *Advances in Global Change Research: Biomass burning and its inter-relationships with the climate system*. Kluwer Academic Publishers, London, UK.

Catchpole, W. (2002), 'Fire properties and burn patterns in heterogeneous landscapes', *Flammable Australia: the fire regimes and biodiversity of a continent*, 49–75.

Cheney, N. P.; Gould, J. S.; McCaw, W. L. & Anderson, W. R. (2012), 'Predicting fire behaviour in dry eucalypt forest in southern Australia', *Forest Ecology and Management* 280, 120–131.

Feunekes, U. (1991), 'Error analysis in fire simulation models', PhD thesis, University of New Brunswick (Canada).

- Geiger, R. Aron, R. H. & Todhunter, P. (2009), *The climate near the ground*, Rowman & Littlefield.
- Gignoux, J. Davies, I. Flint, S. & Zucker, J.-D. e. (2011), 'The Ecosystem in Practice: Interest and Problems of an Old Definition for Constructing Ecological Models', *Ecosystems* 14(7), 1039–1054.
- Gill, A. M. (1975), 'Fire and the Australian flora: a review', *Australian forestry* 38(1), 4–25. Gould, J.; McCaw, W.; Cheney, N.; Ellis, P.; Knight, I.; Sullivan, A. & others (2007), 'Project Vesta: Fire in Dry Eucalypt Forest', CSIRO.
- Grimm, V.; Berger, U.; Bastiansen, F.; Eliassen, S.; Ginot, V.; Giske, J.; Goss-Custard, J.; Grand, T.; Heinz, S. K.; Huse, G. & others (2006), 'A standard protocol for describing individual-based and agent-based models', *Ecological modelling* 198(1), 115–126.
- Grimm, V.; Berger, U.; DeAngelis, D. L.; Polhill, J. G.; Giske, J. & Railsback, S. F. (2010), 'The ODD protocol: a review and first update', *Ecological Modelling* 221(23), 2760–2768.
- Hirsch, K. G. (1996), *Canadian forest fire behavior prediction (FBP) system: user's guide*, Vol. 7.
- Johnston, P. Kelso, J. & Milne, G. J. (2008), 'Efficient simulation of wildfire spread on an irregular grid', *International Journal of Wildland Fire* 17(5), 614–627. Keetch, J. J. & Byram, G. M. (1968), A drought index for forest fire control, US Department of Agriculture, Forest Service, Southeastern Forest Experiment Station.
- McArthur, A. G. (1973), 'Forest Fire Danger Meter Mark V', Commonwealth of Australia Forestry and Timber Bureau, Canberra.
- McCaw, W. Gould, J. & Cheney, N. (2008), 'Existing fire behaviour models under- predict the rate of spread of summer fires in open jarrah (*Eucalyptus marginata*) forest', *Australian Forestry* 71(1), 16–26.
- McRae, R. H. (1992), 'Prediction of areas prone to lightning ignition', *International Journal of Wildland Fire* 2(3), 123–130.
- Mount, A. (1972), *The derivation and testing of a soil dryness index using run-off data*, Forestry Commission, Tasmania.

Noble, I. Gill, A. & Bary, G. (1980), 'McArthur's fire-danger meters expressed as equations', *Australian Journal of Ecology* 5(2), 201–203.

Olsen, J. (1963), 'Energy storage and the balance of producers and consumers in ecological systems', *Ecology* 44, 322–32.

Sharples, J. J. (2009), 'An overview of mountain meteorological effects relevant to fire behaviour and bushfire risk', *International Journal of Wildland Fire* 18(7), 737–754.

Sirakoff, C. (1985), 'A correction to the equations describing the McArthur forest fire danger meter', *Australian journal of ecology* 10(4), 481–481.

Walker, J. (1981), 'Fuel dynamics in Australian vegetation', *Fire and the Australian biota*, 101–127.

Wallace, G. (1993), 'A numerical fire simulation-model', *International Journal of Wildland Fire* 3(2), 111–116.

Wood, S. W. Murphy, B. P. & Bowman, D. M. (2011), 'Firescape ecology: how topography determines the contrasting distribution of fire and rain forest in the south- west of the Tasmanian Wilderness World Heritage Area', *Journal of Biogeography* 38(9), 1807–1820.